UNDERSTANDING THE PHYSIOLOGY OF STRIGOLACTONES IN *ARABIDOPSIS THALIANA*: A MULTI-ANGLE APPROACH

CEDRICK MATTHYS

PROMOTERS: PROF. DR. SOFIE GOORMACHTIG, PROF. DR. TOM BEECKMAN

Dissertation submitted in partial fulfilment of the requirements
to obtain the degree of Doctor of Science:
Biochemistry and Biotechnology

Academic year: 2016 – 2017

Ghent University – Department of Plant Biotechnology and Bioinformatics
Vlaams Instituut voor Biotechnologie – Center of Plant Systems Biology

This work was supported by Bijzonder Onderzoeksfonds (BOF) through the PhD fellowship 01D39311.

Examination board

Chair

Prof. Dr. Lieven De Veylder

Ghent University – Faculty of Sciences, Department of Plant Biotechnology and Bioinformatics

VIB – Center of Plant Systems Biology

Secretary

Prof. Dr. Bartel Vanholme

Ghent University – Faculty of Sciences, Department of Plant Biotechnology and Bioinformatics

VIB – Center of Plant Systems Biology

Promoters

Prof. Dr. Sofie Goormachtig

Ghent University – Faculty of Sciences, Department of Plant Biotechnology and Bioinformatics

VIB – Center of Plant Systems Biology

Prof. Dr. Tom Beeckman

Ghent University – Faculty of Sciences, Department of Plant Biotechnology and Bioinformatics

VIB – Center of Plant Systems Biology

Other members

Dr. Sandrine Bonhomme

Institut Jean-Pierre Bourgin, INRA – AgroParisTech – CNRS - Université Paris-Saclay

Dr. Danny Vereecke

Ghent University - Faculty of Bio-engineers; Department of Applied Biosciences

Dr. Boris Parizot

Ghent University – Faculty of Sciences, Department of Plant Biotechnology and Bioinformatics

VIB – Center of Plant Systems Biology

Prof. Dr. Bert De Rybel

Ghent University – Faculty of Sciences, Department of Plant Biotechnology and Bioinformatics

VIB – Center of Plant Systems Biology

SUMMARY

Multiple functions have been identified for the plant hormones strigolactones (SLs) during plant growth and development. However, due to their recent discovery, much still needs to be investigated about the SL signaling cascades and detailed knowledge about their physiological effects is lacking. In this PhD, we aimed to obtain a profound mechanistic and molecular insight into how SL signaling triggers the downstream physiological responses and focused on the root system architecture of *Arabidopsis thaliana*.

To this end, we studied the effect of SLs on the development of the lateral root (LR) in an in-depth spatiotemporal manner and investigated the SL crosstalk with cytokinin and auxin. We could show that treatment with the SL analog *rac*-GR24 did not affect LR initiation, but negatively influenced LR priming and emergence, the latter especially near the root-shoot junction. The cytokinin module *ARABIDOPSIS HISTIDINE KINASE3 (AHK3)/ARABIDOPSIS RESPONSE REGULATOR1 (ARR1);ARR12* was found to interact with the *rac*-GR24-dependent reduction in LR development, because mutants in this pathway made the LR development insensitive to *rac*-GR24. Additionally, pharmacological analyses, mutant analyses, and gene expression analyses indicated that the affected polar auxin transport stream in mutants of the *AHK3/ARR1;ARR12* module could be the underlying cause. We were also able to determine that the influence of *rac*-GR24 on the LR density requires the recognition of the two *rac*-GR24 enantiomers by both the DWARF14 and KARRIKIN-INSENSITIVE2 receptors.

To obtain a genome-wide overview of the transcriptomic changes brought about by the *rac*-GR24 treatment and to identify the downstream players in the physiological responses of SLs on the root system architecture, we applied RNA sequencing on root tissues. SLs were found to influence various pathways, such as the hormonal crosstalk, drought responses, and light harvesting and sensitivity, and to modulate the plant's secondary metabolism. Based on the obtained datasets, we could characterize the transcription factor TARGET OF MONOPTEROS5 LIKE 1 (TMO5L1) as a downstream component of the SL pathway in the root. Genetic and molecular evidence revealed that TMO5L1 plays a key role in the

regulation of the SL-mediated root responses, such as influence of the LR development and impact on the flavonol content of the root.

Finally, we also initiated a chemical genetics screen with the aim to identify new SL antagonists that could be helpful in the further deciphering of the SL actions. By screening a compound library for molecules that inhibit the *rac*-GR24-induced reduction in hypocotyl elongation, we identified various lead compounds. Of these lead compounds, three were also found to prevent the *rac*-GR24-induced germination of parasitic seeds, whereas two others possibly influence the impact of *rac*-GR24 on LR development.

In conclusion, by combining the results obtained via these various approaches, we contributed greatly to a better understanding on how the SL signaling network results in the execution of the downstream physiological responses. In addition, the newly identified lead compounds provide a new tool for further research on the molecular SL signaling mechanisms.

SAMENVATTING

Strigolactonen (SLs) zijn plantenhormonen waarvoor verscheidene functies geïdentificeerd werden tijdens de groei en ontwikkeling van de plant. Vanwege hun recente ontdekking moet er nog veel onderzocht worden over de SL signalisatiecascades en gedetailleerde kennis over hun fysiologische effecten ontbreekt. Dit doctoraat had tot doel om een diepgaand mechanistisch en moleculair inzicht te verwerven in de manier waarop SL signalisatie zorgt voor de stroomafwaartse fysiologische responsen, waarbij we de focus op de wortelarchitectuur van *Arabidopsis thaliana* legden.

Daartoe hebben we het effect van SLn op de ontwikkeling van de zijwortel (ZW) onderzocht via een diepgaande spatiotemporele analyse en hebben we de interactie van SLn met cytokinine en auxine bestudeerd. We konden aantonen dat behandeling met het SL analoog *rac*-GR24 geen effect had op ZW initiatie, maar een negatieve invloed had op zowel ZW *priming* als uitgroei, dit laatste voornamelijk in de buurt van de overgang van de wortel naar de scheut. De cytokinine module *ARABIDOPSIS HISTIDINE KINASE3 (AHK3)/ARABIDOPSIS RESPONSE REGULATOR1 (ARR1);ARR12* bleek te interageren met de *rac*-GR24-afhankelijke verlaging van ZW uitgroei, omdat mutanten in deze module een ongevoeligheid vertoonden voor het effect van *rac*-GR24 op ZW ontwikkeling. Bovendien toonden farmacologische analyses, analyses van mutanten en genexpressie-analyses aan dat het verstoorde polaire auxine transport in mutanten van de *AHK3/ARR1;ARR12* module de onderliggende oorzaak zou kunnen zijn. We konden ook vast stellen dat de invloed van *rac*-GR24 op de ZW densiteit de herkenning van de twee *rac*-GR24 enantiomeren vereist, door zowel de DWARF14 als de KARRIKIN-INSENSITIVE2 receptor.

Om een genoom-wijd overzicht van de transcriptionele veranderingen ten gevolge van *rac*-GR24-behandeling te bekomen, en om stroomafwaartse spelers in de fysiologische responsen van SLn op de wortelarchitectuur te identificeren, pasten we RNA sequenering toe op wortelweefsel. SLn bleken verscheidene *pathways* te beïnvloeden, zoals hormonale interacties, droogteresponsen, capteren van licht en lichtgevoeligheid, en het secundaire metabolisme. Op basis van de verkregen datasets, konden we de transcriptiefactor TARGET OF MONOPTEROS5 LIKE 1 (TMO5L1) karakteriseren als een

stroomafwaartse component van het SL signalisatienetwerk in de wortel. Genetisch en moleculair bewijs toonde aan dat TMO5L1 een sleutelrol speelt in de regulatie van de SL-gemedieerde responsen in de wortel, zoals een invloed op de ZW ontwikkeling en de flavonol inhoud van de wortel.

Tenslotte initieerden we ook een chemisch genetische *screen* met als doel nieuwe SL antagonisten te identificeren die nuttig kunnen zijn bij de verdere ontcijfering van de SL activiteiten. Door het screenen van een chemische bibliotheek naar moleculen die de *rac*-GR24-geïnduceerde verlaging van hypocotylelongatie verhinderen, identificeerden we verscheidene *lead* moleculen. Van deze *lead* moleculen waren er drie die ook de *rac*-GR24-geïnduceerde kieming van parasitaire zaden konden voorkomen, terwijl twee anderen mogelijk ook de impact van *rac*-GR24 op LR ontwikkeling beïnvloedden.

Samenvattend, door het combineren van de resultaten verkregen via deze verschillende benaderingen konden we sterk bijdragen tot een beter begrip van hoe het SL signalisatienetwerk resulteert in de uitvoering van de stroomafwaartse fysiologische reacties. Bovendien bieden de nieuw geïdentificeerde *lead* moleculen een nieuw instrument voor het verdere onderzoek naar de moleculaire SL signalisatiemechanismen.

Table of Contents

List of abbreviations

4CL	4-coumarate-CoA ligase
ACT	actin
AHK	arabidopsis histidine kinase
AMF	arbuscular mycorrhizal fungi
ANOVA	analysis of variance
ap	acropetal
ARR	arabidopsis response regulator
BAP	6-benzylaminopurine
BBX	B-box domain protein
bHLH	basic helix-loop-helix
bp	basipetal
BRC	branched
bZIP	basic leucine zipper
CCD	carotenoid cleavage dioxygenase
cDNA	complement DNA
ChIP	chromatin immunoprecipitation
CHS	chalcon synthase
CHX	cycloheximide
CO	carlactone oxidase
Col-0	Columbia-0
COP	constitutive photomorphogenic
CRE	cytokinin response
CRY	cryptochrome
Ct	cycle threshold
D	dwarf
DAD	decreased apical dominance
DAG	days after germination
DLK	D14-like
DMSO	dimethyl sulfoxide
DNA	deoxyribonucleic acid
DSF	differential scanning fluorimetry
EAR	ETHYLENE-RESPONSIVE FACTOR Amphiphilic Repression
EIN	ethylene insensitive
ETR	ethylene response
FC	fold change
FDR	false discovery rate
FLS	flavonol synthase
GAMMA-TIP	gamma tonoplast intrinsic protein
GFP	green fluorescent protein
GUS	β-glucuronidase

HEPES	4-(2-hydroxyethyl)-1-piperazineethanesulfonic acid
HTD	high tillering dwarf
HTL	hyposensitive to light
HY	long hypotocyl
HYH	HY5 homolog
IAA	indole-3-acetic acid
IBA	indole-3-butyric acid
KAI	karrikin insensitive
KAI2c	conserved KAI2 clade
KAI2d	divergent KAI2 clade
KAI2i	intermediate KAI2 clade
KAR	karrikin
KL	KAI2 ligand
KUF	KAR-up F-box
Ler	Landsberg erecta
LHCB	light harvesting complex B
LHW	LONESOME HIGHWAY
LOG	LONELY GUY
LR	lateral root
LRD	lateral root density
LRP	lateral root primordium
M	molar
MAKR	membrane-associated kinase regulator
MAX	more axillary branching
mes	methyl esterase
MS	Murashige & Skoog
NAA	1-Naphthyl acetic acid
NIT	nitrilase
NPA	1-N-naphthylphthalamic acid
OS	orobanchol synthase
PAL	Phe ammonia lyase
PAR	photosynthetically active radiation
PATS	polar auxin transport stream
PDR	pleiotropic drug resistance
PHOT	phototropin
PHY	phytochrome
PIF	phytochrome interacting factor
PIN	pin-formed
PIN1ox	PIN1-overexpressing
PIP	plasma membrane intrinsic protein
PS	photosystem
qRT-PCR	quantitative real-time polymerase chain reaction
RD	response to dessication
RMS	ramosus

RNA	ribonucleic acid
RSA	root system architecture
SAR	structure-activity relationship
SAUR	small auxin up RNA
SCF	Skp, cullin, F-box
SCR	scarecrow
SDS	sodium dodecyl sulfate
SE	standard error
SHY	short hypocotyl
SL	strigolactone
SMAX	suppressor of max2
SMXL	suppressor of max2 like
spp.	species pluralis
TB	TEOSINTE BRANCHED
TF	transcription factor
TIR	transport inhibitor response
TMO	target of monopteros
TMO5L	target of monopteros 5 like
TPL	topless
TPR	topless related
TT	transparent testa
UV	ultraviolet
UVR	UVB-resistance
WT	wild type
XPP	xylem pole pericycle
YFP	yellow fluorescent protein
YLG	Yoshimulactone green

PART I:

INTRODUCTION

CHAPTER 1:

INTRODUCTION THE WHATS, THE WHERES AND THE HOWS OF STRIGOLACTONE ACTION

CEDRICK MATTHYS*, ALAN WALTON*, SYWIA STRUK, ELISABETH STES, FRANCOIS-DIDIER BOYER, KRIS GEVAERT, AND SOFIE GOORMACHTIG

*This chapter is adapted from: **Matthys, C.,*** *Walton, A.,* et al. (2016). Planta 243, 1327-1337.*

Author's contribution: * These authors contributed equally to this work

Abstract

Strigolactones are a group of plant secondary metabolites that have been assigned multiple roles, of which the most recent is hormonal activity. Over the last decade, these compounds have been shown to regulate various aspects of plant development, such as shoot branching and leaf senescence, but a growing body of literature suggests that these hormones play an equally important role in the root. In this chapter, we present the biosynthesis and signaling and discuss the most important strigolactone-related phenotypes, with a main focus on all known root phenotypes linked to strigolactones. We examine the expression and presence of the main players in the biosynthesis and signaling of these hormones and bring together the available information that allows us to explain how strigolactones act to modulate the root system architecture.

1.1. Strigolactone biosynthesis and transport

Much of the initial progress made in unraveling both the strigolactone (SL) biosynthesis and signaling pathways has been based on a set of high-branching/tillering mutants identified in multiple species, such as the high-branching phenotypes of *decreased apical dominance1* (*dad1*) in petunia (*Petunia hybrida*), *ramosus1* (*rms1*) to *rms5* in pea (*Pisum sativum*), *more axillary branching1* (*max1) to max4* in thale cress (*Arabidopsis thaliana)*, and *dwarf* (*d*) and *high tillering dwarf* (*htd*) mutants in rice (*Oryza sativa*) that directed the focus toward research aiming at deciphering the SL mode of action on lateral shoot branching (Beveridge et al., 1996; Bainbridge et al., 2005; Zou et al., 2006; Stirnberg et al., 2007; Alder et al., 2008; Drummond et al., 2009; Vogel et al., 2010). Indeed, mutants in the SL pathway show a bushy phenotype that can be rescued by application of synthetic SLs for the biosynthesis, but not for the signaling mutants.

Originally, all natural SLs were discovered in root exudates and consist of a tricyclic lactone group (ABC-rings), connected by an enol-ether bridge to a butenolide group (D-ring) (Figure 1). Generally, one or two methyl groups are coupled to the A-ring and one or more hydroxyl or acetoxyl groups to the A/B-part (Xie et al., 2010; Al-Babili and Bouwmeester, 2015). The most rudimentary molecule is 5-deoxystrigol and is, therefore, considered as the general precursor of the other SLs. Besides the natural SLs, also synthetic bioactive analogs exist, such as the commonly used *rac*-GR24 (Figure 1) (Yoneyama et al., 2009; Zwanenburg et al., 2009).

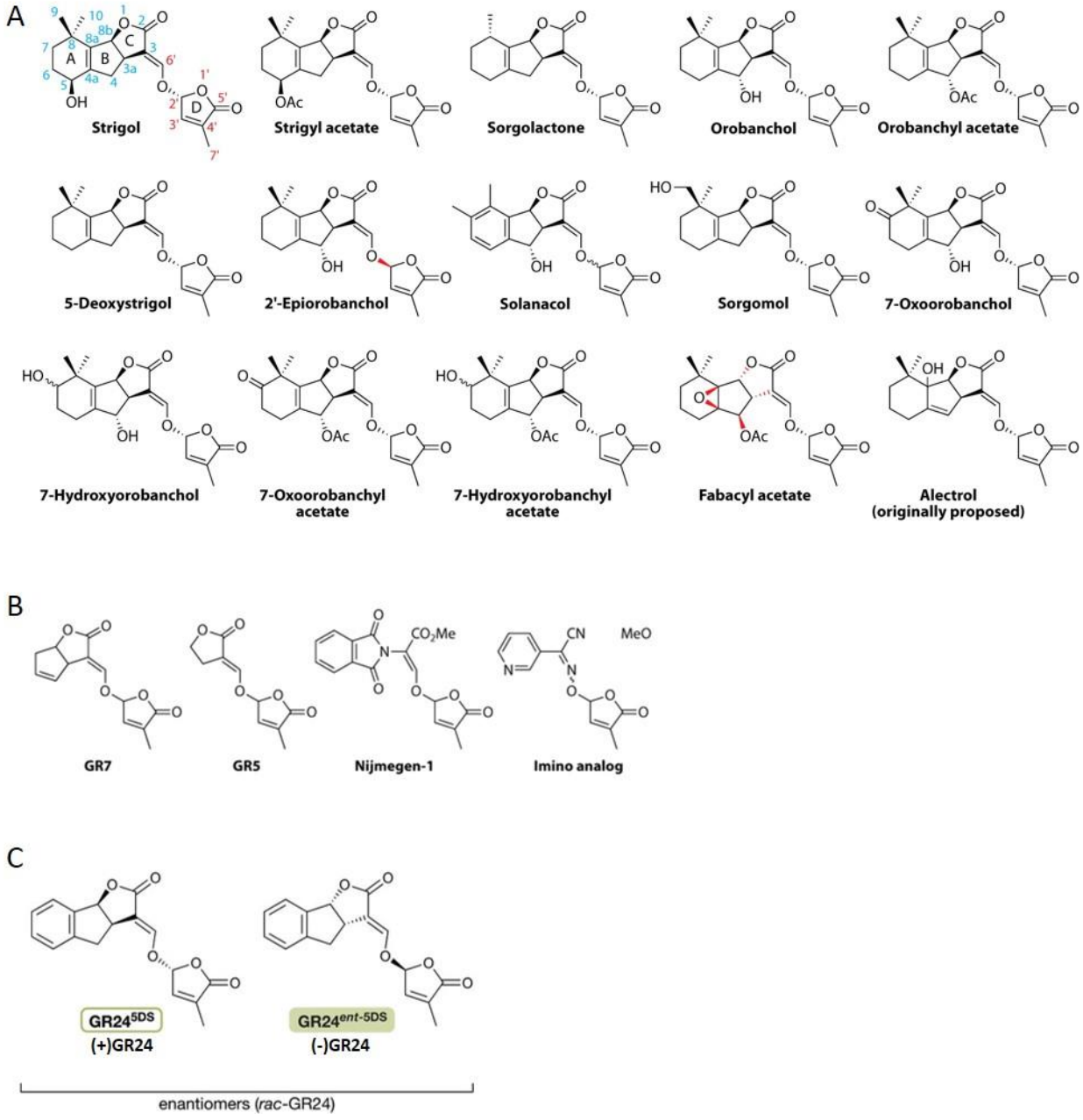

Figure 1. Structure of natural SL molecules and synthetic SL analogs. (A) A selection of various occurring natural SLs. **(B)** Synthetic SL analogs, GR7, GR5, Nijmegen-1, and imino analog. **(C)** Structure of the commonly used synthetic SL analog *rac*-GR24, consisting of two enantiomers: $GR24^{5DS}$ or (+)GR24, and $GR24^{ent\text{-}5DS}$ or (-)GR24. Figure modified from Xie et al., 2010 and Scaffidi et al., 2014.

The first step in the SL biosynthesis pathway is catalyzed by DWARF27 (D27) inside the plastids, namely by isomerization of all-*trans*-β-carotene into 9-*cis*-β-carotene (Figure 2) (Lin et al., 2009; Waters et al., 2012). The next steps in the biosynthesis also occur in the plastids and are catabolized by the

carotenoid cleavage dioxygenases MAX3 and MAX4, giving rise to carlactone, a known SL biosynthesis intermediate, which is the substrate of MAX1 (Figure 2) (Booker et al., 2005; Scaffidi et al., 2013; Seto et al., 2014). In *Arabidopsis*, MAX1 converts carlactone to carlactonoic acid, which, in turn, is a precursor of SLs and methyl carlactonoate, a compound shown to exhibit SL-related activity (Figure 2) (Abe et al., 2014).

Several decisive initial studies provided the foundations for the SL biosynthesis pathway, mainly in pea (for a review, see Beveridge et al., 2009), but also in *Arabidopsis*, in which grafting of wild-type (WT) rootstocks to the scions of either *max1, max3,* or *max4* can rescue the high-branching phenotype (Turnbull et al., 2002; Sorefan et al., 2003; Booker et al., 2004). These data underline the importance of the root for (at least a precursor of) SL production, because the root is sufficient to rescue entirely the shoot branching phenotype in these grafting experiments. However, the SLs are not exclusively produced in the root, because *d27*, *max3,* and *max4* rootstocks do not lead to an increased branching phenotype in WT scions, a phenotype expected to occur when the SL production would completely be abolished (Turnbull et al., 2002; Sorefan et al., 2003).

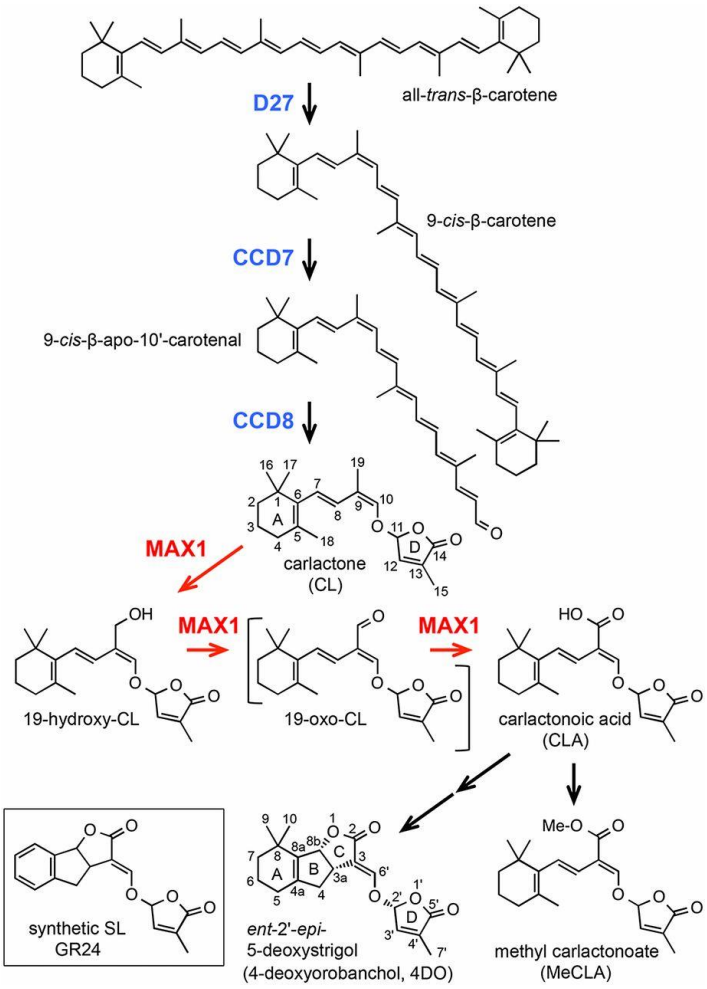

Figure 2. Proposed SL biosynthesis pathway. The first step is the reversible, D27-catalyzed 9-cis/all-trans isomerization of β-carotene. Carotenoid cleavage dioxygenase 7 (CCD7) (MAX3) then mediates the stereospecific cleavage of 9-*cis*-β-carotene at the C9′-C10′ double bond in the *trans*-moiety of the substrate, yielding the intermediate 9-*cis*-β-apo-10′-carotenal and β-ionone. In one step, CCD8 (MAX4) converts 9-*cis*-β-apo-10′-carotenal into carlactone. In *Arabidopsis*, MAX1 converts carlactone to carlactonoic acid, which, in turn, is a precursor of SLs and methyl carlactonoate. Figure modified from Abe et al., 2014.

More clues about SL production came from the expression patterns of the biosynthesis genes. Although the grafting experiments hinted at the roots as important SL production sites, the relative expression of the first biosynthetic gene *D27* is lower in the roots than in the aboveground tissue (Lin et al., 2009). Additionally, the *d27* mutant rootstock, similar to that of the *max3* and *max4* mutants, does

not increase the branching of grafted WT scions, suggesting that the D27 activity in the shoot is sufficient to inhibit branching (Waters et al., 2012). Hence, these data indicate that the root is not the main site for the first committed step in the SL biosynthesis pathway. Still, by means of mRNA *in situ* hybridization in rice, *D27* was shown within the root tissue to be specifically expressed in the lateral roots (LRs) and in the vascular tissue of the crown roots (Figure 3) (Lin et al., 2009). However, an overview of the expression pattern along the primary root is urgently needed. The expression pattern of the *MAX3* and *MAX4* genes also points to a general production of SLs in several tissues, nonetheless with a main production site in the root. Detailed analysis of the p*MAX4*:*GUS* lines in *Arabidopsis* revealed that, although a weak expression could be detected in the hypocotyl, petioles, and somewhat in nodal tissue, most staining occurred in the primary root tip as early as the first day post germination and in the tips of emerged LRs (Figure 3) (Sorefan et al., 2003; Bainbridge et al., 2005). Additionally, detailed comparative analysis of the *MAX3* expression in multiple tissues hints at a predominant expression in the roots, although relatively high levels are also detected in siliques, primary inflorescence stems, and, to a lesser extent, in secondary inflorescence stems and petioles (Booker et al., 2004). Finally, the *MAX1* gene, coding for a cytochrome P450 enzyme, involved in the last documented step(s) of a bioactive SL formation (Figure 2), was expressed all over the plant, more particularly within the vascular tissues (Booker et al., 2005). In the root, the expression starts in the developing vascular tissue above the differentiation zone of the root tip, a pattern that does not overlap with the *MAX4* expression within the root tip (Figure 3) (Booker et al., 2005). However, the nonoverlapping expression patterns are in agreement with the demonstrated mobile nature of the SL intermediate carlactone (Booker et al., 2005; Scaffidi et al., 2013; Seto et al., 2014). The general *MAX1* expression suggests that SLs can be produced everywhere in the plant, thus also in the root.

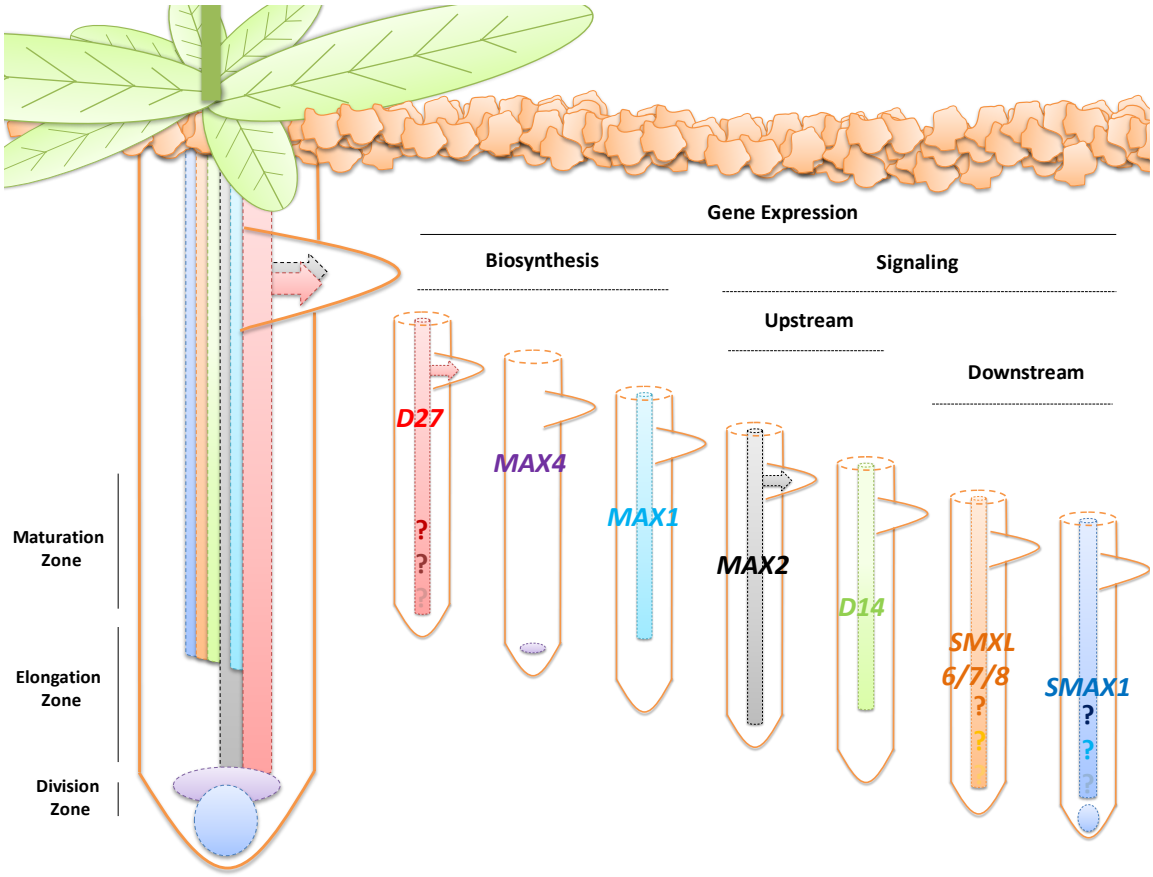

Figure 3. *Arabidopsis* gene expression in the roots for the main SL biosynthesis genes (*D27, MAX4*, and *MAX1)* and the upstream (*MAX2* and *D14*) and downstream (*SMXL6 SMXL7 SMXL8* and *SMAX1*) signaling components. *MAX4* is only expressed in the root tip, whereas *MAX1* is expressed in the vasculature until the differentiation root zone. *MAX2* is expressed in the root vasculature until the root tip, not completely overlapping with the *D14* expression pattern, because *D14* expression is absent in the root tip, but the D14 protein is present in the root tip (data not included in the figure). As no data for *D27* are available in *Arabidopsis*, the current profile is deduced from information available in rice. Because of the lack of spatial information on the *D27* expression along the primary root, the extent of the expression pattern was assumed (indicated by '??'). Also for *SMAX1* and for *SMXL6/7/8,* no information on their expression pattern along the complete main root are known (also indicated by '?').

Altogether, these data imply that SLs are not exclusively produced in the root, but more generally within the vascular tissues of many organs, although long-distance transport from the root toward the shoot has to be considered as well. In agreement, mass spectrometry revealed that SLs occur in the xylem

sap of *Arabidopsis* and tomato (*Solanum lycopersicum*) (Kohlen et al., 2011). However, more recently, the long-distance transport of SLs in a large number of species has been questioned (Xie et al., 2015). In all tested species, both endogenous and exogenous SLs were transported from the root to the shoot, but could never be detected in the xylem sap (Xie et al., 2015), implying that the root-to-shoot transport of SLs happens via active cell-to-cell transport. Valuable information regarding cell-to-cell transport has been obtained from research in petunia that identified an ATP-binding cassette transporter, designated PLEIOTROPIC DRUG RESISTANCE1 (PDR1) as a key SL transporter (Kretzschmar et al., 2012). This transporter is localized asymmetrically in root cells with different expression patterns, depending on the cell type involved (Sasse et al., 2015). In root hypodermal cells, PDR1 is localized on the apical membrane, hinting at an active SL transport mechanism toward the shoot, whereas in the hypodermal passage cells, in which arbuscular mycorrhizal fungi can specifically penetrate the host, the expression is confined to the outer-lateral membrane, indicative for active transport outward into the rhizosphere.

1.2. The strigolactone signaling pathway

The SL signaling pathway is in the process of being unraveled with a central role for the *Arabidopsis* MAX2 protein and its orthologs in various plant species (Beveridge et al., 1996; Ishikawa et al., 2005; Stirnberg et al., 2007; Drummond et al., 2011). This nuclear leucine-rich-repeat-containing F-box protein belongs to the same family as the auxin receptor TRANSPORT INHIBITOR RESPONSE1 (TIR1) and the jasmonate receptor CORONATINE INSENSITIVE1 (Dharmasiri et al., 2005; Stirnberg et al., 2007; Sheard et al., 2010). MAX2 is part of a Skp, Cullin, F-box (SCF)-type E3 ligase complex that ubiquitinates proteins, often to target them for proteasomal degradation (Stirnberg et al., 2007; Vierstra, 2009). In rice and petunia, the MAX2 orthologs interact with the D14 protein, an α/β hydrolase that is able to bind and hydrolyze SLs (Hamiaux et al., 2012; Zhou et al., 2013). The active site of the D14 protein consists of a

hydrophobic pocket containing the highly conserved catalytic triad Ser-Asp-His (Figure 4) (Hamiaux et al., 2012). Binding of *rac*-GR24 in this pocket causes a hydrophilic attack, resulting in the cleavage of the *rac*-GR24 molecule into an ABC-ring part and the D-ring attached to the catalytic Ser (Figure 4) (Zhao et al., 2013). This reaction has a slow enzymatic turnover and destabilizes the D14 protein (Hamiaux et al., 2012; Zhao et al., 2013). As mutation of the catalytic triad abolishes the D14 functionality and because the hydrolyzed products no longer possess any biological activity, the destabilization of the protein is believed to facilitate the interaction with other partner proteins, such as MAX2, followed by proteasomal degradation of target proteins (Figures 4 and 5) (Hamiaux et al., 2012). Based on studies in rice and *Arabidopsis*, DWARF53 (D53) and the eight members of the SUPPRESSOR OF MAX2 1 LIKE (SMXL) family (SMAX1 and SMXL2 to SMXL8), respectively, were proposed to be D3/MAX2 targets (Figure 5) (Jiang et al., 2013; Stanga et al., 2013; Zhou et al., 2013; Kong et al., 2014). For D53, SMXL6, SMXL7, and SMXL8, a *rac*-GR24-induced and for D3/MAX2, a D14-dependent proteasomal degradation were demonstrated, bringing us closer to the understanding of how the MAX2/D14 signaling components give rise to the well-described phenotypes (Figures 4 and 5) (Wang et al., 2015; Soundappan et al., 2015).

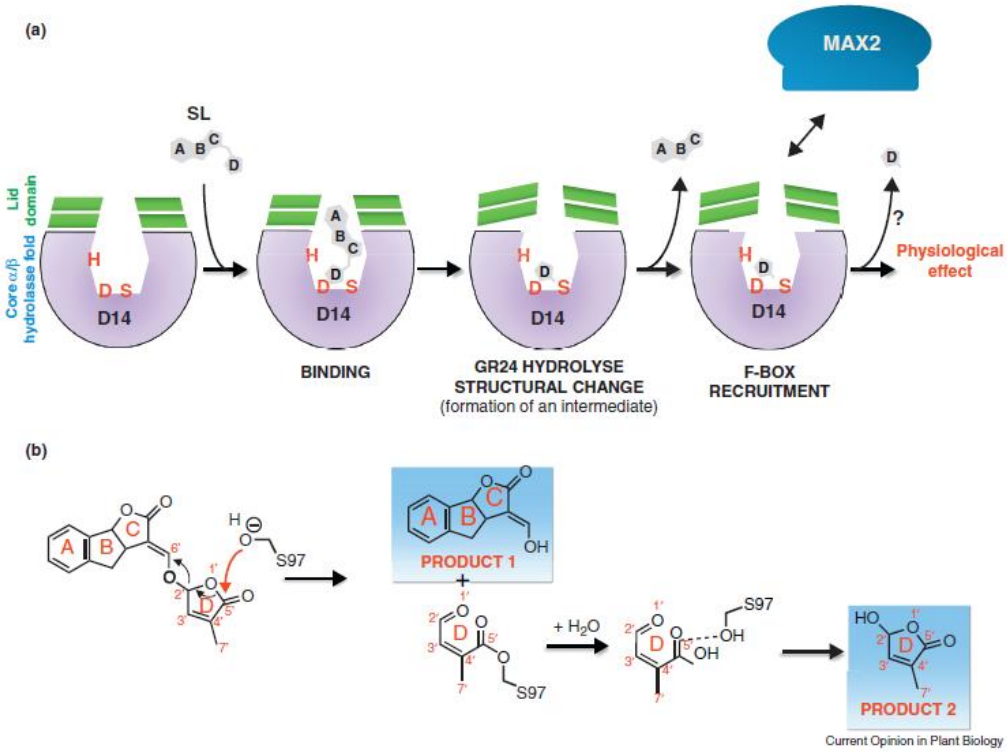

Figure 4. Model for the SL signaling pathway through SL hydrolysis. (a) The proposed SL receptor D14 is an a/b-hydrolase with both binding and enzymatic activities. The hydrophobically active site pocket contains the conserved catalytic triad serine (S), aspartate (D), histidine (H) essential for the D14 enzymatic and binding activities. Structural changes in D14 following SL binding or hydrolysis would trigger MAX2-dependent degradation via the proteasome of SL signaling repressors. How MAX2 binds D14 is still not understood. **(b)** Currently proposed model for *rac*-GR24 hydrolysis by D14 with nucleophilic attack of the D-ring and formation of an intermediate. The hydroxyl group of the serine residue (S97) of the catalytic triad attacks the SL butenolide ring on position C50 leading to the transitory opening of the D ring and the release of product 1. A transient intermediate product is generated, covalently linked to the protein by the serine and rapidly converted into a hydroxyl butenolide (product 2). Figure taken from De Saint Germain et al. (2013).

Both known SL signaling genes *MAX2* and *D14* are expressed in the vascular tissues of several plant organs. MAX2 is mainly localized in the nucleus and distributed in the cells associated with vascular tissues throughout the plant (Shen et al., 2007; Stirnberg et al., 2007). Also in the root, *MAX2* expression occurs in vascular, pericycle, and endodermal cells, with decreasing expression levels toward the root

base (Figure 3) (Stirnberg et al., 2007). In *Arabidopsis*, the expression pattern of *D14* largely ties in with that of *MAX2*. However, inside the root, the *D14* expression is absent in the meristematic zone of the root tip, but appears in the root differentiation and elongation zones, whereafter it progressively gets restricted to the phloem cells (Figure 3) (Chevalier et al., 2014). So, both in the root tip and in the older part of the root vascular bundle, the expression patterns of *MAX2* and *D14* don't appear to overlap. Nevertheless, because the expression pattern of a translational *D14:GUS* fusion is larger than that of a transcriptional fusion, together with a high expression level in the root tip, the D14 protein should be present where *MAX2* is expressed (Chevalier et al., 2014). The subcellular localization of D14 has been found to be both cytoplasmic and nuclear in all investigated tissue types (Chevalier et al., 2014).

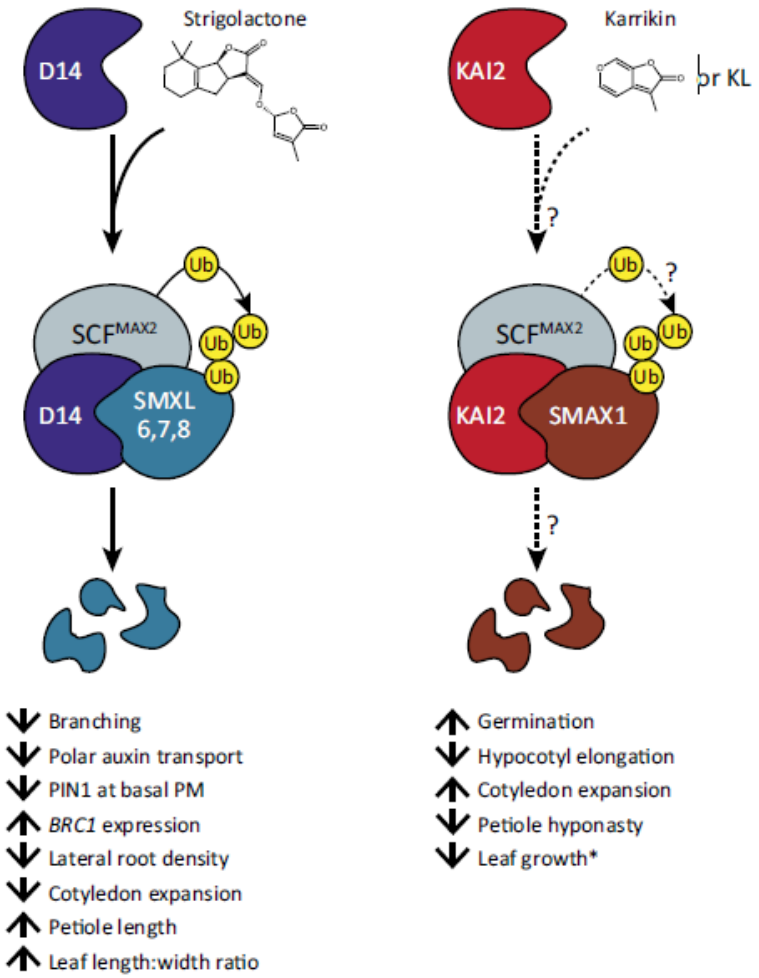

Figure 5. Models of strigolactone (SL) and karrikin (KAR) signaling. SLs are recognized by D14, triggering an association of D14 with SCF^{MAX2} and the SMXL6,SMXL7,SMXL8/D53 proteins that are then targeted for proteasomal degradation, enabling growth responses to SLs. Other carotenoid-derived SL-like molecules, such as methyl carlactonoate, may act similarly through D14. KARs are produced by burning vegetation. Based on genetic evidence and analogy to the SL pathway, we hypothesize that KAR or a putative KARRIKIN INSENSITIVE 2 (KAI2) ligand (KL) are recognized by KAI2, triggering the formation of a SCF^{MAX2}–KAI2–SMAX1 complex. SMAX1 is then polyubiquitinated and degraded by the 26S proteasome, allowing KAR/KL responses, such as increased germination. Dashed lines and question marks indicate that the KAI2-dependent signaling mechanism is an untested hypothesis. Upward and downward arrows mark an increase and decrease in a growth response, respectively. *Leaf growth effects of *kai2* and *smax1* are influenced by photoperiod. Figure modified from Morffy et al. (2016).

This general expression pattern suggests that SL signaling mediated by MAX2 and D14 can happen throughout the plant, although generally restricted to the vascular tissues of the various organs. In the root, it is noteworthy that the signaling components are not always expressed in the specific zones in which SLs play a role, such as in the trichoblasts, *i.e.* the epidermal cells from where root hair cells develop (Stirnberg et al., 2007; Koren et al., 2013; Chevalier et al., 2014). Additionally, reestablishment of the *MAX2* expression specifically in the endodermis via expression through the endodermis-specific *SCARECROW* (*SCR*) promoter could rescue the root hair, lateral root density (LRD), and primary root length phenotypes in the *max2* mutant (Koren et al., 2013). As such, a non-cell-autonomous action of the SL signaling complex in the root is very likely, because of the possible mobility of the D14 protein (Chevalier et al., 2014; Thieme et al., 2015). Alternatively, mobile secondary messengers, other than SLs, might be generated that move to the action site (Kumar et al., 2015). Finally, the expression profiles of the genes encoding four SMXL proteins, responsible for the coordination of the SL signaling downstream of MAX2, have been published (Wang et al., 2015, Soundappan et al., 2015). Through the use of promoter GUS-GFP reporter lines, root-based expression of *SMAX1, SMAX6, SMAX7,* and *SMAX8* has been shown to occur in the vascular tissue of the main root and also, specifically for *SMAX1,* in the root cap (Figure 3) (Soundappan et al., 2015).

A higher level of complexity has appeared concerning the SL signaling network, because some of the core components are also involved in the signaling of other molecules. For instance, KAI2 in *Arabidopsis*, a protein structurally closely related to D14, is responsible for the detection of karrikins, smoke-derived signals that induce seed germination, a process that also appears to require the MAX2 F-box protein and a member of the SMXL gene family, namely SMAX1 (Figure 5) (Nelson et al., 2011; Stanga et al., 2013). Structurally, karrikins share the butenolide D-ring with the strigolactones, but despite their similarity, they show different physiological effects (see below) (Figure 5) (Nelson et al., 2012). Just like D14, KAI2 has a hydrophobic crevice that contains the highly conserved catalytic triad Ser-Asp-His that is

essential for KAI2-functionality and a seemingly similar signaling cascade, although the different shape of the ligang-binding pocket (Figure 5) (Waters et al., 2014, 2015). Moreover, besides a role as a karrikin receptor, KAI2 is also required for the establishment of arbuscular mycorrhization in rice (Gutjahr et al., 2015). Additionally, the commonly used SL analog *rac*-GR24 has been found to trigger non-SL responses as well, making the understanding of the SL signaling and the resulting physiological effects even more tangled (Scaffidi et al., 2014). *rac*-GR24 consists of an equimolar mixture of two enantiomers, (+)GR24 (or $GR24^{5DS}$) and (-)GR24 (or $GR24^{ent\text{-}5DS}$), from which (+)GR24 mimics a natural SL molecule that initiates D14-dependent signaling. However, the unnatural (-)GR24 enantiomer was found to initiate KAI2-specific signaling, rather than a signaling cascade via D14 (Scaffidi et al., 2014). In other words, this enantiomer mimics karrikins and other unknown endogenous compounds that signal via KAI2. Much care should thus be taken when the MAX2-dependent phenotypes resulting from *rac*-GR24 treatment are evaluated, because the outcome might not be SL specific. Furthermore, in parasitic plants, some KAI2 orthologs have evolved to recognize SLs rather than karrikins (see below) (Conn et al., 2015, Tsuchiya et al., 2015).

1.3. The role of strigolactones in rhizosphere communication

SLs have originally been identified as seed germination stimulants for parasitic weeds, such as *Striga* spp. and *Phelypanche* spp. These parasites germinate in the neighborhood of host plant roots, to which they attach themselves to subtract water, photosynthates, and nutrients. The end result is a weakened or dead host, with large agricultural losses worldwide as a consequence (Yoder and Scholes, 2010). These seeds have been known for a long time to only germinate in the presence of host roots (Vaucher, 1823), but it took until 1966 to discover that strigol was the active germination stimulant in root exudates of cotton (*Gossypium hirsutum)* (Cook et al., 1966). Further research identified the CD-moiety of the SL molecule as the bioactiphore for parasitic seed germination, more or less corresponding to the

region that is required for its phytohormonal activity (Zwanenburg and Pospíšil, 2013). Thus, the perception mechanisms might be similar, as indeed in agreement with the recent demonstration that the KAI2 paralogs present in parasites have acquired the ability to sense SLs (Figure 6) (Conn et al., 2015; Tsuchiya et al., 2015; Toh et al., 2015).

The *KAI2* gene has undergone extensive gene duplication in parasites that contain up to 13 copies, whereas *D14* was maintained as a single copy (Conn et al., 2015). Based on their conservation, they can be subdivided into three phylogenetic clades: a conserved clade (KAI2c), an intermediate clade (KAI2i), and a divergent clade (KAI2d), the latter containing the majority of the paralogs (Figure 6). Based on homology modeling and crystal structure, the KAI2d clade is believed to have a larger ligand-binding cavity than KAI2i and KAI2c that is seemingly more similar to the D14 cavity (Conn et al., 2015; Toh et al., 2015). Interestingly, transgenic complementation of the *Arabidopsis kai2* mutant with parasitic KAI2d members confers SL-specific germination to *Arabidopsis*, whereas complementation with a KAI2i member restores specifically karrikin-responsive germination (Conn et al., 2015; Toh et al., 2015). This observation implies that the *KAI2* gene has undergone extensive duplication in the parasite to obtain novel ligand specificities that enables the parasite to respond to various germination stimulants, which, in turn, may influence the host range of the parasite (Figure 6) (Conn et al., 2015).

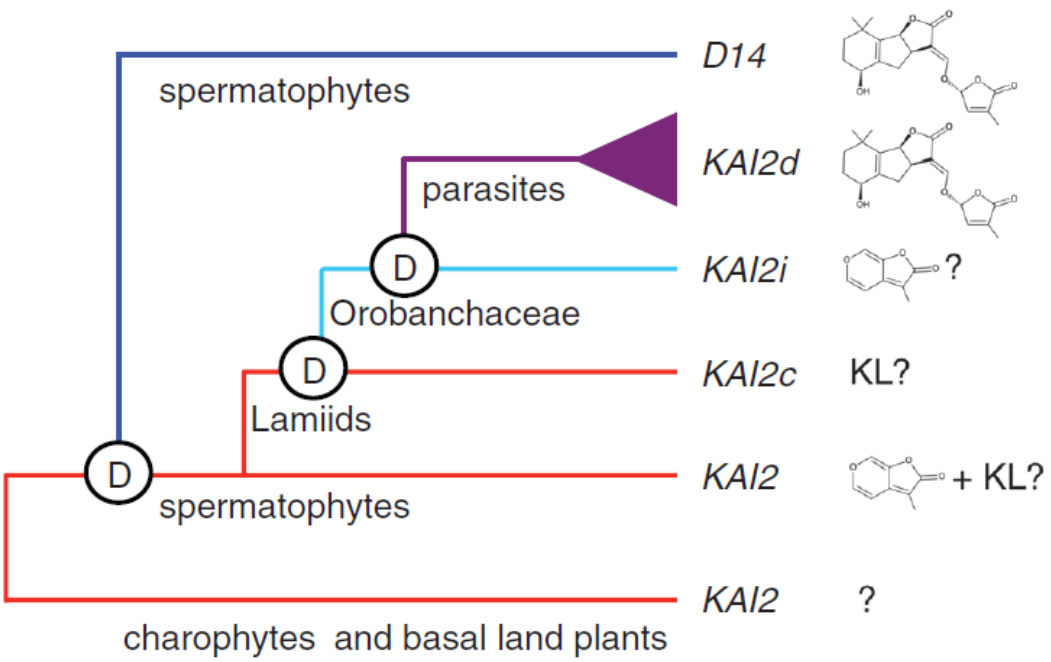

Figure 6. Model of KAI2 and D14 evolution. KAI2 homologs are found in charophyte algae and other basal lineages, but their functions and ligands are unknown. D14 probably arose from a duplication of KAI2 before the evolution of seed plants (spermatophytes). KAI2 of *Arabidopsis* recognizes KAR and probably an endogenous KAI2 ligand (KL). Duplication of KAI2 after the evolution of Lamiids produced KAI2c and KAI2i paralogs in the Lamiales and Solanales. KAI2c may recognize KL and KAI2i possibly also KAR. Further duplication events in the parasitic Orobanchaceae led to a fast evolving clade of KAI2d that recognizes SLs. Figure taken from Conn et al., 2015.

Moreover, the recent development of a probe that activates specifically SL signaling by binding to D14 of *Arabidopsis* and becomes fluorescent after enzymatic hydrolysis has provided more insights into the SL signaling in parasitic seeds (Tsuchiya et al., 2015). This probe, Yoshimulactone Green (YLG), can also be hydrolyzed by several KAI2d paralogs in *Striga*, but not by KAI2c, proving that KAI2d paralogs are indeed responsible for SL-induced germination of parasitic seeds.

From an evolutionary point of view, one could wonder why plants still produce and exude these suicidal compounds into the rhizospere. The question was addressed by the identification of SLs as

branching factors of arbuscular mycorrhizal fungi (AMF) (Akiyama et al., 2005). These fungi form a symbiosis with more than 80% of all land plants to facilitate water and nutrient uptake by the host plants in return for photosynthates for the fungus (Parniske, 2008). The structural requirements for SL molecules to be active as branching factors for AMF seem to be more stringent than those for germination of parasitic seeds and hormonal activity. Indeed, they absolutely need the presence of the ABC-ring part (Akiyama et al., 2010; Cohen et al., 2013), implying that the signaling mechanism of SLs in AMF probably differs from that in plants. However, from the plant side of the symbiosis, KAI2 has been shown to play a pivotal role in the establishment of the symbiotic interaction in rice (Gutjahr et al., 2015). Loss of KAI2 blocks the early colonization process and keeps the plant insensitive for exudates of germinating AMF. Hence, KAI2 might regulate the plant's ability to undergo a symbiotic interaction, although it cannot be excluded that KAI2 might be involved in perception of early communication signals from the fungus (Gutjahr et al., 2015).

1.4. Strigolactones as endogenous phytohormones

Non-host plants of AM fungi, such as *Arabidopsis*, were found to produce SLs, indicating that these molecules must exert an additional endogenous role, because they were found to regulate lateral shoot branching (Gomez-Roldan et al., 2008; Umehara et al., 2008). In the meantime, an increasing amount of research is emerging on the effect of SLs on various other developmental processes, such as germination, photomorphogenesis, and root architecture (Figures 5 and 7) (Woo et al., 2001; Snowden et al., 2005; Shen et al., 2007, 2012; Tsuchiya et al., 2010; Toh et al., 2012).

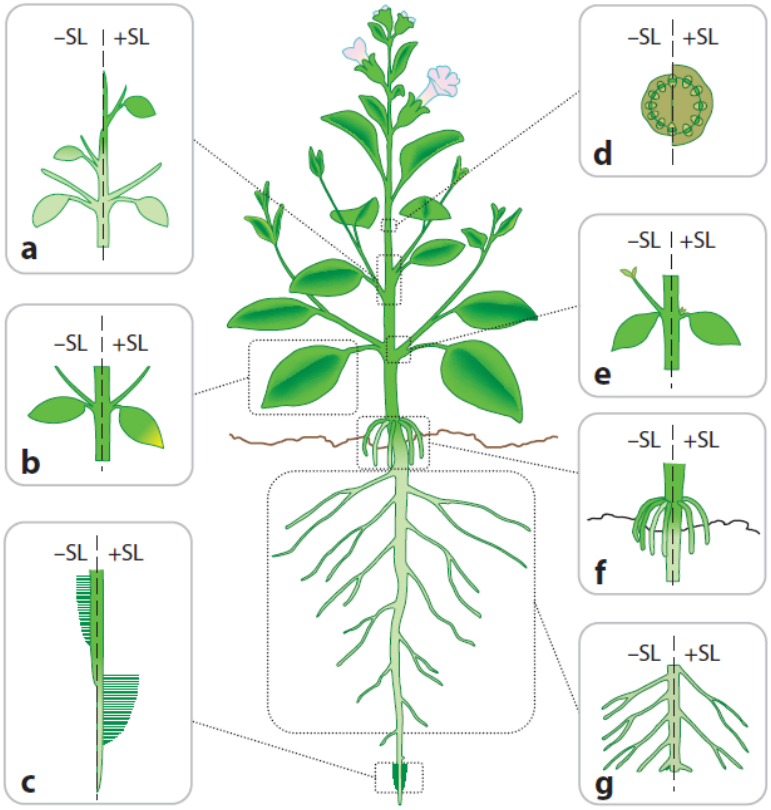

Figure 7. Roles of strigolactones (SLs) in plant development. SLs stimulate internode growth **(a)**, accelerate leaf senescence **(b),** enhance the elongation of root hairs and the growth of primary roots **(c),** increase stem thickness and induce secondary growth **(d),** inhibit the outgrowth of axillary buds (**e),** and inhibit the formation of adventitious roots **(f)** and of lateral roots **(g)**. Figure taken from Al-Babili and Bouwmeester (2015).

1.4.1 Strigolactones control shoot branching

Shoot branching is a major determinant of the plant's architecture and consists of two consecutive processes, namely the formation of buds in the leaf axils and the outgrowth of these axillary buds into branches (Bennett and Leyser, 2006). The outgrowth is tightly regulated by both internal (phytohormones) and external (nutrients, light,…) cues, but, in most cases, the buds stay dormant by a process called apical dominance (Leyser, 2009). This apical dominance is primarily determined by auxin that is mainly produced by young leaves at the tip of the stem and is transported toward the root, although

the apical auxin has been proven to only inhibit branching in an indirect fashion (Thimann and Skoog, 1933; Booker et al., 2003). Besides auxin, also cytokinins influence the shoot architecture by promoting shoot branching instead of inhibiting it (Sachs and Thimann, 1967). Also a third class of phytohormones, SLs, were shown to regulate branching (Gomez-Roldan et al., 2008; Umehara et al., 2008). SL mutants show increased branching, which can be rescued by exogenous *rac*-GR24 in the biosynthetic mutants, but not in the signaling mutants. Also application of the SL intermediate carlactone can rescue this phenotype, but neither in the signaling mutants nor in the biosynthetic *max1* mutant, indicating that carlactone is metabolized in the plant into the bioactive compound in a MAX1-dependent fashion (Scaffidi et al., 2013). For the branching regulation by SLs, SMXL6, SMXL7, and SMXL8 are specifically involved as downstream targets of MAX2 (Soundappan et al., 2015).

Counterintuitively, SLs can both inhibit and promote branching, depending on the applied *rac*-GR24 concentration and the auxin transport status of the plant (Shinohara et al., 2013). Generally, exogenous *rac*-GR24 inhibits branching, but in a genetic background with an altered auxin status (such as in the auxin receptor mutant *transport inhibitor response 3* [*tir3*]) *rac*-GR24 promotes branching at very low concentrations and inhibits branching at higher concentrations (Shinohara et al., 2013).

Currently, two, not mutually exclusive, models can explain the hormonal regulation of shoot branching by auxin, cytokinins, and SLs: the 'secondary messenger' model and the 'auxin transport canalization' model (extensively reviewed by Domagalska and Leyser, 2011). In the secondary messenger model, the reason for indirect inhibition of bud outgrowth by apical auxin is that auxin produces secondary messenger molecules that, in turn, regulate bud outgrowth locally. Both cytokinins and SLs are good candidate secondary messengers, because auxin has been found to regulate their biosynthesis (Hayward et al., 2009; Johnson et al., 2006; Nordström et al., 2004). In agreement with their role as secondary messengers, both hormones can directly regulate bud outgrowth after their application on the buds (Sachs and Thimann, 1967; Brewer et al., 2009).

There is also a lot of supporting evidence for the 'auxin transport canalization model' (Figure 8). In this model, dormant buds are assumed to be a source of auxin that needs to be transported outside the bud to trigger leaf initiation and expansion (Bayer et al., 2009). An initial auxin flux from the buds occurs that eventually develops into a polar auxin transport stream (PATS) by a positive feedback mechanism (Figure 8a) (Balla et al., 2011). The efficiency by which this mechanism takes place depends on the sink capacity of the stem, which is a good auxin sink, to be transported to the roots. However, under normal circumstances, the sink capacity of the stem is already saturated by auxin from the shoot apex, thus preventing bud outgrowth (Figure 8b). Mutants in the SL pathway show an increased accumulation of the PIN-FORMED1 (PIN1) auxin transporter in the PATS with an accompanying enhanced auxin transport capacity (Bennett et al., 2006; Brewer et al., 2009). In addition, the branching phenotype of these mutants can be restored to WT levels by addition of low doses of auxin transport inhibitors (Bennett et al., 2006). SLs are indeed capable of diminishing the auxin transport and the accumulation of PIN1 on the basal membrane of xylem parenchyma cells within 10 minutes after treatment with *rac*-GR24, independent of protein synthesis, but dependent of MAX2 and clathrin (Figure 8b) (Crawford et al., 2010; Shinohara et al; 2013). Based on these data, the canalization model states that SLs act systemically to dampen the PATS in the stem by reducing the PIN1 accumulation on the cell membrane. In this manner, SLs lower the canalization efficiency and enhance the competition between the buds.

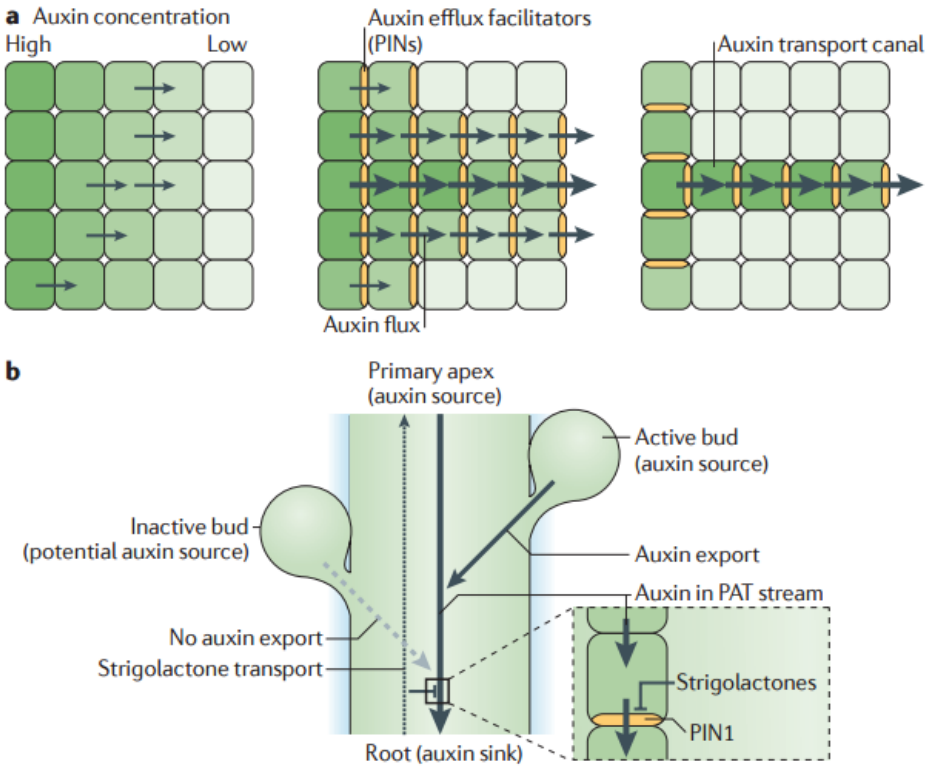

Figure 8. Auxin transport canalization and bud activation. (a) The auxin transport canalization-based model describes a process in which an initial auxin flux from source to sink is gradually canalized into cell files with high levels of highly polarized transporters. Canalization is driven by a positive feedback loop in which the auxin flux upregulates and polarizes the auxin efflux facilitators in the direction of the auxin flow, resulting in the formation of auxin transport canals. **(b)** In the auxin transport canalization-based model, buds act as auxin sources and the stem as an auxin sink owing to its ability to transport auxin away toward the root. Buds must export auxin to be activated and they compete for the common auxin transport pathway through the main stem to the root. Upon bud activation, the auxin transport from active buds reduces the sink strength of the stem and thus prevents other buds from exporting their auxin, allowing auxin to be transported in the PATS, derived either from more apical buds or from the primary apex, to regulate bud activation in an indirect manner. SLs act systemically to dampen the PATS and reduce the accumulation of PIN1 on cell membranes, enhancing competition between buds for the common auxin sink in the stem. Figure taken from Domagalska and Leyser (2011).

1.4.2 The role of strigolactones in photomorphogenesis

Various environmental stimuli regulate plant development, among which light is the most important factor. Depending on the absence or presence of light, plants undergo two different developmental programs: skotomorphogenesis in darkness and photomorphogenesis in the light. Photomorphogenic development is characterized by hypocotyl elongation inhibition, cotyledon opening and greening, and root growth promotion, whereas skotomorphogenesis is associated with an elongated hypocotyl, apical hook maintenance, and closed unexpanded cotyledons (Kami et al., 2010). To be able to respond to various light aspects, such as quality, quantity, duration, and direction, plants are equipped with a vast array of photoreceptors. These receptors are the red/far-red sensing phytochromes (PHYA to PHYE in *Arabidopsis*), cryptochromes (CRY1 and CRY2) and phototropins (PHOT1 and PHOT2) for the UV-A/blue region of the light spectrum, and the UVB-RESISTANCE 8 (UVR8) UV-B receptor (Lin and Shalitin, 2003; Chaves et al., 2011; Rizzini et al., 2011; Burgie and Vierstra, 2014).

Downstream of these photoreceptors, several transcription factors regulate the expression of light-induced genes, of which *LONG HYPOCOTYL5* (*HY5*) is the most important one. *HY5* encodes a basic leucine zipper (bZIP) transcription factor that acts as a positive photomorphogenesis regulator (Chattopadhyay et al., 1998) and its activity is controlled by the negative regulator CONSTITUTIVE PHOTOMORPHOGENIC1 (COP1), an E3 ubiquitin ligase that marks HY5 for proteasomal degradation in the dark (Saijo et al., 2003). Mutations in *HY5* cause pleiotropic phenotypes, such as an elongated hypocotyl in the light and a distorted root architecture (Oyama et al., 1997). This pleiotropism is not unexpected, because HY5 had been identified as a central hub between light and hormone signaling. HY5 has been shown to regulate auxin, gibberellin, and abscisic acid signaling by modulating their biosynthesis or signaling (Cluis et al., 2004; Sibout et al., 2006; Chen et al., 2008; Weller et al., 2009).

For SLs as well, a crosstalk with light signaling during seedling development has been discovered. Indeed, in a genetic screen to identify mutants in the light signaling pathway, MAX2 was retrieved (Shen et al., 2007) and *max2* seedlings show a defective inhibition of the hypocotyl elongation when grown under monochromatic red, far-red and blue light, but do not differ from the WT in the dark. The mutants also develop slightly reduced cotyledons and are hyposensitive to light-induced seed germination (Shen et al., 2007). These responses are regulated downstream of MAX2 by the SMAX1 member of the SMXL family, again indicating that the different physiological responses of SLs are mediated by various SMXL members (Stanga et al., 2013, 2016). Interestingly, the SL biosynthetic mutants *max1*, *max3*, and *max4* do not share these phenotypes with *max2* (Shen et al., 2012). Based on this observation, *MAX2* might regulate photomorphogenesis independently of SLs by modulating several hormonal pathways. Indeed, the *max2* mutant is hyposensitive to gibberellic acid and hypersensitive to abscisic acid during seed germination, accompanied with a misregulation of biosynthetic and catabolic genes of these hormones when compared to the WT (Shen et al., 2012). However, based on these observations, it is hard to fully rule out a role for SLs, because *rac*-GR24 and both pure enantiomers of *rac*-GR24 clearly inhibit the hypocotyl elongation under continuous red light in the WT (Nelson et al., 2011; Scaffidi et al., 2014). The possibility exists that the known SL biosynthetic mutants are leaky or that SLs or related signaling molecules are produced via an alternative, non-canonical biosynthetic pathway. In support of this theory, the *Arabidopsis max1* and *max4* mutants were found to be still capable of inducing germination of *Striga* seeds and a SL biosynthetic mutant of *Physcomitrella patens* of producing SLs (Kohlen et al., 2011; Proust et al., 2011). Also other basal plants known to produce SLs lack some of the canonical biosynthetic genes (Delaux et al., 2012).

SLs and photomorphogenesis have been linked by the fact that *rac*-GR24 inhibits the hypocotyl elongation by preventing the nuclear localization of COP1 and by promoting *HY5* expression and stabilization of the HY5 protein (Tsuchiya et al., 2010). However, the involvement of HY5 in the *rac*-GR24

regulation of photomorphogenesis has been quite controversial. HY5 has been found to be not absolutely required for SL-mediated inhibition of the hypocotyl elongation (Waters and Smith, 2013). Although the *hy5* mutant is less responsive to *rac*-GR24 than the WT, some known transcriptional SL responses were not affected in the *hy5* mutant. In addition, because the double mutant *max2;hy5* had an additive effect on the hypocotyl length, HY5 and MAX2 might act mainly in separate signaling pathways during photomorphogenesis (Waters and Smith, 2013). In contrast, based on more recently available data, a model for the *rac*-GR24-regulated inhibition of the hypocotyl elongation has been proposed with a central role for HY5 (Figure 9) (Jia et al., 2014). *rac*-GR24 inhibits the hypocotyl elongation in a cryptochrome-dependent manner in blue light and in a phytochrome-dependent manner in red and far-red light. Downstream of these photoreceptors, both COP1 and PHYTOCHROME INTERACTING FACTORs (PIFs) appear to be involved as negative regulators of the *rac*-GR24 effects. PIFs are basic helix-loop-helix (bHLH) transcription factors that regulate negatively photomorphogenesis downstream of the phytochromes. Upon activation by light, phytochromes interact with PIF proteins, with their phosphorylation and degradation as a consequence (Leivar et al., 2008; Leivar and Monte, 2014). Whereas the pathway via COP1 requires HY5, the pathway via PIF was found to be independent of HY5 (Figure 9) (Jia et al., 2014). Thus, PIFs are believed to contribute to the *rac*-GR24 response through components different from HY5 that act in a parallel pathway downstream of MAX2, possibly explaining, in part, the previously obtained data on the largely HY5-independent SL-mediated inhibition of the hypocotyl elongation (Waters and Smith, 2013; Jia et al., 2014).

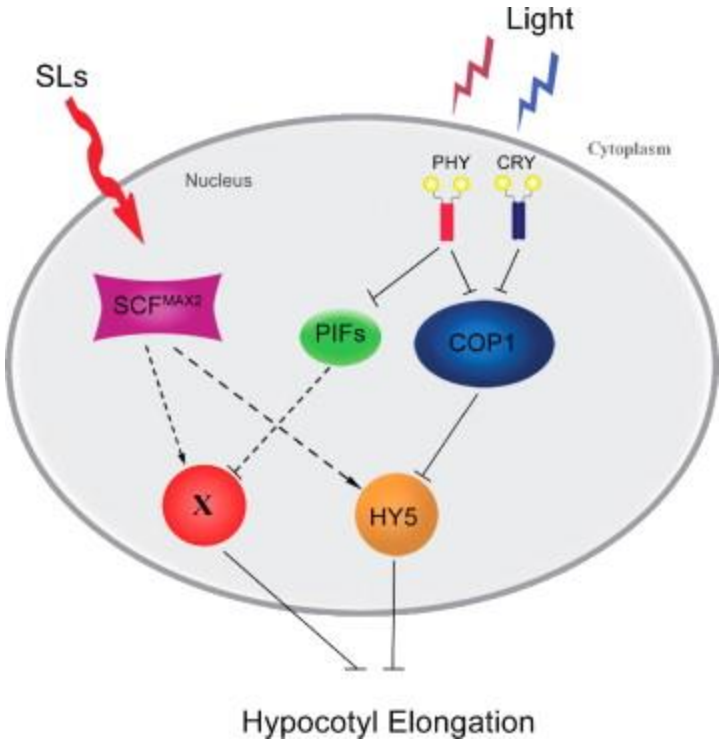

Figure 9. Strigolactone and light signaling pathways coordinately regulate seedling development. Light signals perceived by phytochromes and cryptochromes promote seedling development either by impairing the activity of the negative regulator COP1 that releases downstream positive factors, such as HY5, or by inducing the rapid phosphorylation and degradation of negative transcription factors, such as PIFs. *rac*-GR24 signals, transduced by the SCF^{MAX2} E3 ubiquitin-protein ligase complex, regulate seedling development through MAX2-dependent promotion of *HY5* expression to increase the HY5 accumulation or through an unknown PIF-regulated factor X. Figure taken from Jia et al. (2014).

To complicate matters even more, besides SLs, also karrikins have been shown to regulate the photomorphogenic program of *Arabidopsis* (Nelson et al., 2011). Based on the long hypocotyl phenotype of the *kai2* mutant, which resembles that of *max2* and differs from the WT hypocotyl phenotype of *d14*, the role of endogenous SLs in this phenotype is believed to be subordinate to the endogenous molecule that signals via KAI2 (Scaffidi et al., 2014). Furthermore, the exogenous SL precursor carlactone is at least tenfold less active than *rac*-GR24 in inhibiting the hypocotyl elongation, suggesting that endogenous SLs

-in contrast to exogenous *rac*-GR24- might be less important for photomorphogenesis (Nelson et al., 2011; Scaffidi et al., 2013, 2014).

1.4.3 Strigolactones influence *Arabidopsis* seed germination

Seeds provide a strong protection niche to the vulnerable embryo. Therefore, it is not surprising that seed germination happens under a tight environmental and hormonal control (Penfield and King, 2009). Abscisic acid plays a pivotal role in the establishment of dormancy in seeds, whereas gibberellins are known to counteract these abscisic acid responses, making them powerful germination activators (Yamaguchi et al., 2007). Besides these two key regulators, also a positive role for ethylene and cytokinins in seed germination have been described, although the effect of cytokinins is believed to be due to ethylene production (Lieberman, 1979; Ghassemian et al., 2000).

Recently, also a positive role in seed germination has been attributed to SLs in *Arabidopsis* (Nelson et al., 2011; Toh et al., 2012). In *Arabidopsis*, dormancy is generally weak, so that seeds germinate easily under normal conditions. However, seed germination can be suppressed by supra-optimal temperature conditions, a process called thermoinhibition (Toh et al., 2008). Exogenous *rac*-GR24 overcomes this inhibition, by both decreasing and increasing abscicic acid and gibberellic acid levels in seeds, respectively. In accordance with a role for SL during thermoinhibition, the SL signaling mutant *max2* and the biosynthetic mutant *max1* (but not *max3*) show a hypersensitive phenotype that, in the case of *max1*, can be rescued by *rac*-GR24 addition. Additionally, SLs also overcome secondary dormancy after a prolonged imbibition period at high temperature (Toh et al., 2012). Freshly harvested *Arabidopsis* seeds undergo primary dormancy that can be repressed by karrikins, but also by *rac*-GR24 addition, albeit with a tenfold lower efficiency than that of karrikins (Nelson et al., 2011). Besides the photomorphogenic responses, this response was also shown to be regulated downstream of MAX2 by SMAX1 (Stanga et al., 2013, 2016).

However, later only the non-natural (-)GR24, which is perceived by KAI2, has been found to be responsible for this germination phenotype in primary dormant seeds (Scaffidi et al., 2014). This clarification implies that not endogenous SLs, but karrikins or endogenous molecules that signal via KAI2, are involved in the germination of primary dormant seeds, in agreement with the observation that exogenous carlactone is unable to induce *Arabidopsis* germination (Scaffidi et al., 2013, 2014). The question remains to be answered whether the observed effect of *rac*-GR24 during thermoinhibition is also not due to SLs. However, the fact that the SL biosynthesis mutant *max1* doesn't have a WT phenotype might indicate that endogenous SLs really play a role at least during thermoinhibition.

1.4.4 Regulation of the root system architecture by strigolactones

The root system architecture of *Arabidopsis thaliana*

In *Arabidopsis*, the root system architecture (RSA) is dominated by the primary root. This root is formed already during embryogenesis and, after germination, it grows by cell divisions in the root apical meristem, followed by cell elongation in a specific root zone. After a short while, the one-dimensional growth of the root system expands by the formation of lateral roots (LRs). In contrast to the shoot, no axillary meristems are formed in the root that can give rise to branches. Instead, LRs develop from the pericycle, a tissue comprising the inner cell layer of the root that lines the vascular bundle (Figure 11a). The pericycle is not a homogenous tissue, but consists of different cell types. The cells that are located opposite of the xylem poles are shorter and are radially expanded when compared to the other cells (Laskowski et al., 1995; Dubrovsky et al., 2000). In *Arabidopsis*, LRs only develop from these cell types, thus, only in front of the xylem poles (Dolan et al., 1993).

LR development has been described as consisting of consecutive developmental programs (Figure 10) (Péret et al., 2009). The process starts with priming of the root xylem pole pericycle cells in the root

meristem zone, followed by LR initiation through asymmetric cell division of primed pericycle cells and then by a well-controlled pattern of cell division to finally form the dome-shaped LR primordium (LRP) that pierces through the primary root during LR emergence (Péret et al., 2009).

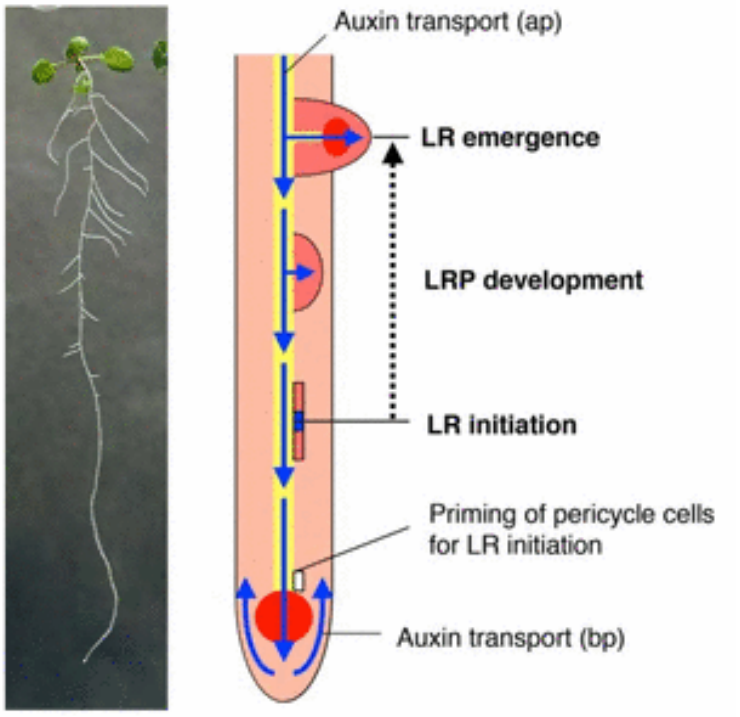

Figure 10. Developmental events during LR formation. First, pericycle cells are primed for the future LR initiation at the basal meristem, followed by LR initiation (anticlinal cell divisions to produce shorter and longer cells) and LR primordium (LRP) development, and finally by LR emergence. Auxin is transported toward the young root tip (acropetal transport; ap), and then, at the root tip, it is redirected to the basal part of the root (basipetal transport; bp). Both acropetal and basipetal auxin transport are required for LR formation. The apical meristem of primary and lateral roots is indicated by red ovals. On the left, a photograph shows a 10-day-old wild-type *Arabidopsis* seedling (Columbia accession). Figure taken from Fukaki and Tasaka (2009).

Priming of pericycle cells – LRs are formed along the primary root according to a highly structured pattern (Lucas et al., 2008). Indeed, not every xylem pole pericycle cell gives rise to a LRP. The first step

during LR formation starts with an oscillatory gene expression in the basal meristem of the primary root, a transition zone between the meristem and the elongation zone (De Smet et al., 2007; Moreno-Risueno et al., 2010). This process is called priming and creates so-called prebranch sites, containing cells able to form a LRP later on and characterized by the expression of the early LR marker *GATA23* (De Rybel et al., 2010). The oscilations in the basal meristem can be visualized by the activity of the synthetic auxin-inducible DR5 promoter and seem to occur with an interval of approximately 6 hours (Moreno-Risueno et al., 2010). Due to the cell divisions in the root meristem, these prebranch sites move shootward, where some of these pericycle cells become specified as founder cells. Recently, the local conversion of indole-3-butyric acid (IBA) into indole-3-acetic acid (IAA) in the root cap has been found to serve as a auxin source that is required to regulate the amplitude of the oscillatory auxin response in the basal meristem and, in turn, the prebranch site formation (Xuan et al., 2015). Moreover, the MEMBRANE-ASSOCIATED KINASE REGULATOR 4 (MAKR4) has been identified to act downstream of the IBA-to-IAA conversion to transform the prebranch sites into founder cells (Xuan et al., 2015). Besides auxin, also a carotenoid-derived signal was shown to be involved in priming (Van Norman et al., 2014), of which the identity remains elusive, because pharmacological experiments and mutant analyses have excluded the involvement of both abscisic acid and SLs (Van Norman et al., 2014).

Lateral root initiation – Immediately after the specification of founder cells, the next step in the LR formation takes place, called the initiation and is characterized by an asymmetric and anticlinal cell division (Casimiro et al., 2001). As such, two smaller daughter cells are generated to form the center of the future LRP. Also during this LR formation step, auxin plays a central role. Just before and during the asymmetric division, auxin accumulates and/or responds in the small daughter cells, together with the induction of various auxin-related genes (Benková et al., 2003; Tatematsu et al., 2004).

Lateral root primordium development – Next, the smaller daughter cells undergo various specifically oriented cell divisions, so that a primordium will develop that eventually will pierce through

the epidermis of the primary root. Based on the cell division patterns, eight different stages can be distinguished (Figures 11b and 11d) (Malamy and Benfey, 1997). First, the smaller daughter cells undergo several rounds of anticlinal divisions by which a cell file of maximally 10 cells develop, characterizing stage I. Then, these cells divide periclinally giving rise to a two-cell--layered structure (stage II). Subsequently, the outer cell layer divides periclinally to generate a stage-III LRP. As not all cells of the primordium divide, the characteristic dome-shape of the LRP arises from this stage on. After this step, a fourth cell layer is formed by another round of periclinal divisions of the inner cells (stage IV). Stage V is characterized by some additional rounds of cell divisions, so that the developing LRP has migrated already half way through the parental cortex. At stage VI, the primordium starts to penetrate into the epidermis and its size has expanded so much that it becomes difficult to trace and define all occurring cell division events. At stage VII, the primordium is on the verge to emerge from the primary root and the actual emergence (stage VIII) is mainly brought about by cell expansion instead of cell division.

As auxin plays a crucial role during LRP development, the PIN1 proteins, which are the most important auxin efflux transporters, are directionally relocalized to cause a lateral auxin flux toward the developing LRP. The subsequent formation of an auxin gradient with a maximum at the primordium tip is crucial for the correct organogenesis of LRs (Figure 11c) (Benková et al., 2003).

Emergence of the LRP is believed to be coupled with the activation of the newly formed LR meristem. From this point on, the primordium is considered to be a mature emerged LR, because their own meristematic cells are responsible for future growth (Malamy and Benfey 1997). However, acropetal transport of the shoot-derived auxin is still required to support the further LR elongation at the early stage (Wu et al., 2007).

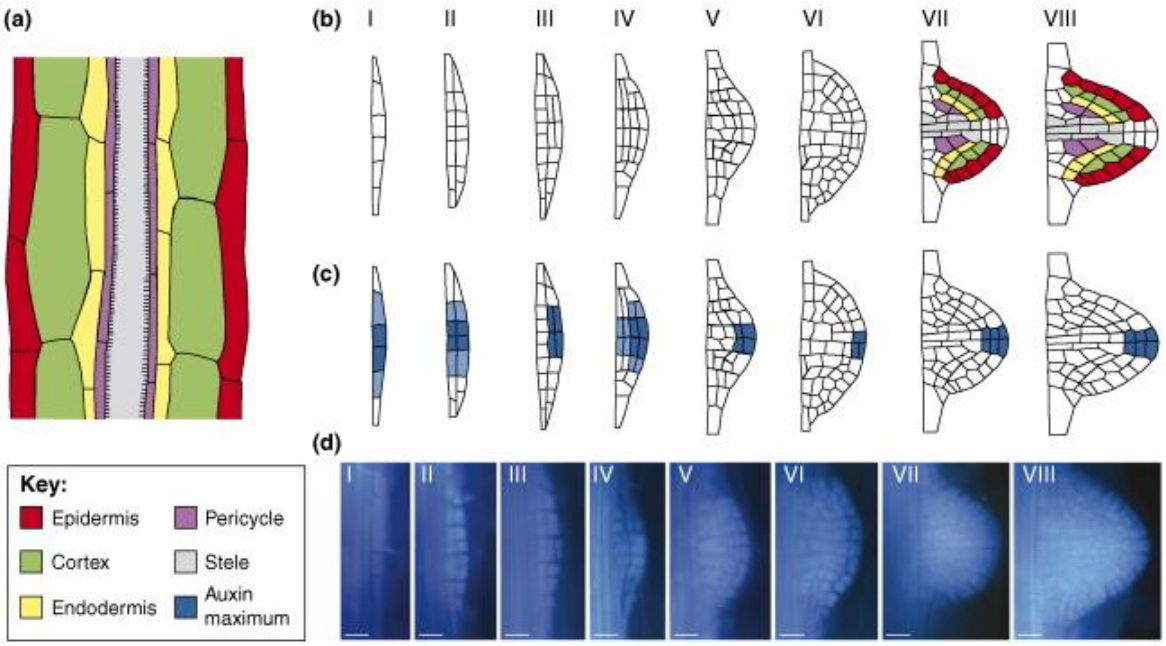

Figure 11. Morphological changes during lateral root development. (a) Section of the *Arabidopsis* primary root. Lateral roots originate deep within the primary root from the pericycle cells. **(b)** The eight stages of primordium development (roman numbers) are shown. **(c)** Establishment of the auxin signaling maximum, as demonstrated with the DR5:GUS reporter (blue gradient). **(d)** The cartoons were drawn from aniline blue-stained roots for each stage of lateral root development. The scale bars represent 20 µm. Figure taken from Péret et al. (2009).

Hormonal regulation of lateral root development

Besides the dominant role of auxin during LR development, other hormones have been shown to be involved in the regulation of this process. Cytokinins, for instance, are known to inhibit the auxin-induced expression of *PIN* genes and to distort the formation of an auxin gradient during LR initiation (Reviewed in Vanstraelen and Benková 2012). As such, cytokinins inhibit both the initial asymmetrical cell divisions of the founder cells and the patterning during the LRP development. Also abscisic acid inhibits LR development, but, in contrast, it prevents the emergence and further outgrowth (De Smet et al., 2006). Ethylene seems to exert a dual role. At high concentrations, it enhances both the acropetal and basipetal auxin transport in the root and, as such, it inhibits auxin accumulation and formation of an auxin maximum

(Negi et al., 2008). Instead, low concentrations promote LR initiation by enhancing auxin biosynthesis (Ivanchenko et al., 2008). Brassinosteroids have also been attributed a role during LR development: they promote LR initiation by enhancing the acropetal auxin transport (Bao et al., 2004). Finally, SLs have been shown to play a role in the RSA regulation (see below).

Which are the effects of strigolactones in the root?

Although the involvement of SLs in shaping the RSA has been demonstrated in various species, including *Arabidopsis*, pea, *Medicago truncatula* (barrel medic), rice, and tomato, most research has been done on *Arabidopsis* (Kapulnik et al., 2011a; Koltai, 2011; Ruyter-Spira et al., 2011; Rasmussen et al., 2012) and the impact of SLs has been identified on all important aspects of the RSA, such as primary root length, root hair formation, LRD, and adventitious rooting (Figure 12). The influence of SLs on the primary root growth has been reported to be subtle and to depend on the growth conditions and the plant species used. Addition of *rac*-GR24 increased the primary root length of *Arabidopsis* with an increase in cortical cells in the primary root meristem as a consequence, especially when plants were grown in the absence of exogenous sucrose (Ruyter-Spira et al., 2011), and coinciding with an increase in size of the meristem and the primary root transition zone (Ruyter-Spira et al., 2011). In agreement, the biosynthetic SL mutants *max1* and *max4* and the signaling mutant *max2* have a shorter primary root than that of the WT, with correspondingly fewer cortical cells in the primary root meristem, suggesting that endogenous SLs control root growth (Ruyter-Spira et al., 2011). However, high concentrations of *rac*-GR24 (> 2.5 µM) lead to a MAX2-independent inhibition of primary root growth, probably due to the toxicity of the nonphysiological concentrations (Ruyter-Spira et al., 2011; Shinohara et al., 2013). Alternatively, it is possible that the *max2* mutant is not completely flawed in SL signaling and starts to respond at higher concentrations of *rac*-GR24. Also in rice, similar effects have been reported, although the primary root of SL mutants was only shorter than that of the WT under low phosphate and low nitrate conditions, demonstrating that the effect of

endogenous SLs is influenced by the growth conditions (Sun et al., 2014). Under both normal and nutrient-poor conditions, application of *rac*-GR24 results in an elongation of the primary root of the WT and of the SL mutants, except for the signaling mutant *d3* (Sun et al., 2014). However, *rac*-GR24 has no effect on the seminal root length (Arite et al., 2012) or on the primary root length of tomato and *M. truncatula* (Koltai et al., 2010; De Cuyper et al., 2015). For tomato, only a combined treatment with auxin uncovered an effect on the primary root length: the inhibitory effect of auxin on root growth diminished with the addition of increased concentrations of *rac*-GR24 (Koltai et al., 2010). In contrast, in *Lotus japonicus* (birdsfoot trefoil) upon silencing of the MAX3 ortholog, the length of the primary root had increased instead of decreased (Liu et al., 2013). Hence, it is difficult to make general conclusions on the SL influence on the primary root length, probably because of subtle phenotypes, the influence of growth conditions, or even varying endogenous hormonal backgrounds between different species.

The effect of SLs is more pronounced on LR development. Treatment with *rac*-GR24 affects LR initiation or outgrowth in a MAX2-dependent manner (Kapulnik et al., 2011a; Ruyter-Spira et al., 2011). Accordingly, the LRD is higher in *max2* than in the WT, indicative of a negative effect of SLs on LR development. However, the LR phenotypes of the SL biosynthetic mutants *max3* and *max4* are still unclear, because the phenotypes do not differ from the WT, although an intermediate phenotype between that of the WT and that of the *max2* mutant has been reported (Kapulnik et al., 2011a; Ruyter-Spira et al., 2011). This observation might indicate that signals other than SLs are at play in the regulation of the phenotype or that some residual SL metabolites are present in the used biosynthesis mutants. Just as for the root length, at high *rac*-GR24 concentrations, a MAX2-independent decrease of the LRD has been observed that could hint at a toxicity effect when *rac*-GR24 is applied at concentrations higher than 1 µM (Ruyter-Spira et al., 2011). Similar to *Arabidopsis*, the LRD of WT rice is reduced after treatment with various concentrations of *rac*-GR24 (Sun et al., 2014). Comparable to the effect on the primary root length, growth conditions also influence the SL impact, because enhanced auxin levels or signaling as obtained

through growth under low phosphate conditions, revert the negative effect of *rac*-GR24 on the LRD into a positive one (Ruyter-Spira et al., 2011). The molecular basis for these observations is still unknown, but could reflect the influence of the auxin landscape on the outcome of the SL treatments, as observed during shoot lateral branching (Ruyter-Spira et al., 2011; Shinohara et al., 2013).

Root hair development is an inherent part of the RSA, because root hairs play an essential role in taking up nutrients from the soil (Gilroy and Jones, 2000; López-Bucio et al., 2003). In both *Arabidopsis* and tomato, *rac*-GR24 elongates the root hairs (Koltai et al., 2010; Kapulnik et al., 2011a). However, SL mutants (*max2*, *max3,* and *max4*) do not seem to exhibit shorter root hairs than the WT under control conditions, indicating that this phenotype might not be controlled by endogenous SLs (Kapulnik et al., 2011a; Koren et al., 2013; Pandya-Kumar et al., 2014). On the contrary, under phosphate-limiting conditions, the root hair density of the SL-biosynthetic mutant *max4* and signaling mutant *max2* appears to be lower than that of the WT, an effect that can be complemented with a high dose of exogenous *rac*-GR24 (Mayzlish-Gati et al., 2012).

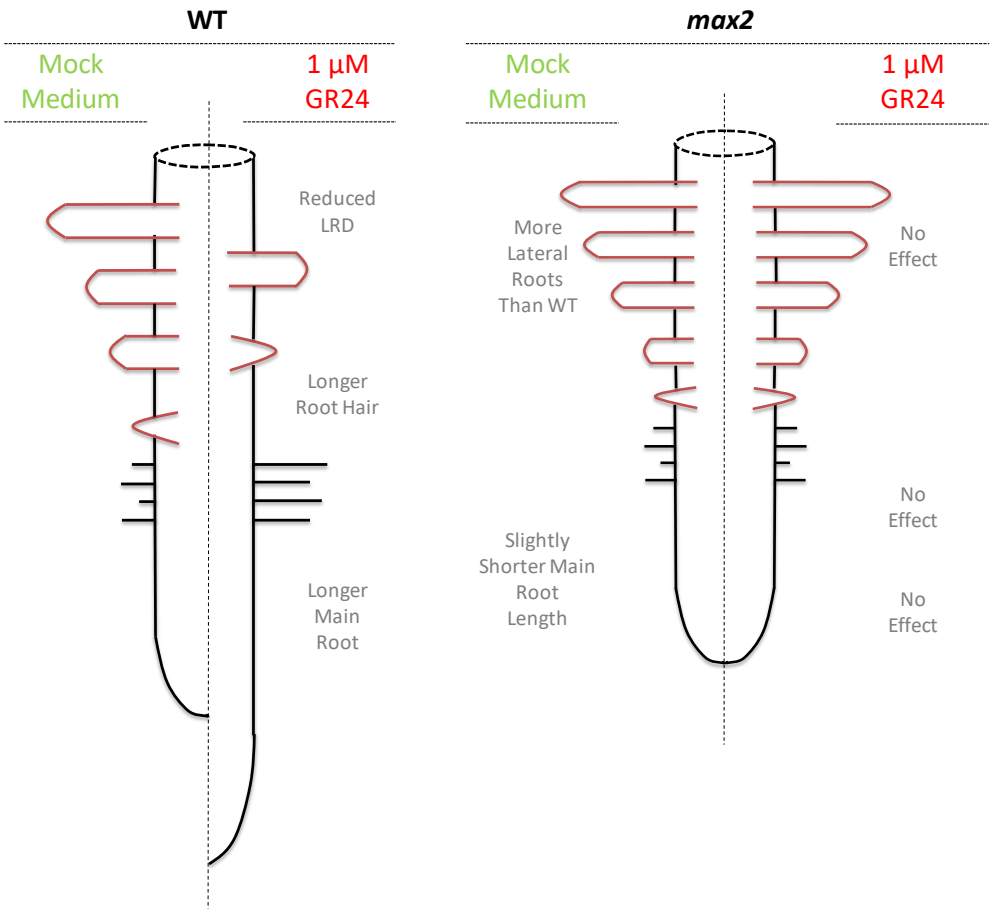

Figure 12. Known effects of *rac*-GR24 on WT and *max2* mutant *Arabidopis* roots when grown in nutrient-rich media.

Finally, an effect on root initiation from nonroot tissue in *Arabidopsis*, pea (adventitious roots), and rice (crown roots) has been attributed to SLs (Arite et al., 2012; Rasmussen et al., 2012). In *Arabidopsis* and pea, both SL biosynthesis and signaling mutants show a higher adventitious rooting capacity than the WT, suggesting that endogenous SLs suppress the formation of adventitious roots (Rasmussen et al., 2012). Likewise, application of *rac*-GR24 results in a clear dose-dependent decrease in adventitious roots, but not in the signaling mutants (Rasmussen et al., 2012). In dark-grown pea, the SL biosynthesis mutants, but not the SL signaling mutants, show a reduced number of adventitious roots, pointing to a potential role of SLs, independently of MAX2, in adventitious root formation in the dark (Urquhart et al., 2015). In rice,

the crown roots of all SL mutants seem to be shorter than those of the WT and are fewer in number, a phenotype that is rescued by *rac*-GR24 in a concentration-dependent manner for all biosynthesis mutants (Arite et al., 2012; Sun et al., 2014), suggesting that SLs regulate crown root development positively in rice, rather than negatively in *Arabidopsis* and in light-grown pea.

Hence, thus far, of the four root-specific SL-triggered phenotypes that have been observed, two seem directly related to SLs, namely increased primary root length and adventitious rooting. For the effect on root hairs and LRD, more research needs to be done. For the time being, it cannot be excluded that a yet unknown signal, mimicked by *rac*-GR24 and signaling through MAX2, might also be at play (Gutjahr et al., 2015).

How do plants regulate the physiological responses in the roots?

Phytohormones are known to interact with each other to regulate specific phenotypes. A large body of research has revealed that, just as for other organs, the action of SLs in the root often takes place in concert with other phytohormones. The best studied case is the tight crosstalk between SLs and auxin for the action of SLs on shoot branching (Crawford et al., 2010; Domagalska and Leyser, 2011; Shinohara et al., 2013). For instance, exogenous auxin can directly affect the key SL biosynthesis genes, inducing the expression of both *MAX3* and *MAX4* (Foo et al., 2005; Hayward et al., 2009). Inversely, *rac*-GR24 leads to a significant decrease in expression of *INDOLE-3-ACETIC ACID INDUCIBLE 1* (*IAA1*), an auxin-responsive gene, for which the mutant is known to be resistant to inhibition of root and hypocotyl elongation and stimulation of LR growth by auxin (Park et al., 2002; Yang et al., 2004; Mashiguchi et al., 2009). Additionally, in the root tip, prolonged treatments with *rac*-GR24 result in a down-regulation of the auxin efflux carriers PIN1, PIN3, and PIN7 (Ruyter-Spira et al., 2011). However, in-depth research on the *PIN1* expression revealed that, in contrast to SLs that induce the PIN1 endocytosis from the plasma membrane in shoots,

roots are not responsive to short SL treatments, both regarding the total PIN1 protein levels and subcellular localization (Shinohara et al., 2013). This observation could indicate that the crosstalk between SLs and auxin might be differentially regulated in the shoot and in the root, or that some root responses might be the indirect result of PIN1-affecting SLs in the shoot (Shinohara et al., 2013).

The effect of *rac*-GR24 on the LRD of *Arabidopsis* is influenced by the auxin status of the plant (Ruyter-Spira et al., 2011). At low auxin concentrations, the addition of *rac*-GR24 leads to a decreased LRD, whereas at high auxin concentration this treatment causes an increased LRD (Ruyter-Spira et al., 2011). As an explanation, *rac*-GR24 might cause auxin levels to sink below an optimum for LR development, through a reduction in auxin flow via modified PIN recycling at the membrane in the xylem parenchyma cells, leading to a decreased LRD. However, at high auxin concentrations, the *rac*-GR24--triggered reduction in the auxin flow would set off the total auxin content to reach the given optimum, thereby giving rise to an increased LRD (Ruyter-Spira et al., 2011; Shinohara et al., 2013). Nevertheless, more research will be required to fully understand these observations.

The crosstalk between auxin and SL signaling in root hair elongation is less clear, albeit the active role of both hormones. An independent action mechanism would be expected, because auxin treatments enhance the root hair responses to *rac*-GR24 and the *max2* mutant remains responsive to auxin in its root hair phenotype (Kapulnik et al., 2011b). Nevertheless, some crosstalk might occur, because the auxin receptor mutant *tir1* was less responsive to *rac*-GR24 (Kapulnik et al., 2011b). Recently, a link between SLs and auxin transport has been established that controls root hair elongation. Indeed, *rac*-GR24 increases the PIN2 abundance at the epidermal plasma membrane during root hair elongation, suggesting that *rac*-GR24 affects PIN2 endocytosis and endosomal trafficking via actin dynamics in a MAX2-dependent manner (Pandya-Kumar et al., 2014). Besides the auxin-SL link, a role for ethylene in the SL-induced root hair elongation has been elucidated (Kapulnik et al., 2011b). SLs seem not to be necessary for the root hair response to ethylene, but both the ethylene signaling mutants *ethylene insensitive2* (*ein2*)

and *ethylene response1* (*etr1*) are less responsive to *rac*-GR24 in their root hair phenotype, implying that ethylene is epistatic to SLs for this phenotype. Furthermore, as the *rac*-GR24 effect could be abolished by blocking ethylene biosynthesis, ethylene might be required for the *rac*-GR24 impact on root hair elongation (Kapulnik et al., 2011b).

The effect of *rac*-GR24 on adventitious rooting in *Arabidopsis* has been studied as well by the interaction between SLs and auxin and has been found to act mainly independently in the regulation of this process (Rasmussen et al., 2013). Moreover, a possible interaction between cytokinins and SLs has been investigated and ruled out, because SL mutants are responsive to cytokinins and cytokinin mutants to *rac*-GR24 for the adventitious rooting phenotype (Rasmussen et al., 2013).

The previous experiments allow insight into the SL effects at the physiological level, but information on the mechanism at the molecular level is scarce. The next challenge in understanding SL signaling in roots is to bridge the gap between the hormonal crosstalk network and MAX2 targets. As MAX2 acts in an SCF complex to degrade specific SL targets, a considerable research effort has been directed toward uncovering these elusive targets, of which the degradation might explain some of the SL-induced MAX2-dependent phenotypes. Recently, the high LRD observed in the *max2* mutant has been shown to be rescued in the *max2,smxl6,smxl7,smxl8* quadruple mutant, indicating that signaling through these SMXL proteins controls the effects on LR development (Soundappan et al., 2015). Now, it would be interesting to assess the response of this quadruple mutant for other known *rac*-GR24 responses, such as root hair elongation or effect on primary root length.

Additionally, whereas the involvement of MAX2 in the different root responses is well established, the role of the SL receptor D14 has not been investigated either for root length, LR development, root hair elongation, or adventitious root phenotype. This research is all the more relevant when recent findings are taken into account, namely that the commonly used racemic GR24 mixture is apparently not specific

to SLs, but can mimic other naturally occurring signaling compounds as well, such as karrikins and unknown endogenous ones, that are perceived through the D14 homolog KAI2 (Guo et al., 2013; Gutjahr et al., 2015; Conn and Nelson, 2016). To solve this problem, it would be useful to investigate first whether any of the known root phenotypes are either specific to a given *rac*-GR24 enantiomer or a given receptor protein. As indicated above, the *smxl6/smxl7/smxl8* mutant can rescue the naturally increased LRD of the *max2* mutant (Soundappan et al., 2015). Hence, although not tested yet, these data would predict that D14 is involved in the SL impact on the LRD.

1.5. Concluding remarks

Thanks to contributions made in several new studies, we progressively gain more insights into the intricate SL signaling networks in the roots. The importance of SLs in shaping the RSA is clear from the various phenotypes that have been identified across multiple species. Detailed information is now available describing the elaborate crosstalk between SLs and other plant hormones. Furthermore, it is becoming clear that SLs act in concert with at least auxin, cytokinins, and ethylene for several of the known root phenotypes. Two main challenges remain to be tackled to fully unravel the role of SLs in the root. The first task will be to bridge the gap between the MAX2 F-BOX targets and the known root phenotypes and the second to investigate the possibility that compounds other than SLs could be at play in some of the described *max2* phenotypes.

References

Abe, S., Sado, A., Tanaka, K., Kisugi, T., Asami, K., Ota, S., Kim, H.I., Yoneyama, K., Xie, X., Ohnishi, T., Seto, Y., Yamaguchi, S., Akiyama, K., Yoneyama, K., and Nomura, T. (2014). Carlactone is converted to carlactonoic acid by MAX1 in *Arabidopsis* and its methyl ester can directly interact with AtD14 in vitro. Proc. Natl. Acad. Sci. USA 111, 18084-18089.

Akiyama, K., Matsuzaki, K.-i., and Hayashi, H. (2005). Plant sesquiterpenes induce hyphal branching in arbuscular mycorrhizal fungi. Nature 435, 824-827.

Akiyama, K., Ogasawara, S., Ito, S., and Hayashi, H. (2010). Structural requirements of strigolactones for hyphal branching in AM fungi. Plant Cell Physiol. 51, 1104-1117.

Al-Babili, S., and Bouwmeester, H.J. (2015). Strigolactones, a novel carotenoid-derived plant hormone. Annu. Rev. Plant Biol. 66, 161-186.

Alder, A., Holdermann, I., Beyer, P., and Al-Babili, S. (2008). Carotenoid oxygenases involved in plant branching catalyse a highly specific conserved apocarotenoid cleavage reaction. Biochem. J. 416, 289-296.

Arite, T., Kameoka, H., and Kyozuka, J. (2012). Strigolactone positively controls crown root elongation in rice. J. Plant Growth Regul. 31, 165-172.

Bainbridge, K., Sorefan, K., Ward, S., and Leyser, O. (2005). Hormonally controlled expression of the Arabidopsis MAX4 shoot branching regulatory gene. Plant J. 44, 569-580.

Balla, J., Kalousek, P., Reinöhl, V., Friml, J., and Procházka, S. (2011). Competitive canalization of PIN-dependent auxin flow from axillary buds controls pea bud outgrowth. Plant J. 65, 571-577.

Bao, F., Shen, J., Brady, S.R., Muday, G.K., Asami, T., and Yang, Z. (2004). Brassinosteroids interact with auxin to promote lateral root development in Arabidopsis. Plant Physiol. 134, 1624-1631.

Bayer, E.M., Smith, R.S., Mandel, T., Nakayama, N., Sauer, M., Prusinkiewicz, P., and Kuhlemeier, C. (2009). Integration of transport-based models for phyllotaxis and midvein formation. Genes Dev. 23, 373-384.

Bennett, T., and Leyser, O. (2006). Something on the side: axillary meristems and plant development. Plant Mol. Biol. 60, 843-854.

Bennett, T., Sieberer, T., Willett, B., Booker, J., Luschnig, C., and Leyser, O. (2006). The Arabidopsis MAX pathway controls shoot branching by regulating auxin transport. Curr. Biol. 16, 553-563.

Beveridge, C.A., Dun, E.A., and Rameau, C. (2009). Pea has its tendrils in branching discoveries spanning a century from auxin to stringolactones. Plant Physiol. 151, 985-990.

Beveridge, C.A., Ross, J.J., and Murfet, I.C. (1996). Branching in pea. Action of genes Rms3 and Rms4. Plant Physiol. 110, 859-865.

Booker, J., Auldridge, M., Wills, S., McCarty, D., Klee, H., and Leyser, O. (2004). MAX3/CCD7 is a carotenoid cleavage dioxygenase required for the synthesis of a novel plant signaling molecule. Curr. Biol. 14, 1232-1238.

Booker, J., Chatfield, S., and Leyser, O. (2003). Auxin acts in xylem-associated or medullary cells to mediate apical dominance. Plant Cell 15, 495-507.

Booker, J., Sieberer, T., Wright, W., Williamson, L., Willett, B., Stirnberg, P., Turnbull, C., Srinivasan, M., Goddard, P., and Leyser, O. (2005). MAX1 encodes a cytochrome P450 family member that acts downstream of MAX3/4 to produce a carotenoid-derived branch-inhibiting hormone. Dev. Cell 8, 443-449.

Brewer, P.B., Dun, E.A., Ferguson, B.J., Rameau, C., and Beveridge, C.A. (2009). Strigolactone acts downstream of auxin to regulate bud outgrowth in pea and Arabidopsis. Plant Physiol. 150, 482-493.

Burgie, E.S., and Vierstra, R.D. (2014). Phytochromes: an atomic perspective on photoactivation and signaling. Plant Cell 26, 4568-4583.

Casimiro, I., Marchant, A., Bhalerao, R.P., Beeckman, T., Dhooge, S., Swarup, R., Graham, N., Inzé, D., Sandberg, G., Casero, P.J., and Bennett, M. (2001). Auxin transport promotes Arabidopsis lateral root initiation. Plant Cell 13, 843-852.

Chattopadhyay, S., Ang, L.-H., Puente, P., Deng, X.-W., and Wei, N. (1998). Arabidopsis bZIP protein HY5 directly interacts with light-responsive promoters in mediating light control of gene expression. Plant Cell 10, 673-683.

Chaves, I., Pokorny, R., Byrdin, M., Hoang, N., Ritz, T., Brettel, K., Essen, L.-O., van der Horst, G.T.J., Batschauer, A., and Ahmad, M. (2011). The cryptochromes: blue light photoreceptors in plants and animals. Annu. Rev. Plant Biol. 62, 335-364.

Chen, H., Zhang, J., Neff, M.M., Hong, S.-W., Zhang, H., Deng, X.-W., and Xiong, L. (2008). Integration of light and abscisic acid signaling during seed germination and early seedling development. Proc. Natl. Acad. Sci. USA 105, 4495-4500.

Chevalier, F, Nieminen, K, Sánchez-Ferrero, J.C., Rodríguez, M.L., Chagoyen, M., Hardtke, C.S., and Cubas, P. (2014). Strigolactone promotes degradation of DWARF14, an α/β hydrolase essential for strigolactone signaling in Arabidopsis. Plant Cell 26, 1134-1150.

Cluis, C.P., Mouchel, C.F., and Hardtke, C.S. (2004). The Arabidopsis transcription factor HY5 integrates light and hormone signaling pathways. Plant J. 38, 332-347.

Cohen, M., Prandi, C., Occhiato, E.G., Tabasso, S., Wininger, S., Resnick, N., Steinberger, Y., Koltai, H., and Kapulnik, Y. (2013). Structure—function relations of strigolactone analogs: activity as plant hormones and plant interactions. Mol. Plant 6, 141-152.

Conn, C.E., and Nelson, D.C. (2016). Evidence that KARRIKIN-INSENSITIVE2 (KAI2) receptors may perceive an unknown signal that is not karrikin or strigolactone. Front. Plant Sci. 6, 1219.

Conn, C.E., Bythell-Douglas, R., Neumann, D., Yoshida, S., Whittington, B., Westwood, J.H., Shirasu, K., Bond, C.S., Dyer, K.A., and Nelson, D.C. (2015). Convergent evolution of strigolactone perception enabled host detection in parasitic plants. Science 349, 540-543.

Cook, C.E., Whichard, L.P., Turner, B., Wall, M.E., and Egley, G.H. (1966). Germination of witchweed (Striga lutea Lour.): isolation and properties of a potent stimulant. Science 154, 1189-1190.

Crawford, S., Shinohara, N., Sieberer, T., Williamson, L., George, G., Hepworth, J., Müller, D., Domagalska, M.A., and Leyser, O. (2010). Strigolactones enhance competition between shoot branches by dampening auxin transport. Development 137, 2905-2913.

De Cuyper, C., Fromentin, J., Yocgo, R.E., De Keyser, A., Guillotin, B., Kunert, K., Boyer, F.-D., and Goormachtig, S. (2015). From lateral root density to nodule number, the strigolactone analogue GR24 shapes the root architecture of Medicago truncatula. J. Exp. Bot. 66, 137-146. [Corrigendum J. Exp. Bot. 66, 4091].

De Rybel, B., Vassileva, V., Parizot, B., Demeulenaere, M., Grunewald, W., Audenaert, D., Van Campenhout, J., Overvoorde, P., Jansen, L., Vanneste, S., Möller, B., Wilson, M., Holman, T., Van Isterdael, G., Brunoud, G., Vuylsteke, M., Vernoux, T., De Veylder, L., Inzé, D., Weijers, D., Bennett, M.J., and Beeckman, T. (2010). A novel Aux/IAA28 signaling cascade activates GATA23-dependent specification of lateral root founder cell identity. Curr. Biol. 20, 1697-1706.

De Saint Germain, A., Bonhomme, S., Boyer, F.-D., and Rameau, C. (2013). Novel insights into strigolactone distribution and signalling. Curr. Opin. Plant Biol. 16, 583-589.

De Smet, I., Tetsumura, T., De Rybel, B., Frey dit Frei, N., Laplaze, L., Casimiro, I., Swarup, R., Naudts, M., Vanneste, S., Audenaert, D., Inzé, D., Bennett, M.J., and Beeckman, T. (2007). Auxin-dependent regulation of lateral root positioning in the basal meristem of Arabidopsis. Development 134, 681-690.

De Smet, I., Zhang, H., Inzé, D., and Beeckman, T. (2006). Novel role for abscisic acid emerges from underground. Trends Plant Sci. 11, 434-439.

Delaux, P.-M., Xie, X., Timme, R.E., Puech-Pages, V., Dunand, C., Lecompte, E., Delwiche, C.F., Yoneyama, K., Bécard, G., and Séjalon-Delmas, N. (2012). Origin of strigolactones in the green lineage. New Phytol. 195, 857-871.

Dharmasiri, N., Dharmasiri, S., and Estelle, M. (2005). The F-box protein TIR1 is an auxin receptor. Nature 435, 441-445.

Dolan, L., Janmaat, K., Willemsen, V., Linstead, P., Poethig, S., Roberts, K., and Scheres, B. (1993). Cellular organisation of the Arabidopsis thaliana root. Development 119, 71-84.

Domagalska, M.A., and Leyser, O. (2011). Signal integration in the control of shoot branching. Nat. Rev. Mol. Cell Biol. 12, 211-221.

Drummond, R.S.M., Martínez-Sánchez, N.M., Janssen, B.J., Templeton, K.R., Simons, J.L., Quinn; B.D., Karunairetnam, S., and Snowden, K.C. (2009). Petunia hybrida CAROTENOID CLEAVAGE DIOXYGENASE7 is involved in the production of negative and positive branching signals in petunia. Plant Physiol. 151, 1867-1877.

Drummond, R.S.M., Sheehan, H., Simons, J.L., Martínez-Sánchez, N.M., Turner, R.M., Putterill, J., and Snowden, K.C. (2011). The expression of petunia strigolactone pathway genes is altered as part of the endogenous developmental program. Front. Plant Sci. 2, 115.

Dubrovsky, J.G., Doerner, P.W., Colón-Carmona, A., and Rost, T.L. (2000). Pericycle cell proliferation and lateral root initiation in Arabidopsis. Plant Physiol. 124, 1648-1657.

Foo, E., Bullier, E., Goussot, M., Foucher, F., Rameau, C., and Beveridge, C.A. (2005). The branching gene RAMOSUS1 mediates interactions among two novel signals and auxin in pea. Plant Cell 17, 464-474.

Fukaki, H., and Tasaka, M. (2009). Hormone interactions during lateral root formation. Plant Mol Biol. 69, 437-449.

Ghassemian, M., Nambara, E., Cutler, S., Kawaide, H., Kamiya, Y., and McCourt, P. (2000). Regulation of abscisic acid signaling by the ethylene response pathway in Arabidopsis. Plant Cell 12, 1117-1126.

Gilroy, S., and Jones, D.L. (2000). Through form to function: root hair development and nutrient uptake. Trends Plant Sci. 5, 56-60.

Gomez-Roldan, V., Fermas, S., Brewer, P.B., Puech-Pagès, V., Dun, EA., Pillot, J.-P., Letisse, F., Matusova, R., Danoun, S., Portais, J-C., Bouwmeester, H., Bécard, G., Beveridge, C.A., Rameau, C., and Rochange, S.F. (2008). Strigolactone inhibition of shoot branching. Nature 455, 189-194.

Guo, Y., Zheng, Z., La Clair, J.J., Chory, J., and Noel, J.P. (2013). Smoke-derived karrikin perception by the α/β-hydrolase KAI2 from Arabidopsis. Proc. Natl. Acad. Sci. USA 110, 8284-8289.

Gutjahr, C., Gobbato, E., Choi, J., Riemann, M., Johnston, M.G., Summers, W., Carbonnel, S., Mansfield, C., Yang, S.-Y., Nadal, M., Acosta, I., Takano, M., Jiao, W.-B., Schneeberger, K., Kelly, K.A., and Paszkowski, U. (2015). Rice perception of symbiotic arbuscular mycorrhizal fungi requires the karrikin receptor complex. Science 350, 1521-1524.

Hamiaux, C., Drummond, R.S.M., Janssen, B.J., Ledger, S.E., Cooney, JM., Newcomb, R.D., and Snowden, K.C. (2012). DAD2 is an α/β hydrolase likely to be involved in the perception of the plant branching hormone, strigolactone. Curr. Biol. 22, 2032-2036.

Hayward, A., Stirnberg, P., Beveridge, C., and Leyser, O. (2009). Interactions between auxin and strigolactone in shoot branching control. Plant Physiol. 151, 400-412.

Ishikawa, S., Maekawa, M., Arite, T., Onishi, K., Takamure, I., and Kyozuka, J. (2005). Suppression of tiller bud activity in tillering dwarf mutants of rice. Plant Cell Physiol. 46, 79-86.

Ivanchenko, M.G., Muday, G.K., and Dubrovsky, J.G. (2008). Ethylene–auxin interactions regulate lateral root initiation and emergence in Arabidopsis thaliana. Plant J. 55, 335-347.

Jia, K.-P., Luo, Q., He, S.-B., Lu, X.-D., and Yang, H.-Q. (2014). Strigolactone-regulated hypocotyl elongation is dependent on cryptochrome and phytochrome signaling pathways in Arabidopsis. Mol. Plant 7, 528-540.

Jiang, L., Liu, X., Xiong, G., Liu, H., Chen, F., Wang, L., Meng, X., Liu, G., Yu, H., Yuan, Y., Yi, W., Zhao, L., Ma, H., He, Y., Wu, Z., Melcher, K., Qian, Q., Xu, H.E., Wang, Y., and Li, J. (2013). DWARF 53 acts as a repressor of strigolactone signalling in rice. Nature 504, 401-405.

Jiang, L., Matthys, C., Marquez-Garcia, B., De Cuyper, C., Smet, L., De Keyser, A., Boyer, F.-D., Beeckman, T., Depuydt, S., and Goormachtig, S. (2016). Strigolactones spatially influence lateral root development through the cytokinin signaling network. J. Exp. Bot. 67, 379–389.

Johnson, X., Brcich, T., Dun, E.A., Goussot, M., Haurogné, K., Beveridge, C.A., and Rameau, C. (2006). Branching genes are conserved across species. Genes controlling a novel signal in pea are coregulated by other long-

distance signals. Plant Physiol. 142, 1014-1026.

Kami, C., Lorrain, S., Hornitschek, P., and Fankhauser, C. (2010). Light-regulated plant growth and development. Curr. Topics Dev. Biol. 91, 29-66.

Kapulnik, Y., Delaux, P.-M., Resnick, N., Mayzlish-Gati, E., Wininger, S., Bhattacharya, C., Séjalon-Delmas, N., Combier, J.-P., Bécard, G., Belausov, E., Beeckman, T., Dor, E., Hershenhorn, J., and Koltai, H. (2011a). Strigolactones affect lateral root formation and root-hair elongation in Arabidopsis. Planta 233, 209-216.

Kapulnik, Y., Resnick, N., Mayzlish-Gati, E., Kaplan, Y., Wininger, S., Hershenhorn, J., and Koltai, H. (2011b). Strigolactones interact with ethylene and auxin in regulating root-hair elongation in Arabidopsis. J. Exp. Bot. 62, 2915-2924.

Kohlen, W., Charnikhova, T., Liu, Q., Bours, R., Domagalska, M.A., Beguerie, S., Verstappen, F., Leyser, O., Bouwmeester, H., and Ruyter-Spira, C. (2011). Strigolactones are transported through the xylem and play a key role in shoot architectural response to phosphate deficiency in nonarbuscular mycorrhizal host Arabidopsis. Plant Physiol. 155, 974-987.

Koltai, H. (2011). Strigolactones are regulators of root development. New Phytol 190, 545-549.

Koltai, H., Dor, E., Hershenhorn, J., Joel, D.M., Weininger, S., Lekalla, S., Shealtiel, H., Bhattacharya, C., Eliahu, E., Resnick, N., Barg, R., and Kapulnik, Y. (2010). Strigolactones' effect on root growth and root-hair elongation may be mediated by auxin-efflux carriers. J. Plant Growth Regul. 29, 129-136.

Kong, X., Zhang, M., and Ding, Z. (2014). D53: the missing link in strigolactone signaling. Mol. Plant 7, 761-763.

Koren, D., Resnick, N., Mayzlish Gati, E., Belausov, E., Weininger, S., Kapulnik, Y., and Koltai, H. (2013). Strigolactone signaling in the endodermis is sufficient to restore root responses and involves SHORT HYPOCOTYL 2 (SHY2) activity. New Phytol. 198, 866-874.

Kretzschmar, T., Kohlen, W., Sasse, J., Borghi, L., Schlegel, M., Bachelier, J.B., Reinhardt, D., Bours, R., Bouwmeester, H.J., and Martinoia, E. (2012). A petunia ABC protein controls strigolactone-dependent symbiotic signalling and branching. Nature 483, 341-344.

Kumar, M., Pandya-Kumar, N., Dam, A., Haor, H., Mayzlish-Gati, E., Belausov, E., Wininger, S., Abu-Abied, M., McErlean, C.S.P., Bromhead, L.J., Prandi, C., Kapulnik,Y., and Koltai, H. (2015). Arabidopsis response to low-phosphate conditions includes active changes in actin filaments and PIN2 polarization and is dependent on strigolactone signalling. J. Exp. Bot. 66, 1499-1510.

Laskowski, M.J., Williams, M.E., Nusbaum, H.C., and Sussex, I.M. (1995). Formation of lateral root meristems is a two-stage process. Development 121, 3303-3310.

Leivar, P., and Monte, E. (2014). PIFs: systems integrators in plant development. Plant Cell 26, 56-78.

Leivar, P., Monte, E., Oka, Y., Liu, T., Carle, C., Castillon, A., Huq, E., and Quail, P.H. (2008). Multiple phytochrome-interacting bHLH transcription factors repress premature seedling photomorphogenesis in darkness. Curr. Biol. 18, 1815-1823.

Leyser, O. (2009). The control of shoot branching: an example of plant information processing. Plant Cell Environ. 32, 694-703.

Lieberman, M. (1979). Biosynthesis and action of ethylene. Annu. Rev. Plant Physiol. 30, 533-591.

Lin, C., and Shalitin, D. (2003). Cryptochrome structure and signal transduction. Annu. Rev. Plant Biol. 54, 469-496.

Lin, H., Wang, R., Qian, Q., Yan, M., Meng, X., Fu, Z., Yan, C., Jiang, B., Su, Z., Li, J., and Wang, Y. (2009). DWARF27: an iron-containing protein required for the biosynthesis of strigolactones, regulates rice tiller bud outgrowth. Plant Cell 21, 1512-1525.

Liu, J., Novero, M., Charnikhova, T., Ferrandino, A., Schubert, A., Ruyter-Spira, C., Bonfante, P., Lovisolo, C., Bouwmeester, H.J., and Cardinale, F. (2013). CAROTENOID CLEAVAGE DIOXYGENASE 7 modulates plant growth, reproduction, senescence, and determinate nodulation in the model legume Lotus japonicus. J. Exp. Bot. 64, 1967-1981.

López-Bucio, J., Cruz-Ramírez, A., and Herrera-Estrella, L. (2003). The role of nutrient availability in regulating root architecture. Curr. Opin. Plant Biol. 6, 280-287.

Lucas, M., Guédon, Y., Jay-Allemand, C., Godin, C., and Laplaze, L. (2008). An auxin transport-based model of root branching in Arabidopsis thaliana. PLoS ONE 3, e3673.

Malamy, J.E., and Benfey, P.N. (1997). Organization and cell differentiation in lateral roots of Arabidopsis thaliana. Development 124, 33-44.

Mashiguchi, K., Sasaki, E., Shimada, Y., Nagae, M., Ueno, K., Nakano, T., Yoneyama, K., Suzuki, Y., and Asami, T. (2009). Feedback-regulation of strigolactone biosynthetic genes and strigolactone-regulated genes in Arabidopsis. Biosci. Biotechnol. Biochem. 73, 2460-2465.

Mayzlish-Gati, E., De-Cuyper, C., Goormachtig, S., Beeckman, T., Vuylsteke, M., Brewer, P.B., Beveridge, C.A., Yermiyahu, U., Kaplan, Y., Enzer, Y., Wininger, S., Resnick, N., Cohen, M., Kapulnik, Y., and Koltai, H. (2012). Strigolactones are involved in root response to low phosphate conditions in Arabidopsis. Plant Physiol. 160, 1329-1341.

Moreno-Risueno, M.A., Van Norman, J.M., Moreno, A., Zhang, J., Ahnert, S.E., and Benfey, P.N. (2010). Oscillating gene expression determines competence for periodic Arabidopsis root branching. Science 329, 1306-1311.

Morffy, N., Faure, L., and Nelson, D.C. (2016). Smoke and hormone mirrors: action and evolution of karrikin and strigolactone signaling. Trends Genet. 32, 176-188.

Negi, S., Ivanchenko, M.G., and Muday, G.K. (2008). Ethylene regulates lateral root formation and auxin transport in *Arabidopsis thaliana*. Plant J. 55, 175-187.

Nelson, D.C., Flematti, G.R., Ghisalberti, E.L., Dixon, K.W., and Smith, S.M. (2012). Regulation of seed germination and seedling growth by chemical signals from burning vegetation. Annu. Rev. Plant Biol. 63, 107-130.

Nelson, D.C., Scaffidi, A., Dun, E.A., Waters, M.T., Flematti, G.R., Dixon, K.W., Beveridge, C.A., Ghisalberti, E.L., and Smith, S.M. (2011). F-box protein MAX2 has dual roles in karrikin and strigolactone signaling in Arabidopsis thaliana. Proc. Natl. Acad. Sci. USA 108, 8897-8902.

Nordström, A., Tarkowski, P., Tarkowska, D., Norbaek, R., Åstot, C., Dolezal, K., and Sandberg, G. (2004). Auxin regulation of cytokinin biosynthesis in Arabidopsis thaliana: a factor of potential importance for auxin--cytokinin-regulated development. Proc. Natl. Acad. Sci. USA 101, 8039-8044.

Oyama, T., Shimura, Y., and Okada, K. (1997). The Arabidopsis HY5 gene encodes a bZIP protein that regulates stimulus-induced development of root and hypocotyl. Genes Dev. 11, 2983-2995.

Pandya-Kumar, N., Shema, R., Kumar, M., Mayzlish-Gati, E., Levy, D., Zemach, H., Belausov, E., Wininger, S., Abu-Abied, M., Kapulnik, Y., and Koltai, H. (2014). Strigolactone analog GR24 triggers changes in PIN2 polarity, vesicle trafficking and actin filament architecture. New Phytol. 202, 1184-1196.

Park, J.-Y., Kim, H.-J., and Kim, J. (2002). Mutation in domain II of IAA1 confers diverse auxin-related phenotypes and represses auxin-activated expression of Aux/IAA genes in steroid regulator-inducible system. Plant J. 32, 669-683.

Parniske, M. (2008). Arbuscular mycorrhiza: the mother of plant root endosymbioses. Nat. Rev. Microbiol. 6, 763-775.

Penfield, S., and King, J. (2009). Towards a systems biology approach to understanding seed dormancy and germination. Proc. R. Soc. B 276, 3561-3569.

Péret, B., De Rybel, B., Casimiro, I., Benková, E., Swarup, R., Laplaze, L., Beeckman, T., and Bennett, M.J. (2009). Arabidopsis lateral root development: an emerging story. Trends Plant Sci. 14, 399-408.

Proust, H., Hoffmann, B., Xie, X., Yoneyama, K., Schaefer, D.G., Yoneyama, K., Nogué, F., and Rameau, C. (2011). Strigolactones regulate protonema branching and act as a quorum sensing-like signal in the moss Physcomitrella patens. Development 138, 1531-1539.

Rasmussen, A., Heugebaert, T., Matthys, C., Van Deun, R., Boyer, F.-D., Goormachtig, S., Stevens, C., and Geelen, D. (2013). A fluorescent alternative to the synthetic strigolactone GR24. Mol. Plant 6, 100-112.

Rasmussen, A., Mason, M.G., De Cuyper, C., Brewer, P.B., Herold, S., Agusti, J., Geelen, D., Greb, T., Goormachtig, S., Beeckman, T., and Beveridge, C.A. (2012). Strigolactones suppress adventitious rooting in Arabidopsis and pea. Plant Physiol. 158, 1976-1987.

Rizzini, L., Favory, J.-J., Cloix, C., Faggionato, D., O'Hara, A., Kaiserli, E., Baumeister, R., Schäfer, E., Nagy, F., Jenkins, G.I., and Ulm, R. (2011). Perception of UV-B by the Arabidopsis UVR8 protein. Science 332, 103-106.

Ruyter-Spira, C., Kohlen, W., Charnikhova, T., van Zeijl, A., van Bezouwen, L., de Ruijter, N., Cardoso, C., Lopez-Raez, J.A., Matusova, R., Bours, R., Verstappen, F., and Bouwmeester, H. (2011). Physiological effects of the synthetic strigolactone analog GR24 on root system architecture in Arabidopsis: another belowground role for strigolactones? Plant Physiol. 155, 721-734.

Sachs, T., and Thimann, K.V. (1967). The role of auxins and cytokinins in the release of buds from dominance. Am. J. Bot. 54, 136-144.

Saijo, Y, Sullivan, J.A., Wang, H., Yang, J., Shen, Y., Rubio, V., Ma, L., Hoecker, U., and Deng, X.W. (2003). The COP1--SPA1 interaction defines a critical step in phytochrome A-mediated regulation of HY5 activity. Genes Dev. 17, 2642-2647.

Sasse, J., Simon, S., Gübeli, C., Liu, G.-W., Cheng, X., Friml, J., Bouwmeester, H., Martinoia, E., and Borghi, L. (2015). Asymmetric localizations of the ABC transporter PaPDR1 trace paths of directional strigolactone transport. Curr. Biol. 25, 647-655.

Scaffidi, A., Waters, M.T., Ghisalberti, E.L., Dixon, K.W., Flematti, G.R., and Smith, S.M. (2013). Carlactone-independent seedling morphogenesis in Arabidopsis. Plant J. 76, 1-9.

Scaffidi, A., Waters, M.T., Sun, Y.K., Skelton, B.W., Dixon, K.W., Ghisalberti, E.L., Flematti, G.R., and Smith, S.M. (2014). Strigolactone hormones and their stereoisomers signal through two related receptor proteins to induce different physiological responses in Arabidopsis. Plant Physiol. 165, 1221 1232.

Seto, Y., Sado, A., Asami, K., Hanada, A., Umehara, M., Akiyama, K., and Yamaguchi, S. (2014). Carlactone is an endogenous biosynthetic precursor for strigolactones Proc. Natl. Acad. Sci. USA 111, 1640-1645.

Sheard, L.B., Tan, X., Mao, H., Withers, J., Ben-Nissan, G., Hinds, T.R., Kobayashi, Y., Hsu, F.-F., Sharon, M., Browse, J., He, S.Y., Rizo, J., Howe, G.A., and Zheng, N. (2010). Jasmonate perception by inositol-phosphate-potentiated COI1—JAZ co-receptor. Nature 468, 400-405.

Shen, H., Luong, P., and Huq, E. (2007). The F-Box protein MAX2 functions as a positive regulator of photomorphogenesis in Arabidopsis. Plant Physiol. 145, 1471-1483.

Shen, H., Zhu, L., Bu, Q.-Y., and Huq, E. (2012). MAX2 affects multiple hormones to promote photomorphogenesis. Mol. Plant 5, 750-762.

Shinohara, N., Taylor, C., and Leyser, O. (2013). Strigolactone can promote or inhibit shoot branching by triggering rapid depletion of the auxin efflux protein PIN1 from the plasma membrane. PLoS Biol. 11, e1001474.

Sibout, R., Sukumar, P., Hettiarachchi, C., Holm, M., Muday, G.K., and Hardtke, C.S. (2006). Opposite root growth phenotypes of hy5 versus hy5 hyh mutants correlated with increased constitutive auxin signaling. PLoS Genet. 2, e202, 1898-1911.

Snowden, K.C., Simkin, A.J., Janssen, B.J., Templeton, K.R., Loucas, H.M., Simons, J.L., Karunairetnam, S., Gleave, A.P., Clark, D.G., and Klee, H.J. (2005). The Decreased apical dominance1/Petunia hybrida CAROTENOID CLEAVAGE DIOXYGENASE8 gene affects branch production and plays a role in leaf senescence, root growth, and flower development. Plant Cell 17, 746-759.

Sorefan, K., Booker, J., Haurogné, K., Goussot, M., Bainbridge, K., Foo, E., Chatfield, S., Ward, S., Beveridge, C., Rameau, C., and Leyser, O. (2003). MAX4 and RMS1 are orthologous dioxygenase-like genes that regulate shoot branching in Arabidopsis and pea. Genes Dev. 17, 1469-1474.

Soundappan, I., Bennett, T., Morffy, N., Liang, Y., Stanga, J.P., Abbas, A., Leyser, O., and Nelson, D.C. (2015). SMAX1-LIKE/D53 family members enable distinct MAX2-dependent responses to strigolactones and karrikins in Arabidopsis. Plant Cell 27, 3143-3159.

Stanga, J.P., Morffy, N., and Nelson, D.C. (2016). Functional redundancy in the control of seedling growth by the karrikin signaling pathway. Planta 243, 1397-1406.

Stanga, J.P., Smith, S.M., Briggs, W.R., and Nelson, D.C. (2013). SUPPRESSOR OF MORE AXILLARY GROWTH2 1 controls seed germination and seedling development in Arabidopsis. Plant Physiol. 163, 318-330.

Stirnberg, P., Furner, I.J., and Leyser, H.M.O. (2007). MAX2 participates in an SCF complex which acts locally at the node to suppress shoot branching. Plant J. 50, 80-94.

Sun, H., Tao, J., Liu, S., Huang, S., Chen, S., Xie, X., Yoneyama, K., Zhang, Y., and Xu, G. (2014). Strigolactones are involved in phosphate- and nitrate-deficiency-induced root development and auxin transport in rice. J. Exp. Bot. 65, 6735-6746.

Tatematsu, K., Kumagai, S., Muto, H., Sato, A., Watahiki, M.K., Harper, R.M., Liscum, E., and Yamamoto, K.T. (2004). MASSUGU2 encodes Aux/IAA19, an auxin-regulated protein that functions together with the transcriptional activator NPH4/ARF7 to regulate differential growth responses of hypocotyl and formation of lateral roots in Arabidopsis thaliana. Plant Cell 16, 379-393.

Thieme, C.J., Rojas-Triana, M., Stecyk, E., Schudoma, C., Zhang, W., Yang, L., Miñambres, M., Walther, D., Schulze, W.X., Paz-Ares, J., Scheible, W.-R., and Kragler, F. (2015). Endogenous Arabidopsis messenger RNAs transported to distant tissues. Nat. Plants 1, 15025 [Erratum Nat. Plants 1, 15088].

Thimann, K.V., and Skoog, F. (1933). Studies on the growth hormone of plants. III. The inhibiting action of the growth substance on bud development. Proc. Natl. Acad. Sci. USA 19, 714-716.

Toh, S., Holbrook-Smith, D., Stogios, P.J., Onopriyenko, O., Lumba, S., Tsuchiya, Y., Savchenko, A., and McCourt, P. (2015). Structure-function analysis identifies highly sensitive strigolactone receptors in Striga. Science 350, 203-207.

Toh, S., Imamura, A., Watanabe, A., Nakabayashi, K., Okamoto, M., Jikumaru, Y., Hanada, A., Aso, Y., Ishiyama, K., Tamura, N., Iuchi, S., Kobayashi, M., Yamaguchi, S., Kamiya, Y., Nambara, E., and Kawakami, N. (2008). High temperature-induced abscisic acid biosynthesis and its role in the inhibition of gibberellin action in Arabidopsis seeds. Plant Physiol. 146, 1368–1385.

Toh, S., Kamiya, Y., Kawakami, N., Nambara, E., McCourt, P., and Tsuchiya, Y. (2012). Thermoinhibition uncovers a role for strigolactones in Arabidopsis seed germination. Plant Cell Physiol. 53, 107-117.

Tsuchiya, Y., Vidaurre, D., Toh, S., Hanada, A., Nambara, E., Kamiya, Y., Yamaguchi, S., and McCourt, P. (2010). A small-molecule screen identifies new functions for the plant hormone strigolactone. Nat. Chem. Biol. 6, 741-749.

Tsuchiya, Y., Yoshimura, M., Sato, Y., Kuwata, K., Toh, S., Holbrook-Smith, D., Zhang, H., McCourt, P., Itami, K., Kinoshita, T., and Hagihara, S. (2015). Probing strigolactone receptors in Striga hermonthica with fluorescence. Science 349, 864-868.

Turnbull, C.G.N., Booker, J.P., and Leyser, H.M.O. (2002). Micrografting techniques for testing long-distance signalling in Arabidopsis. Plant J. 32, 255-262.

Umehara, M., Hanada, A., Yoshida, S., Akiyama, K., Arite, T., Takeda-Kamiya, N., Magome, H., Kamiya, Y., Shirasu, K., Yoneyama, K., Kyozuka, J., and Yamaguchi, S. (2008). Inhibition of shoot branching by new terpenoid plant hormones. Nature 455, 195-200.

Urquhart, S., Foo, E., and Reid, J.B. (2015). The role of strigolactones in photomorphogenesis of pea is limited to adventitious rooting. Physiol. Plant. 153, 392-402.

Van Norman, J.M., Zhang, J., Cazzonelli, C.I., Pogson, B.J., Harrison, P.J., Bugg, T.D.H., Chan, K.X., Thompson, A.J., and Benfey, P.N. (2014). Periodic root branching in Arabidopsis requires synthesis of an uncharacterized carotenoid derivative. Proc. Natl. Acad. Sci. USA 111, E1300-1309.

Vanstraelen, M., and Benková, E. (2012). Hormonal interactions in the regulation of plant development. Annu. Rev. Cell Dev. Biol. 28, 463-487.

Vaucher, J.P. (1823). Mémoire sur la germination des orobanches. Mém. Mus. Hist. Nat. Paris 10, 261-273.

Vierstra, R.D. (2009). The ubiquitin-26S proteasome system at the nexus of plant biology. Nat. Rev. Mol. Cell Biol. 10, 385-397.

Vogel, J.T., Walter, M.H., Giavalisco, P., Lytovchenko, A., Kohlen, W., Charnikhova, T., Simkin, A.J., Goulet, C., Strack, D., Bouwmeester, H.J., Fernie, A.R., and Klee, H.J. (2010). SlCCD7 controls strigolactone biosynthesis, shoot branching and mycorrhiza-induced apocarotenoid formation in tomato. Plant J. 61, 300-311.

Wang, L., Wang, B., Jiang, L., Liu, X., Li, X., Lu, Z., Meng, X., Wang, Y., Smith, S.M., and Li, J. (2015). Strigolactone signaling in Arabidopsis regulates shoot development by targeting D53-like SMXL repressor proteins for ubiquitination and degradation. Plant Cell 27, 3128-3142.

Waters, M.T., and Smith, S.M. (2013). KAI2- and MAX2-mediated responses to karrikins and strigolactones are largely independent of HY5 in Arabidopsis seedlings. Mol. Plant 6, 63-75.

Waters, M.T., Brewer, P.B., Bussell, J.D., Smith, S.M., and Beveridge, C.A. (2012). The Arabidopsis ortholog of rice DWARF27 acts upstream of MAX1 in the control of plant development by strigolactones. Plant Physiol. 159, 1073-1085.

Waters, M.T., Scaffidi, A., Moulin, S.L.Y., Sun, Y.K., Flematti, G.R., and Smith, S.M. (2015b). A Selaginella moellendorffii ortholog of KARRIKIN INSENSITIVE2 functions in Arabidopsis development but cannot mediate responses to karrikins or strigolactones. Plant Cell 27, 1925-1944.

Waters, M.T., Scaffidi, A., Sun, Y.K., Flematti, G.R., and Smith, S.M. (2014). The karrikin response system of Arabidopsis. Plant J. 79, 623-631.

Weller, J.L., Hecht, V., Vander Schoor, J.K., Davidson, S.E., and Ross, J.J. (2009). Light regulation of gibberellin biosynthesis in pea is mediated through the COP1/HY5 pathway. Plant Cell 21, 800-813.

Woo, H.R., Chung, K.M., Park, J.-H., Oh, S.A., Ahn, T., Hong, S.H., Jang, S.K., and Nam, H.G. (2001). ORE9, an F-box protein that regulates leaf senescence in Arabidopsis. Plant Cell 13, 1779-1790.

Wu, G., Lewis, D.R., and Spalding, E.P. (2007). Mutations in Arabidopsis multidrug resistance-like ABC transporters separate the roles of acropetal and basipetal auxin transport in lateral root development. Plant Cell 19, 1826-1837.

Xie, X., Yoneyama, K., and Yoneyama, K. (2010). The strigolactone story. Annu. Rev. Phytopathol. 48, 93-117.

Xie, X., Yoneyama, K., Kisugi, T., Nomura, T., Akiyama, K., Asami, T., and Yoneyama, K. (2015). Strigolactones are transported from roots to shoots, although not through the xylem. J. Pestic. Sci. 40, 214-216.

Xuan, W., Audenaert, D., Parizot, B., Möller, B.K., Njo, M.F., De Rybel, B., De Rop, G., Van Isterdael, G., Mähönen, A.P., Vanneste, S., and Beeckman, T. (2015). Root cap-derived auxin pre-patterns the longitudinal axis of the Arabidopsis root. Curr. Biol. 25, 1381-1388.

Yang, X., Lee, S., So, J.-h., Dharmasiri, S., Dharmasiri, N., Ge, L., Jensen, C., Hangarter, R., Hobbie, L., and Estelle, M. (2004). The IAA1 protein is encoded by AXR5 and is a substrate of SCFTIR1. Plant J. 40, 772-782.

Yoder, J.I., and Scholes, J.D. (2010). Host plant resistance to parasitic weeds; recent progress and bottlenecks. Curr. Opin. Plant Biol. 13, 478-484.

Yoneyama, K., Xie, X., Yoneyama, K., and Takeuchi, Y. (2009). Strigolactones: structures and biological activities. Pest Manag. Sci. 65, 467-470.

Zhao, L.H., Zhou, X.E., Wu, Z.-S., Yi, W., Xu, Y., Li, S., Xu, T.-H., Liu, Y., Chen, R.-Z., Kovach, A., Kang, Y., Hou, L., He, Y., Xie, C., Song, W., Zhong, D., Xu, Y., Wang, Y., Li, J., Zhang, C., Melcher, K., and Xu, H.E. (2013). Crystal structures of two phytohormone signal-transducing α/β hydrolases: karrikin-signaling KAI2 and strigolactone-signaling DWARF14. Cell Res. 23, 436-439.

Zhou, F., Lin, Q., Zhu, L., Ren, Y., Zhou, K., Shabek, N., Wu, F., Mao, H., Dong, W., Gan, L., Ma, W., Gao, H., Chen, J., Yang, C., Wang, D., Tan, J., Zhang, X., Guo, X., Wang, J., Jiang, L., Liu, X., Chen, W., Chu, J., Yan, C., Ueno, K., Ito, S., Asami, T., Cheng, Z., Wang, J., Lei, C., Zhai, H., Wu, C., Wang, H., Zheng, N., and Wan, J. (2013). D14--SCFD3-dependent degradation of D53 regulates strigolactone signalling. Nature 504, 406-410.

Zou, J., Zhang, S., Zhang, W., Li, G., Chen, Z., Zhai, W., Zhao, X., Pan, X., Xie, Q., and Zhu, L. (2006). The rice HIGH-TILLERING DWARF1 encoding an ortholog of Arabidopsis MAX3 is required for negative regulation of the outgrowth of axillary buds. Plant J. 48, 687-698.

Zwanenburg, B., and Pospíšil, T. (2013). Structure and activity of strigolactones: new plant hormones with a rich future. Mol. Plant 6, 38-62.

Zwanenburg, B., Mwakaboko, A.S., Reizelman, A., Anilkumar, G., and Sethumadhavan, D. (2009). Structure and function of natural and synthetic signalling molecules in parasitic weed germination. Pest Manag. Sci. 65, 478-491.

PART II:

SCOPE AND OBJECTIVES

Plants are complex multicellular organisms and, as such, require a tight control of their developmental processes. An important manner by which this tight developmental regulation can be coordinated is via the action of hormones. Plants only possess a limited number of hormones that most often can target almost all cell types. In addition, phytohormones frequently have different functions and, on top of that, their impact can be influenced by the activity of other hormones. Therefore, unraveling the complex hormonal signaling pathways in plants that result in various physiological responses is a very important research theme. Besides the classic hormones auxin, cytokinins, ethylene, gibberellin, and abscisic acid, several new plant hormones were discovered, of which strigolactones (SLs) are one of the most recent ones. SLs had originally been identified as signaling molecules in the rhizosphere and endogenously they regulate important processes, such as shoot branching, photomorphogenesis, and root architecture. Because of their various roles in defining the plant's morphology and communication with organisms in the rhizosphere, SLs have become a cutting-edge topic in plant biology and agronomy, with great potential in modern agriculture. Due to their recent discovery, much is still undetermined about the SL signaling cascades and detailed knowledge about their physiological effects is lacking.

The main objective of this PhD is to obtain a profound mechanistic and molecular insight into how SL signaling results in the downstream physiological responses with a focus on the root system architecture of *Arabidopsis thaliana*. To this end, we study the effect of *rac*-GR24, a synthetic SL analog, on lateral root development in an in-depth spatiotemporal manner and explore a possible crosstalk with cytokinin and auxin, two other hormones, known to shape the root system architecture. The results are presented in **Chapter 2**. In addition, we wanted to obtain a genome-wide overview of the transcriptomic changes brought about by *rac*-GR24 treatment by means of RNA sequencing (**Chapter 3)**. Furthermore, in **Chapter 4**, we elaborate on the identification of a downstream player in the physiological responses of SLs on the root system architecture. An additional objective of this PhD is to initiate a chemical genetics screen, by which we aimed at characterizing new SL antagonists that can aid in further deciphering the SL

signaling network. These results will be covered in **Chapter 5**. Finally, we will discuss our findings, place our results in a broad context, and address future research perspectives in **Chapter 6**.

PART III:

RESULTS

CHAPTER 2:

STRIGOLACTONES SPATIALLY INFLUENCE LATERAL ROOT DEVELOPMENT THROUGH THE CYTOKININ SIGNALING NETWORK

LING-XIANG JIANG*, **CEDRICK MATTHYS***, BELEN MARQUEZ-GARCIA, CAROLIEN DE CUYPER, LIEN SMET, ANNICK DE KEYSER, FRANCOIS-DIDIER BOYER, TOM BEECKMAN, STEPHEN DEPUYDT, AND SOFIE GOORMACHTIG

Modified from: Jiang, L., **Matthys, C.,*** et al. (2016). J. Exp. Bot. 67, 379-389*

Author's contribution: * These authors contributed equally to this work

Abstract

Strigolactones (SLs) are important rhizosphere signals that act as phytohormones and have multiple functions, including modulation of lateral root (LR) development. Here, we show that treatment with the SL analog *rac*-GR24 did not affect LR initiation, but negatively influenced LR priming and emergence, the latter especially near the root-shoot junction. The cytokinin module ARABIDOPSIS HISTIDINE KINASE3 (AHK3)/ARABIDOPSIS RESPONSE REGULATOR1 (ARR1);ARR12 was found to interact with the *rac*-GR24-dependent reduction in LR development, because mutants in this pathway rendered LR development insensitive to *rac*-GR24. Additionally, pharmacological analyses, mutant analyses and gene expression analyses indicated that the affected polar auxin transport stream in mutants of the AHK3/ARR1;ARR12 module could be the underlying cause. Altogether, the data reveal that the *rac*-GR24 effect on LR development depends on the hormonal landscape that results from the intimate connection with auxins and cytokinins, two main players in LR development.

2.1. Introduction

Strigolactones (SLs) are phytohormones that affect lateral branching of the shoot (Gomez-Roldan et al., 2008; Umehara et al., 2008) and many other processes, such as drought tolerance, leaf senescence, and secondary growth, among others (Woo et al., 2001; Snowden et al., 2005; Shen et al., 2007, 2012; Tsuchiya et al., 2010; Agusti et al., 2011; Bu et al., 2014). In the rhizosphere, SLs influence interactions of the host plant with neighboring organisms, such as root-parasitic plants, mycorrrhizal fungi, and rhizobia (for review, see Xie et al., 2010; Rasmussen et al., 2013a). The root system architecture itself is also affected by SLs, because SLs influence adventitious root development, main root growth, root hair development, and lateral root (LR) development (Kapulnik et al., 2011a, 2011b; Ruyter-Spira et al., 2011; Mayzlish-Gati et al., 2012; Rasmussen et al., 2012, 2013a; Sun et al., 2014). The ontogenesis of LRs consists of several successive steps that are highly regulated (reviewed by Péret et al., 2009). The first step is priming of the LR that occurs in the xylem pole pericycle (XPP) cells in the basal meristem zone of the root tip. These primed XPP cells, also designated prebranch sites, have acquired the developmental program to become a LR. As the root grows, the primed XPP cells enter the elongation zone, where they undergo asymmetric cell division, a process designated LR initiation. Through further well controlled division patterns, an LR primordium (LRP) will be formed that will ultimately develop into a typical dome-shaped primordium that will pierce through the main root and will form an emerged LR.

Regarding LR development, addition of the SL analog *rac*-GR24 was found to reduce the LR density (LRD), because of a diminished LR initiation and LR outgrowth (Koltai et al., 2010; Ruyter-Spira et al., 2011; Kapulnik et al., 2011b). In *Arabidopsis thaliana*, mutants in the F-box protein MORE AXILLARY GROWTH2 (MAX2) are perturbed in SL perception and display higher LRDs than the wild-type (WT) plants (Kapulnik et al., 2011b; Kohlen et al., 2011; Ruyter-Spira et al., 2011). When the MAX2 function was restored specifically in the root endodermis of *max2* mutants, their insensitivity could be partially complemented

(Koren et al., 2013). SLs are perceived by an α/β-hydrolase, DWARF14 (D14), that binds and hydrolyzes SLs and plays a central role in downstream signaling activation (Hamiaux et al., 2012; Zhao et al., 2013). In petunia (*Petunia hybrida*) and rice (*Oryza sativa*), D14 interacts with MAX2/D3, a nuclear-localized F-box protein that participates in the Skp-Cullin-F-box (SCF) complexes and, thus, can mediate the ubiquitin-dependent degradation of signaling proteins (Hamiaux et al., 2012; Zhao et al., 2013).

The interaction of SLs with auxins and cytokinins in regulation of shoot lateral branching has been thoroughly studied mainly in pea (*Pisum sativum*) and *Arabidopsis* (for a review, see Stirnberg et al., 2010; Cheng et al., 2013; Rasmussen et al., 2013a). Indeed, SL biosynthesis and signaling are intimately connected with auxin transport regulation (Foo et al., 2005; Bennett et al., 2006; Brewer et al., 2009; Ferguson and Beveridge, 2009; Hayward et al., 2009; Crawford et al., 2010; Koltai et al., 2010; Shinohara et al., 2013; Pandya-Kumar et al., 2014). The application of *rac*-GR24 reduces the basipetal auxin transport and the accumulation of PIN-FORMED1 (PIN1) in the plasma membrane of xylem parenchyma cells in the shoot in a MAX2-dependent manner (Crawford et al., 2010). Moreover, in buds, SLs promote PIN1 endocytosis through a clathrin-dependent mechanism that occurs independently of de novo protein synthesis (Shinohara et al., 2013). In pea, SLs have been demonstrated to act also independently of auxin (Brewer et al., 2015). Interestingly, SLs could inhibit shoot lateral branching only when a competing auxin source was available (Crawford et al., 2010; Liang et al., 2010). The auxin landscape also influences the SL control on branching, because the negative effect on shoot lateral branching disappeared and even became positive when the auxin homeostasis was changed (Shinohara et al., 2013). In buds, SLs and cytokinins are known to interact antagonistically and locally (Dun et al., 2012; Zhang et al., 2010; Hu et al., 2014), probably through their common target, BRANCHED1 (BRC1) in Arabidopsis (Minakuchi et al., 2010; Braun et al., 2012; Dun et al., 2012).

Also in the root, the interaction of SLs with auxins has been investigated. PIN1, PIN3 and PIN7 protein levels are reduced upon prolonged treatment with *rac*-GR24 (Ruyter-Spira et al., 2011).

Additionally, during *rac*-GR24-induced root hair elongation, the PIN2 abundance increases at the apical plasma membrane of epidermal cells, suggesting that SLs affect PIN2 endocytosis and endosomal trafficking via actin dynamics in a MAX2-dependent manner (Pandya-Kumar et al., 2014). The inhibitory effect of *rac*-GR24 on LR development can be reverted to an induction rather than a reduction of LRD by applying a high dose of auxin, or under low phosphate conditions that may increase the auxin sensitivity (Pérez-Torres et al., 2008; Ruyter-Spira et al., 2011). These observations suggest that, just as for branching, changes in the auxin landscape could modulate the impact of *rac*-GR24 (Ruyter-Spira et al., 2011).

Cytokinins are also well known to influence the root architecture (reviewed in Vanstraelen and Benková, 2012). Cytokinin signaling negatively affects LR development by impinging on PIN-dependent auxin transport (Laplaze et al., 2007; Bishopp et al., 2011; Marhavý et al., 2011, 2014; Bielach et al., 2012; Chang et al., 2013; Moreira et al., 2013). Interaction of SLs with cytokinins during LR development has been poorly studied, but *max2-1* mutants have been reported to have a reduced sensitivity to the syntethic cytokinin 6-benzylaminopurine (BAP) (Koren et al., 2013).

Here, LR priming as well as outgrowth are shown to be modulated by treatment with *rac*-GR24, the latter in a spatiotemporal manner, mainly affecting the emergence of the LRs, which are the closest to the root-shoot junction. In addition, the ARABIDOPSIS HISTIDINE KINASE3 (AHK3)/ARABIDOPSIS RESPONSE REGULATOR1 (ARR1)/ARR12 cytokinin signaling module interacts with SLs to affect LR development, probably through changes in polar auxin transport. Altogether, the results put the SL action on LR development in the auxin landscape context via cross-talk mechanisms with cytokinin signaling.

2.2. Results

2.2.1. rac-GR24 reduces lateral rooting in Arabidopsis by affecting LR emergence, especially near the root-shoot junction in a MAX2-dependent manner

The overall MAX2-dependent reduction in LRD caused by *rac*-GR24 application had already been reported (Kapulnik et al., 2011b; Kohlen et al., 2011; Ruyter-Spira et al., 2011), but phenotypical insights into this event are still lacking. Upon *rac*-GR24 treatment, the first emerged LR had an altered position and this effect was abolished in the *max2-1* mutant. When plants were grown without *rac*-GR24 (mock), the distance from the hypocotyl to the first emerged LR was on average 3.37 mm, whereas when grown in the presence of *rac*-GR24 it increased to 6.27 mm in WT plants (Fig. 1A).

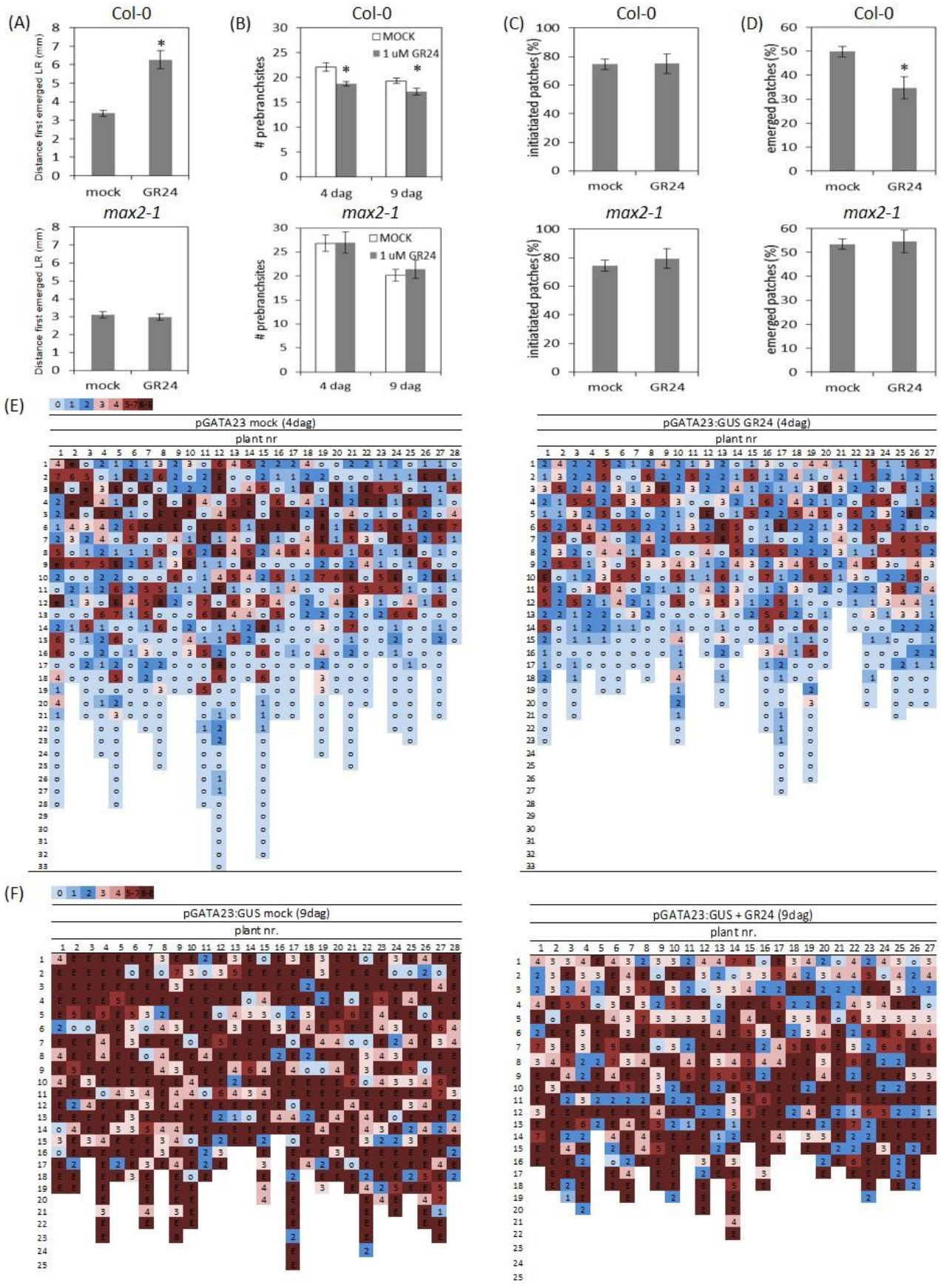
(A)
Col-0
Distance first emerged LR (mm)
mock
GR24
max2-1
(B)
Col-0
prebranchsites
MOCK
1 uM GR24
4 dag
9 dag
max2-1
(C)
Col-0
initiated patches (%)
max2-1
(D)
Col-0
emerged patches (%)
max2-1
(E)
pGATA23 mock (4dag)
pGATA23:GUS GR24 (4dag)
plant nr
(F)
pGATA23:GUS mock (9dag)
pGATA23:GUS + GR24 (9dag)
plant nr.

Fig. 1. Effect of exogenous *rac*-GR24 on LR development near the root-shoot junction. (A) Distance to the first emerged LR in Col-0 (top) and *max2-1* (bottom). Data presented are means ± SE of three biological repeats ($n > 20$). *$P < 0.001$, according to the Student's *t*-test. **(B)** Total number of prebranch sites under mock (white bars) and *rac*-GR24 treatment (grey bars), 4 and 9 DAG in Col-0 (top) and *max2-1* (bottom). Data presented are means ± SE of three biological repeats ($n > 20$). *$P < 0.05$, according to the Student's *t*-test. **(C)** Percentage of initiated patches under mock and 1 μM *rac*-GR24 treatments in Col-0 (top) and *max2-1* (bottom) at 9 DAG. **(D)** Percentage of emerged patches under mock and *rac*-GR24 treatment in Col-0 (top) and *max2-1* (bottom). Data presented are means ± SE of three biological repeats ($n > 20$). *$P < 0.05$, according to the Student's *t*-test. **(E, F)** Stages of LR primordia via *GATA23:GUS* staining in Col-0 under mock (left) and *rac*-GR24 treatment (right) at 4 DAG **(E)** and 9 DAG **(F)**. All events, possibly leading to emerged LRs, were scored in individual plants, color-coded, and for each plant, vertically ordered from the closest to the hypocotyl (up) downward to the meristem (down). The staging of the LR primordia was done according to Malamy and Benfey 1997. Stage '0' refers to a prebranch site, which is hallmarked by *GATA23:GUS* expression prior to cell division events. The root fragments used for analysis were comparable in length. Data of one representative experiment are shown. The experiments were repeated three times with similar results.

To understand this effect, the LR development was spatiotemporally followed, with specific focus on the upper root zone. Therefore, the expression of the early LR marker *GATA23* that indicates prebranch sites (Supplementary Fig. S1) (De Rybel et al., 2010), was used and combined with the staging of the LR primordia (Malamy and Benfey, 1997), in both WT and max2-1 plants, under mock and *rac*-GR24 treatments (Fig. 1E, F; Supplementary Fig. S2). As such, all sites in which a LR could develop were visualized from the root-shoot junction down to the root meristem at 4 DAG (Fig. 1E; Supplementary Fig. S2A). The progression in LR development was subsequently analyzed at 9 DAG (Fig. 1F; Supplementary Fig. S2B) to obtain a spatiotemporal view of how the LR primordium development was affected by *rac*-GR24 treatment. Fewer *GATA23*-marked sites were observed at 9 DAG than at 4 DAG, implying that not all primed sites developed into a LR primordium. When the number of LR sites between mock and *rac*-GR24-grown plants was compared, slightly, but significantly, fewer sites were counted upon *rac*-GR24 treatment, both at 4 and 9 DAG (Fig. 1B), indicating that *rac*-GR24 treatment reduced the total number of prebranch

sites in WT, but not in *max2-1* seedlings (Fig. 1B). Concerning initiated patches (see Materials and Methods), mock and *rac*-GR24-grown roots of both WT and *max2-1* seedlings did not differ, suggesting that *rac*-GR24 had no effect on LR initiation, once the prebranch site had been formed (Fig. 1C). *rac*-GR24 treatment also affected LR outgrowth (Kapulnik et al., 2011b; Ruyter-Spira et al., 2011; Kohlen et al., 2011). When the percentage of emerged patches was calculated, significantly fewer sites were counted on *rac*-GR24-grown roots than on control roots, but again not on *max2-1* roots (Fig. 1D). Interestingly, when the emergence pattern was analyzed at 9 DAG (Fig. 1F), the LR outgrowth inhibition was most pronounced at positions 1-8, corresponding to the LR primordia closest to the root-shoot junction, but did not occur in the *max2-1* mutant (Supplementary Fig. S2B). These data indicate that mainly the first formed LR primordia, thus those near the root-shoot junction, do not develop when plants are grown in the presence of *rac*-GR24 and that this effect depends on MAX2.

2.2.2. The cytokinin signaling components AHK3, ARR1 and ARR12 mediate the effect of *rac*-GR24 on LR development

Both cytokinins and SLs have been described as negative regulators of LR development in Arabidopsis (Benková et al., 2003; Li et al., 2006; Laplaze et al., 2007; Kapulnik et al., 2011b; Ruyter-Spira et al., 2011). Therefore, the link between the *rac*-GR24-mediated LRD reduction and the cytokinin-mediated LRD inhibition was investigated in further detail. Firstly, the LRD of several cytokinin signaling mutants, single and higher-order mutants affected in the cytokinin receptors CYTOKININ RESPONSE1 (CRE1)/AHK4, AHK2, and/or AHK3 (see Materials and Methods) was examined upon treatment with 1 µM *rac*-GR24 (Fig. 2A, B). For all tested genotypes, *rac*-GR24 treatment did not significantly affect the main root length (Supplementary Fig. S3). For Col-0, *cre1/ahk4*, and *ahk2*, the LRD was significantly reduced upon *rac*-GR24 treatment, but not for the *ahk3* mutant (Fig. 2A). In the double cytokinin receptor mutant

ahk2;ahk4, the LRD decreased significantly upon *rac*-GR24 treatment, whereas no significant changes in LRD were observed for *ahk2;ahk3* and *ahk3;ahk4* between mock and *rac*-GR24 treatment (Fig. 2B). Taken together, these data show that in mutants specifically affected in one member of the cytokinin receptor family, i.e. AHK3 (*ahk3*, *ahk2;ahk3*, and *ahk3;ahk4*), the *rac*-GR24 impact on LRD was abolished, whereas other cytokinin receptor mutants responded as WT plants. The *AHK3* expression was unaffected by *rac*-GR24 treatment (Supplementary Fig. S4).

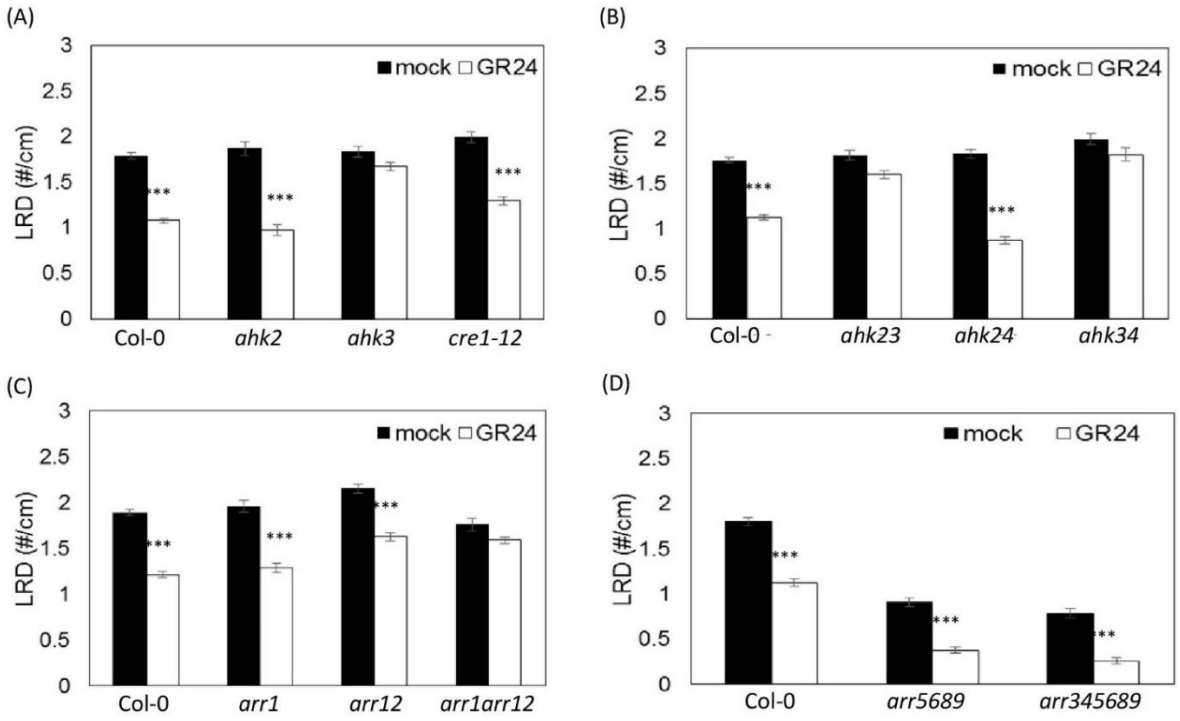

Fig. 2. Effects of *rac*-GR24 on cytokinin perception and signaling mutants. LRD of single cytokinin receptor mutants **(A)**, double cytokinin receptor mutants **(B)**, B-type response regulators *ARR1*, *ARR12* and *ARR1;ARR12* **(C)**, and mutants in higher-order A-type response regulators **(D)** upon *rac*-GR24 treatment. Data presented are means ± SE of three biological repeats ($n > 20$). ***$P < 0.001$, according to ANOVA mixed-model statistical analyses.

These observations prompted the investigation of the downstream signaling components of the cytokinin perception machinery. As the B-type response regulators ARR1 and ARR12 are involved in

mediating the AHK3-dependent effects in the root elongation zone (Dello Ioio et al., 2007, 2008). The *rac*-GR24 impact on the LRD was tested in mutants of these response regulators. The single mutants *arr1* and *arr12* displayed a sensitivity to *rac*-GR24 similar to that of Col-0 (Fig. 2C), but the double mutant *arr1;arr12* did not, indicating that both ARRs need to be disrupted to interfere with the *rac*-GR24 effect on LR development (Fig. 2C).

Having established that AHK3, ARR1 and ARR12 are involved in the GR24-mediated reduction of LRD, we analyzed whether mutants affected in A-type response regulators would affect the GR24-mediated LRD reduction. Therefore, the sensitivity was tested of higher-order A-type ARR mutants to *rac*-GR24, because these negative regulators of the cytokinin response are known to act redundantly in root architecture control (To et al., 2004; Zhang et al., 2011). The *arr5;arr6;arr8;arr9* and *arr3;arr4;arr5;arr6;arr8;arr9* mutants showed a significant increase in sensitivity to *rac*-GR24: LRD decreased by 37% in WT and by 58% and 67% in *arr5;arr6;arr8;arr9* and *arr3;arr4;arr5;arr6;arr8;arr9*, respectively (Fig. 2D). Hence, these data support the hypothesis that an altered cytokinin responsiveness can enhance (A-type ARRs) or repress (B-type ARRs or AHK3) the *rac*-GR24 effect on LR development. Taken together, these experiments demonstrate that specific cytokinin signaling components are needed for the *rac*-GR24 action on LR development.

2.2.3. The modified sensitivity to GR24 of *ahk3*/*arr1*;*arr12*/*shy2* mutants is due to changes in the auxin landscape

The AHK3/ARR1/ARR12 cytokinin signaling pathway has been shown to act upstream of SHORT HYPOCOTYL2 (SHY2) to control root differentiation (Dello Ioio et al., 2007, 2008) and, additionally, the *shy2* loss-of-function mutant has been shown to be insensitive to *rac*-GR24 as well (Koren et al., 2013). To elucidate why mutants in the AHK3/ARR1/ARR12/SHY2 module are affected in their *rac*-GR24 sensitivity,

the *rac*-GR24 phenotype of different *pin* mutants was examined, because SHY2 has been described to specifically repress *PIN1*, *PIN3*, *PIN5*, and *PIN7*, whereas cytokinin treatment downregulated *PIN1* and *PIN3*, but upregulated *PIN7* expression (Dello Ioio et al., 2007; Růžička et al., 2009). First, the *rac*-GR24 effect on LRD of mutations in PIN1, PIN3, PIN5, or PIN7 was analyzed. The decrease in LRD of the *pin7* mutants was only minor upon *rac*-GR24 treatment, indicating that mutation in PIN7 reduced the root sensitivity to GR24 (Fig. 3A), but the LRD reduction of the *pin1-613* mutants however was significantly higher than that in WT plants (Fig. 3B). For the *pin3-3* and *pin5-3* mutants, the LRD did not differ from that of WT plants (Fig. 3C).

Hence, these results provide the first genetic evidence that the LR response to exogenous *rac*-GR24 is modulated by interference with the polar auxin transport through PIN1 and, to a lesser extent of PIN7. Previously, prolonged, but not short *rac*-GR24 treatments, had been demonstrated to influence the expression of PIN1, PIN3 and PIN7 in the root meristem; however, the expression in root parts other than the meristem had not been assessed (Ruyter-Spira et al., 2011; Shinohara et al., 2013). Therefore, the *rac*-GR24 effect was investigated on the transcription of *PIN1* in the mature root, at the hypocotyl-root junction, where LR emergence is mostly affected by the *rac*-GR24 treatment (Fig 3). The impact of GR24 on the *PIN1* expression was analyzed after 7 days of growth of *proPIN1::GUS* seedlings. Interestingly, *PIN1* expression was affected in a spatial way as especially closest to the shoot, the expression in the vasculature was lower upon *rac*-GR24 treatment than under mock conditions (Fig. 3E, F). This observation was confirmed by analyzing the *PIN1* gene expression by qRT-PCR of roots grown either in the presence or the absence of *rac*-GR24 and by assessing the mature versus younger regions of the root (Fig. 3D). Moreover, the *PIN1* expression was also lower in the developing LRs from the upper part of *rac*-GR24-treated plants than that of mock-grown roots, in contrast to developing LRs at younger stages, i.e. near the root meristem (Fig. 3F).

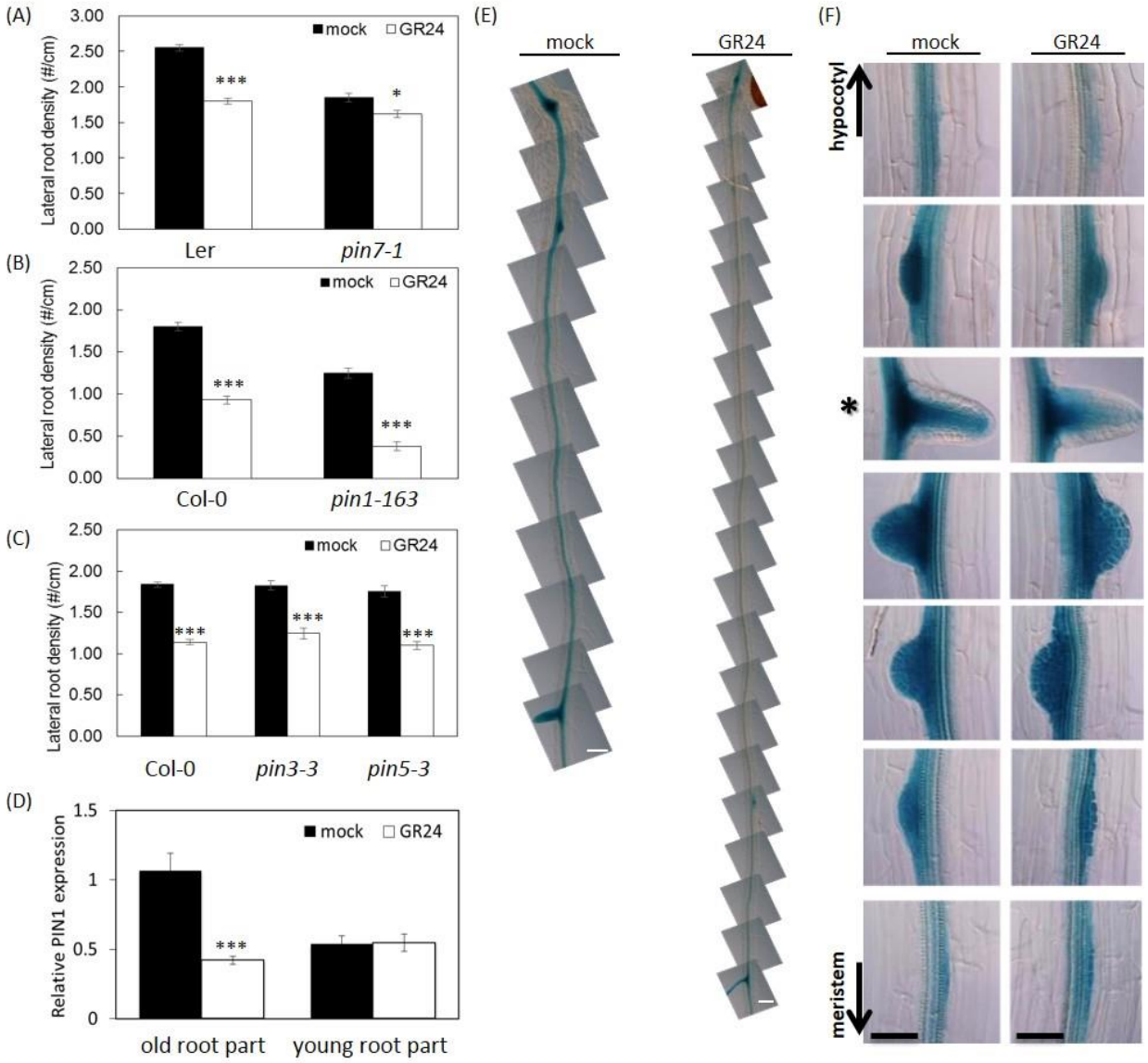

Fig. 3. Interrelation between the polar auxin transport and the *rac*-GR24 effect on LR development. (A-C) LRD of *pin7-1*, *pin1-613*, *pin3-3,* and *pin5-3* mutants compared to WT grown in the presence or absence of *rac*-GR24. Data presented are means ± SE of three biological repeats ($n > 20$). **(D)** Relative *PIN1* expression in 5-day-old seedlings under mock and *rac*-GR24 treatment as determined by qRT-PCR. Material was harvested separately from the upper part (old, above the first emerged LR) and the lower part (young) of the root. **(E)** p*PIN1:GUS* expression patterns of plants grown with and without *rac-GR24*, 7 days after growth. Frames until the first emerged LR are shown. **(F)** Expression of *PIN1* with pro*PIN1:GUS* plants during different stages of LR development under mock and *rac*-GR24 treatment. The panels indicated by the asterisk display the first emerged LR and those above the asterisk correspond to the LR primordia near the root-shoot junction. ***$P < 0.001$, *$P < 0.05$, according to ANOVA mixed-model statistical analyses. Black scale bars = 40 µm; white scale bars = 100 µm.

Thus far, our data demonstrate that mutations in the AHK3/ARR1/ARR12 cytokinin signaling module and in the auxin transport gene PIN1 and PIN7 affects the root sensitivity to *rac*-GR24, and that *rac*-GR24 influences auxin homeostasis by downregulating the expression of *PIN1* near the shoot-root junction which complements the reported decreased PIN protein levels in the root upon prolonged treatments with high concentrations of *rac*-GR24 (Ruyter-Spira et al., 2011).

To further investigate how the auxin environment alters the *rac*-GR24 effect, the *rac*-GR24 response was examined in plants that overexpressed YUCCA with concomitantly increased free auxin levels (Zhao et al., 2001). The LRD of *YUCCA1-D* plants did not decrease upon *rac*-GR24 treatment, indicating that enhanced endogenous auxin levels also modulate the *rac*-GR24 response in roots (Fig. 4A). Also PIN1-overexpressing (*PIN1ox*) plants that have highly increased frequencies of root primordia with retarded growth were analyzed (Benková et al., 2003). The typical *rac*-GR24-mediated decrease in LRD was no longer visible, but rather an increase in LRD was observed (Fig. 4B). Moreover, when the foliar auxin source that determines the outgrowth potential of LRs (Bhalerao et al., 2002; Ljung et al., 2005) was removed by decapitation after 6 days of growth and when these plants were subsequently treated with *rac*-GR24 for 5 days, the effects disappeared on both the *PIN1ox* lines (increase in LRD) and the WT (decrease in LRD), indicating that shoot-derived auxin is important for the *rac*-GR24 responses in roots (Fig. 4C). Application of IAA in these experiments (see Materials and Methods) revealed that shoot-derived auxin mediated the effect, because it complemented the phenotype of decapitated plants (Fig. 4D). Altogether, the functional data demonstrate that shoot-derived auxin controls the effect of *rac*-GR24 on lateral rooting in *Arabidopsis*, as previously hypothesized (Ruyter-Spira et al., 2011).

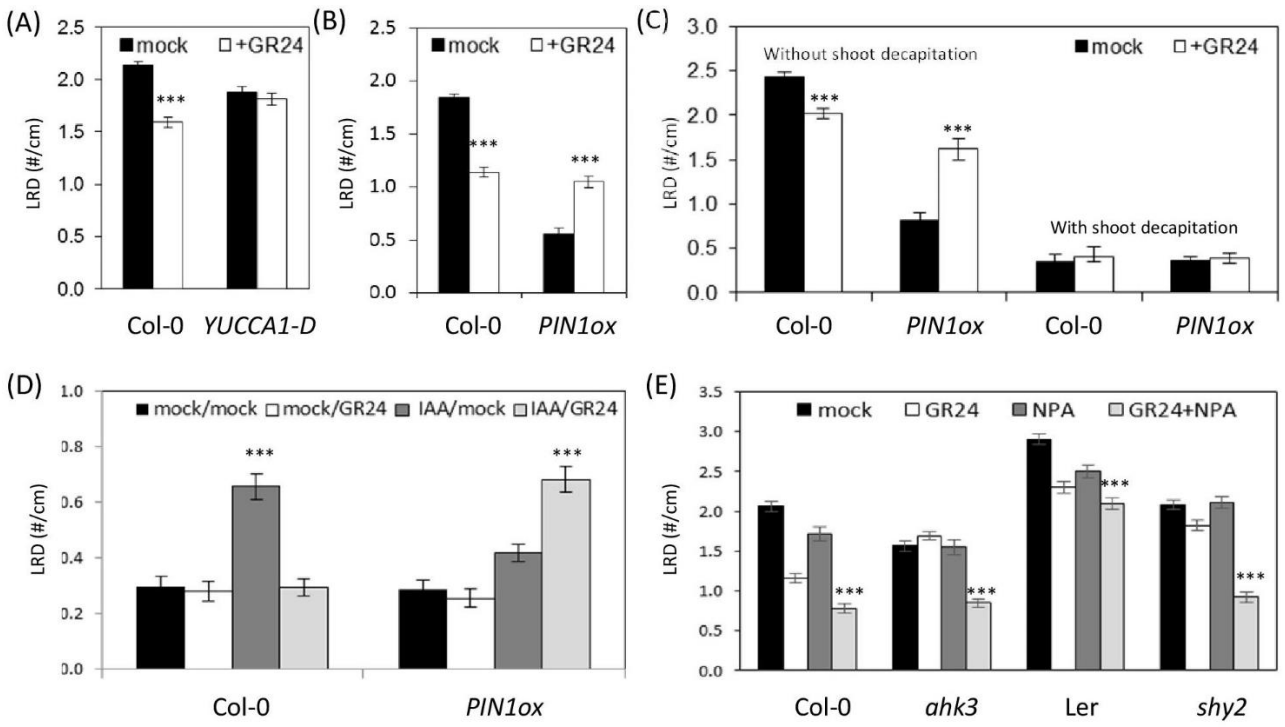

Fig. 4. Dependence of *rac*-GR24 action on the plant auxin status. (A) LRD of WT and *YUCCA*-overexpressing (*YUCCA1-D*) plants, grown with and without *rac*-GR24. **(B)** LRD of WT and *PIN1*-overexpressing (*PIN1ox*) plants, grown with and without *rac*-GR24. **(C)** LRD of Col-0 and *35S:PIN1* (PIN1ox) plants with and without shoot decapitation, grown in the presence or absence of *rac*-GR24. **(D)** LRD of Col-0 and *PIN1ox* plants with decapitation and with and without apically applied IAA grown in the presence or absence of *rac*-GR24. Mock/mock: decapitated plants grown in the absence of *rac*-GR24 and without applied IAA; mock/+GR24: decapitated plants grown in the presence of *rac*-GR24 and without applied IAA; IAA/mock: decapitated plants grown in absence of *rac*-GR24 and with apically applied IAA; IAA/+GR24: decapitated plants grown in the presence of GR24 and with apically applied IAA. **(E)** LRD of Col-0, *ahk3,* L*er* and *shy2-24* mutants upon treatment with mock, *rac*-GR24, NPA, or NPA+ *rac*-GR24. Data presented are means ± SE of three biological repeats ($n > 20$). ***$P < 0.001$, according to ANOVA mixed-model statistical analyses.

All mutants with *rac*-GR24-insensitive root responses, i.e. *ahk3*, *arr1;arr12*, and *shy2-24*, display an enhanced PIN1 expression (Dello Ioio et al., 2007, 2008; Zhang et al., 2011) that might cause their insensitivity towards *rac*-GR24. This hypothesis was tested by applying low concentrations (100 nM) of NPA, a polar auxin transport inhibitor (Himanen et al., 2002). The LRD response was analyzed under mock

and *rac*-GR24 treatment after 9 days of growth (Fig. 4E). Addition of this low concentration of NPA had no clear effect on *PIN1* expression in the main root, although a slight increase in *PIN1* gene expression was observed in the root tip (Supplementary Fig. S5). However, when the *ahk3* and *shy2-24* mutants were grown on plates supplemented with NPA as well as *rac*-GR24, the LRD was lower than that of roots grown under mock conditions or supplemented with *rac*-GR24 or NPA alone, implying that treatment with NPA rendered the mutant plants responsive to *rac*-GR24 again. For Col-0, no additional effect was seen when the roots were treated with both NPA and *rac*-GR24.

2.3. Discussion

Several aspects of the root system architecture are modulated by SLs (for reviews, see Cheng et al., 2013; Rasmussen et al., 2013a; Koltai, 2014). Here, *rac*-GR24 was found to control LR development spatiotemporally and to interplay with cytokinin that, just like SLs, regulates LR development. A summarizing model is presented (Fig. 5).

The method established to build a developmental map of all possible initiated LRs combines the *GATA23* marker gene for induction of prebranching sites, i.e. pericycle-derived LR founder cells that are predestined to start cell division for LR development, and LR positioning (Malamy and Benfey, 1997; De Rybel et al., 2010). Together with the determination of the position of each event along the main root, a precise developmental map provides location and developmental stage of each LR event, thereby revealing that the main effect of *rac*-GR24 on the development of LRs concerns their emergence. This observation concurs with previously published work, although the proposed specific interruption at stage V of LR development was not detected (Ruyter-Spira et al., 2011). The fact that these authors used a higher concentration of 2.5 µM *rac*-GR24, a different growth medium and growth conditions could be the underlying cause of of this discrepancy, as the effect of SLs on the root system arachitecture has been shown to be influenced by the environment (Ruyter-Spira et al., 2011; Shinohara et al., 2013).

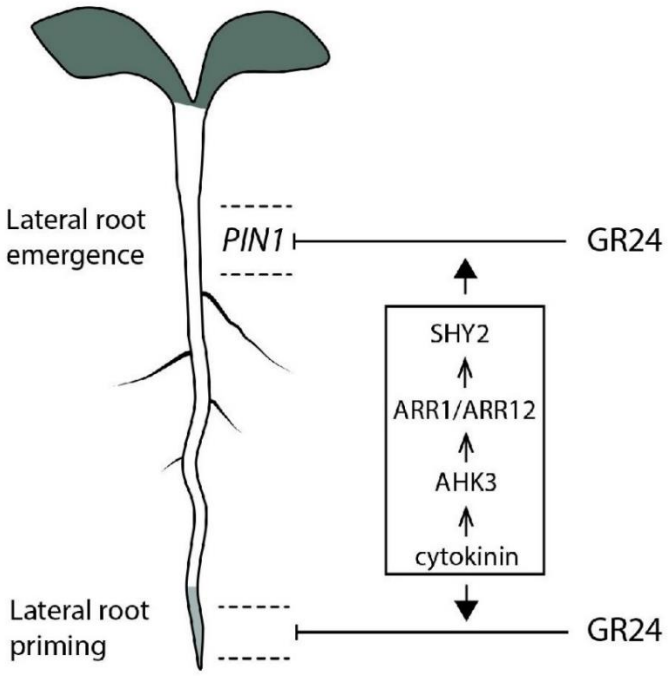

Fig. 5. Working model on the interaction of cytokinins with the SL analogue *rac*-GR24 to control lateral root development. *rac*-GR24 treatment results in an inhibition of lateral root emergence, mainly but not exclusively near the root-shoot junction, and to a minor extent in an inhibition of lateral root priming in the root meristem zone. In the region of the root near the root-shoot junction, this coincides with a spatial downregulation of *PIN1* expression by *rac*-GR24 treatment. The cytokinin module that signals via AHK3, through the response regulators ARR1/ARR12, and ultimately to SHY2, influences the effect of GR24 on lateral root development. Mutants in this pathway are insensitive to *rac*-GR24 probably due to their reported higher PIN1 levels since reducing the auxin flux by NPA treatment renders the mutants sensitive again to *rac*-GR24.

On the 9-DAG map, it were the LRs that were mainly, but not exclusively, situated close to the root-shoot junction that did no longer emerge under *rac*-GR24 treatment. Accordingly, the distance between the hypocotyl-shoot junction and the first emerged LR was longer in *rac*-GR24-grown roots than in control roots. This MAX2-dependent effect is in accordance with its essential function in SL signaling. Hence, *rac*-GR24 might affect specifically the emergence of the LRs that develop first and are positioned in the older part of the root. This spatiotemporal effect was also seen on the *PIN1* expression pattern in

the root. Although the reason for this effect still needs to be investigated, the disappearance of the SL receptor might be the underlying cause, because *rac*-GR24 treatment reduces the D14 protein abundance in roots (Chevalier et al., 2014).

Additionally, a small, but significant, decrease in prebranch sites was visible, whereas *rac*-GR24 had no appreciable effect on LR initiation. Hence, the previously detected *rac*-GR24 effect on LR initiation (Kapulnik et al., 2011b; Ruyter-Spira et al., 2011) is possibly due to an impact on prebranching, which could have been misinterpreted as an effect on initiation. Indeed, the authors did not score for an effect of priming, as this can only be visualized using the early LR marker GATA23. Prebranch sites are established by a periodic oscillation of auxin concentrations accompanied by fluctuations in specific gene expression (De Smet et al., 2007; Moreno-Risueno et al., 2010). This oscillating pattern has been found to be mediated by a carotenoid compound, distinct from SLs (Van Norman et al., 2014). In agreement with the data presented, the *max2* mutants also exhibited an increased LR capacity (Van Norman et al., 2014). It would be interesting to analyze whether *rac*-GR24, as a mimic of SLs or related compounds, modulates the periodic oscillation of auxin to cause the small effect on prebranching. Furthermore, independently of SLs, at 9 DAG, fewer LR events are observed on the same main root part than at 4 DAG, possibly indicating that not all primed sites develop into LRs. Cytokinins have been identified as endogenous repressors of LR development in a close interplay with auxin (Benková et al., 2003; Li et al., 2006; Laplaze et al., 2007). Here, the *rac*-GR24 effect on LR development required the functional cytokinin receptor AHK3, but not AHK2 and AHK4/CRE1. The dependence on AHK3 and not on AHK4 is remarkable, because AHK4 has been implicated in LR patterning along the main root (Marhavý et al., 2011), whereas AHK3 and the two immediately downstream B-type response regulator genes, ARR1 and ARR12, play an important role in determining the root meristem size (Dello Ioio et al., 2007, 2008). Also in the experimental setup, the double mutant *arr1;arr12* had no LR response toward *rac*-GR24, implying that the same cytokinin module (AHK3/ARR1/ARR12) that determines the root meristem differentiation also governs the *rac*-

GR24 action on LR development. AHK3 is involved in meristem differentiation by transcriptional control of the auxin-induced *SHY2/IAA3* gene (Dello Ioio et al., 2007, 2008). The typical reduction in lateral rooting upon *rac*-GR24 treatment was indeed not seen in the *shy2-24* loss-of-function mutants (Koren et al., 2013), supporting the hypothesis that the AHK3/ARR1/ARR12 module acts through SHY2 to result in *rac*-GR24 insensitivity.

The AHK3/ARR1/ARR12/SHY2 module negatively influences *PIN1/PIN3/PIN5/PIN7* expression (Dello Ioio et al., 2007, 2008), whereas cytokinin treatment downregulates *PIN1/PIN3/PIN5,* but upregulates *PIN7* expression (Laplaze et al., 2007; Růžička et al., 2009). These changes in *PIN* gene expression and their consequences on the polar auxin transport might be the underlying cause for the *rac*-GR24 insensitivity of the mutants. Several PIN mutants had a modified sensitivity to *rac*-GR24: *pin3* and *pin5* mutants still displayed a reduced LR development upon *rac*-GR24 treatment, whereas *pin7* mutants were only slightly responsive to GR24 and *pin1-613* mutants were hypersensitive in agreement with the opposite influence of cytokinins on their expression. In addition, treatment of *ahk3* and *shy2-24* with NPA made them sensitive again to *rac*-GR24. Hence, the changes in PIN gene expression, such as the *PIN1* overexpression observed in these mutants (Dello Ioio et al., 2007, 2008; Zhang et al., 2011) with an enhanced polar auxin transport as a result, might be the reason that *rac*-GR24 does not reduce the LRD in these mutants.

Moreover, the data support the central role of auxin transport for the SL action. Based on exogenous auxin and phosphate level modulation, the auxin content in roots has been shown to determine its responsiveness toward *rac*-GR24 (Ruyter-Spira et al., 2011). Indeed, endogenous overproduction of auxin via overexpression of YUCCA could make lateral root development unresponsive to *rac*-GR24. As auxin is well known to positively regulate its own efflux from cells, less PIN1 internalization in the *YUCCA1-D* mutant was observed, resulting in the accumulation of PIN1 on the plasma membrane (Paciorek et al., 2005). Hence, the observation on the *YUCCA1-D* mutant fits with the theory that mutants

with an enhanced PIN1 expression are insensitive to *rac*-GR24. Interestingly, PIN1-overexpressing plants no longer displayed a reduced LRD when treated with *rac*-GR24, but an opposite phenotype with an increased LRD. The difference in phenotypes between the plants overexpressing YUCCA1-D and PIN1 is intruiging, but might be due to differences in the severity of the PIN1 accumulation. Also in the shoot, depending on the auxin transport landscape, *rac*-GR24 could have positive or negative effects on the shoot lateral branching by depleting PIN1 from the membranes of xylem parenchyma cells of inflorescence stems (Shinohara et al., 2013). In addition, *rac*-GR24 has been shown to have a different effect on LR development that depends on the growth conditions: inhibition under sufficient and induction under low phosphate conditions or with exogenous IAA (Ruyter-Spira et al., 2011). Hence, overexpression of PIN1 has an effect on *rac*-GR24 responses similar to that of phosphate-limiting conditions: an increase, rather than a decrease, in LRD.

In conclusion, the data presented imply that *rac*-GR24 regulates LR development in a spatiotemporal manner with the strongest effect on emergence of the first developed LR positioned close to the root-shoot junction. This effect is tightly integrated into the auxin-cytokinin network that rules the root architecture with the polar auxin transport capacity as a central player on which both cytokinin and *rac*-GR24 act.

2.4. Materials and methods

Plant material and growth conditions

The *pin7-1* mutant from *Arabidopsis thaliana* (L.) Heyhn. is in Landsberg erecta (Ler) background, whereas the other lines described are in Columbia-0 (Col-0) background. The plant material used has been described previously: *ahk2-2*, *cre1-12*, and *ahk3-3* (Higuchi et al., 2004); *ahk2;ahk3, ahk2;ahk4,* and *ahk3;ahk4* (Riefler et al., 2006); *arr1*, *arr12* and *arr1;arr12* (Mason et al., 2005); *arr3;arr4;arr5;arr6*, and *arr3;arr4;arr5;arr6;arr8;arr9* (To et al., 2004); *pin1-613* (Bennett et al., 2006); *35S:PIN1-GFP (PIN1ox)* (Růžička et al., 2007); *pin3-3* (Friml et al., 2002); *pin5-3* (Mravec et al., 2009); *pin7-1* (Friml et al., 2003); *shy2-24* (Tian and Reed, 1999); *proAHK3:GUS* (Higuchi et al., 2004); *proPIN1:GUS* and *pGATA23:NLS-GFP-GUS* (De Rybel et al., 2010); and *YUCCA1-D* (Zhao et al., 2001).

Seeds were surface-sterilized for 5 min in 70% (v/v) ethanol, 0.05% (v/v) sodium dodecyl sulfate (SDS) solution, then incubated in 95% (v/v) ethanol for 5 min, and plated on half-strength Murashige and Skoog (½MS) medium (1% [w/v] sucrose and 0.8% [w/v] agar). Plants were stratified at 4°C for 2 days, transferred to a growth chamber at 21°C (16-h light/8-h dark photoperiod). A racemic mixture of GR24 (*rac*-GR24) was supplemented to the growth medium at the start of the experiment and plants were grown for the indicated time. All the experiments were repeated three times. Chemical compounds were added in the following concentrations, except indicated otherwise: 1 µM GR24 and 0.1 µM 1-N-naphthylphthalamic acid (NPA).

Phenotypic analysis and statistics

After 9 days of growth, LRs were counted under a binocular S4E microscope (Leica Microsystems) and root length was measured with ImageJ (http://rsb.info.nih.gov/ij). Both values were used to calculate the LRD. For the decapitation experiments, seedlings were grown for 6 days, where after the shoot was

removed as described (Forsyth and Van Staden, 1981). The bottom part was transferred to ½MS medium with or without 1 µM *rac*-GR24. For the complementation with indole-3-acetic acid (IAA), agar blocks (0.5 cm3) containing solidified growth medium with and without 10 µM IAA were added to the decapitated site and the LRD was analyzed 5 days later. Replicate means were subjected to statistics by analysis of variance (ANOVA; SAS Institute Inc., Cary, North Carolina, USA).

Stage determination by GATA23 expression analysis

pGATA23:NLS-GFP-GUS seeds were put on medium supplemented with 1 µM *rac*-GR24 or with the same volume of acetone as control and were stratified for 2 days at 4°C. Seedlings were grown vertically under continuous white light at 21°C. At 4 days after germination (DAG), half the seedlings were harvested for analysis, whereas for the remaining seedlings, the position of the main root tip was marked and the plates were transferred back to the growth room. At 9 DAG, the root parts above the mark were harvested. Samples were stained with β-glucuronidase (GUS), cleared as described (Malamy and Benfey, 1997) and analyzed under the microscope (see below). For the calculations of the percentage of initiated sites, the total average of initiations at 9 DAG was divided by the total average sites present at 4 DAG (i.e. the sum of all events, from 'stage 0' (prebranch site) to 'E' (emerged LR), divided by the amount of plants analyzed). Likewise for the calculations of the percentage of emerged sites, the total average of emerged LRs at 9 DAG was divided by the total average sites present at 4 DAG.

Histochemical analysis of GUS activity

Whole seedlings were stained in multiwell plates as described (Jefferson et al., 1987). Samples were cleared as described (Malamy and Benfey, 1997) and were analyzed by a differential interference contrast BX51 microscope (Olympus). Alternatively, samples were mounted directly in chloral hydrate solution (chloral hydrate:water:glycerol, 8:3:1) and microscopically analyzed.

RNA isolation, qRT-PCR and statistical analysis of *PIN1* expression

Arabidopsis *proPIN1::GUS* seeds were sown on ½MS medium with or without 1 µM *rac*-GR24. Seeds were stratified for 2 days at 4°C and then grown in vertical position at 21°C (16-h light/8-h dark photoperiod). After 7 days, root material was harvested and flash-frozen in liquid nitrogen. The region between the root-shoot junction and the first emerged LR was harvested separately from the remaining root system. Approximately 100 seedlings were used for each treatment and the experiment was repeated three times.

RNA preparation, cDNA synthesis, real-time qRT-PCR, and statistical analysis of expression profiling were done as described (Rasmussen et al., 2013b). The primers used are the following: PIN1_forward GGCATGGCTATGTTCAGTCTTGGG and PIN1_reverse ACGGCAGGTCCAACGACAAATC; ACTIN_forward CGCCATCCAAGCTGTTCTC and ACTIN_reverse TCACGTCCAGCAAGGTCAAG.

Accession numbers

The *Arabidopsis* Genome Initiative locus identifiers for the genes characterized in this study are: *AHK3* (AT1G27320), *SHY2* (AT1G04240), *PIN1* (AT1G73590), *PIN7* (AT1G23080), and *YUCCA1* (AT4G32540). Germplasm identification numbers for the seeds are: *ahk2* (*ahk2-2tk*), *ahk3-3* (SALK_069269), *cre1-12* (SALK_048970), *ahk2;ahk3* (*ahk2-5ahk3-7*), *ahk2;ahk4* (*ahk2-5cre1-12*), *ahk3;ahk4* (*ahk3-7;cre1-2*), *arr1-2* (N6368), *arr12-1* (CS6978), *arr1;arr12* (*arr1-3;arr12-1*), *pin1-613* (SALK_047613), and *pin5-3* (SALK_021738).

2.5. References

Agusti, J., Herold, S., Schwarz, M., Sanchez, P., Ljung, K., Dun, E.A., Brewer, P.B., Beveridge, C.A., Sieberer, T., Sehr, E.M., and Greb, T. (2011). Strigolactone signaling is required for auxin-dependent stimulation of secondary growth in plants. Proc. Natl. Acad. Sci. USA 108, 20242-20247 [Err. Proc. Natl. Acad. Sci. USA 109, 14277].

Benková, E., Michniewicz, M., Sauer, M., Teichmann, T., Seifertová, D., Jürgens, G., and Friml, J. (2003). Local, efflux-dependent auxin gradients as a common module for plant organ formation. Cell 115, 591-602.

Bennett, T., Sieberer, T., Willett, B., Booker, J., Luschnig, C., and Leyser, O. (2006). The *Arabidopsis MAX* pathway controls shoot branching by regulating auxin transport. Curr. Biol. 16, 553-563.

Bhalerao, R.P., Eklöf, J., Ljung, K., Marchant, A., Bennett, M., and Sandberg, G. (2002). Shoot-derived auxin is essential for early lateral root emergence in *Arabidopsis* seedlings. Plant J. 29, 325-332.

Bielach, A., Duclercq, J., Marhavý, P., and Benková, E. (2012). Genetic approach towards the identification of auxin-cytokinin crosstalk components involved in root development. Phil. Trans. R. Soc. B 367, 1469-1478.

Bishopp, A., Benková, E., and Helariutta, Y. (2011). Sending mixed messages: auxin-cytokinin crosstalk in roots. Curr. Opin. Plant Biol. 14, 10-16.

Braun, N., de Saint Germain, A., Pillot, J.-P., Boutet-Mercey, S., Dalmais, M., Antoniadi, I., Li, X., Maia-Grondard, A., Le Signor, C., Bouteiller, N., Luo, D., Bendahmane, A., Turnbull, C., and Rameau, C. (2012). The pea TCP transcription factor PsBRC1 acts downstream of strigolactones to control shoot branching. Plant Physiol. 158, 225-238.

Brewer, P.B., Dun, E.A., Ferguson, B.J., Rameau, C., and Beveridge, C.A. (2009). Strigolactone acts downstream of auxin to regulate bud outgrowth in pea and Arabidopsis. Plant Physiol. 150, 482-493.

Brewer, P.B., Dun, E.A., Gui, R., Mason, M.G., and Beveridge, C.A. (2015). Strigolactone inhibition of branching independent of polar auxin transport. Plant Physiol. 168, 1820-1829.

Bu, Q., Lv, T., Shen, H., Luong, P., Wang, J., Wang, Z., Huang, Z., Xiao, L., Engineer, C., Kim, T.H., Schroeder, J.I., and Huq, E. (2014). Regulation of drought tolerance by the F-box protein MAX2 in Arabidopsis. Plant Physiol. 164, 424-439.

Chang, L., Ramireddy, E., and Schmülling, T. (2013). Lateral root formation and growth of *Arabidopsis* is redundantly regulated by cytokinin metabolism and signalling genes. J. Exp. Bot. 64, 5021-5032.

Cheng, X., Ruyter-Spira, C., and Bouwmeester, H. (2013). The interaction between strigolactones and other plant hormones in the regulation of plant development. Front. Plant Sci. 4, 199.

Chevalier, F., Nieminen, K., Sánchez-Ferrero, J.C., Rodríguez, M.L., Chagoyen, M., Hardtke, C.S., and Cubas, P. (2014). Strigolactone promotes degradation of DWARF14, an α/β hydrolase essential for strigolactone signaling in *Arabidopsis*. Plant Cell 26, 1134-1150.

Crawford, S., Shinohara, N., Sieberer, T., Williamson, L., George, G., Hepworth, J., Müller, D., Domagalska, M.A., and Leyser, O. (2010). Strigolactones enhance competition between shoot branches by dampening auxin transport. Development 137, 2905-2913.

De Rybel, B., Vassileva, V., Parizot, B., Demeulenaere, M., Grunewald, W., Audenaert, D., Van Campenhout, J., Overvoorde, P., Jansen, L., Vanneste, S., Möller, B., Wilson, M., Holman, T., Van Isterdael, G., Brunoud, G., Vuylsteke, M., Vernoux, T., De Veylder, L., Inzé, D., Weijers, D., Bennett, M.J., and Beeckman, T. (2010). A novel Aux/IAA28 signaling cascade activates GATA23-dependent specification of lateral root founder cell identity. Curr. Biol. 20, 1697-1706.

De Smet, I., Tetsumura, T., De Rybel, B., Frey dit Frei, N., Laplaze, L., Casimiro, I., Swarup, R., Naudts, M., Vanneste, S., Audenaert, D., Inzé, D., Bennett, M.J., and Beeckman, T. (2007). Auxin-dependent regulation of lateral root positioning in the basal meristem of *Arabidopsis*. Development 134, 681-690.

Dello Ioio, R., Nakamura, K., Moubayidin, L., Perilli, S., Taniguchi, M., Morita, M.T., Aoyama, T., Costantino, P., and Sabatini, S. (2008). A genetic framework for the control of cell division and differentiation in the root meristem. Science 322, 1380-1384.

Dello Ioio, R., Scaglia Linhares, F., Scacchi, E., Casamitjana-Martinez, E., Heidstra, R., Costantino, P., and Sabatini, S. (2007). Cytokinins determine *Arabidopsis* root-meristem size by controlling cell differentiation. Curr. Biol. 17, 678-682.

Dun, E.A., de Saint, Germain, A., Rameau, C., and Beveridge, C.A. (2012). Antagonistic action of strigolactone and cytokinin in bud outgrowth control. Plant Physiol. 158, 487-498.

Ferguson, B.J., and Beveridge, C.A. (2009). Roles for auxin, cytokinin, and strigolactone in regulating shoot branching. Plant Physiol. 149, 1929-1944.

Foo, E., Bullier, E., Goussot, M., Foucher, F., Rameau, C., and Beveridge, C.A. (2005). The branching gene *RAMOSUS1* mediates interactions among two novel signals and auxin in pea. Plant Cell 17, 464-474.

Forsyth, C., and Van Staden, J. (1981). The effects of root decapitation on lateral root formation and cytokinin production in Pisum sativum. Physiol Plant. 51, 375-379.

Friml, J., Vieten, A., Sauer, M., Weijers, D., Schwarz, H., Hamann, T., Offringa, R., and Jürgens, G. (2003). Efflux-dependent auxin gradients establish the apical--basal axis of *Arabidopsis*. Nature 426, 147-153.

Friml, J., Wiśniewska, J., Benková, E., Mendgen, K., and Palme, K. (2002). Lateral relocation of auxin efflux regulator PIN3 mediates tropism in *Arabidopsis*. Nature 415, 806-809.

Gomez-Roldan, V., Fermas, S., Brewer, P.B., Puech-Pagès, V., Dun, EA., Pillot, J.-P., Letisse, F., Matusova, R., Danoun, S., Portais, J-C., Bouwmeester, H., Bécard, G., Beveridge, C.A., Rameau, C., and Rochange, S.F. (2008). Strigolactone inhibition of shoot branching. Nature 455, 189-194.

Hamiaux, C., Drummond, R.S.M., Janssen, B.J., Ledger, S.E., Cooney, JM., Newcomb, R.D., and Snowden, K.C. (2012). DAD2 is an α/β hydrolase likely to be involved in the perception of the plant branching hormone, strigolactone. Curr. Biol. 22, 2032-2036.

Hayward, A., Stirnberg, P., Beveridge, C., and Leyser, O. (2009). Interactions between auxin and strigolactone in shoot branching control. Plant Physiol. 151, 400-412.

Higuchi, M., Pischke, M.S., Mähönen, A.P., Miyawaki, K., Hashimoto, Y., Seki, M., Kobayashi, M., Shinozaki, K., Kato, T.,

Tabata, S., Helariutta, Y., Sussman, M.R., and Kakimoto, T. (2004). *In planta* functions of the *Arabidopsis* cytokinin receptor family. Proc. Natl. Acad. Sci. USA 101, 8821-8826.

Himanen, K., Boucheron, E., Vanneste, S., de Almeida Engler, J., Inzé, D., and Beeckman, T. (2002). Auxin-mediated cell cycle activation during early lateral root initiation. Plant Cell 14, 2339-2351.

Hu, Z., Yamauchi, T., Yang, J., Jikumaru, Y., Tsuchida-Mayama, T., Ichikawa, H., Takamure, I., Nagamura, Y., Tsutsumi, N., Yamaguchi, S., Kyozuka, J., and Nakazono, M. (2014). Strigolactone and cytokinin act antagonistically in regulating rice mesocotyl elongation in darkness. Plant Cell Physiol. 55, 30-41.

Jefferson, R.A., Kavanagh, T.A., and Bevan, M.W. (1987). GUS fusions: β-glucuronidase as a sensitive and versatile gene fusion marker in higher plants. EMBO J. 6, 3901-3907.

Kapulnik, Y., Resnick, N., Mayzlish-Gati, E., Kaplan, Y., Wininger, S., Hershenhorn, J., and Koltai, H. (2011a). Strigolactones interact with ethylene and auxin in regulating root-hair elongation in *Arabidopsis*. J. Exp. Bot. 62, 2915-2924.

Kapulnik, Y., Delaux, P.-M., Resnick, N., Mayzlish-Gati, E., Wininger, S., Bhattacharya, C., Séjalon-Delmas, N., Combier, J.-P., Bécard, G., Belausov, E., Beeckman, T., Dor, E., Hershenhorn, J., and Koltai, H. (2011b). Strigolactones affect lateral root formation and root-hair elongation in *Arabidopsis*. Planta 233, 209-216.

Kohlen, W., Charnikhova, T., Liu, Q., Bours, R., Domagalska, M.A., Beguerie, S., Verstappen, F., Leyser, O., Bouwmeester, H., and Ruyter-Spira, C. (2011). Strigolactones are transported through the xylem and play a key role in shoot architectural response to phosphate deficiency in nonarbuscular mycorrhizal host Arabidopsis. Plant Physiol. 155, 974-987.

Koltai, H. (2014). Receptors, repressors, PINs: a playground for strigolactone signaling. Trends Plant Sci. 19, 727-733.

Koltai, H., Dor, E., Hershenhorn, J., Joel, D.M., Weininger, S., Lekalla, S., Shealtiel, H., Bhattacharya, C., Eliahu, E., Resnick, N., Barg, R., and Kapulnik, Y. (2010). Strigolactones' effect on root growth and root-hair elongation may be mediated by auxin-efflux carriers. J. Plant Growth Regul. 29, 129-136.

Koren, D., Resnick, N., Mayzlish Gati, E., Belausov, E., Weininger, S., Kapulnik, Y., and Koltai, H. (2013). Strigolactone signaling in the endodermis is sufficient to restore root responses and involves SHORT HYPOCOTYL 2 (SHY2) activity. New Phytol. 198, 866-874.

Laplaze, L., Benkova, E., Casimiro, I., Maes, L., Vanneste, S., Swarup, R., Weijers, D., Calvo, V., Parizot, B., Herrera-Rodriguez, M.B., Offringa, R., Graham, N., Doumas, P., Friml, J., Bogusz, D., Beeckman, T., and Bennett, M. (2007). Cytokinins act directly on lateral root founder cells to inhibit root initiation. Plant Cell 19, 3889-3900.

Li, X., Mo, X., Shou, H., and Wu, P. (2006). Cytokinin-mediated cell cycling arrest of pericycle founder cells in lateral root initiation of *Arabidopsis*. Plant Cell Physiol. 47, 1112-1123.

Liang, J., Zhao, L., Challis, R., and Leyser, O. (2010). Strigolactone regulation of shoot branching in chrysanthemum (*Dendranthema grandiflorum*). J. Exp. Bot. 61, 3069-3078.

Ljung, K., Hull, A.K., Celenza, J., Yamada, M., Estelle, M., Normanly, J., and Sandberg, G. (2005). Sites and regulation of auxin biosynthesis in Arabidopsis roots. Plant Cell 17, 1090-1104.

Malamy, J.E., and Benfey, P.N. (1997). Organization and cell differentiation in lateral roots of *Arabidopsis thaliana*. Development 124, 33-44.

Minakuchi, K., Kameoka, H., Yasuno, N., Umehara, M., Luo, L., Kobayashi, K., Hanada, A., Ueno, K., Asami, T., Yamaguchi, S., and Kyozuka, J. (2010). *FINE CULM1* (*FC1*) works downstream of strigolactones to inhibit the outgrowth of axillary buds in rice. Plant Cell Physiol. 51, 1127-1135.

Marhavý, P., Bielach, A., Abas, L., Abuzeineh, A., Duclercq, J., Tanaka, H., Pařezová, M., Petrášek, J., Friml, J., Kleine-Vehn, J., and Benková, E. (2011). Cytokinin modulates endocytic trafficking of PIN1 auxin efflux carrier to control plant organogenesis. Dev. Cell 21, 796-804.

Marhavý, P., Duclercq, J., Weller, B., Feraru, E., Bielach, A., Offringa, R., Friml, J., Schwechheimer, C., Murphy, A., and Benková, E. (2014). Cytokinin controls polarity of PIN1-dependent auxin transport during lateral root organogenesis. Curr. Biol. 24, 1031-1037.

Mason, M.G., Mathews, D.E., Argyros, D.A., Maxwell, B.B., Kieber, J.J., Alonso, J.M., Ecker, J.R., and Schaller, G.E. (2005). Multiple type-B response regulators mediate cytokinin signal transduction in *Arabidopsis*. Plant Cell 17, 3007-3018.

Mayzlish-Gati, E., De-Cuyper, C., Goormachtig, S., Beeckman, T., Vuylsteke, M., Brewer, P.B., Beveridge, C.A., Yermiyahu, U., Kaplan, Y., Enzer, Y., Wininger, S., Resnick, N., Cohen, M., Kapulnik, Y., and Koltai, H. (2012). Strigolactones are involved in root response to low phosphate conditions in Arabidopsis. Plant Physiol. 160, 1329-1341.

Moreira, S., Bishopp, A., Carvalho, H., and Campilho, A. (2013). AHP6 inhibits cytokinin signaling to regulate the orientation of pericycle cell division during lateral root initiation. PLoS ONE 8, e56370.

Moreno-Risueno, M.A., Van Norman, J.M., Moreno, A., Zhang, J., Ahnert, S.E., and Benfey, P.N. (2010). Oscillating gene expression determines competence for periodic *Arabidopsis* root branching. Science 329, 1306-1311.

Mravec, J., Skůpa, P., Bailly, A., Hoyerová, K., Křeček, P., Bielach, A., Petrášek, J., Zhang, J., Gaykova, V., Stierhof, Y.-D., Dobrev, P.I., Schwarzerová, K., Rolčík, J., Seifertová, D., Luschnig, C., Benková, E., Zažímalová, E., Geisler, M., and Friml, J. (2009). Subcellular homeostasis of phytohormone auxin is mediated by the ER-localized PIN5 transporter. Nature 459, 1136-1140.

Paciorek, T., Zažímalová, E., Ruthardt, N., Petrášek, J., Stierhof, Y.-D., Kleine-Vehn, J., Morris, D.A., Emans, N., Jürgens, G., Geldner, N., and Friml, J. (2005). Auxin inhibits endocytosis and promotes its own efflux from cells. Nature 435, 1251-1256.

Pandya-Kumar, N., Shema, R., Kumar, M., Mayzlish-Gati, E., Levy, D., Zemach, H., Belausov, E., Wininger, S., Abu-Abied, M., Kapulnik, Y., and Koltai, H. (2014). Strigolactone analog GR24 triggers changes in PIN2 polarity, vesicle trafficking and actin filament architecture. New Phytol. 202, 1184-1196.

Péret, B., De Rybel, B., Casimiro, I., Benková, E., Swarup, R., Laplaze, L., Beeckman, T., and Bennett, M.J. (2009). *Arabidopsis* lateral root development: an emerging story. Trends Plant Sci. 14, 399-408.

Pérez-Torres, C.-A., López-Bucio, J., Cruz-Ramírez, A., Ibarra-Laclette, E., Dharmasiri, S., Estelle, M., and Herrera-Estrella, L. (2008). Phosphate availability alters lateral root development in *Arabidopsis* by modulating auxin sensitivity via a mechanism involving the TIR1 auxin receptor. Plant Cell 20, 3258-3272.

Růžička, K., Ljung, K., Vanneste, S., Podhorská, R., Beeckman, T., Friml, J., and Benková, E. (2007). Ethylene regulates root growth through effects on auxin biosynthesis and transport-dependent auxin distribution. Plant Cell 19, 2197-2212.

Růžička, K., Šimášková, M., Duclercq, J., Petrášek, J., Zažímalová, E., Simon, S., Friml, J., Van Montagu, M.C.E., and Benková, E. (2009). Cytokinin regulates root meristem activity via modulation of the polar auxin transport. Proc. Natl. Acad. Sci. USA 106, 4284-4289.

Rasmussen, A., Depuydt, S., Goormachtig, S., and Geelen, D. (2013b). Strigolactones fine-tune the root system. Planta 238, 615-626.

Rasmussen, A., Heugebaert, T., Matthys, C., Van Deun, R., Boyer, F.-D., Goormachtig, S., Stevens, C., and Geelen, D. (2013). A fluorescent alternative to the synthetic strigolactone GR24. Mol. Plant 6, 100-112.

Rasmussen, A., Mason, M.G., De Cuyper, C., Brewer, P.B., Herold, S., Agusti, J., Geelen, D., Greb, T., Goormachtig, S., Beeckman, T., and Beveridge, C.A. (2012). Strigolactones suppress adventitious rooting in Arabidopsis and pea. Plant Physiol. 158, 1976-1987.

Riefler, M., Novak, O., Strnad, M., and Schmülling, T. (2006). *Arabidopsis* cytokinin receptor mutants reveal functions in shoot growth, leaf senescence, seed size, germination, root development, and cytokinin metabolism. Plant Cell 18, 40-54.

Ruyter-Spira, C., Kohlen, W., Charnikhova, T., van Zeijl, A., van Bezouwen, L., de Ruijter, N., Cardoso, C., Lopez-Raez, J.A., Matusova, R., Bours, R., Verstappen, F., and Bouwmeester, H. (2011). Physiological effects of the synthetic strigolactone analog GR24 on root system architecture in Arabidopsis: another belowground role for strigolactones? Plant Physiol. 155, 721-734.

Shen, H., Luong, P., and Huq, E. (2007). The F-Box protein MAX2 functions as a positive regulator of photomorphogenesis in Arabidopsis. Plant Physiol. 145, 1471-1483.

Shen, H., Zhu, L., Bu, Q.-Y., and Huq, E. (2012). MAX2 affects multiple hormones to promote photomorphogenesis. Mol. Plant 5, 750-762.

Shinohara, N., Taylor, C., and Leyser, O. (2013). Strigolactone can promote or inhibit shoot branching by triggering rapid depletion of the auxin efflux protein PIN1 from the plasma membrane. PLoS Biol. 11, e1001474.

Snowden, K.C., Simkin, A.J., Janssen, B.J., Templeton, K.R., Loucas, H.M., Simons, J.L., Karunairetnam, S., Gleave, A.P., Clark, D.G., and Klee, H.J. (2005). The *Decreased apical dominance1/Petunia hybrida CAROTENOID CLEAVAGE DIOXYGENASE8* gene affects branch production and plays a role in leaf senescence, root growth, and flower development. Plant Cell 17, 746-759.

Stirnberg, P., Ward, S., and Leyser, O. (2010). Auxin and strigolactones in shoot branching: intimately connected? Biochem. Soc. Trans. 38, 717-722.

Sun, H., Tao, J., Liu, S., Huang, S., Chen, S., Xie, X., Yoneyama, K., Zhang, Y., and Xu, G. (2014). Strigolactones are involved in phosphate- and nitrate-deficiency-induced root development and auxin transport in rice. J. Exp. Bot. 65, 6735-6746.

Tian, Q., and Reed, J.W. (1999). Control of auxin-regulated root development by the *Arabidopsis thaliana SHY2/IAA3* gene. Development 126, 711-721.

To, J.P.C., Haberer, G., Ferreira, F.J., Deruère, J., Mason, M.G., Schaller, G.E., Alonso, J.M., Ecker, J.R., and Kieber, J.J. (2004). Type-A Arabidopsis response regulators are partially redundant negative regulators of cytokinin signaling. Plant Cell 16, 658-671.

Tsuchiya, Y., Vidaurre, D., Toh, S., Hanada, A., Nambara, E., Kamiya, Y., Yamaguchi, S., and McCourt, P. (2010). A small-molecule screen identifies new functions for the plant hormone strigolactone. Nat. Chem. Biol. 6, 741-749.

Umehara, M., Hanada, A., Yoshida, S., Akiyama, K., Arite, T., Takeda-Kamiya, N., Magome, H., Kamiya, Y., Shirasu, K., Yoneyama, K., Kyozuka, J., and Yamaguchi, S. (2008). Inhibition of shoot branching by new terpenoid plant hormones. Nature 455, 195-200.

Van Norman, J.M., Zhang, J., Cazzonelli, C.I., Pogson, B.J., Harrison, P.J., Bugg, T.D.H., Chan, K.X., Thompson, A.J., and Benfey, P.N. (2014). Periodic root branching in *Arabidopsis* requires synthesis of an uncharacterized carotenoid derivative. Proc. Natl. Acad. Sci. USA 111, E1300-1309.

Vanstraelen, M., and Benková, E. (2012). Hormonal interactions in the regulation of plant development. Annu. Rev. Cell Dev. Biol. 28, 463-487.

Woo, H.R., Chung, K.M., Park, J.-H., Oh, S.A., Ahn, T., Hong, S.H., Jang, S.K., and Nam, H.G. (2001). ORE9, an F-box protein that regulates leaf senescence in Arabidopsis. Plant Cell 13, 1779-1790.

Xie, X., Yoneyama, K., and Yoneyama, K. (2010). The strigolactone story. Annu. Rev. Phytopathol. 48, 93-117.

Zhang, S., Li, G., Fang, J., Chen, W., Jiang, H., Zou, J., Liu, X., Zhao, X., Li, X., Chu, C., Xie, Q., Jiang, X., and Zhu, L. (2010). The interactions among *DWARF10*, auxin and cytokinin underlie lateral bud outgrowth in rice. J. Integr. Plant Biol. 52, 626-638.

Zhang, W., To, J.P.C., Cheng, C.-Y., Schaller, G.E., and Kieber, J.J. (2011). Type-A response regulators are required for proper root apical meristem function through post-transcriptional regulation of PIN auxin efflux carriers. Plant J. 68, 1-10.

Zhao, L.H., Zhou, X.E., Wu, Z.-S., Yi, W., Xu, Y., Li, S., Xu, T.-H., Liu, Y., Chen, R.-Z., Kovach, A., Kang, Y., Hou, L., He, Y., Xie, C., Song, W., Zhong, D., Xu, Y., Wang, Y., Li, J., Zhang, C., Melcher, K., and Xu, H.E. (2013). Crystal structures of two phytohormone signal-transducing α/β hydrolases: karrikin-signaling KAI2 and strigolactone-signaling DWARF14. Cell Res. 23, 436-439.

Zhao, Y., Christensen, S.K., Fankhauser, X., Cashman, J.R., Cohen, J.D., Weigel, D., and Chory, J. (2001). A role for flavin monooxygenase-like enzymes in auxin biosynthesis. Science 291, 306-309.

2.6. Supplementary data

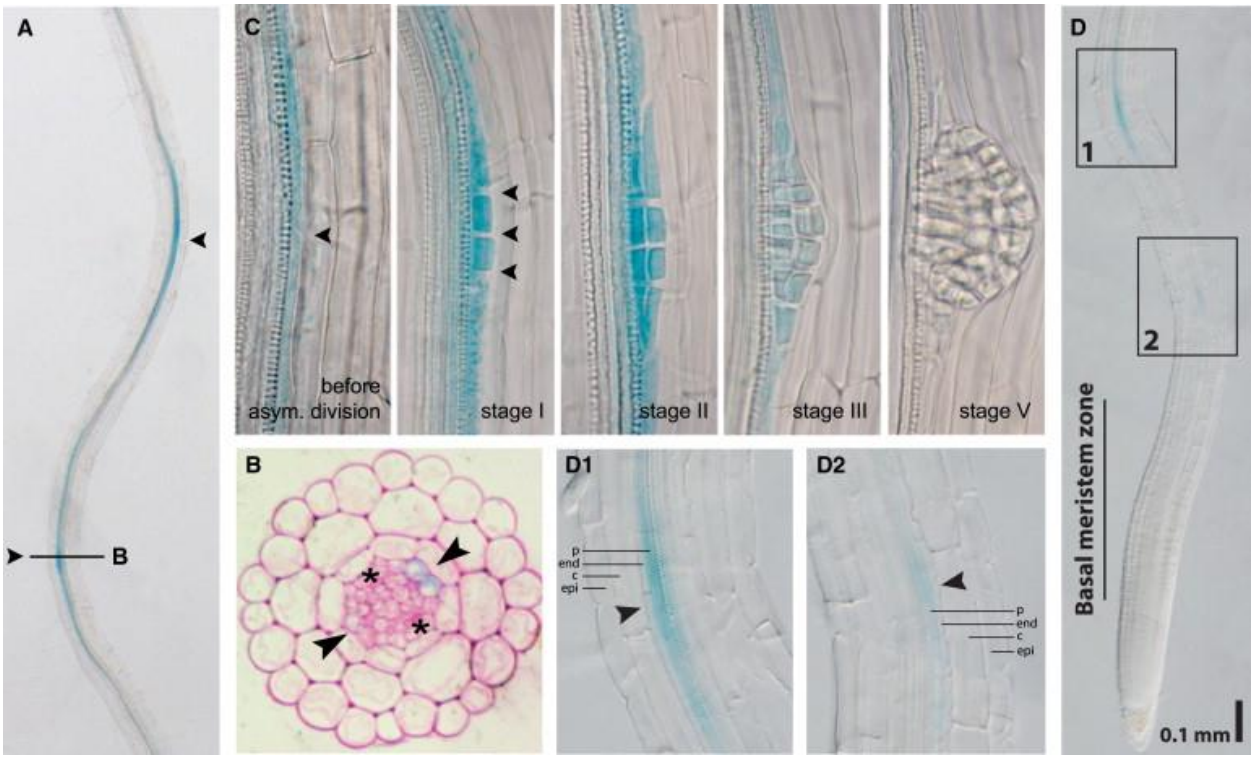

Supplementary Figure S1. Expression pattern of the p*GATA23:GUS* reporter line. (A) *pGATA23:GUS* expression in the mature root at sites of lateral root initiation (arrowheads). The horizontal black line represents the location of the section shown in (B). **(B)** Section through a stage I lateral root primordium showing *pGATA23:GUS* expression at one side of the xylem pole pericycle (XPP). Asterisks and arrowheads indicate phloem pole and XPP cells, respectively. **(C)** Detailed expression analysis of *GATA23* during stages of lateral root initiation. **(D)** Before the first asymmetric division, *GATA23* is expressed in patches in the root (arrowheads in D1 and D2). The vertical black line in (D) indicates the basal meristem. (D1) and (D2) show magnifications of boxed areas in (D) (epi, epidermis; c, cortex; endo, endodermis; p, pericycle). Figure taken from De Rybel et al., 2009.

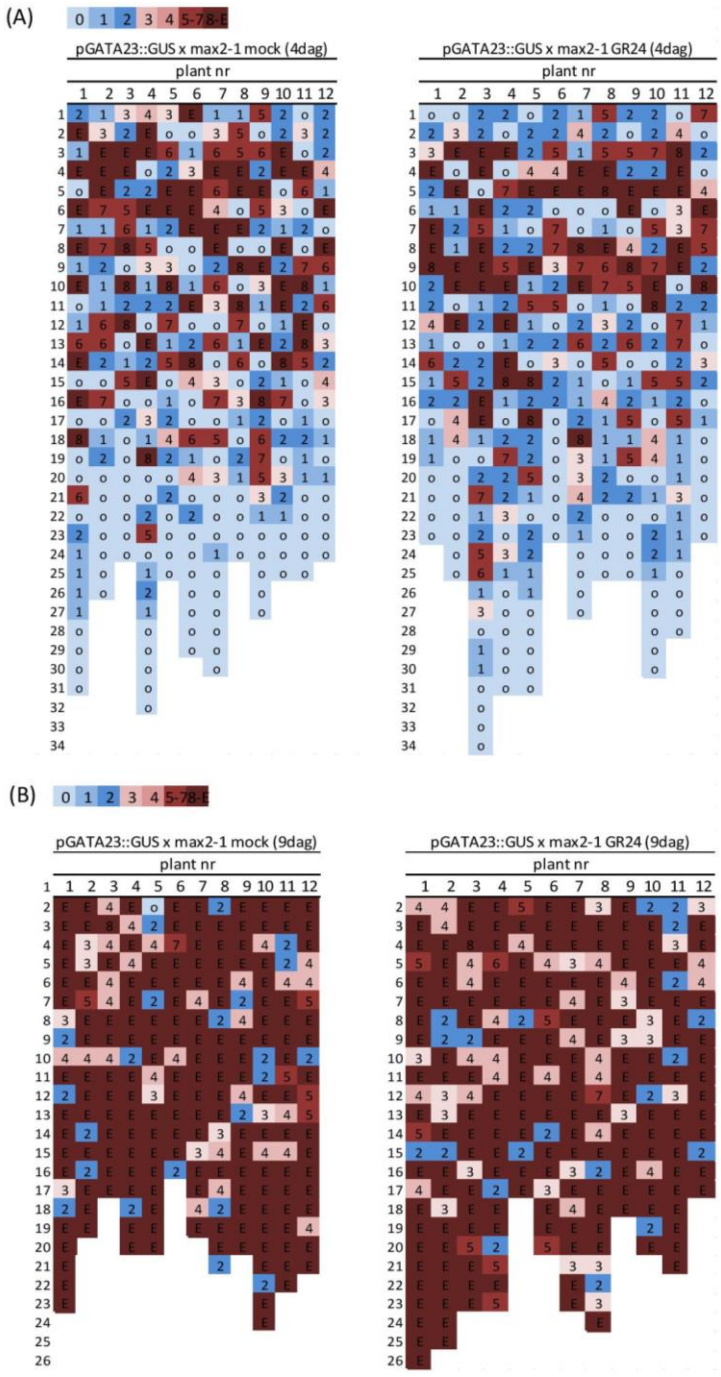

Supplementary Figure S2. Stages of lateral root primordia via *GATA23:GUS* staining in *max2-1* under mock and *rac*-GR24 treatment at 4 and 9 DAG. Stages of LR primordia via *GATA23:GUS* staining in *max2-1* under mock (left) and *rac*-GR24 treatment (right) at 4 DAG (A) and 9 DAG (B). All events, possibly leading to emerged LRs, were scored in individual plants, color-coded, and for each plant, vertically ordered from the closest to the hypocotyl (up) downward to the meristem (down). The root fragments used for analysis were comparable in length.

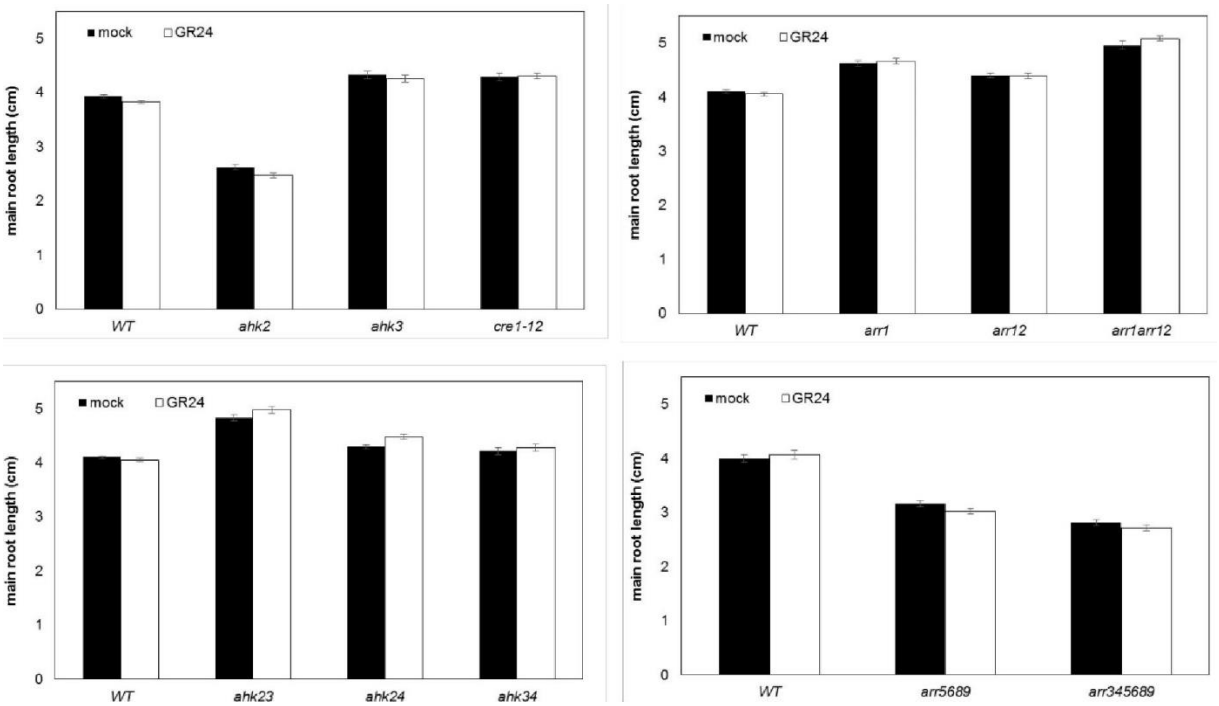

Supplementary Figure S3. Main root lengths of WT and cytokinin receptor and signal transduction mutants under mock and *rac*-GR24 treatment. Main root lenght of single cytokinin receptor mutants (*ahk2*, *ahk3* and *cre1*), double cytokinin receptor mutants (*ahk2;3*; *ahk2;4* and *ahk3;4*), B-type response regulators (*arr1*, *arr12* and *arr1;12*), and mutants in higher-order A-type response regulators (*arr5;6;8;9* and *arr3;4;5;6;8;9*) upon *rac*-GR24 treatment. Data presented are means ± SE of three biological repeats (n > 20).

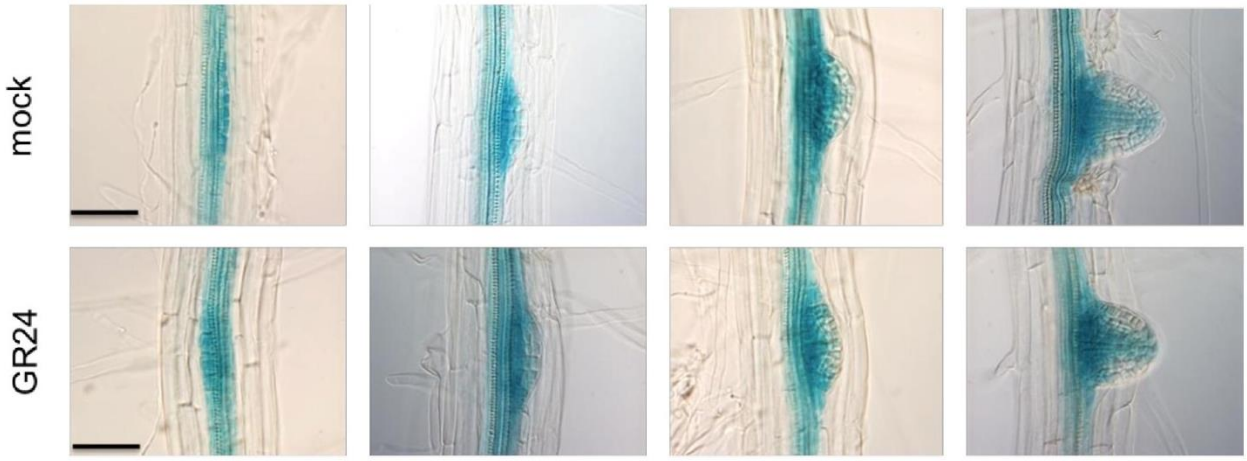

Supplementary Figure S4. pAHK3-GUS expression patterns of lateral root primordia at different developmental stages under mock and GR24 treatment. *pAHK3:GUS* expression patterns of lateral root primordia of plants grown with and without *rac*-GR24, 7 days after growth.

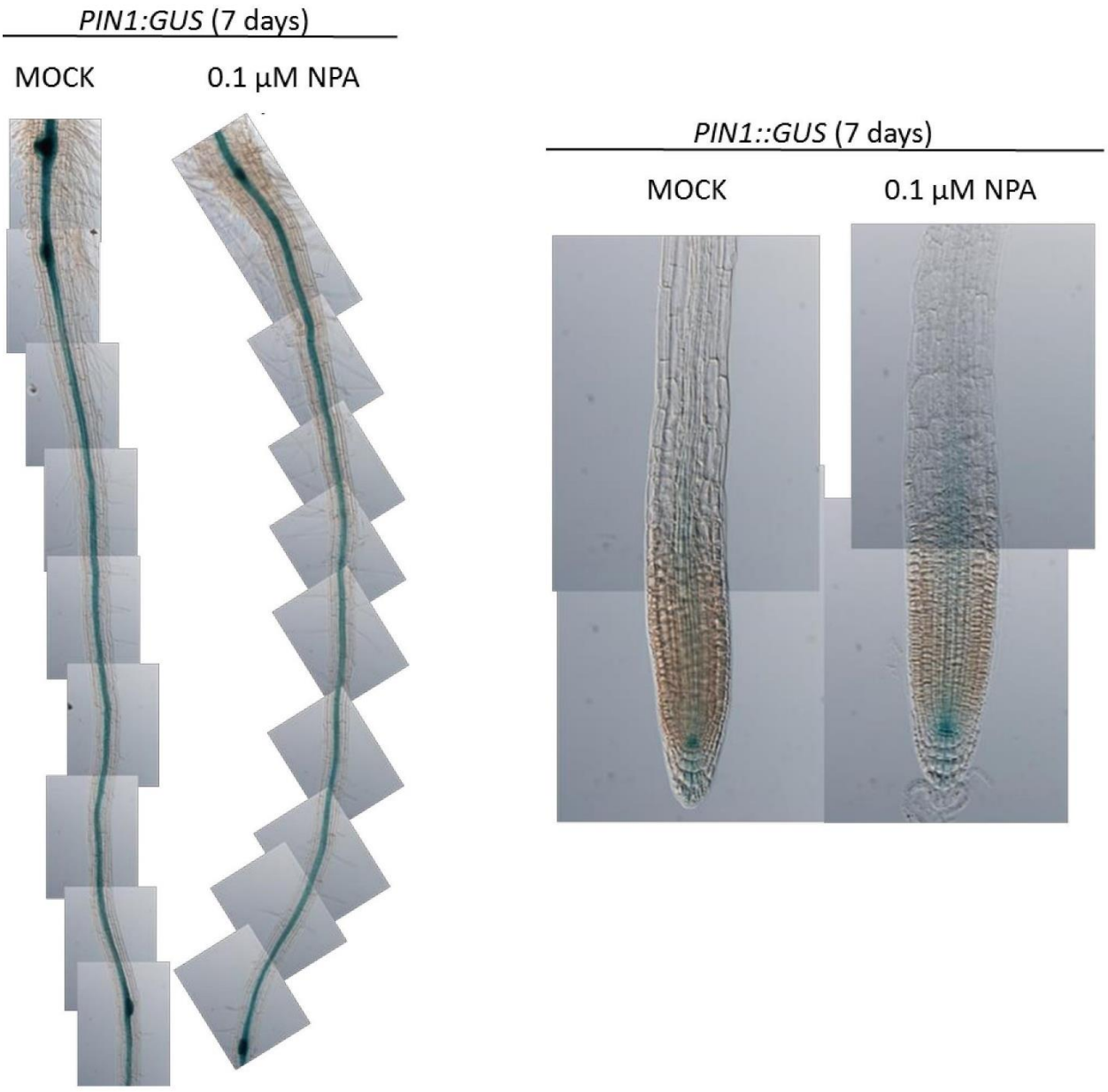

Supplementary Figure S5. *pPIN1:GUS* expression pattern after treatment with 0.1 µM NPA around the root-shoot junction (left) and the root meristem zone (right). p*PIN1:GUS* expression patterns of plants grown with and without *0.1 µM NPA,* 7 days after growth. The region around the root-shoot junction until the first emerged lateral root primordium (left) and the root meristem zone (right) are shown.

CHAPTER 3

A TRANSCRIPTOME-WIDE ANALYSIS OF *rac*-GR24 TREATMENT ON THE ROOT OF *ARABIDOPSIS THALIANA*

CEDRICK MATTHYS, BORIS PARIZOT, VERONIQUE STORME, TOM BEECKMAN, AND SOFIE GOORMACHTIG

In preparation

Author's contribution: Cedrick Matthys was the main researcher involved in the work displayed in this chapter.

Abstract

Multiple functions have been identified for the plant hormones strigolactones during plant growth and development. In the root system architecture as well, strigolactones play an important role, but an in-depth understanding of the responses in the root at the transcriptional level is lacking. Here, we present a transcriptome-wide overview on the changes brought about by treatment with the synthetic strigolactone analog *rac*-GR24 in the roots of *Arabidopsis thaliana* and on the differences in the root transcriptome of the signaling mutant *more axillary growth2* compared to the wild type. Strigolactones were found to influence various pathways, such as the hormonal crosstalk, drought responses, and light harvesting and sensitivity, and to modulate the plant's secondary metabolism. Additionally, we show that the influence of *rac*-GR24 on the lateral root density and root length requires both the recognition of the two enantiomers of *rac*-GR24 by either the DWARF14 or KARRIKIN-INSENSITIVE2 receptor. Altogether, the data imply that the *rac*-GR24 signaling involves the alteration of different pathways to regulate its impact on the root system architecture.

3.1. Introduction

Strigolactones (SLs) have recently been identified as plant hormones with potentially important agricultural applications. The phytohormonal action of SLs is mainly assessed in the context of the shoot architecture, because SLs play a role in the inhibition of lateral bud outgrowth (Gomez-Roldan et al., 2008; Umehara et al., 2008). However, the phytohormonal effects on leaf senescence, drought tolerance, biotic stress responses, seed germination, and secondary growth have been reported as well (Snowden et al., 2005; Tsuchiya et al., 2010; Agusti et al., 2011; Toh et al., 2012a, 2012b; Bu et al., 2014; Ha et al., 2014). Moreover, besides their function as phytohormones, SLs are also known for their role in the rhizosphere, because they influence arbuscular mycorrhizal associations, induce parasitic plant germination, and affect nodulation (Soto et al., 2010; Xie et al., 2010; Foo and Davies, 2011; Foo et al., 2013).

Additionally, SLs influence the root system architecture. The widely used treatment with the synthetic strigolactone *rac*-GR24 that consists of two enantiomers has been shown to increase the primary root length, due to a size enhancement of the meristem and transition zone (Ruyter-Spira et al., 2011). Furthermore, *rac*-GR24 has a positive effect on root hair elongation and plays an inhibitory role on lateral root development and adventitious rooting (Kapulnik et al., 2011a, 2011b; Ruyter-Spira et al., 2011; Rasmussen et al., 2012; Chapter 2). In agreement, mutants in the F-box protein MORE AXILLARY GROWTH 2 (MAX2), perturbed in SL perception, have a shorter main root, display a higher adventitious rooting capacity, and have a higher lateral root density than those of wild-type (WT) plants (Ruyter-Spira et al., 2011; Kapulnik et al., 2011a; Rasmussen et al., 2012). Moreover, accordingly with being a main signaling factor, *max2* mutants do not display the characteristic *rac*-GR24-dependent phenotypes (Kapulnik et al., 2011a; Ruyter-Spira et al 2011). Concerning the effect on the lateral root density, restoring the MAX2 function specifically in the root endodermis was sufficient to complement the response (Koren et al., 2013).

The divergent effects of *rac*-GR24 on the root system architecture imply that the regulation occurs on various tissues and maybe via different mechanisms. Additionally, the interpretation of the observations is complicated by the fact that *rac*-GR24 consists of two enantiomers from which one, the (+)GR24 is recognized by the SL receptor DWARF 14 (D14), whereas the other, the (-)GR24 by the karrikin receptor, KARRIKIN INSENSITIVE 2 (KAI2) (Scaffidi et al., 2014). As a result, the *rac*-GR24 effects are a combination of signaling through both D14 and KAI2, whereafter the signaling of both pathways converge on MAX2 (Scaffidi et al., 2014). Thus far, it is not clear which is the contribution of D14 or KAI2 in the root responses.

Recently, much insights have been obtained into the perception of SLs, but it is currently unclear what happens thereafter (Soundappan et al., 2015; Wang et al., 2015; Bennett et al., 2016; Liang et al., 2016;). Transcription-dependent, as well as transcription-independent signaling mechanisms have been proposed (Shinohara et al., 2013; Liang et al., 2016). Insights into the transcription-dependent approaches can be obtained via genome-wide transcriptome studies, of which a few related to SLs have been published (Mashiguchi et al., 2009; Mayzlish-Gati et al., 2010; Nelson et al., 2010; Ha et al., 2014). The first microarray analysis on whole *Arabidopsis max1* seedlings, affected in SL biosynthesis, after treatment with *rac*-GR24 revealed a limited amount of differentially expressed genes (Mashiguchi et al., 2009). From this dataset, an intensive crosstalk between SLs and auxin was demonstrated, because the majority of the downregulated genes were related to auxin. Additionally, a modest link with light was suggested, due to the upregulation of some transcription factors (TFs) putatively involved in light signaling (Mashiguchi et al., 2009). This molecular link was later confirmed in another microarray study on tomato (*Solanum lycopersicum*) root tissue treated for 48 h with *rac*-GR24 (Mayzlish-Gati et al., 2010). A substantial amount of the upregulated genes was involved in light harvesting, as part of the photosystems I and II. Finally, comparison of the transcriptome of *max2* and WT leaves via microarray analysis, both under normal conditions and after drought stress (Ha et al., 2014) revealed a role for MAX2 (and *rac*-GR24) in drought stress. Indeed, nearly 20% of the downregulated genes in *max2* under well-watered conditions were inducible by

drought, a percentage that increased even more under drought stress. Accordingly, treatment with *rac*-GR24 enhanced the drought tolerance of *Arabidopsis*, whereas mutants in the SL pathway were hypersensitive to drought, confirming the molecular data (Bu et al., 2014; Ha et al., 2014). A transcriptome dataset of *Arabidopsis* seeds treated for 24 h with karrikins (KARs) can potentially also be related to the *rac*-GR24 treatment, because of the presence of the (-)GR24 enantiomer (Nelson et al., 2010; Scaffidi et al., 2014). KAR treatment was shown to induce rather than repress transcripts and the upregulated genes to be enriched for light-responsive genes (Nelson et al., 2010). Thus, besides *rac*-GR24, also KAR influences light signaling in *Arabidopsis*.

Taking into account the diverse physiological effects that are attributed to *rac*-GR24 in the *Arabidopsis* root, we can assume that they are coordinated by various transcriptional networks, which are connected to D14 and/or to KAI2-based signaling. However, transcriptome-wide changes in the *Arabidopsis* root have not been investigated yet, creating a gap between the observable physiological responses of *rac*-GR24 treatment on the root system architecture and their molecular basis. Here we investigate the involvement of D14 and KAI2 on the influence of SLs on the lateral root density and present the *rac*-GR24-dependent transcriptome profile of the *Arabidopsis* WT and *max2* root tissue. Our data imply that both D14 and KAI2 via MAX2 control the influence of *rac*-GR24 on the lateral root density and that *rac*-GR24 treatment of roots does not influence one pathway, but modulates various pathways to affect the root system architecture.

3.2. Results and discussion

3.2.1. The *Arabidopsis* root shows physiological responses to *rac*-GR24 and to both pure enantiomers

The involvement of MAX2 in the impact of the commonly used *rac*-GR24 mixture on the LRD is well established, but neither the effect of the pure enantiomers nor the role of D14 or KAI2 has been investigated. Previously, both enantiomers have been shown to be effective in hypocotyl elongation inhibition in *Arabidopsis* and in germination of parasitic seeds, whereas only the (-)GR24 can alleviate primary dormancy for the *Arabidopsis* seed germination (Scaffidi et al., 2014). The two enantiomers also affect the suppression of shoot branching, although (+)GR24 is much more potent (Scaffidi et al., 2014). To distinguish between the impact on the LRD of the two different enantiomers, *Arabidopsis* seedlings were grown for 9 days in the presence of 1 µM purified (+)GR24, (-)GR24, or *rac*-GR24 and the LRD was analyzed (see Materials and Methods). In the WT, both enantiomers and *rac*-GR24 similarly reduced the LRD, by 37% for *rac*-GR24 and (+)GR24 and by 33% for (-)GR24 (Figure 1). These effects depended on MAX2, because no reduction was observed in the *max2* mutant.

In a next step, the involvement of the receptors D14 and KAI2 was analyzed. Treatment with *rac*-GR24 reduced the LRD of the *d14* mutant by 19%, which is significantly lower than the 37% decrease observed in WT plants (P <0.001), indicating that the *d14* mutant was partially insensitive to *rac*-GR24. The same was true for the effect of (+)GR24, because the decrease in LRD in *d14* was lower than that in the WT (14% vs 37%; P <0.001). However, when treated with (-)GR24, a reduction of 29% was obtained for *d14,* which did not significantly differ from that of the WT (33%) (Figure 1). Because *d14* was still partially sensitive to *rac*-GR24 and (+)GR24, an additional receptor is expected to be involved to provoke the effects on LRD. KAI2 could be a possible candidate. To investigate this, the *hyposensitive to light* (*htl-3*) mutant, which is a mutant *KAI2* allele in Col-0 background, was analyzed. To avoid further confusion regarding gene names, we will use 'kai2' when referring to the *htl-3* mutant. Indeed, *kai2* appeared partially insensitive to (+)GR24 with a reduction in LRD of 26% compared to

37% in the WT, but this difference turned out not to be significant (*P* = 0.06). Moreover, the *d14;kai2* double mutant displayed an insensitivity to (+)GR24 likewise as *max2*. Hence, to perceive the LRD-affecting (+)GR24 enantiomer, both KAI2 and D14 are involved. Regarding the effect of the (-)GR24 enantiomer, compared to the 33% decrease in LRD observed in the WT, still a 20% reduction occurs in the *kai2* mutant, showing that the *kai2* mutant remained partially sensitive to (-)GR24 (*P* <0.01). Thus, KAI2 might not be the sole receptor to perceive the (-) enantiomer to act on the LRD. When both receptor genes were mutated in the *d14;kai2* double mutant, *Arabidopsis* was insensitive to (-)GR24 and phenocopied the *max2* mutant, hinting at an additional involvement of D14 in the (-)GR24 perception. However, the observation that the *d14* mutant was fully sensitive to (-)GR24 is not in agreement with this hypothesis. More research is required to fully understand this phenotype. One hypothesis would be that both receptors are redundant, and that the relative importance of the functional receptor increases when the other receptor is non-functional. Indeed, biochemical research in pea (*Pisum sativum*) showed that RAMOSUS 3 (RMS3), the D14 ortholog, has a high affinity for (+)GR24, but a low affinity for (-)GR24, and that both enantiomers are hydrolyzed by RMS3 (de Saint Germain et al., 2016). This result is in agreement with previous data revealing that D14 in rice (*Oryza sativa*) selectively consumes (+)GR24 over (-)GR24, when *rac*-GR24 is supplied, but also that (-)GR24 is hydrolyzed over time (Nakamura et al., 2013). Also in *Arabidopsis*, D14 is capable of hydrolyzing both enantiomers, but with a much higher efficiency for (+)GR24, whereas KAI2 also hydrolyzes both enantiomers, but inversely has a much higher efficiency for (-)GR24 (Flematti et al., 2016). Hence, our experiments are in agreement with these biochemical data, but are not in line with earlier findings on the hypocotyl phenotype (Scaffidi et al., 2014). There, a complete separation between D14 and KAI2 as responsible for the perception of (+)GR24 and (-)GR24, respectively, was proposed. A difference in sensitivity between the two bioassays could be the underlying cause of this discrepancy.

Nevertheless, we can conclude that both enantiomers can cause a decrease in LRD and that both D14 and KAI2 receptors are involved in the perception of the natural (+)GR24 enantiomer and that KAI2 plays a main role in (-)GR24 perception, but also in (+)GR24 perception.

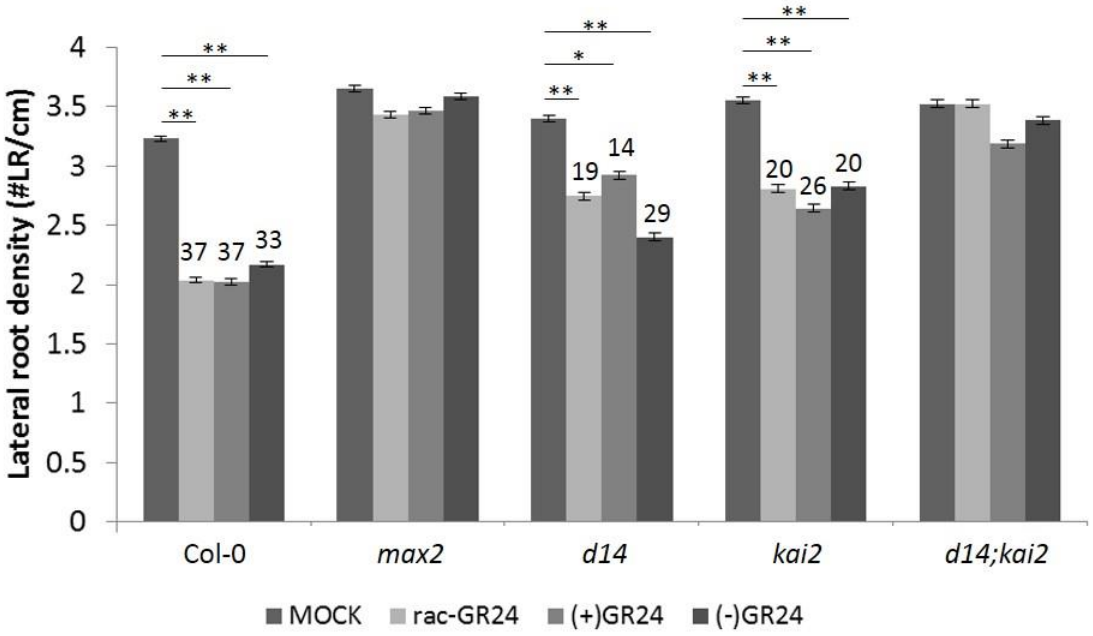

Figure 1. Effects of 1 µM *rac*-GR24, (+)GR24, and (-)GR24 on the LRD of WT, *d14, kai2*, *max2*, and the *d14;kai2* double mutant. Plants were grown for 9 days under continuous light conditions at 21°C on half-strength Murashige and Skoog medium with 1% [w/v] sucrose. Error bars represent the standard error (SE), based on three independent biological repeats (n > 20). * *P* <0.05; ** *P* <0.001, according to ANOVA mixed modeling; the treatments were compared to the MOCK condition for each genotype. Numbers above the bars represent the % reduction compared to the MOCK control for each genotype. *P*-values regarding the differences in LRD reductions between different genotypes and different treatments are indicated in the text, where appropriate.

The previous data showed the effects of exogenous *rac*-GR24 on the LRD. In agreement, *max2* mutants displayed an increased LRD. To get an initial idea of the importance of the two receptors in the SL-induced LRD reduction, we compared the phenotypes of the different mutants. The LRD of the *kai2* and the *d14;kai2* mutants was higher than that of the WT, similarly to the *max2* mutant (Table 1). In contrast, the LRD of *d14* was not significantly different from that of the WT (Table 1). This finding could indicate that endogenously, KAI2 plays an important role in the control of the LRD. However, staging of the LR primordia in the different receptor mutants should additionally be performed, as this will give a better insight into the lateral root forming potential of the mutants. Indeed, genetical studies have indicated that mainly the D14 signaling pathway via SMXL6, SMXL7 and SMXL8 could play

an important role in the regulation of LRD (Soundappan et al., 2015). The SL biosynthesis mutants *max3* and *max4* do not share the same strong phenotype as the *max2* mutant (Kapulnik et al., 2011a; Ruyter-Spira et al., 2011). This could indicate that the biosynthesis mutants still produce some residual SLs or the existence of a non-canonical pathway for SL synthesis (Chapter 1). Alternatively, it could be that the LRD is not regulated by SLs, but by currently unknown components that signal through KAI2, D14 and MAX2. These signals might be the same as those that control hypocotyl elongation and *Arabidopsis* seed germination. These two previously annotated SL phenotypes caused by unknown endogenous molecules signal through the MAX2 signaling cascade (Scaffidi et al., 2013; Waters et al. 2014; Conn and Nelson, 2016; Sun et al., 2016). Hence, the next challenge will be to discover the metabolites, produced independently from MAX3 and MAX4, but mimicked by (+)- and (-)GR24 that use the D14/KAI2/MAX2 signaling cascade (Sun et al., 2016).

In summary, the LRD is likely controlled through both the D14 and the KAI2 signaling pathway that perceive unknown molecules and/or SLs and exogenous *rac*-GR24 mimicks this effect.

Table 1. LRD of SL signaling mutants compared to WT plants. Plants were grown for 9 days under continuous light conditions at 21°C on half-strength Murashige and Skoog medium with 1% [w/v] sucrose. Student's *t* test was used to show statistical differences between the WT and a specific mutant.

Genotype	LRD ± SE	% Increase[a]	*P* value[b]
Col-0 (WT)	3.23 ± 0.02	-	-
d14	3.40 ± 0.03	5.19	(0,21)
kai2	3.55 ± 0.03	9.97	**
d14;kai2	3.52 ± 0.03	9.06	*
max2	3.65 ± 0.03	13.16	***

[a] Percentage increase in LRD relative to the WT.

[b] Student's *t* test compared to the WT; * *P value* <0.05; ** *P* value <0.01; *** *P* value <0.001; n.s., not significant

3.2.2. The root responds transcriptionally to *rac*-GR24 treatment in a manner different from that of the shoot

Previously, several SL markers have been delivered via a transcriptomic experiment on whole seedlings that are frequently used in SL and karrikin research (Mashiguchi et al., 2009; Nelson et al., 2011; Waters et al., 2012). In a first step to analyze the transcriptional responses especially in the root, we selected 10 published SL marker genes and examined whether they were also valid SL markers in root tissue. To this end, 5-day-old *Arabidopsis* seedlings were transferred to medium containing 1 µM *rac*-GR24 or to mock medium and after 0, 6, 24, and 48 h of treatment, the whole root was isolated for qRT-PCR analysis. Five of the 10 tested genes had a transcriptional response upon *rac*-GR24 treatment: *KAR-UP F-BOX 1* (*KUF1*; AT1G31350); a *DREB* TF (AT1G64380); *B-BOX DOMAIN PROTEIN 20* (*BBX20;* AT4G39070); *D14-LIKE 2* (*DLK2;* AT3G24420), and *MORE AXILLARY BRANCHING 4 (MAX4;*

AT4G32810) (Figure 2). The SL biosynthetic gene *MAX4* was subjected to negative feedback regulation in the root at all investigated time points, in agreement with previous results obtained on whole seedlings (Mashiguchi et al., 2009). The expression of *KUF1* and *BBX20* was already induced after 6 h of treatment and was maintained until at least 48 h oftreatment. The effect on *DLK2* expression was also induced from 6 h of treatment onward, but was only statistically different going from 24 h of treatment with *rac*-GR24. Finally, for the *DREB* TF an induction of expression was seen from 24 h of treatment onward, but was only statistically different after 48 h of treatment. Of the five genes that are not root SL markers, one gene, *RESPONSE REGULATOR 16* (*ARR16;* AT2G40670), was not expressed in root tissues, whereas the other four genes had no transcriptional response upon the *rac*-GR24 treatment in the root, namely *SMALL AUXIN UP RNA 63 (SAUR63;* AT1G29440); *SAUR15* (AT4G38850); AT3G60290, and *CYTOCHROME P450, FAMILY 707, SUBFAMILY A, POLYPEPTIDE 3* (*CYP707A3*) (Supplementary Figure 1).

These data indicate that the *Arabidopsis* root is responsive to transcriptional changes brought about by *rac*-GR24 treatment, although they also reveal that roots have a distinct response compared with whole seedlings. Some shoot marker genes were not transcriptionally modified in root tissues, indicative of the existence of shoot-specific SL markers. In contrast, also yet to be discovered root-specific SL markers may exist.

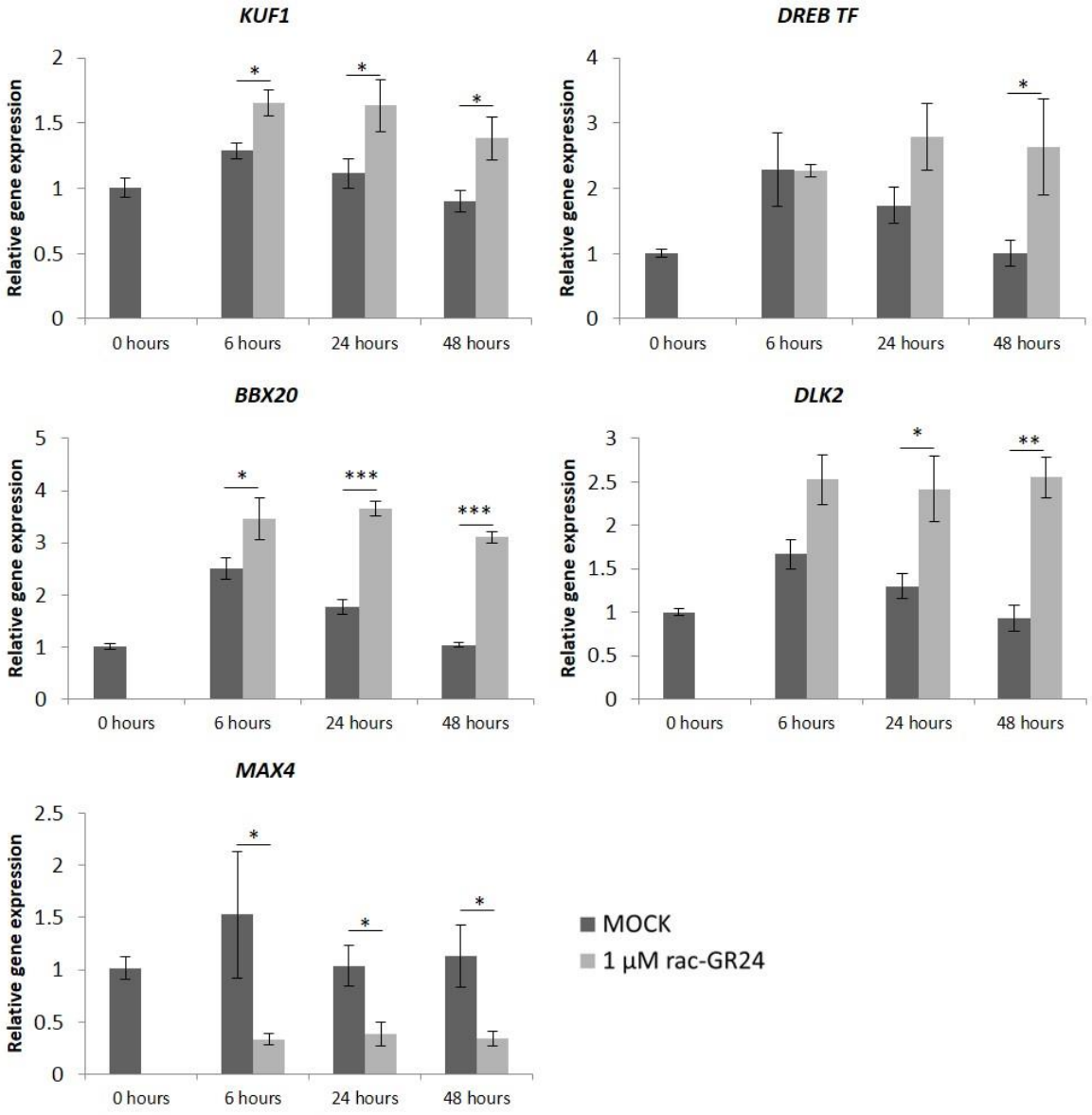

Figure 2. Effect of 1 µM *rac*-GR24 on the expression levels of various SL markers in the *Arabidopsis* root. Plants were grown for 5 days under continuous light conditions at 21°C on half-strength Murashige and Skoog medium with 1% [w/v] sucrose whereafter they were transferred to fresh medium containing 1 µM *rac*-GR24 or to MOCK medium. Root material was harvested 6 h, 24 h, and 48 h after transfer. Transcript levels were measured in root tissues by qRT-PCR and normalized to *ACTIN2*. Error bars represent the standard error (SE), based on three independent biological repeats, approximately 100 seedlings were pooled for each sample. An ANOVA-mixed model was used for the statistical analysis. * P <0.05; ** P <0.01; *** P <0.001. For each timepoint, statistical differences between the MOCK and the treated samples are depicted.

3.2.3. *rac*-GR24 has no high impact on lateral root marker gene expression

Next, we wanted to identify additional genes in the root for which the expression is influenced by *rac*-GR24 treatment. Previously (Chapter 2), we showed that *rac*-GR24 affects the LR development at two levels, with a minor and major effect on LR priming and LR outgrowth, respectively. To discover *rac*-GR24-induced LR markers, we made an educated guess and used a dataset containing marker genes specific for different developmental stages during LR development (Supplementary Table 1) (data published by Voβ et al. [2015] and further analyzed by Boris Parizot). To obtain synchronized root material for this microarray analysis, LRs had been induced by a gravitropical stimulant and root tissue had been harvested after several time points (Ditengou et al., 2008; Voß et al., 2015). Genes with a clear induction at a specific time point during development were considered as potential LR marker genes (Supplementary Table 1). First, from the original list of 178 genes, the expression of the 106 most clear markers was confirmed by qRT-PCR. These genes were selected based on some criteria such as clear induction of expression, without multiple or broad peaks in the expression pattern during LR development. We used RNA derived from synchronized root material by means of the lateral root inducing system (Himanen et al., 2002). To this end, seedlings were first grown for 72 h on NPA-containing medium to prevent LR development and then transferred to NAA-containing medium to induce synchronized LR development along the primary root. Harvest at specific time points after transfer to auxin-containing medium (i.e. after 0, 2, 6, 12, 18, 24, or 48 h) allows enrichment of the LR material at specific developmental stages. By using this material for qRT-PCR, we could validate 46 of the 106 marker genes in two independent repeats (Supplementary Table 2). Finally, the expression of these 46 genes was tested for the root response to the *rac*-GR24 treatment. Five-day-old seedlings were transferred to fresh medium containing 1 µM *rac*-GR24 or to MOCK medium and were treated for 6, 24, or 48 h and material of the whole root was harvested. Only one single gene, *AT2G22590*, encoding a UDP-glycosyltransferase superfamily protein was responsive to the *rac*-GR24 treatment (Figure 3). The glycosyltransferase was also a transcriptional target of the MYB12 TF, one of the key regulators of flavonol biosynthesis in *Arabidopsis* (Stracke et al., 2007). The fact that this gene, and

thus probably downstream flavonol biosynthesis, was upregulated is in agreement with the investigated effect of the *rac*-GR24 treatment on the root proteome (Walton et al., 2016). Multiple proteins involved in flavonol biosynthesis have demonstrated to accumulate upon treatment wih *rac*-GR24 in a MAX2-dependent manner and this effect has been implied to be caused by an impact on the transcript level (Walton et al., 2016). However, the *rac*-GR24-responsive gene that we identified is not part of that dataset.

In summary, *rac*-GR24 does not seem to affect greatly the direct transcriptional regulation of the developmental LR program, although the clear physiological effects on the root system architecture. As such, a genome-wide view on the transcriptomic changes is required to identify more *rac*-GR24 responsive transcripts in the root.

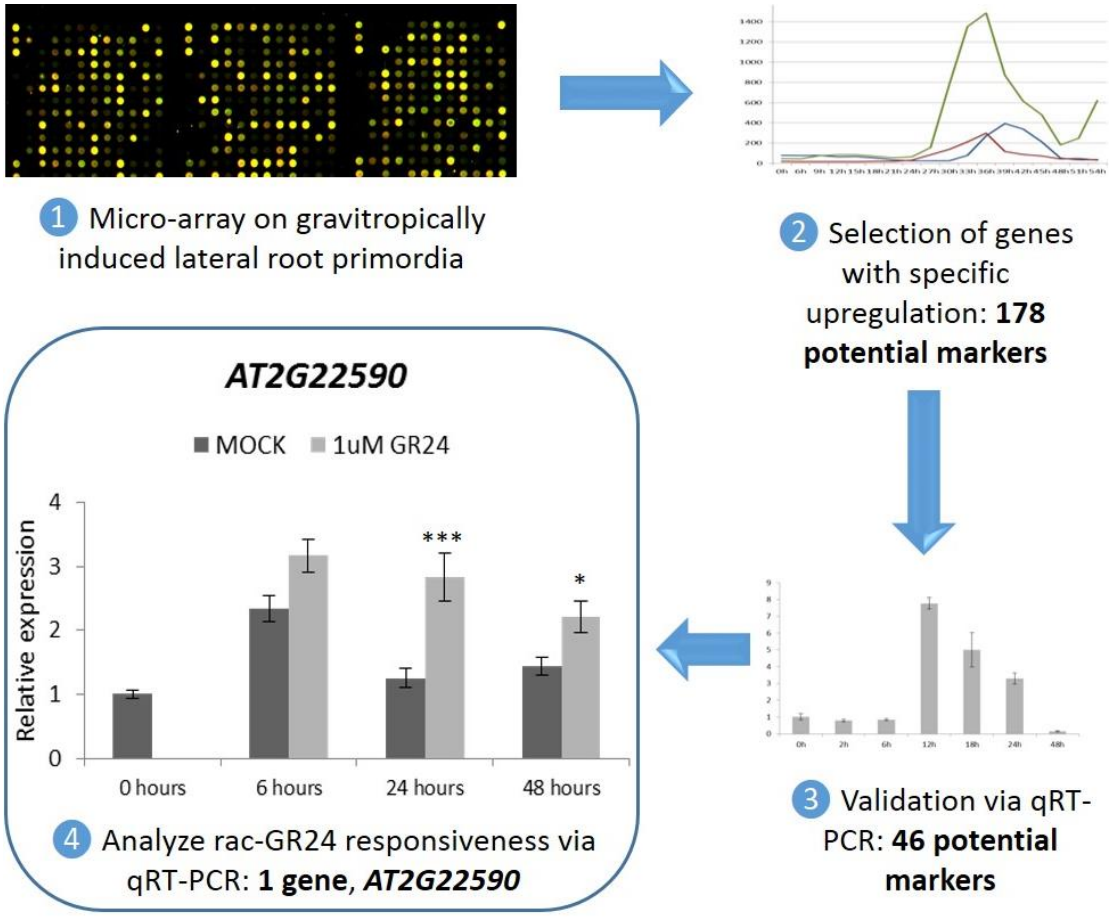

Figure 3. Identification of a *rac*-GR24-responsive potential root marker gene. A microarray analysis was done on gravitropically induced LR primordia at different stages of development (1). From this dataset, 178 genes with an upregulated expression at one specific time point were selected as potential LR markers (2). From this subset, 46 genes could be validated via qRT-PCR with synchronized LR material (for details, see text) (3). One single potential marker gene appeared to be responsive to *rac*-GR24 treatment (4). Plants were grown for 5 days under continuous light conditions at 21°C on half-strength Murashige and Skoog medium with 1% [w/v] sucrose whereafter they were transferred to fresh medium containing 1 µM *rac*-GR24 or to MOCK medium. Root material was harvested 6 h, 24 h, and 48 h after transfer. Transcript levels were measured in root tissues by qRT-PCR and normalized to *ACTIN2*. Error bars represent the standard error (SE), based on three independent biological repeats. An ANOVA-mixed model was used for the statistical analysis. * P <0.05; *** P <0.001.

3.2.4. An RNAseq analysis of transcriptome-wide *rac*-GR24 effects in the *Arabidopsis* root

Previous results indicate that additional molecular data are needed to thoroughly understand the effects of *rac*-GR24 on the root system architecture. To obtain a profound insight into the transcriptome-wide changes, we carried out an RNAseq experiment on the whole root of *Arabidopsis,* of plants treated with *rac*-GR24. At the time when the RNAseq was initiated, very few to no molecular data was available on the effect of SLs on root development. As such, we first wanted to obtain a general and complete view of the transcriptomic changes that are brought about by *rac*-GR24 treatment. Because SLs are known to affect the root architecture at different developmental processes such as LR development, primary root growth and root hair elongation (Chapter 2; Kapulnik et al., 2011; Ruyter-Spira et al., 2011), we decided to analyze the effect of *rac*-GR24 on the complete root. Additionally, the role of D14 in SL signaling was not clear at that time, the KAI2 signaling pathway via MAX2 was still unknown and the different activity of the two enantiomers of *rac*-GR24 were still to be discovered. As such, we decided to include only the WT and the *max2* mutant for analysis, and used *rac*-GR24 instead of the pure enantiomers. To this end, seedlings of both Col-0 and *max2* were grown for 5 days, whereafter they were transferred to fresh medium supplemented with 1 µM *rac*-GR24 or to MOCK medium for 6 h. In comparison with other plant hormones, this time frame could be considered as fairly late, because for many hormones, the first transcriptional events happen within several minutes after treatment as illustrated with the jasmonate responses (Pauwels et al., 2010). The signaling cascade of SLs is not initiated so rapidly. Indeed, the degradation of the direct target proteins SMXL6, SMXL7, and SMXL8 occurs only 30 minutes to 1 hour after treatment (Zhao et al., 2013; Soundappan et al., 2015; Wang et al., 2015). Thus, harvesting after 6 h of treatment will ensure picking up transcriptional responses, based on the effects of *rac*-GR24 on the expression of previously published SL marker genes (Figure 2). Although in general the transcriptional responses of the analyzed markers was stronger after 24 h compared to 6 h of treatment, we decided to select the

earliest possible timepoint in order to minimize secondary effects. To enrich for statistically and biologicaly significant differentially expressed genes, we applied as selection criteria a corrected *P*-value < 0.05 and a fold change cutoff of 1.2. Treatment with *rac*-GR24 is known for its relative weak effect on expression levels (Mashiguchi et al., 2009). For our analyses, selection of this fold change cut-off was justified by the confirmation of genes that are known to be regulated by *rac*-GR24 in the root, such as the flavonol biosynthesis genes and genes of the SMXL family (See below) (Walton et al., 2016).

For Col-0 treated with *rac*-GR24, 146 differentially expressed genes were obtained, 63 induced and 83 repressed genes (Supplementary dataset 1), whereas for the *max2* mutant, 107 genes were differentially expressed, of which 87 were upregulated and 20 were downregulated (Supplementary dataset 2). The fact that there are differentially expressed genes in the *max2* mutant after *rac*-GR24 treatment is unexpected, and will be discussed later on. Finally, comparison of *max2* to the WT grown under normal growth conditions resulted in 2,011 differentially expressed genes, of which 882 were upregulated and 1,129 were downregulated (Supplementary dataset 3). The latter dataset will be referred to as the *max2*-MOCK dataset. As extra information, the datasets with a FC cutoff of 2 is also made available via supplementary data: WT treated with *rac*-GR24 (Supplementary Dataset 4), *max2* treated with *rac*-GR24 (Supplementary Dataset 5) and the max2-MOCK dataset (Supplementary Dataset 6). Clearly, the *max2*-MOCK dataset contains much more genes compared to the *rac*-GR24 dataset. This is not completely unexpected, because *max2* is a mutant and has a distinct phenotype compared to the WT (Shen et al., 2007), as such many differentially expressed genes could be secondary effects, compared to the short time *rac*-GR24-treatment. In part, it could also be that *rac*-GR24, compared to natural SLs or endogenous molecules that signal via D14 and KAI2, is not the most potent SL mimick to induce changes in the transcriptome.

Clearly, a lot of genes had a perturbed expression, requiring an in-depth analysis of the content of these datasets. First, the overlap with published SL-related datasets was analyzed.

Compared to a dataset of *rac*-GR24-treated two-week-old *max1* seedlings, 3 genes were also present in the dataset of the WT roots treated with *rac*-GR24 (*CYCLING DOF FACTOR 4* [*AT2G34140*], *SMXL2* and *SMXL7*) (Figure 4A) (Mashiguchi et al., 2009). A dataset of KAR-treated seeds had 4 genes in common with the WT roots treated with *rac*-GR24 (*URIDINE DIPHOSPHATE GLYCOSYLTRANSFERASE 74E2* [*AT1G05680*], *RAFFINOSE SYNTHASE 2* [*AT3G57520*], a *Leucine-rich repeat family protein* [*AT1G33590*] and a receptor-like protein kinase-related family protein [AT5G48540]) (Figure 4B) (Nelson et al., 2010). Finally, a microarray analysis comparing 24-day-old shoot tissue of WT and max2 displayed 230 genes in common with the max2-MOCK dataset of root tissue. As such, based on the relatively small overlaps, it could be that the response on the transcriptome is different depending on the timing and the type of tissue that is assayed.

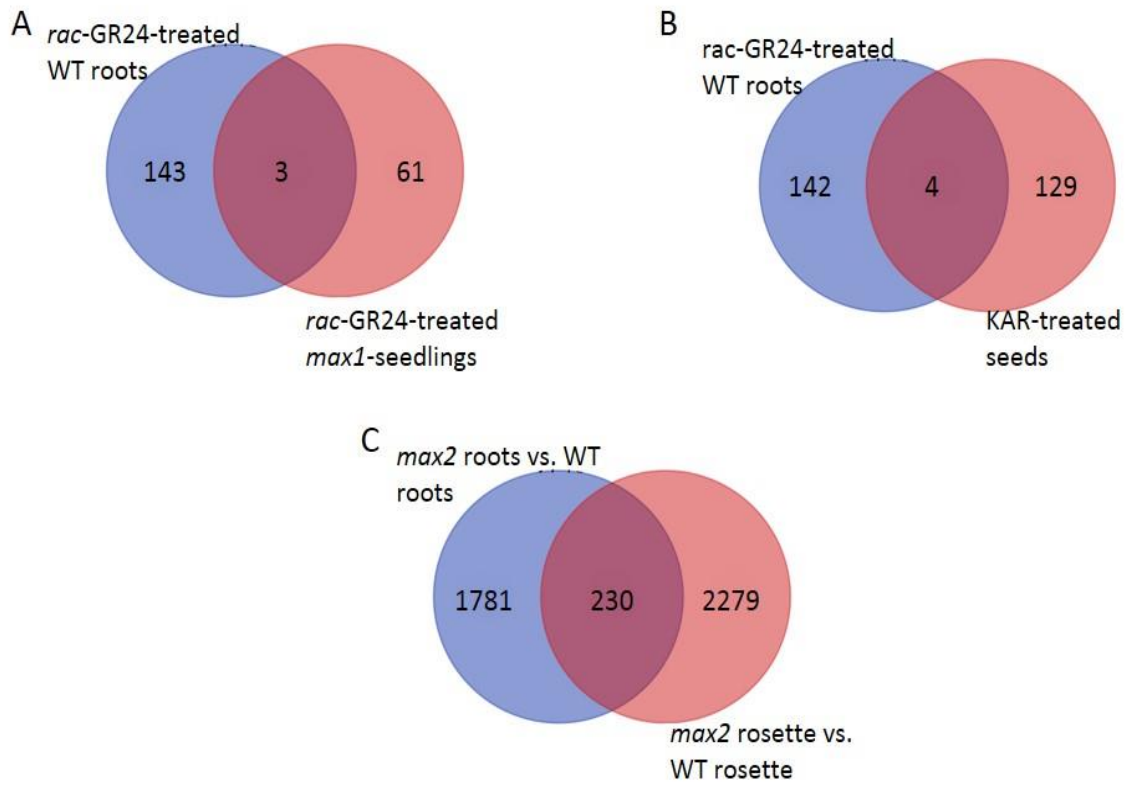

Figure 4. Overlap of datasets with published SL-related datasets. (A) Overlap of the *rac*-GR24-treated WT root dataset with a dataset of *max1*-seedlings treated with *rac*-GR24 (Mashiguchi et al., 2009). **(B)** Overlap of the *rac*-GR24-treated WT root dataset with a dataset of KAR-treated seeds (Nelson et al., 2010). **(C)** Overlap of the *max2*-roots compared to WT root tissue

under mock conditions with a dataset comparing the *max2* rosette with WT rosette (Ha et al., 2014). Genes were selected based on a FC cutoff of 1.2 and *P*-value < 0.05.

Various processes affected by *rac*-GR24 treatment in Col-0 are also affected by a mutation in *max2* under normal growth conditions

To interpret and simultatenously get a clear visualization of the content of the datasets, we used the MapMan software that allows the organization and display of genes onto schemes of metabolic pathways or biological processes (Thimm et al., 2004). Figure 5A gives a general overview of the transcriptomic changes brought about by *rac*-GR24 treatment of WT root tissue, whereas Figure 5B summarizes this general overview for the *max2* root grown under normal conditions compared to the WT (the *max2*-MOCK dataset). The biologically most relevant processes are those that are both affected by the *rac*-GR24 treatment in the WT as well as differentially expressed in *max2* under normal conditions. Therefore, we first focused on these common processes.

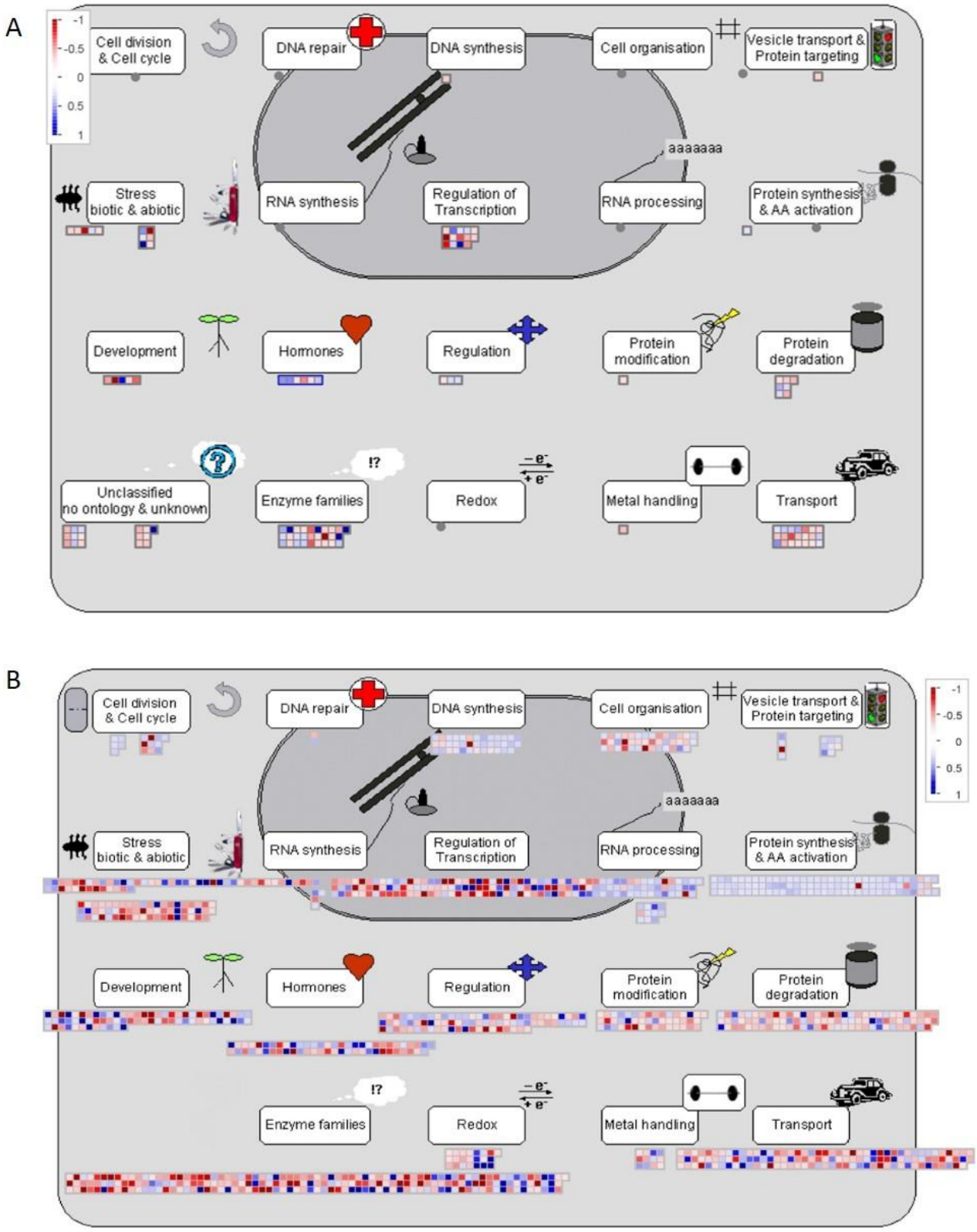

Figure 5. General overview of the transcriptomic changes in WT by the *rac*-GR24 treatment in root tissue, and in the *max2* mutant root compared to the WT grown under normal growth conditions. **(A)** MapMan-generated overview that summarizes the cellular processes that were perturbed by *rac*-GR24 in the WT and (B) in the *max2* mutant under normal

growth conditions compared to the WT. Each square represents one gene. Color coding according to the LOG2 scale: blue, upregulated; red, downregulated. Data were manually curated. For the gene identity, see Supplementary Table 3 (for figure 5A) and Supplementary Table 4 (for Figure 5B).

Several transcriptional regulators appeared to be differentially expressed after *rac*-GR24 treatment (Figure 5; Supplementary Table 3, '*regulation of transcription'*). When the overlap with the *max2*-MOCK dataset was taken in account, only five transcriptional regulators were retained (Table 2). Besides this selection, also a full list of overlapping genes between the *max2*-MOCK dataset and the WT treated with *rac*-GR24 is available via Supplementary Table 5. From the transcriptional regulators, the TF *TARGET OF MONOPTEROS 5 LIKE1* (*TMO5L1*) showed the strongest downregulation by *rac*-GR24 and was upregulated in the *max2* root grown under normal growth conditions. Interestingly, also its closest homolog *TMO5* had the same pattern, albeit slightly weaker. The role of these TFs in the regulation of the SL physiology will be covered in Chapter 4. Besides these two TFs, also two members of the *SUPPRESSOR OF MAX2* (*SMAX*) family were upregulated by *rac*-GR24 and downregulated in the *max2*-MOCK dataset: *SMAX1 LIKE 2* (*SMXL2*) and *SMXL7* (Table 4). Additionally, also SMAX1 was downregulated in the *max2*-MOCK dataset (Table 3, '*regulation of transcription*'). These three genes, *SMAX1*, *SMXL2,* and *SMXL7*, are involved in downstream SL/KAR signaling (Stanga et al., 2013, 2016; Soundappan et al., 2015; Wang et al., 2015). As under normal circumstances SMXL7, and probably also SMAX1 and SMXL2, is degraded by MAX2 upon SL signaling, downregulation of these genes in *max2* suggests that the SMAX proteins negatively regulate their own expression (Soundappan et al., 2015; Wang et al., 2015). In agreement, the expression of *SMXL2* and *SMXL7*, but not of *SMAX1,* was induced by *rac*-GR24 in the WT (Supplementary dataset 1; Table 4). As validation, the expression of *SMAX1*, *SMXL2*, and *SMXL7* was reconfirmed by qRT-PCR. After 5 days of growth, seedlings were transferred to 1 µM *rac*-GR24-containing medium or to mock medium and the roots were harvested for analysis at different time points. All three genes were induced after 6 h of *rac*-GR24 treatment and, compared to the mock treatment, they were upregulated until 48 h after treatment, the last

investigated time point (Figure 6). For *SMXL2* and *SMXL7*, *GUS* reporter lines were constructed and confirmed the induction of transcription after *rac*-GR24 treatment (Supplementary Figures 2 and 3; LX. Jiang, unpublished data). In other plant hormonal pathways, in which ubiquitin-dependent proteasomal degradation plays an essential role, as during auxin and jasmonate signaling, the genes encoding the repressor proteins are often transcriptionally self-regulated as part of a feedback loop (Chini et al., 2007; Kepinski and Leyser, 2005).

Table 2. Transcriptional regulators shared between the Col-0 *rac*-GR24-treated and the *max2*-MOCK datasets

AGI code	FDR (WT, *rac*-GR24)	FC (WT, *rac*-GR24)	FDR (mock, *max2*)	FC (mock, *max2*)	Description	aver. counts (WT MOCK)	aver. counts (WT *rac*-GR24)	aver. counts (*max2* MOCK)
AT1G68810	6.85E-27	0.4871788	6.65492E-06	1.3089518	TMO5L1	377	179	563
AT3G25710	0.0234167	0.7939342	0.001548477	1.24559262	TMO5	334	259	480
AT1G66140	0.0308496	0.8080716	6.75539E-10	1.42480574	zinc finger protein 4	314	248	513
AT4G30350	0.0017711	1.2056147	1.07106E-62	0.45298929	SMXL2	781	917	405
AT2G29970	1.439E-12	1.4473004	2.06843E-08	0.73860528	SMXL7	540	761	457

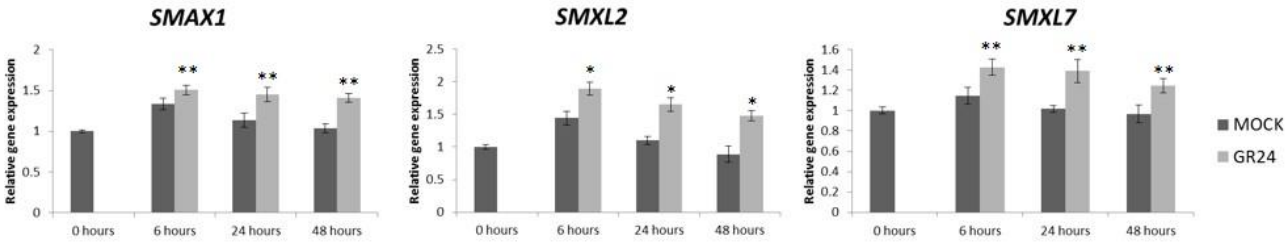

Figure 6. Relative transcriptional levels of SMXL1, SMXL2, and SMXL7 in the presence of *rac*-GR24 at different time points.
Plants were grown for 5 days under continuous light conditions at 21°C on half-strength Murashige and Skoog medium with 1% [w/v] sucrose whereafter they were transferred to fresh medium containing 1 µM *rac*-GR24 or to MOCK medium. Root material was harvested 6 h, 24 h, and 48 h after transfer. Transcript levels were measured in root tissues by qRT-PCR and normalized to *ACTIN2*. Error bars represent the standard error (SE), based on three independent biological repeats. An ANOVA-mixed model was used for the statistical analysis. * P <0.01; ** P <0.001; comparisons of MOCK and treatment within each timepoint are depicted.

Also various hormonal pathways were perturbed, but only a few by the *rac*-GR24 treatment itself (Figure 5A; Supplementary Table 3, '*hormones*'), whereas quite a large group of genes related to phytohormone biosynthesis and signaling were differentially expressed in the *max2* mutant compared to the WT (Figure 5B; Supplementary Table 4, '*hormones*'). Although only a few genes involved in auxin transport and signaling were affected by *rac*-GR24, nearly one third (18 of 57) of the 'hormone' gene cluster that is differentially expressed in *max2* was related to auxin (Table 3, '*hormones*'). The majority of these auxin-related genes was upregulated, pointing to an increased auxin flux and signaling in *max2*. Indeed, the intimate crosstalk between SLs (*rac*-GR24) and auxin has been reported (Foo et al., 2005; Bennett et al., 2006; Brewer et al., 2009; Ferguson and Beveridge 2009; Hayward et al., 2009; Crawford et al., 2010; Koltai et al., 2010; Shinohara et al., 2013; Pandya-Kumar et al., 2014;). However, this enhanced auxin flux seems also to be balanced by reduction of the available free or active auxin. METHYL ESTERASE 17 (MES17) was downregulated in *max2*, which is known to methylate IAA to an inactive form, whereas NITRILASE1 (NIT1), which catalyzes the terminal activation step in indole-acetic acid (IAA) biosynthesis, was downregulated and genes that affect auxin homeostasis were upregulated (AT1G05680 and AT4G27260) (Supplementary Table 4, '*hormones*'). Nevertheless, the fact that only a few genes related to auxin were differentially expressed by *rac*-GR24 in the WT is in contrast with previous results (Mashiguchi et al., 2009), in which via microarray analysis of whole seedlings a vast amount of the by *rac*-GR24 differentially expressed genes were found to be related to auxin. This discrepancy might be due to the use of whole plantlets instead of root tissues and, as already suggested, the *rac*-GR24 effects on auxin dynamics might be less pronounced or slower in root tissues than in the shoot (Shinohara et al., 2013). Besides auxin, also a minor link with brassinosteroids, salicylic acid, and ethylene were detected after treatment of the WT with *rac*-GR24, each represented by one single gene (Table 2, '*hormones*'). In contrast, in the *max2* mutant, the levels and signaling of abscisic acid, cytokinin, and gibberellin were both positively and negatively affected, pointing to a complex hormonal network, as already demonstrated (Supplementary Table 4, 'hormones') (Shen et al., 2012). For crosstalk with SLs in the root, mainly auxin, but more recently, also cytokinins have been

identified (see Chapter 2). However, this interaction is not fully supported by transcriptional effects, probably because the effects on the crosstalk of *rac*-GR24 with cytokinins have been demonstrated to occur locally in the upper, and not in the younger, part of the root (see Chapter 2). As such, transcriptomic changes might not be visible when tissue samples of the whole root are considered.

A substantial amount of genes involved in transport activities and metabolic processes were also differentially regulated (Figure 5; Supplementary Table 2 and 3, '*transport*'). Regarding transport, strikingly six genes encoding for water channels were downregulated by *rac*-GR24 in the roots: *PLASMA MEMBRANE INTRINSIC PROTEIN 1* (*PIP1*), *PIP1a*, *PIP2B*, *RESPONSE TO DESSICATION 28* (*RD28*), *GAMMA TONOPLAST INTRINSIC PROTEIN* (*GAMMA-TIP*), and *TIP2;2*. Downregulation of aquaporins helps the plant to cope with drought or salt stress (Aharon et al., 2013). This result fits with previous studies that showed that *rac*-GR24 has a positive effect on drought tolerance of plants, although the effect on drought tolerance depended on the shoot and not the root (Bu et al., 2014; Ha et al., 2014). So, although root-related traits are not affected, the transcriptome of the root seemingly still responds to *rac*-GR24 to protect the plant from drought and salinity stress. Inversly and accordingly, in the *max2* root grown under normal conditions, various aquaporin-coding genes were upregulated compared to the WT (Supplementary Table 4, '*transport*'). Also numerous other genes, known to be upregulated by salt and drought, were downregulated in *max2* (Supplementary Table 4, '*abiotic stress'*).

Next, we considered the metabolic processes that are represented in the dataset of WT roots treated with *rac*-GR24 (Figure 7; Table 5) and in the *max2*-MOCK dataset (Figure 8; Table 6). Light perception and signaling are an essential part of plant survival and have already been linked to MAX2 and SLs (see Chapter 1). Also the results from these datasets support this role for MAX2 (and *rac*-GR24). Various genes involved in the light reactions of light-harvesting complex II were highly upregulated by the *rac*-GR24 treatment: *LIGHT HARVESTING COMPLEX B1.1* (*LHCB1.1; AT1G29920*), *LHCB1.2*, *LHCB1.4* (*AT2G34430*), and *LHCB2.2* (Figure 7; Table 5). Also in tomato, *rac*-GR24 and light-harvesting gene expression have been positively correlated in the root as well as in the shoot

(Mayzlish-Gati et al., 2012). However, genes involved in the light reactions were upregulated in the *max2* mutant as well (Figure 8; Table 6, '*Light reactions*'). Genes of which the expression is positively regulated by *rac*-GR24, are not expected to be upregulated in the *max2* signaling mutant under normal growth conditions. Of course, it can be that the expression of these genes is upregulated because of feedback mechanisms or because of secondary effects taking place in the *max2*-mutant. To investigate this, we determined the expression levels via qRT-PCR in the WT and the *max2* mutant, but could not confirm an enhanced expression of *LHCB1.4* and *LHCB1.1* (Supplementary Figure 4). However, when looking at the average counts for these genes in the RNAseq (Supplementary Tables 3 and 4) they are very lowly expressed under normal conditions, and are slightly upregulated by both *rac*-GR24 and the *max2* mutation. This leads to very high fold changes, but are maybe not very biologically relevant. Furthermore, and in agreement with the hyposensitivity of *max2* to light, several genes related to light perception and signaling were downregulated in the *max2* mutant, among which the key TF *ELONGATED HYPOCOTYL 5* (*HY5*) and its homolog *HY5-HOMOLOG* (*HYH*), whereas the negative regulator *CONSTITUTIVE PHOTOMORPHOGENIC 2* (*COP2*) was upregulated in *max2* (see Table 3, '*regulation/signaling*').

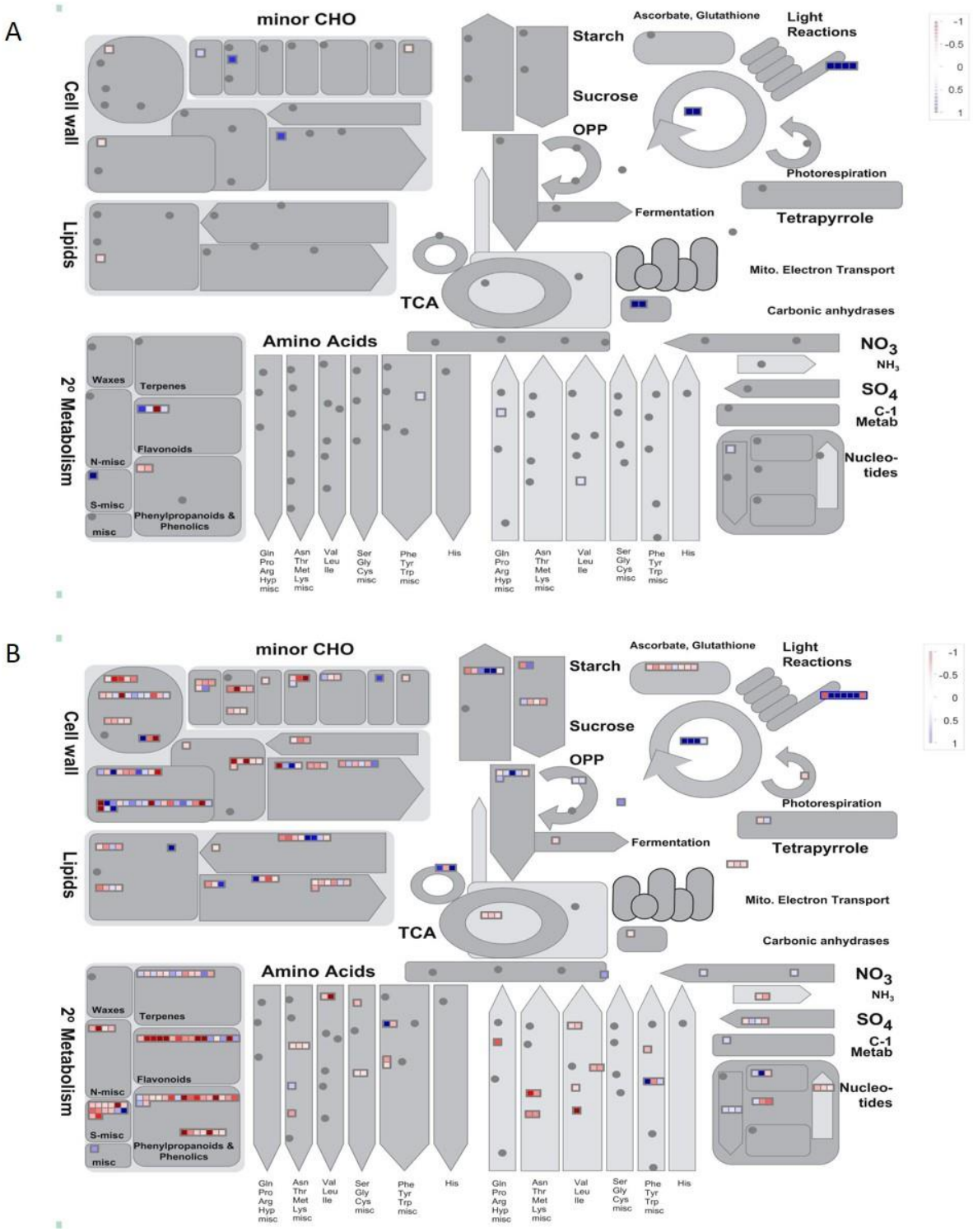

Figure 7. Overview of the transcriptomic changes in the WT by *rac*-GR24 treatment in the root related to cell metabolism, and in the *max2* mutant root compared to the WT grown under normal growth conditions. **(A)** MapMan-generated overview that summarizes the metabolic pathways that were perturbed by the *rac*-GR24 treatment in the WT. (B) MapMan-generated overview of the metabolic pathways that were perturbed in the max2 mutant compared to the WT. Each square

represents one gene. Color coding according to the LOG2 scale: blue, upregulated; red, downregulated. Data were manually curated. For the gene identity, see Supplementary Table 6 and 7.

When the overview of the changes in the general metabolism of *max2* is considered, an obvious negative effect on the secondary metabolism could be observed (Figure 7B; Supplementary Table 7, *'secondary metabolism'*). The majority of the genes involved in the phenylpropanoid pathway to flavonoid/lignin production in the dataset were downregulated in *max2*. A complementary effect was also present in the *rac*-GR24-treated WT dataset: several genes in flavonoid production were upregulated after treatment with *rac*-GR24 (Figure 7B, Supplementary Table 6, *'secondary metabolism'*). Two genes involved in flavonoid biosynthesis were upregulated: *TRANSPARANT TESTA 7* (*TT7*) and the *UDP-GLYCOSYLTRANSFERASE SUPERFAMILY PROTEIN* (*AT2G22590)*, which had previously been identified as a *rac*-GR24-responsive gene from the LR marker dataset (Figure 3). Accordingly, both genes were strongly downregulated in the *max2* roots grown under normal conditions (Figure 7B; Supplementary Table 7, '*secondary metabolism*'). One flavonoid-related gene did not follow this pattern: the *AT1G25460* gene that was downregulated after the *rac*-GR24 treatment. However, the possible involvement of this gene in flavonoid biosynthesis might derive from weak structural similarities with a dihydroflavonol-4-reductase and not from biochemical evidence (Zhou et al. 2010). Hence, because its actual functionality in flavonoid biosynthesis is not yet proven and also, because its gene expression profile in the RNAseq dataset that does not fit that of the other genes involved in flavonoid biosynthesis, we suggest that this gene does probablly not function in this process. In addition, the average counts of this gene in the RNAseq are very low compared to the other genes. These data are in agreement with the increased flavonoid production in the root after treatment with *rac*-GR24 found via via proteomic and metabolomic analyses (Walton et al., 2016), whereas in *max2* it was lower than that of the WT, in line with protein and transcript levels of flavonoid biosynthetic genes (Walton et al., 2016). These effects in the *max2* mutant were validated and checked whether they were the result of signaling via the D14- and/or the KAI2-

mediated pathway by means of qRT-PCR on root tissues of WT, *max2*, *d14*, *kai2,* and the *d14;kai2* double mutant grown for 5 days (Figure 8). As such, in analogy to their transcriptional repression in the *max2* mutant background, the expression levels of these genes could give a first impression by which receptor their expression might be regulated. For the majority of the tested genes, a similar pattern could be observed: a downregulation in the *max2* and in the *kai2* mutant background as well as in the double *d14*;*kai2* mutant (Figure 8A-8D). However, the expression of these genes was not affected by a mutation in *D14*. Only for *PHENYLALANINE AMMONIA-LYASE1* (*PAL1*) and *4-COUMARATE-CoA LIGASE3* (*4CL3*), the expression was not (statistically significantly) reduced in the *kai2* single mutant, but only in the *d14*;*kai2* double mutant and in *max2* (Figures 8E and 8F). These results indicate that the negative impact on the secondary metabolism in *max2* could be mainly the result of distorted signaling via the KAI2 receptor, because a mutation in this receptor only gave a similar effect. Although the expression of these genes in the single *d14* mutant was unaffected, a slight role for the D14 receptor in this process cannot be ruled out, given that the *PAL1* and *4CL3* expression was affected in the *d14;kai2* double mutant and not in the *kai2* mutant, implying some redundancy between these two receptors, with a potential major role for KAI2 and a minor role for D14. Certainly, analysis of gene expression in the different mutants treated with *rac*-GR24 or pure enantiomers will give stronger clues to which signaling pathway(s) is involved. Nevertheless, this observation broadly fits with a previous demonstration that both pure enantiomers of *rac*-GR24 were capable of enhancing the flavonoid levels in the roots of *Arabidopsis* (Walton et al., 2016). Although a strict separation between the perception of (–)GR24 and (+)GR24 by KAI2 and D14 had been suggested previously, we found that, at least in regulating the LRD phenotype, KAI2 could perceive both pure enantiomers (Figure 1). This fact, together with the redundancy between D14 and KAI2, might be reason that both pure enantiomers are (equally) capable of positively affecting the flavonoid content in *Arabidopsis* roots (Walton et al., 2016).

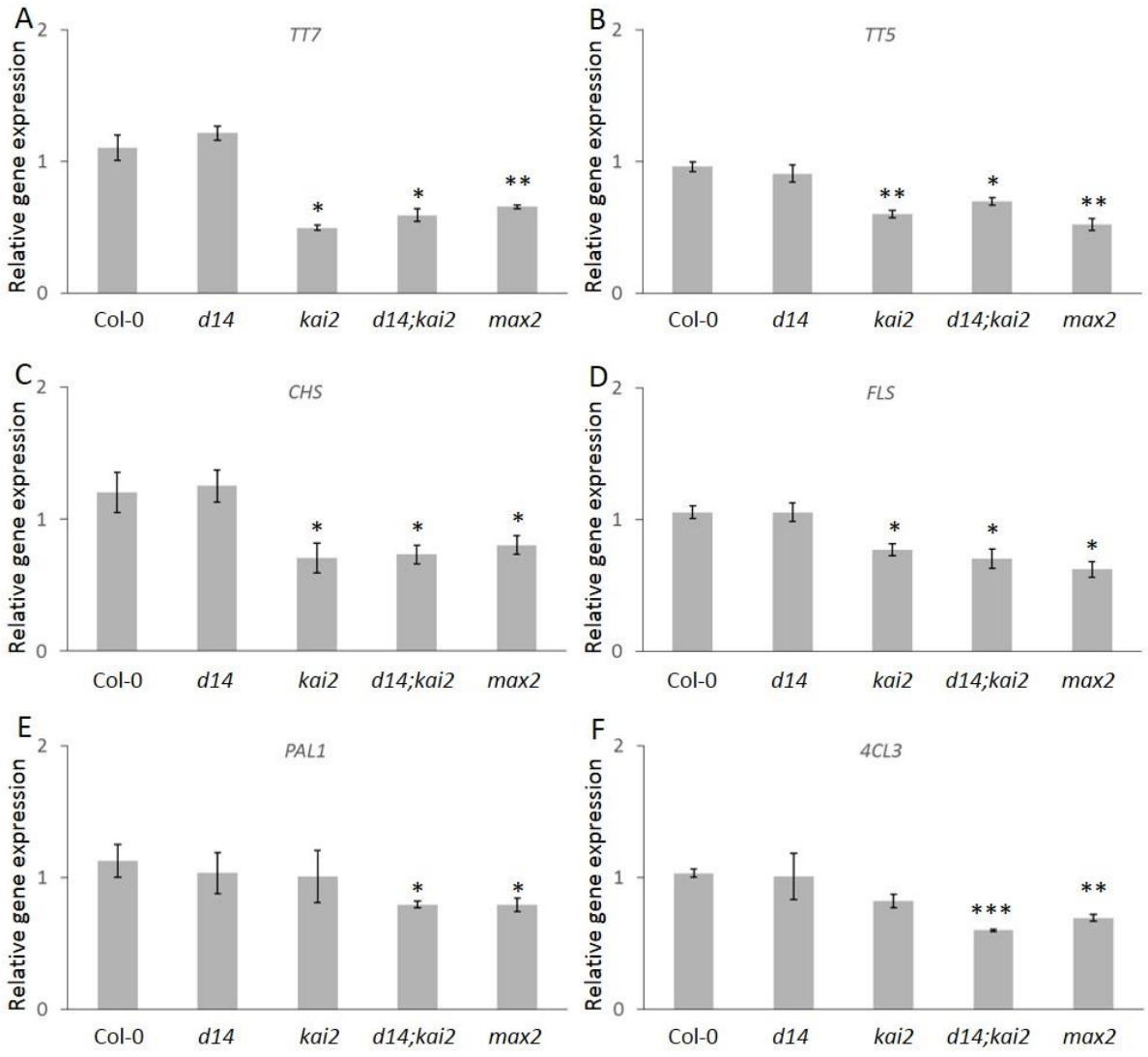

Figure 9. Expression in the root of several genes involved in flavonoid biosynthesis in the different SL signaling mutants. Plants of Col-0, *d14*, *kai2, d14;kai2,* and *max2* were grown under continuous light conditions at 21°C on nylon meshes placed on half-strength Murashige and Skoog medium with 1% [w/v] sucrose. Root tissue was harvested after 5 days of growth. Transcript levels were measured by qRT-PCR and normalized to *ACTIN2*. Error bars represent the standard error (SE), based on three independent biological repeats. A one-way ANOVA was used for the statistical analysis. * P <0.05; ** P <0.01; *** P <0.001; the expression levels in the different mutants were compared to that of the WT.

In conclusion, the the *MAX2* gene mutation caused a great change in the transcriptome of the *Arabidopsis* root, in contrast to a rather slight effect of the *rac*-GR24 treatment on WT roots. Generally, various common pathways seemed to be affected, both by the *rac*-GR24 treatment and by a mutation

in *max2*, such as hormonal crosstalk, water housekeeping (response to drought and salinity), photosynthesis, and secondary metabolism. Not the distortion of one specific pathway is seemingly responsible for the physiological effects on the root system architecture. Instead, *rac*-GR24 and MAX2 signaling might influence many different physiological processes and, as such, regulate complex traits.

The *max2* mutant seems responsive to *rac*-GR24

Despite already a few microarray analyses related to SL actions, none checked changes in the *max2* transcriptome upon the *rac*-GR24 treatment, because this mutant is presumed to be insensitive to *rac*-GR24. However, based on the RNAseq results, the *max2* mutant seemed not at all completely insensitive to *rac*-GR24 at the transcriptional level, because 107 genes were differentially expressed (Supplementary Dataset 2). This could either mean that the *max2* mutant is not completely flawed in SL signaling, or shows the existence of a MAX2-independent *rac*-GR24 signaling pathway in the plant. The commonly used *max2* mutant in literature is the *max2-1*, which accounts for a point mutation. Indeed, the max2 mutant was earlier reported to respond phenotypically when higher concentrations of rac-GR24 were applied, which could imply a remnant of SL signaling (Ruyter-Spira et al., Shinohara et al., 2013). This should be investigated by using a *max2* knock out mutant, such as *max2-3*.

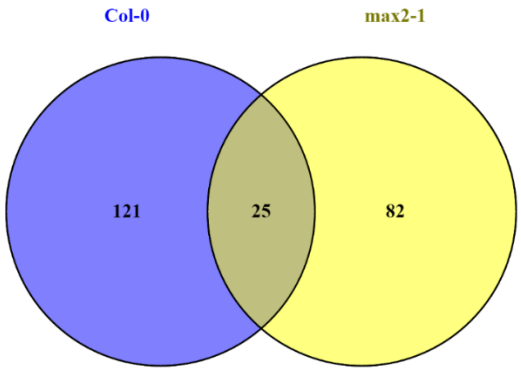

Figure 10. Overlap between the datasets of the *rac*-GR24-treated WT (Col-0) vs. the *rac*-GR24-treated *max2* mutant. Genes were selected based on a FC cutoff of 1.2 and *P*-value < 0.05. Content for the 3 gene sets can be retrieved in Supplementary Tables 8 (WT unique), 9 (overlap) and 10 (*max2* unique).

The overlap between the treated WT and *max2-1* datasets contained 25 genes (Figure 10; Supplementary Table 9), which at least indicates that the majority of the responsive genes in WT depend on MAX2 (Supplementary Table 8). On the other hand, this also suggests that the 82 genes that are uniquely differentially expressed in *max2* upon treatment with *rac*-GR24 were not responsive in WT (Supplementary Table 10). The latter result is completely unexpected. To further investigate this, these 82 genes were searched for in the full dataset of the WT treated with *rac*-GR24 (without fold change- and *P*-value cutoffs). When applying a less restrictive *P*-value of $P < 0.1$, 15 of the 82 genes were found to be potentially also differentially expressed in the WT (As indicated in yellow in Supplementary Table 9), amongst which the *MAX4* gene (P = 0,0508 in WT). Even after this step, still 67 genes are uniquely differentially expressed in *max2* after *rac*-GR24 treatment. In the *max2* mutant, many pathways are perturbed, which could be the underlying cause of an apparent enhanced sensitivity towards *rac*-GR24. In an attempt to confirm this, we selected *MAX4* (which was originally in the *max2*-unique dataset) and five additional genes from the list of genes that are expected to be specifically differentially expressed in the *max2* mutant upon treatment with *rac*-GR24 and investigated their expression pattern via qRT-PCR (Figure 11). The *MAX4* gene was differentially regulated in the WT upon the *rac*-GR24 treatment and this trend seems also present in the *max2*-mutant, but was not statistically significant (Figure 11A). For the other genes, no significant differences could be observed, despite a certain trend in the data (Figure 11 B-F). To investigate this further, these experiments should be repeated on material with less variation between the different biological repeats, and in addition more genes should be included for confirmation.

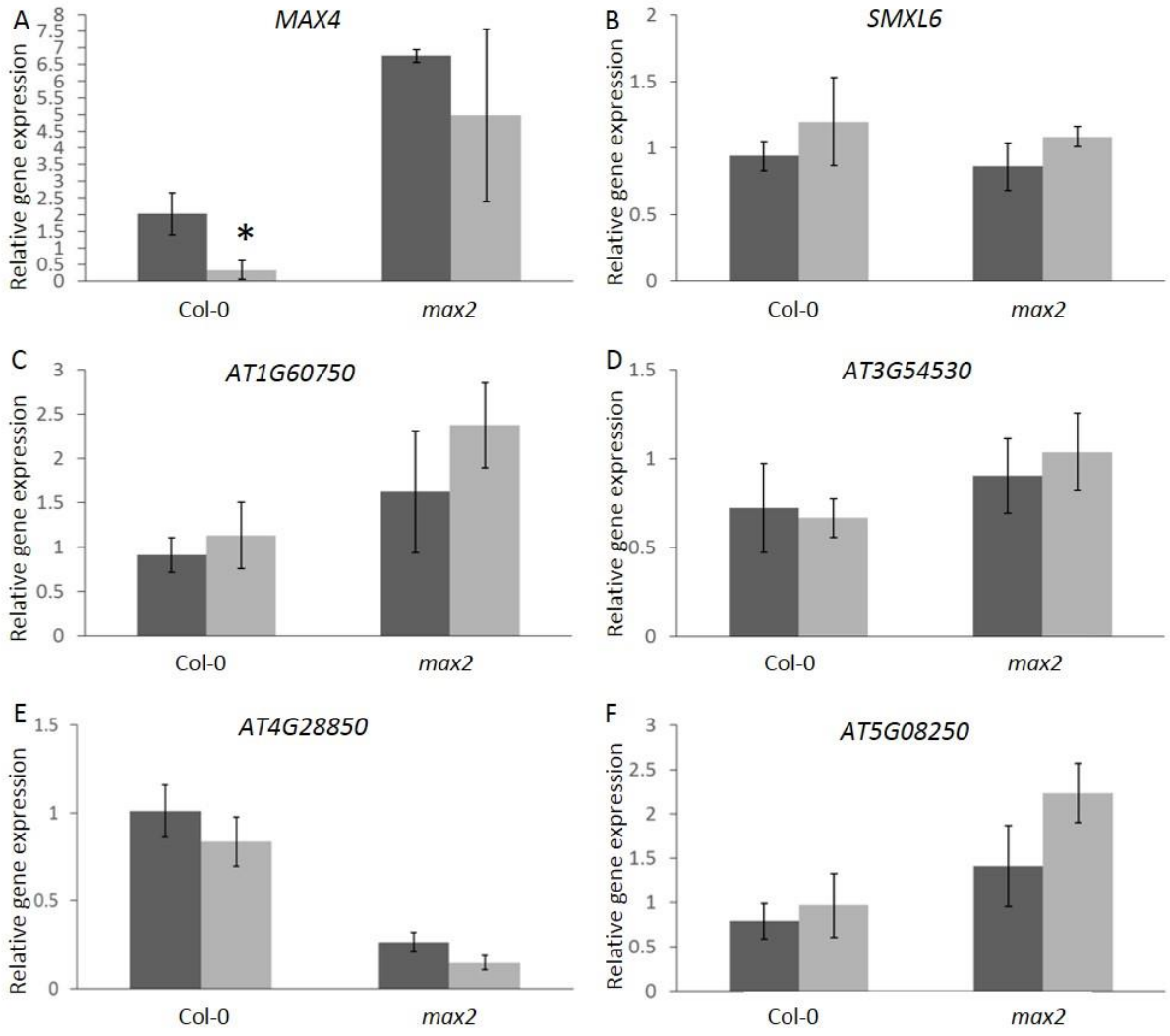

Figure 11. qRT-PCR analysis of a subset of genes that were specifically downregulated by *rac*-GR24 in *max2,* but not in the WT. Col-0 and *max2* seedlings were grown for 5 days under continuous light conditions at 21°C on half-strength Murashige and Skoog medium with 1% [w/v] sucrose whereafter they were transferred to fresh medium containing 1 µM *rac*-GR24 or to MOCK medium. Root material was harvested 6 h after transfer. Transcript levels were measured in root tissue by qRT-PCR and normalized to *ACTIN2*. Error bars represent the standard error (SE), based on three independent biological repeats. An ANOVA-mixed model was used for the statistical analysis. * P <0.05.

The RNAseq also reveals the involvement of MAX2 in processes that are not regulated via D14 or KAI2

The dataset comparing the *max2* mutant with the WT under untreated conditions contains over 2,000 genes, which was far more than the differentially expressed genes after the *rac*-GR24 treatment. Besides the common processes disturbed both after the *rac*-GR24 treatment of the WT and in the *max2* compared to the WT under untreated conditions, also various unique processes are perturbed in the latter. Generally, the *max2* mutant seemed to have a higher cellular activity than that of the WT root tissue (Figure 5; Supplementary Table 4). Most cell cycle-related genes that were differentially expressed in *max2* compared to WT were upregulated and, correspondingly, also the expression of genes involved in DNA synthesis and histone production was higher in *max2* than in the WT. A possible link might be the higher LR-forming potential in the *max2* mutant than in the WT: more LR primordia are formed, implying that more cell division should take place. Coupled with more dividing cells, most of the genes involved in RNA and protein synthesis were upregulated in the *max2* mutant; more specifically, a large amount of genes encoding ribosomal proteins were slightly upregulated in *max2*. Inversely, the expression of the majority of the differentially expressed genes involved in protein degradation was rather low. To validate and to get some initial insights whether these effects in the *max2* mutant result from signaling via the D14- and/or the KAI2-mediated pathway, we selected some genes and analyzed their expression in the root tissue of the WT, *max2*, *d14*, kai2, and the *d14;kai2* double mutant grown for 5 days via qRT-PCR. For the B-type cyclin gene *CYCB2;1*, the *60S RIBOSOMAL PROTEIN L9* gene, and the *HISTONE 3* gene (*AT5G10390*), we could confirm an upregulation in *max2*, but no differential expression in either one of the receptor mutants or double mutant (Figures 12A-12C), suggesting that the upregulation in *max2* roots does not occur via signaling through the receptors for *rac*-GR24, in agreement with their unaffected expression by the *rac*-GR24 treatment. Hence, these *max2* effects are either late downstream effects of blocked *rac*-GR24 signaling or caused by the blocked signaling pathway of an unknown compound that also signals via MAX2. Another gene homologous to D14 and KAI2 is D14-LIKE 2 (DLK2), to which no function has been

attributed yet (Arite et al., 2009). Although for all known phenotypes related to SL and KAR, a role for DLK2 has been excluded, these findings suggest that the *dlk2* mutant should be carefully analyzed for phenotypes related to these genes (Waters et al., 2012; Bennett et al., 2016). Alternatively, it can also be that MAX2 is involved in other pathways and processes, besides the *rac*-GR24-signaling cascade, resulting in differential expression of these gene classes in *max2*.

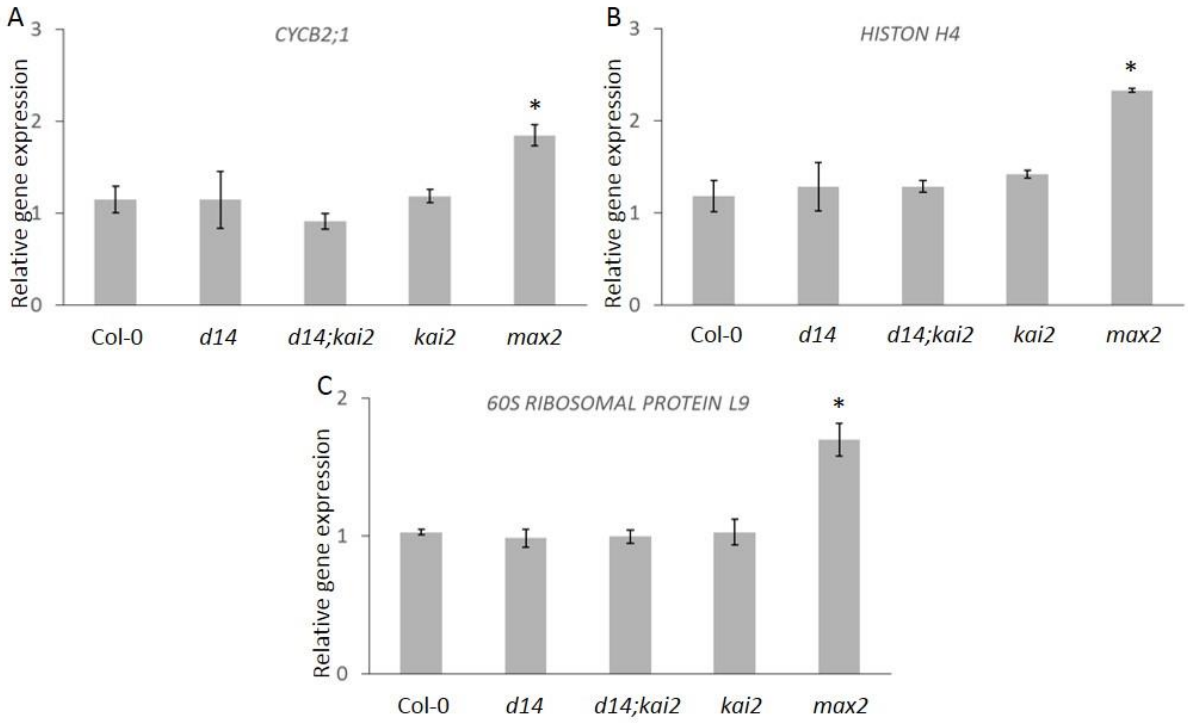

Figure 12. Expression in the root of several genes involved in cellular activities in the different SL signaling mutants. Plants of Col-0, *d14*, *kai2, d14;kai2,* and *max2* were grown under continuous light conditions at 21°C on nylon meshes placed on half-strength Murashige and Skoog medium with 1% [w/v] sucrose. Root tissue was harvested after 5 days of growth. Transcript levels were measured by qRT-PCR and normalized to *ACTIN2*. Error bars represent the standard error (SE), based on three independent biological repeats. A one-way ANOVA was used for the statistical analysis. * *P* <0.05.

3.2.5. Concluding remarks

Strigolactones play an important role in the root system architecture, regulating LRD, adventitious root formation, primary root growth and root hair elongation. However, an in-depth understanding of the responses in the root at the transcriptional level were lacking. Here, we investigated the transcriptome-wide changes brought about by treatment with *rac*-GR24 in the roots of *Arabidopsis thaliana* and the differences in the root transcriptome of the *max2* signaling mutant compared to the wild type. Strigolactones were found to influence various pathways, such as the hormonal crosstalk, drought responses, and light harvesting and sensitivity, and to modulate the plant's secondary metabolism. Additionally, we showed that the influence of *rac*-GR24 on the LRD requires both the recognition of the two enantiomers of *rac*-GR24 by either the DWARF14 or KARRIKIN-INSENSITIVE2 receptor. Altogether, the data imply that the *rac*-GR24 signaling involves the alteration of different pathways to regulate its impact on the root system architecture.

3.3. Materials and methods

Phenotypic root analysis

Arabidopsis thaliana (L.) Heynh. (Columbia accession [Col-0]) WT plants and *max2-1 (*Stirnberg et al., 2002*), d14-1* (Arite et al., 2009)*, htl-3 (i.e. a mutant allele of KAI2 in Col-0 background),* and *d14-1;htl-3* (Toh et al., 2014) mutants were grown for 9 days under continuous light conditions at 21°C on half-strength Murashige and Skoog medium with 1% [w/v] sucrose, supplemented with either 1 µM *rac*-GR24, 1 µM (+)GR24, or 1 µM (-)GR24 (kind gifts of Dr. F.-D. Boyer). Lateral roots (LRs) were counted under a binocular S4E microscope (Leica Microsystems) and root length was measured with ImageJ (http://rsb.info.nih.gov/ij). Both values were used to calculate the lateral root density (LRD). For the statistical analysis, the number of LRs was modelled by Poisson regression with the root length as offset variable. In the presence of overdispersion, the negative binomial distribution was preferred over the Poisson distribution. For the analysis, the GLIMMIX procedure (SAS Institute, Cary, NC, USA) was used that allows random effects. The whole experiment was repeated three times. To account for the correlation between the observations within one repeat, a random intercept for repeat was included in the model. The fixed factors were genotype and treatment. The model included both factors as well as the interaction term. User-defined contrasts were estimated with the PLM procedure (SAS Institute). To check for a family-wise error rate of 0.05, the MAXT method was applied through the simulation method implemented in the PLM procedure.

Expression analyses

For the expression analyses of the *Arabidopsis* Col-0 seeds treated for 0 h, 6 h, 24 h, and 48 h with *rac*-GR24, the seeds were set on nylon meshes (20 µM) to facilitate their transfer to half-strength Murashige and Skoog medium with 1% [w/v] sucrose media. The plates were incubated at 4°C for 2 days, then transferred and grown vertically for 5 days under continuous light conditions at 21°C. Plants were subsequently shifted onto either mock or medium containing 1 µM *rac*-GR24 and

returned to the growth room for 0, 6, 24, or 48 h. The complete root was harvested, flash-frozen in liquid nitrogen and stored at –80°C until processing. Approximately 100 seedlings were used for each treatment and the experiment was repeated three times.

For the expression analyses of Col-0 and *max2* seeds treated for 6 h with *rac*-GR24 or mock treated, *Arabidopsis* WT and *max2-1* seeds were sown, grown, transferred, and harvested similarly as described above after 6 h of mock treatment or treatment with 1 µM *rac*-GR24.

For the expression analyses on Col-0, *max2*, *d14*, *kai2,* and *d14;kai2, Arabidopsis* WT, *max2-1*, *d14-1*, *htl-3 (kai2* allele in Col-0 background*),* and *d14-1;htl-3* seeds were set on half-strength Murashige and Skoog medium with 1% [w/v] sucrose. The plates were incubated at 4°C for 2 days, then transferred, and grown vertically for 5 days under continuous light conditions at 21°C. The whole root was harvested and flash-frozen in liquid nitrogen. Approximately 100 seedlings were used for each treatment and the experiment was repeated three times.

For the validation of the potential LR marker genes by means of synchronized LR material according to the 'Lateral Root Inducing System' (Himanen et al., 2002), *Arabidopsis* WT seeds were set on nylon meshes (20 µm) on half-strength Murashige and Skoog medium with 1% [w/v] sucrose supplemented with 10 µM naphthylphtalamic acid (NPA) to prevent LR primordia development and to synchronize the pericycle. The plates were incubated at 4°C for 2 days, transferred, and grown vertically for 3 days under continuous light conditions at 21°C. Plants were subsequently shifted onto medium containing 10 µM 1-naphthyl acetic acid (1-NAA) to induce synchronously LR development along the main root and returned to the growth room for 0, 2, 6, 12, 18, 24, or 48 h. The whole root excluding the root tip was harvested, flash-frozen in liquid nitrogen, and stored at -80°C until processing. Approximately 100 seedlings were used for each treatment and the experiment was repeated twice.

Total RNA was extracted with the RNeasy Plant Mini Kit (Qiagen) according to the manufacturer's protocol. Genomic DNA was removed by DNase treatment and the RNA samples were

purified through NH_4Ac (final concentration of 2.5 M) precipitation. Samples were quality-controlled and quantified with a Nano-Drop Spectrophotometer (Isogen). One microgram of RNA was reverse-transcribed into cDNA with the iScript cDNA synthesis Kit (BioRad) and subsequently diluted 25 times. Real-time quantitative reverse transcription-polymerase chain reaction (qRT–PCR) was run on a LightCycler 480 (Roche Diagnostics) with SYBR Green for detection. The experiment was done in triplicate on a 384-multiwell plate in a total volume of 5 µl and 10% cDNA fractions. Cycle threshold (Ct) values were obtained with the accompanying software, analyzed with the 2–ΔΔCT method (Livak and Schmittgen, 2001), and normalized against those of ACTIN2 (ACT2, AT3G18780), which was used as an internal standard.

Statistics were done as previously described (Rasmussen et al., 2012).

RNAseq analysis

Arabidopsis Col-0 and *max2-1* seeds were put together on nylon meshes (20 µM) in a square plate divided in two to facilitate transfer to half-strength Murashige and Skoog medium with 1% [w/v] sucrose. The plates were incubated at 4°C for 2 days, transferred, and grown vertically for 5 days under continuous light conditions at 21°C. Plants were subsequently put on either mock or 1 µM *rac*-GR24-containing medium and returned to the growth room for 6 h. The whole root was harvested, flash-frozen in liquid nitrogen, and stored at -80°C until processing. Approximately 100 seedlings were used for each treatment and the experiment was repeated three times.

RNA sequencing (RNAseq) was done after RNA quality control and in-house library preparation to enrich for mRNA. The samples were run on an Illumina HiSeq 2000 platform with a paired-end sequencing mode and a read length of 50 base pairs. The raw data files contained 15-18 million reads per sample. First, these data files were quality checked and filtered to remove reads with a globally insufficient sequencing quality, to trim read ends with poor quality, and to discard overrepresented sequences (such as adaptor sequences). Next, the reads were mapped on the

Arabidopsis genome by means of the annotated genome of The Arabidopsis Information Resource (TAIR10). Only the reads that met specific requirements that reflected their mapping quality were considered, such as those uniquely mapped or with both the mapped forward and the reverse reads in the correct orientation and distance. Each of these reads were then assigned to a specific gene, resulting in a table with raw counts per gene. The raw data and following differential expression analysis was normalized with EdgeR, a plugin for R software, and with the default settings. After statistical analysis, the fold-change threshold was set between 1.2 and 0.83 to select potentially biologically relevant genes.

Mapman analyses

Excel datasets consisting of the differentially expressed genes for each condition were constructed containing the AGI code accompanied with the Log(2) fold change. These files served as input for the MapMan software (http://mapman.gabipd.org/web/guest/mapman). The imported dataset was selected for which the genes were mapped onto the desired MapMan pathway. For each functional category, the genes and description were manually selected and collected into a new table. The constructed lists were finally manually curated with the most recent data available on arabidopsis.org.

3.4. References

Agusti, J., Herold, S., Schwarz, M., Sanchez, P., Ljung, K., Dun, E.A., Brewer, P.B., Beveridge, C.A., Sieberer, T., Sehr, E.M., and Greb, T. (2011). Strigolactone signaling is required for auxin-dependent stimulation of secondary growth in plants. Proc. Natl. Acad. Sci. USA 108, 20242-20247 [Err. Proc. Natl. Acad. Sci. USA 109, 14277].

Aharon, R., Shahak, Y., Wininger, S., Bendov, R., Kapulnik, Y., and Galili, G. (2003). Overexpression of a plasma membrane aquaporin in transgenic tobacco improves plant vigor under favorable growth conditions but not under drought or salt stress. Plant Cell 15, 439-447.

Arite, T., Umehara, M., Ishikawa, S., Hanada, A., Maekawa, M., Yamaguchi, S., and Koyzuka, J. (2009). *d14*, a strigolactone-insensitive mutant of rice, shows an accelerated outgrowth of tillers. Plant Cell Physiol. 50, 1416-1424.

Bennett, T., Liang, Y., Seale, M., Ward, S., Müller, D., and Leyser, O. (2016). Strigolactone regulates shoot development through a core signalling pathway. Biol. Open 5, 1806-1820.

Bennett, T., Sieberer, T., Willett, B., Booker, J., Luschnig, C., and Leyser, O. (2006). The *Arabidopsis MAX* pathway controls shoot branching by regulating auxin transport. Curr. Biol. 16, 553-563.

Brewer, P.B., Dun, E.A., Ferguson, B.J., Rameau, C., and Beveridge, C.A. (2009). Strigolactone acts downstream of auxin to regulate bud outgrowth in pea and Arabidopsis. Plant Physiol. 150, 482-493.

Bu, Q., Lv, T., Shen, H., Luong, P., Wang, J., Wang, Z., Huang, Z., Xiao, L., Engineer, C., Kim, T.H., Schroeder, J.I., and Huq, E. (2014). Regulation of drought tolerance by the F-box protein MAX2 in Arabidopsis. Plant Physiol. 164, 424-439.

Chevalier, F, Nieminen, K, Sánchez-Ferrero, J.C., Rodríguez, M.L., Chagoyen, M., Hardtke, C.S., and Cubas, P. (2014). Strigolactone promotes degradation of DWARF14, an α/β hydrolase essential for strigolactone signaling in *Arabidopsis*. Plant Cell 26, 1134-1150.

Chini, A., Fonseca, S., Fernández, G., Adie, B., Chico, J.M., Lorenzo, O., García-Casado, G., López-Vidriero, I., Lozano, F.M., Ponce, M.R., Micol, J.L., and Solano, R. (2007). The JAZ family of repressors is the missing link in jasmonate signalling. Nature 448, 666-671.

Conn, C.E., and Nelson, D.C. (2016). Evidence that KARRIKIN-INSENSITIVE2 (KAI2) receptors may perceive an unknown signal that is not karrikin or strigolactone. Front. Plant Sci. 6, 1219.

Crawford, S., Shinohara, N., Sieberer, T., Williamson, L., George, G., Hepworth, J., Müller, D., Domagalska, M.A., and Leyser, O. (2010). Strigolactones enhance competition between shoot branches by dampening auxin transport. Development 137, 2905-2913.

de Saint Germain, A., Clavé, G., Badet-Denisot, M.-A., Pillot, J.-P., Cornu, D., Le Caer, J.-P., Burger, M., Pelissier, F., Retailleau, P., Turnbull, C., Bonhomme, S., Chory, J., Rameau, C., and Boyer, F.-D. (2016). An histidine covalent receptor and butenolide complex mediates strigolactone perception. Nat. Chem. Biol. 12, 787-794.

Ditengou, F.A., Teale, W.D., Kochersperger, P., Flittner, K.A., Kneuper, I., van der Graaff, E., Nziengui, H., Pinosa, F., Li, X., Nitschke, R., Laux, T., and Palme, K. (2008). Mechanical induction of lateral root initiation in *Arabidopsis thaliana*. Proc. Natl. Acad. Sci. USA 105, 18818-18823.

Ferguson, B.J., and Beveridge, C.A. (2009). Roles for auxin, cytokinin, and strigolactone in regulating shoot branching. Plant Physiol. 149, 1929-1944.

Foo, E., and Davies, N.W. (2011). Strigolactones promote nodulation in pea. Planta 234, 1073-1081.

Foo, E., Bullier, E., Goussot, M., Foucher, F., Rameau, C., and Beveridge, C.A. (2005). The branching gene *RAMOSUS1* mediates interactions among two novel signals and auxin in pea. Plant Cell 17, 464-474.

Foo, E., Yoneyama, K., Hugill, C.J., Quittenden, L.J., and Reid, J.B. (2013). Strigolactones and the regulation of pea symbioses in response to nitrate and phosphate deficiency. Mol. Plant 6, 76-87.

Flematti, G.R., Scaffidi, A., Waters, M.T., and Smith, S.M. (2016). Stereospecificity in strigolactone biosynthesis and perception. Planta 243, 1361-1373.

Gomez-Roldan, V., Fermas, S., Brewer, P.B., Puech-Pagès, V., Dun, EA., Pillot, J.-P., Letisse, F., Matusova, R., Danoun, S., Portais, J-C., Bouwmeester, H., Bécard, G., Beveridge, C.A., Rameau, C., and Rochange, S.F. (2008). Strigolactone inhibition of shoot branching. Nature 455, 189-194.

Ha, C.V., Leyva-González, M.A., Osakabe, Y., Tran, U.T., Nishimaya, R., Watanabe, Y., Tanaka, M., Seki, M., Yamaguchi, S., Dong, N.V., Yamaguchi-Shinozaki, K., Shinozaki, K., Herrera-Estrella, L., and Tran, L.-S.P. (2014). Positive regulatory role of strigolactone in plant responses to drought and salt stress. Proc. Natl. Acad. Sci. USA 111, 851-856.

Hayward, A., Stirnberg, P., Beveridge, C., and Leyser, O. (2009). Interactions between auxin and strigolactone in shoot branching control. Plant Physiol. 151, 400-412.

Himanen, K., Boucheron, E., Vanneste, S., de Almeida Engler, J., Inzé, D., and Beeckman, T. (2002). Auxin-mediated cell cycle activation during early lateral root initiation. Plant Cell 14, 2339-2351.

Kapulnik, Y., Delaux, P.-M., Resnick, N., Mayzlish-Gati, E., Wininger, S., Bhattacharya, C., Séjalon-Delmas, N., Combier, J.-P., Bécard, G., Belausov, E., Beeckman, T., Dor, E., Hershenhorn, J., and Koltai, H. (2011a). Strigolactones affect lateral root formation and root-hair elongation in Arabidopsis. Planta 233, 209-216.

Kapulnik, Y., Resnick, N., Mayzlish-Gati, E., Kaplan, Y., Wininger, S., Hershenhorn, J., and Koltai, H. (2011b). Strigolactones interact with ethylene and auxin in regulating root-hair elongation in *Arabidopsis*. J. Exp. Bot. 62, 2915-2924.

Kepinski, S., and Leyser, O. (2005). The *Arabidopsis* F-box protein TIR1 is an auxin receptor. Nature 435, 446-451.

Koltai, H., Dor, E., Hershenhorn, J., Joel, D.M., Weininger, S., Lekalla, S., Shealtiel, H., Bhattacharya, C., Eliahu, E., Resnick, N., Barg, R., and Kapulnik, Y. (2010). Strigolactones' effect on root growth and root-hair elongation may be mediated by auxin-efflux carriers. J. Plant Growth Regul. 29, 129-136.

Koren, D., Resnick, N., Mayzlish Gati, E., Belausov, E., Weininger, S., Kapulnik, Y., and Koltai, H. (2013). Strigolactone signaling in the endodermis is sufficient to restore root responses and involves SHORT HYPOCOTYL 2 (SHY2) activity. New Phytol. 198, 866-874.

Liang, Y., Ward, S., Li, P., Bennett, T., and Leyser, O. (2016). SMAX1-LIKE7 signals from the nucleus to regulate shoot development in Arabidopsis via partially EAR motif-independent mechanisms. Plant Cell 28, 1581-1601.

Livak, K.J., and Schmittgen, T.D. (2001). Analysis of relative gene expression data using real-time quantitative PCR and the $2^{-\Delta\Delta C_T}$ method. Methods 25, 402-408.

Mashiguchi, K., Sasaki, E., Shimada, Y., Nagae, M., Ueno, K., Nakano, T., Yoneyama, K., Suzuki, Y., and Asami, T. (2009). Feedback-regulation of strigolactone biosynthetic genes and strigolactone-regulated genes in Arabidopsis. Biosci. Biotechnol. Biochem. 73, 2460-2465.

Mayzlish-Gati, E., De-Cuyper, C., Goormachtig, S., Beeckman, T., Vuylsteke, M., Brewer, P.B., Beveridge, C.A., Yermiyahu, U., Kaplan, Y., Enzer, Y., Wininger, S., Resnick, N., Cohen, M., Kapulnik, Y., and Koltai, H. (2012). Strigolactones are involved in root response to low phosphate conditions in Arabidopsis. Plant Physiol. 160, 1329-1341.

Mayzlish-Gati, E., LekKala, S.P., Resnick, N., Wininger, S., Bhattacharya, C., Lemcoff, J.H., Kapulnik, Y., and Koltai, H. (2010). Strigolactones are positive regulators of light-harvesting genes in tomato. J. Exp. Bot. 61, 3129-3136.

Nakamura, H., Xue, Y.-L., Miyakawa, T., Hou, F., Qin, H.-M., Fukui, K., Shi, X., Ito, E., Ito, S., Park, S.-H., Miyauchi, Y., Asano, A., Totsuka, N., Ueda, T., Tanokura, M., and Asami, T. (2013). Molecular mechanism of strigolactone perception by DWARF14. Nat. Commun. 4, 2613.

Nelson, D.C., Flematti, G.R., Riseborough, J.-A., Ghisalberti, E.L., Dixon, K.W., and Smith, S.M. (2010). Karrikins enhance light responses during germination and seedling development in *Arabidopsis thaliana*. Proc. Natl. Acad. Sci. USA 107, 7095-7100.

Nelson, D.C., Scaffidi, A., Dun, E.A., Waters, M.T., Flematti, G.R., Dixon, K.W., Beveridge, C.A., Ghisalberti, E.L., and Smith, S.M. (2011). F-box protein MAX2 has dual roles in karrikin and strigolactone signaling in *Arabidopsis thaliana*. Proc. Natl. Acad. Sci. USA 108, 8897-8902.

Pandya-Kumar, N., Shema, R., Kumar, M., Mayzlish-Gati, E., Levy, D., Zemach, H., Belausov, E., Wininger, S., Abu-Abied, M., Kapulnik, Y., and Koltai, H. (2014). Strigolactone analog GR24 triggers changes in PIN2 polarity, vesicle trafficking and actin filament architecture. New Phytol. 202, 1184-1196.

Pauwels, L., Fernández Barbero, G., Geerinck, J., Tilleman, S., Grunewald, W., Cuéllar Pérez, A., Chico, J.M., Vanden Bossche, R., Sewell, J., Gil, E., García-Casado, G., Witters, E., Inzé, D., Long, J.A., De Jaeger, G., Solano, R., and Goossens, A. (2010). NINJA connects the co-repressor TOPLESS to jasmonate signalling. Nature 464, 788-791.

Rasmussen, A., Mason, M.G., De Cuyper, C., Brewer, P.B., Herold, S., Agusti, J., Geelen, D., Greb, T., Goormachtig, S., Beeckman, T., and Beveridge, C.A. (2012). Strigolactones suppress adventitious rooting in Arabidopsis and pea. Plant Physiol. 158, 1976-1987.

Ruyter-Spira, C., Kohlen, W., Charnikhova, T., van Zeijl, A., van Bezouwen, L., de Ruijter, N., Cardoso, C., Lopez-Raez, J.A., Matusova, R., Bours, R., Verstappen, F., and Bouwmeester, H. (2011). Physiological effects of the synthetic strigolactone analog GR24 on root system architecture in Arabidopsis: another belowground role for strigolactones? Plant Physiol. 155, 721-734.

Scaffidi, A., Waters, M.T., Ghisalberti, E.L., Dixon, K.W., Flematti, G.R., and Smith, S.M. (2013). Carlactone-independent seedling morphogenesis in Arabidopsis. Plant J. 76, 1-9.

Scaffidi, A., Waters, M.T., Sun, Y.K., Skelton, B.W., Dixon, K.W., Ghisalberti, E.L., Flematti, G.R., and Smith, S.M. (2014). Strigolactone hormones and their stereoisomers signal through two related receptor proteins to induce different physiological responses in Arabidopsis. Plant Physiol. 165, 1221 1232.

Shen, H., Luong, P., and Huq, E. (2007). The F-Box protein MAX2 functions as a positive regulator of photomorphogenesis in Arabidopsis. Plant Physiol. 145, 1471-1483.

Shen, H., Zhu, L., Bu, Q.-Y., and Huq, E. (2012). MAX2 affects multiple hormones to promote photomorphogenesis. Mol. Plant 5, 750-762.

Shinohara, N., Taylor, C., and Leyser, O. (2013). Strigolactone can promote or inhibit shoot branching by triggering rapid depletion of the auxin efflux protein PIN1 from the plasma membrane. PLoS Biol. 11, e1001474.

Snowden, K.C., Simkin, A.J., Janssen, B.J., Templeton, K.R., Loucas, H.M., Simons, J.L., Karunairetnam, S., Gleave, A.P., Clark, D.G., and Klee, H.J. (2005). The *Decreased apical dominance1/Petunia hybrida CAROTENOID CLEAVAGE DIOXYGENASE8* gene affects branch production and plays a role in leaf senescence, root growth, and flower development. Plant Cell 17, 746-759.

Soto, M.J., Fernández-Aparicio, M., Castellanos-Morales, V., García-Garrido, J.M., Ocampo, J.A., Delgado, M.J., and Vierheilig, H. (2010). First indications for the involvement of strigolactones on nodule formation in alfalfa (*Medicago sativa*). Soil Biol. Biochem. 42, 383-385.

Soundappan, I., Bennett, T., Morffy, N., Liang, Y., Stanga, J.P., Abbas, A., Leyser, O., and Nelson, D.C. (2015). SMAX1-LIKE/D53 family members enable distinct MAX2-dependent responses to strigolactones and karrikins in Arabidopsis. Plant Cell 27, 3143-3159.

Stanga, J.P., Morffy, N., and Nelson, D.C. (2016). Functional redundancy in the control of seedling growth by the karrikin signaling pathway. Planta 243, 1397-1406.

Stanga, J.P., Smith, S.M., Briggs, W.R., and Nelson, D.C. (2013). *SUPPRESSOR OF MORE AXILLARY GROWTH2 1* controls seed germination and seedling development in Arabidopsis. Plant Physiol. 163, 318-330.

Stirnberg, P., Furner, I.J., and Leyser, H.M.O. (2007). MAX2 participates in an SCF complex which acts locally at the node to suppress shoot branching. Plant J. 50, 80-94.

Stirnberg, P., van de Sande, K., and Leyser, H.M.O. (2002). *MAX1* and *MAX2* control shoot lateral branching in *Arabidopsis*. Development 129, 1131-1141.

Stracke, R., Ishihara, H., Huep, G., Barsch, A., Mehrtens, F., Niehaus, K., and Weisshaar, B. (2007). Differential regulation of closely related R2R3-MYB transcription factors controls flavonol accumulation in different parts of the *Arabidopsis thaliana* seedling. Plant J. 50, 660-677.

Sun, Y.K., Flematti, G.R., Smith, S.M., and Waters, M.T. (2016). Reporter gene-facilitated detection of compounds in *Arabidopsis* leaf extracts that activate the karrikin signaling pathway. Front. Plant Sci. 7, 1799.

Thimm, O., Bläsing, O., Gibon, Y., Nagel, A., Meyer, S., Krüger, P., Selbig, J., Müller, L.A., Rhee, S.Y., and Stitt, M. (2004). MAPMAN: a user-driven tool to display genomics data sets onto diagrams of metabolic pathways and other biological processes. Plant J. 37, 914-939.

Toh, S., Holbrook-Smith, D., Stokes, M.E., Tsuchiya, Y., and McCourt, P. (2014). Detection of parasitic plant suicide germination compounds using a high-throughput *Arabidopsis* HTL/KAI2 strigolactone perception system. Chem. Biol. 21, 988-998.

Toh, S., Kamiya, Y., Kawakami, N., Nambara, E., McCourt, P., and Tsuchiya, Y. (2012a). Thermoinhibition uncovers a role for strigolactones in Arabidopsis seed germination. Plant Cell Physiol. 53, 107-117.

Toh, S., McCourt, P., and Tsuchiya, Y. (2012b). *HY5* is involved in strigolactone-dependent seed germination in Arabidopsis. Plant Signal. Behav. 7, 556-558.

Tsuchiya, Y., Vidaurre, D., Toh, S., Hanada, A., Nambara, E., Kamiya, Y., Yamaguchi, S., and McCourt, P. (2010). A small-molecule screen identifies new functions for the plant hormone strigolactone. Nat. Chem. Biol. 6, 741-749.

Umehara, M., Hanada, A., Yoshida, S., Akiyama, K., Arite, T., Takeda-Kamiya, N., Magome, H., Kamiya, Y., Shirasu, K., Yoneyama, K., Kyozuka, J., and Yamaguchi, S. (2008). Inhibition of shoot branching by new terpenoid plant hormones. Nature 455, 195-200.

Voß, U., Wilson, M.H., Kenobi, K., Gould, P.D., Robertson, F.C., Peer, W.A., Lucas, M., Swarup, K., Casimiro, I., Holman, T.J., Wells, D.M., Péret, B., Goh, T., Fukaki, H., Hodgman, T.C., Laplaze, L., Halliday, K.J., Ljung, K., Murphy, A.S., Hall, A.J., Webb, A.A.R., and Bennett, M.J. (2015). The circadian clock rephases during lateral root organ initiation in *Arabidopsis thaliana*. Nat. Commun. *6*, 7641.

Wang, L., Wang, B., Jiang, L., Liu, X., Li, X., Lu, Z., Meng, X., Wang, Y., Smith, S.M., and Li, J. (2015). Strigolactone signaling in Arabidopsis regulates shoot development by targeting D53-like SMXL repressor proteins for ubiquitination and degradation. Plant Cell 27, 3128-3142.

Waters, M.T., Nelson, D.C., Scaffidi, A., Flematti, G.R., Sun, Y.K., Dixon, K.W., and Smith, S.M. (2012). Specialisation within the DWARF14 protein family confers distinct responses to karrikins and strigolactones in *Arabidopsis*. Development 139, 1285-1295.

Waters, M.T., Scaffidi, A., Moulin, S.L.Y., Sun, Y.K., Flematti, G.R., and Smith, S.M. (2015). A *Selaginella moellendorffii* ortholog of KARRIKIN INSENSITIVE2 functions in Arabidopsis development but cannot mediate responses to karrikins or strigolactones. Plant Cell 27, 1925-1944.

Waters, M.T., Scaffidi, A., Sun, Y.K., Flematti, G.R., and Smith, S.M. (2014). The karrikin response system of Arabidopsis. Plant J. 79, 623-631.

Xie, X., Yoneyama, K., and Yoneyama, K. (2010). The strigolactone story. Annu. Rev. Phytopathol. 48, 93-117.

Zhao, L.H., Zhou, X.E., Wu, Z.-S., Yi, W., Xu, Y., Li, S., Xu, T.-H., Liu, Y., Chen, R.-Z., Kovach, A., Kang, Y., Hou, L., He, Y., Xie, C., Song, W., Zhong, D., Xu, Y., Wang, Y., Li, J., Zhang, C., Melcher, K., and Xu, H.E. (2013). Crystal structures of two phytohormone signal-transducing α/β hydrolases: karrikin-signaling KAI2 and strigolactone-signaling DWARF14. Cell Res. 23, 436-439.

Zhou, C., Yin, Y., Dam, P., and Xu, Y. (2010). Identification of Novel Proteins Involved in Plant Cell-Wall Synthesis Based on Protein−Protein Interaction Data. J. Proteome Res., 9 (10), 5025–5037

3.5. Supplementary data

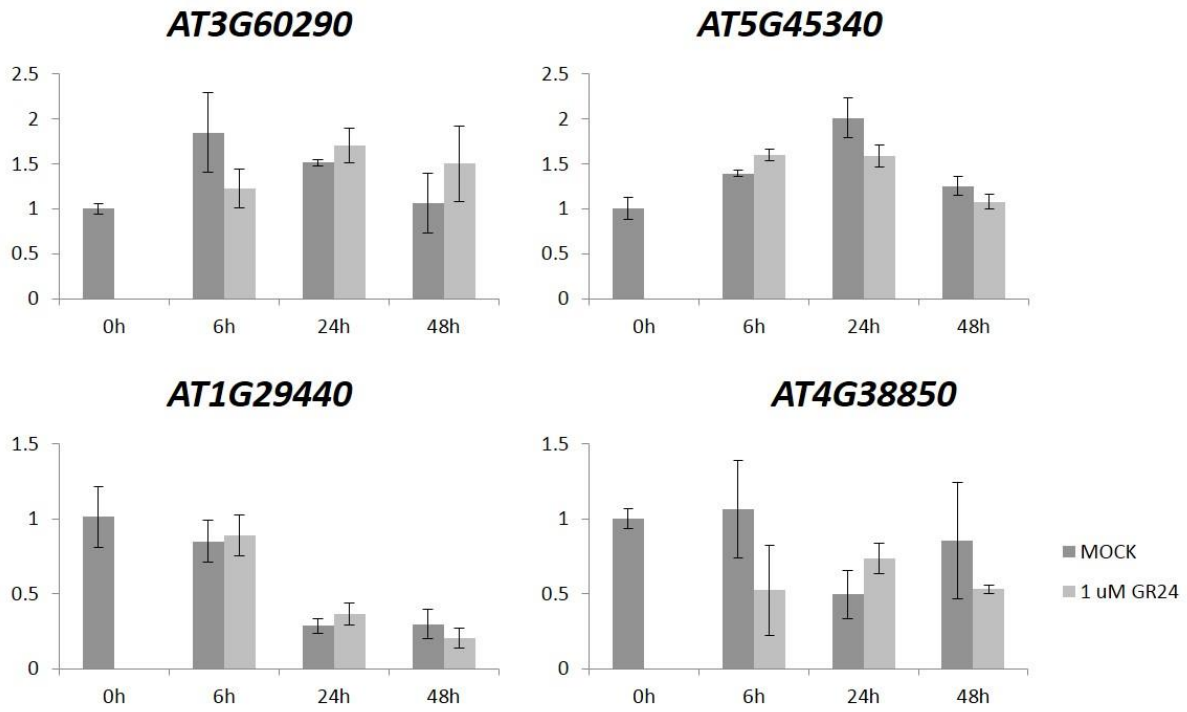

Supplementary Figure 1. Expression levels of several SL markers in the *Arabidopsis* root not affected by *rac*-GR24. Plants were grown for 5 days under continuous light conditions at 21°C on half-strength Murashige and Skoog medium with 1% [w/v] sucrose whereafter they were transferred to fresh medium containing 1 µM *rac*-GR24 or to MOCK medium. Root material was harvested 6 h, 24 h, and 48 h after transfer. Transcript levels were measured in root tissue by qRT-PCR and normalized to *ACTIN2*. Error bars represent the standard error (SE), based on three independent biological repeats. An ANOVA-mixed model was used for the statistical analysis.

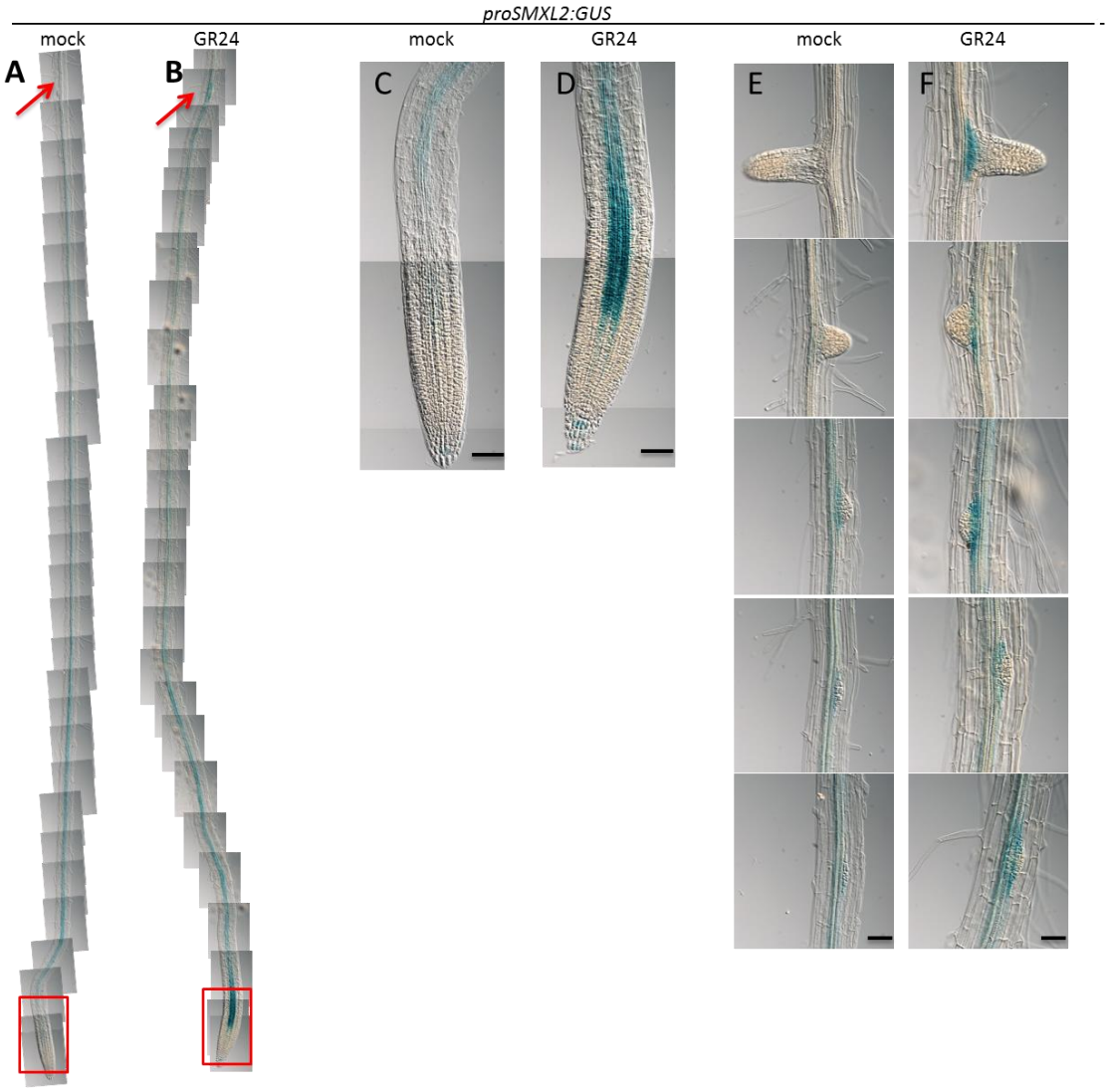

Supplementary Figure 2. Expression pattern of *SMXL2* in the root and upon *rac*-GR24 treatment. Seeds of each line were sown on medium with and without 1 µM *rac*-GR24 for 7 days. **(A, B)** Overview of *proSMXL2:GUS* expression in the root with and without *rac*-GR24 treatment, respectively. Arrows indicate lateral root primodia that do not emerge. (**C, D)** Magnification of the framed regions in **(A)** and **(B)**, respectively (scale bar = 50 µm). **(E, F)** Stages of lateral root primordia of *proSMXL2:GUS* plant with and without *rac*-GR24 treatment, respectively. Scale bar =50 µm. Arrows indicate lateral root primordia that do not emerge. n = 8-12 per repeat. Figure taken from L-X. Jiang, unpublished data.

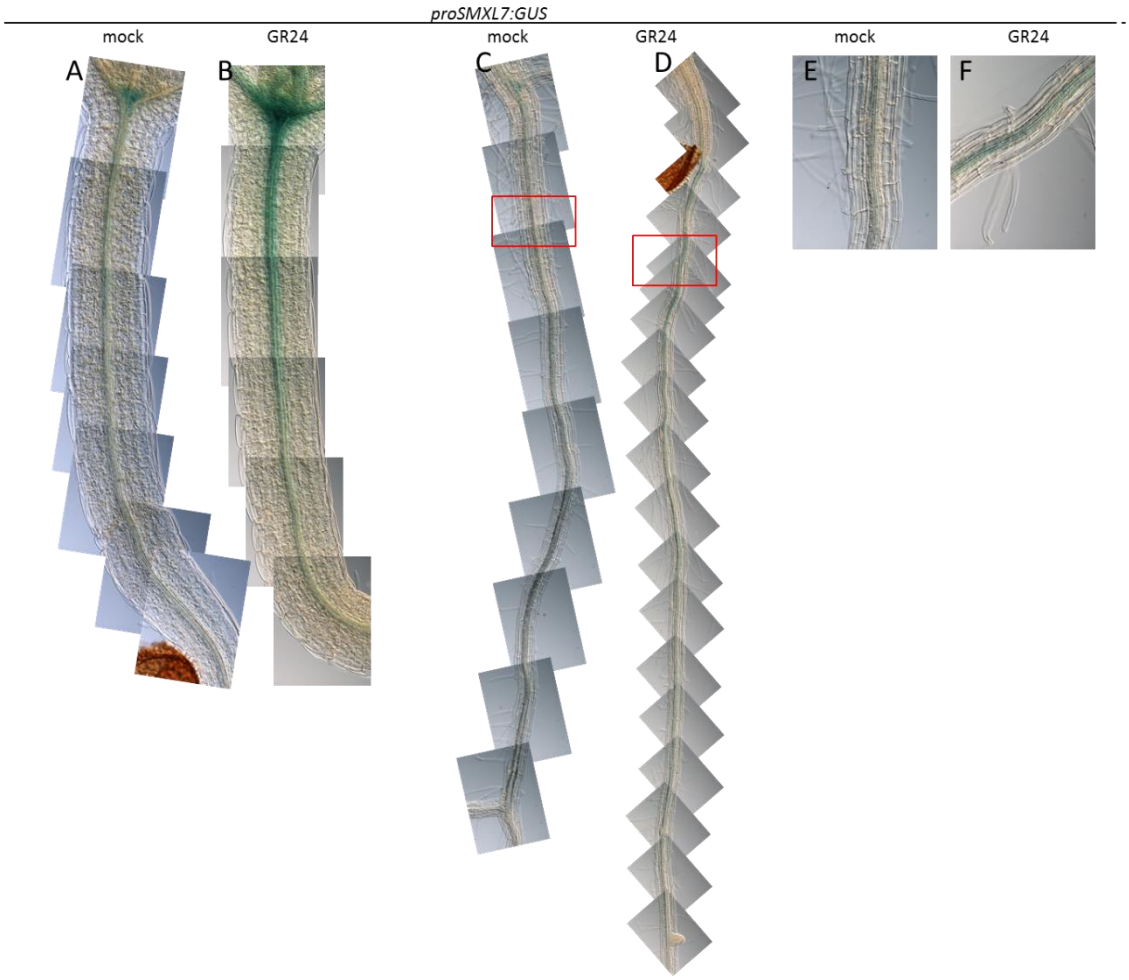

Supplementary Figure 3. Expression pattern of *SMXL7* in the root and upon GR24 treatment. (A, B) Overview of hypocotyl of a *proSMXL7:GUS* plant with and without *rac*-GR24, respectively. **(C, D)** Overview of the *proSMXL7:GUS* expression in the primary root with or without *rac*-GR24. **(E, F)** Magnifications of the framed regions in **(C, D)**; respectively. Three independent lines with three independent repeats were investigated. n = 8-12 per repeat. Figure taken from L-X. Jiang, unpublished data.

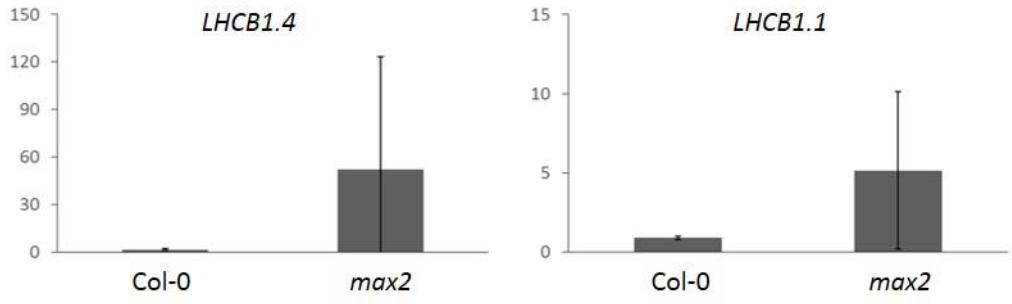

Supplementary Figure 4. Expression of several light-harvesting genes not upregulated in the roots of *max2*. Plants of Col-0 and *max2* were grown under continuous light conditions at 21°C on nylon meshes placed on half-strength Murashige and Skoog medium with 1% [w/v] sucrose. Root tissue was harvested after 5 days of growth. Transcript levels were measured by qRT-PCR and normalized to *ACTIN2*. Error bars represent the standard error (SE), based on three independent biological repeats. A Student's *t*-test was used for the statistical analysis.

Supplementary Table 1. Lateral root marker micro-array dataset upon gravitropical induction of lateral roots. Available via: https://goo.gl/bEs3mx

Supplementary Table 2. Validation of LR markergenes using qRT-PCR. Available via: https://goo.gl/bEs3mx

Supplementary Table 3. Identity of genes covered in Figure 5A. Available via: https://goo.gl/bEs3mx

Supplementary Table 4. Identity of genes covered in Figure 5B. Available via: https://goo.gl/bEs3mx

Supplementary Table 5. Overlapping genes between the *rac*-GR24 treated WT roots and the *max2*-MOCK dataset. Available via: https://goo.gl/bEs3mx

Supplementary Table 6. Identity of genes covered in Figure 7A. Available via: https://goo.gl/bEs3mx

Supplementary Table 7. Identity of genes covered in Figure 7B. Available via: https://goo.gl/bEs3mx

Supplementary Table 8. Genes uniquely differentially expressed by *rac*-GR24 in the WT. Available via: https://goo.gl/bEs3mx

Supplementary Table 9. Genes differentially expressed by *rac*-GR24 in both the WT as in *max2*. Available via: https://goo.gl/bEs3mx

Supplementary Table 10. Genes uniquely differentially expressed by *rac*-GR24 in *max2*. Available via: https://goo.gl/bEs3mx

Supplementary Dataset 1. Differentially Expressed genes after rac-GR24 treatment of WT root tissues with a FC cutoff of 1.2. Available via: https://goo.gl/bEs3mx

Supplementary Dataset 2. Differentially Expressed genes after rac-GR24 treatment of max2 root tissues with a FC cutoff of 1.2. Available via: https://goo.gl/bEs3mx

Supplementary Dataset 3: Differentially Expressed genes in max2 vs. WT root tissues (MOCK condition) with a FC cutoff of 1.2. Available via: https://goo.gl/bEs3mx

Supplementary Dataset 4. Differentially Expressed genes after rac-GR24 treatment of WT root tissues with a FC cutoff of 2. Available via: https://goo.gl/bEs3mx

Supplementary Dataset 5. Differentially Expressed genes after rac-GR24 treatment of max2 root tissues with a FC cutoff of 2. Available via: https://goo.gl/bEs3mx

Supplementary Dataset 6: Differentially Expressed genes in max2 vs. WT root tissues (MOCK condition) with a FC cutoff of 2. Available via: https://goo.gl/bEs3mx

CHAPTER 4:

THE BASIC HELIX-LOOP-HELIX TRANSCRIPTION FACTOR TARGET OF MONOPTEROS 5 LIKE1 COORDINATES STRIGOLACTONE RESPONSES IN THE ROOT

CEDRICK MATTHYS, NICK VANGHELUWE, TOM VIAENE, EUGENIA RUSSINOVA, VERONIQUE STORME, TOM BEECKMAN, AND SOFIE GOORMACHTIG.

In preparation

Author's contribution: Cedrick Matthys was the main researcher involved in the work displayed in this chapter.

Abstract

Multiple roles for strigolactones (SLs) during plant growth and development, such as regulation of shoot and root development, have been uncovered. Despite progress in the unraveling of the early signaling events leading to the degradation of repressor proteins of the SUPPRESSOR OF MORE AXILLLARY BRANCHES2 (MAX2) 1 LIKE (SMXL) family, still no candidate genes further downstream of these SMXL repressors have been identified that control the SL-mediated root responses. Here, we report on the characterization of the transcription factor TARGET OF MONOPTEROS5 LIKE 1 (TMO5L1) as a putative downstream component in the SL pathway in the root. Genetic and molecular evidence indicates that TMO5L1 might play a role in the regulation of the SL-mediated root responses, such as influence on the lateral root development and effect on the flavonol content of the root.

4.1. Introduction

Plants produce a vast variety of low-molecular weight compounds of which some act as hormones, such as the strigolactones (SLs). This class plays multiple roles in plant development and in rhizosphere communication. Thus far, SLs have been mainly studied for their inhibitory effect on axillary bud outgrowth, but they are also known to influence other important plant traits, such as the root system architecture (Gomez-Roldan et al., 2008; Umehara et al., 2008; Kapulnik et al., 2011a; Ruyter-Spira et al., 2011). In the root, SLs inhibit lateral root (LR) development by affecting both priming and the emergence of LRs, but also by altering the primary root length and root hair elongation (Chapter 2; Kapulnik et al., 2011a, 2011b; Ruyter-Spira et al., 2011; Shinohara et al. 2013). Recently, SLs have been shown to positively influence the flavonol content of the root by enhancing transcript and protein levels of various key flavonol biosynthesis genes (Walton et al. 2016). In modern agriculture, biotechnologists as well as breeders seek the most effective plant architecture to obtain the highest yield in specific growth environments. Hence, it is important to understand the SL action and to elucidate the molecular players in SL recognition and signaling.

SLs are derived from apocarotenoids and, in spite of several physiological studies, little is known about the signaling pathways that control SL-dependent functions. DWARF14 (D14), an α/β-fold hydrolase, is able to bind and hydrolyze SLs (Hamiaux et al., 2012; Zhou et al., 2013; de Saint Germain et al., 2016; Yao et al., 2016). Binding of SLs causes the cleavage of the SL molecule into an ABC-ring part and the D-ring that becomes attached to the catalytic serine residue (Zhao et al., 2013). This reaction has a slow enzymatic turnover and destabilizes the D14 protein (Hamiaux et al., 2012; Zhao et al., 2013). This destabilization is believed to facilitate the interaction with other partner proteins, such as MORE AXILLARY BRANCHES2 (MAX2) (Hamiaux et al., 2012; de Saint Germain et al., 2016; Yao et al., 2016). MAX2 is a nuclear localized leucine-rich repeat F-box protein and is, besides D14, a key player in SL signaling

(Stirnberg et al., 2007; Umehara et al., 2008; Gomez-Roldan et al., 2008). Interestingly, karrikins (KARs), which are smoke-derived germination-inducing compounds with a small structural resemblance to SLs , also require MAX2 for signaling (Nelson et al., 2011). Whereas SLs are perceived by D14, KARs and, possibly still elusive, endogenous karrikin-like (KL) compounds, are recognized and bound by KARRIKIN INSENSITIVE2 (KAI2), a protein structurally closely related to D14 (Nelson et al., 2011; Flematti et al., 2013; Soundappan et al., 2015). Recently, the commonly used synthetic bioactive SL, GR24, that consists of a racemic mixture (*rac*-GR24) has been found to be capable of activating both the D14 and the KAI2 signaling pathway (Scaffidi et al., 2014). Genetic and biochemical studies in rice (*Oryza sativa*) and *Arabidopsis thaliana* have revealed that DWARF53 (D53) and members of the *Arabidopsis* SUPPRESSOR OF MAX2 1 LIKE (SMXL) family act as D3/MAX2 targets and are ubiquitinated and degraded upon SL/KAR signaling (Jiang et al., 2013; Stanga et al., 2013; Zhou et al., 2013; Kong et al., 2014). Currently, one of the SMXL family members, SMAX1, is believed to act specifically in the KAR/KL signaling pathway, whereas the SMXL6/SMXL7/SMXL8 clade to be specific for the SL signaling pathway (Stanga et al., 2013; Soundappan et al., 2015; Wang et al., 2015; Liang et al., 2016). SMXL7, as well as the other members of the SMXL clade, contain an ETHYLENE-RESPONSIVE FACTOR Amphiphilic Repression (EAR) domain, indicating that they might act as nuclear repressor proteins. In accordance with this hypothesis, the localization of all the components of the SL signaling complex in the nucleus and the interaction between SMXL7, D14, and MAX2 have been demonstrated (Liang et al., 2016). Interestingly, because this repression domain is not required for every phenotype, the repressing activity of SMXL7 might not be the sole mechanism by which SL signaling occurs (Liang et al., 2016).

In parallel with other hormonal signaling pathways, the SL signaling complex is expected to inhibit the activation of particular transcription factors (TFs) that is relieved upon signaling. In the shoot, the TF TEOSINTE BRANCHED (TB) in maize (*Zea mays*), and its homologs BRANCHED 1 (BRC1) and BRC2 in *Arabidopsis*, FINE CULM1 (FC1) in rice, and *Ps*BRC1 in pea (*Pisum sativum*) have been reported to act

downstream of the SL signaling in bud outgrowth suppression (Aguilar-Martinez et al., 2007; Minakuchi et al., 2010; Braun et al., 2012; Dun et al., 2012). To date, no candidate genes farther downstream of the SMXL repressors have been identified that regulate the SL-mediated root responses. Here, we identified such a TF, *TARGET OF MONOPTEROS5 LIKE1* (*TMO5L1*). *TMO5L1* is a member of a clade of four homologous genes: *TMO5*, *TMO5L1*, *TMO5L2*, and *TMO5L3* (De Rybel et al., 2013). *TMO5* and *TMO5L1* are the closest homologs with a protein identity of 48% and essentially a similar function (De Rybel et al., 2013). They encode basic helix-loop-helix (bHLH) TFs that are expressed in the xylem precursor cells of the root apical meristem. Both TMO5 and TMO5L1 form heterodimers with the bHLH TF LONESOME HIGHWAY (LHW) to become transcriptionally active (Ohashi-Ito and Bergmann, 2007; De Rybel et al., 2013; An et al., 2014). TMO5/LHW and TMO5L1/LHW heterodimers were shown to control the cell divisions that underlie the establishment and indeterminate growth of the root vascular tissue (De Rybel et al., 2013). This effect was accomplished by direct induction of cytokinin biosynthesis genes of the *LONELY GUY* (*LOG*) family, resulting in elevated cytokinin levels in the surrounding cells (De Rybel et al., 2014; Ohashi-Ito et al., 2014). In addition to the cell division control, the TMO5L1/LHW complex also regulates the xylem differentiation and development in the root apical meristem in a negative feedback loop (Vera-Sirera et al., 2015; Katayama et al., 2015). A schematic overview on the role of TMO5/TMO5L1 in vascular development is depicted in Figure 1.

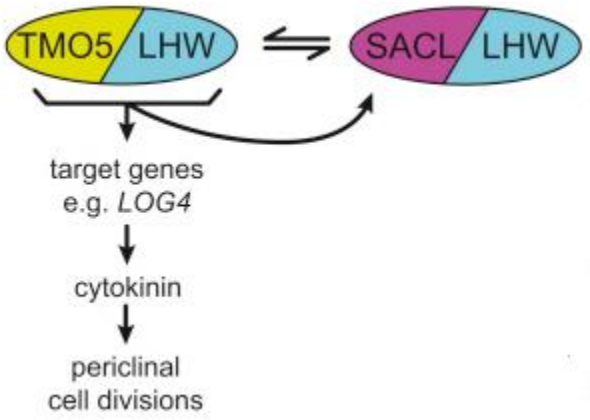

Figure 1. Proposed model for TMO5(L1)-dependent vascular cell proliferation. The bHLH TF's TMO5(L1) and LHW form a heterodimer that results in the expression of target genes, such as LOG4, which leads to cytokinin production. As such, periclinal cell divisions in the vascular tissue are regulated. The action of the TMO5(L1)-LHW dimer is believed to be feedback inhibited by the induction of other bHLH TF's (SAC51-LIKE (SACL)) that can interact with LHW and as such compete with TMO5(L1). Figure modified from Vera-Sirera et al., 2015.

Here, we report on the characterization of the TF TMO5L1 as a downstream component in the SL pathway in the root. Genetic and molecular evidence suggest that TMO5L1 might play a key role in the regulation of the SL-mediated root responses; such as in the impact on the LR development and the flavonol biosynthesis in the root.

4.2. Results

4.2.1 The effect of *rac*-GR24 treatment on the expression of *TMO5L1*

Previously, we have shown via RNA-seq that *rac*-GR24 is able to influence various pathways in the roots of *Arabidopsis* (Chapter 3). As TFs fulfill an important regulatory role, they were selected for further analysis. Various transcriptional regulators were found to be differentially expressed after 6 h of *rac*-GR24 treatment (Chapter 3; Table 1). Interestingly, the *rac*-GR24 treatment repressed the bHLH TF *TMO5L1* most strongly, whereas it was induced in the *max2* mutant grown under normal conditions (Chapter 3; Table 1). The expression of its closest homolog, *TMO5*, was, to a lesser extent, also downregulated upon *rac*-GR24 treatment and upregulated in the max2 mutant (Chapter 3; Table 1). For this reason, we had a closer look at the relation between TMO5L1 and *rac*-GR24 signaling.

Table 1. Transcriptional regulators in the root shared between the Col-0 *rac*-GR24-treated and the *max2*-MOCK datasets

AGI code	FDR (WT, *rac*-GR24)	FC (WT, *rac*-GR24)	FDR (mock, *max2*)	FC (mock, *max2*)	Gene name	aver. counts (WT MOCK)	aver. counts (WT *rac*-GR24)	aver. counts (*max2* MOCK)
AT1G68810	6.85E-27	0.4871788	6.65492E-06	1.3089518	TMO5L1	377	179	563
AT3G25710	0.0234167	0.7939342	0.001548477	1.24559262	TMO5	334	259	480
AT1G66140	0.0308496	0.8080716	6.75539E-10	1.42480574	zinc finger protein 4	314	248	513
AT4G30350	0.0017711	1.2056147	1.07106E-62	0.45298929	SMXL2	781	917	405
AT2G29970	1.439E-12	1.4473004	2.06843E-08	0.73860528	SMXL7	540	761	457

The expression pattern of *TMO5L1* was validated via qRT-PCR (Figure 2). In agreement with the RNA-seq data, a two-fold downregulation could be detected 6 h after *rac*-GR24 treatment of the WT (Figure 2A), but not in the *max2* mutant treated with *rac*-GR24 (Supplementary Figure 1). Compared to

the WT, the *max2* mutant had an enhanced *TMO5L1* expression under normal growth conditions, also confirming the RNA-seq data (Figure 2C). Also after 2 h of *rac*-GR24 treatment, *TMO5L1* was already significantly downregulated, but to a lesser extent than at the 6-h treatment (Figure 2B). We also investigated the expression at later time points after treatment and after 24 h and 48 h of treatment, *TMO5L1* expression remained lower than that of the WT (Figure 2D). Hence, the expression of *TMO5L1* was persistently and not temporarily repressed by the *rac*-GR24 treatment.

Because TMO5 and TMO5L1 are mainly known for their role in vascular development in the root in a heterodimer complex with LHW, the RNA-seq dataset of the *rac*-GR24-treated WT was searched for *LHW* and known downstream target genes of this heterodimer: *LONELY GUY3* (*LOG3*), *LOG4*, *SUPPRESSOR OF ACAULIS 51* (*SAC51*), *SAC51 LIKE 1* (*SACL1*), *SACL2* and *SACL3* (De Rybel et al., 2014; Ohashi-Ito et al., 2014; Katayama et al., 2015; Vera-Sirera et al., 2015). However, none of these genes were found to be differentially expressed by *rac*-GR24. Also in the *max2*-MOCK dataset, only *TMO5L1* and *TMO5* were retrieved as differentially expressed. This could potentially suggest that the effect of *rac*-GR24 might not be related to vascular development. To get more confirmation for this, the expression of these genes should be analyzed by qRT-PCR.

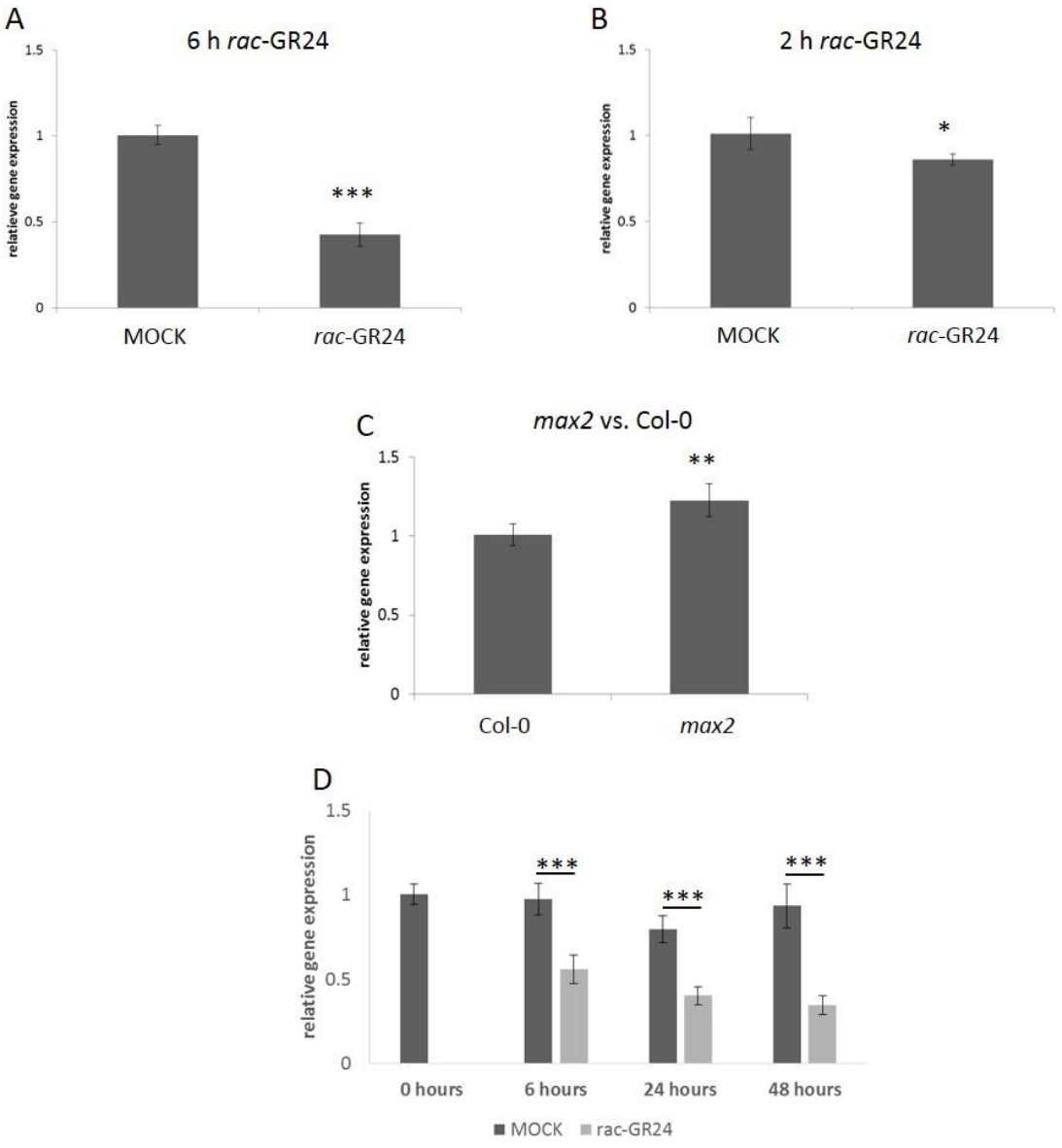

Figure 2. Effect of *rac*-GR24 treatment on the relative gene expression of *TMO5L1* in the root. Five-day-old Col-0 seedlings were transferred to fresh medium containing 1 µM *rac*-GR24 or to control medium (MOCK). Root samples were taken **(A)** after 6 h of treatment, **(B)** after 2 h of treatment, and **(D)** in a time series of 0 h, 6 h, 24 h, and 48 h of treatment. **(C)** Also the expression of *TMO5L1* in *max2* was determined compared to the WT, both grown in the absence of *rac*-GR24. The relative gene expression was determined via qRT-PCR and the expression level was normalized via *ACTIN* (*ACT2*). Means of three independent biological repeats are presented and error bars represent the standard error (SE) of these three independent repeats. Asterisks indicate statistically significant differences compared to the MOCK treatments (* $P < 0.05$; ** $P < 0.01$; *** $P < 0.001$; A to C, Student's *t*-test; D, ANOVA-mixed model).

Because of the recent findings that *rac*-GR24 is not strigolactone specific and can activate signaling via both D14 and KAI2 through MAX2, the question was raised whether the *rac*-GR24 effect on the *TMO5L1* expression was mediated via D14 or via KAI2. To get an initial insight, qRT-PCR was applied on root tissue of WT, *max2*, *d14*, *kai2*, the *d14;kai2* double mutant, and a *MAX2*-overexpressing line grown for 5 days. Confirming the previous data, the *TMO5L1* expression was higher in the *max2* mutant than in the WT and, accordingly, the *MAX2* overexpression caused a slight repression of the *TMO5L1* expression (Figure 3). An increased expression could also be observed in the *d14* mutant background, but not as high as in the *max2* mutant, whereas the expression level in *kai2* was the same as that in the WT (Figure 3). Only in the *d14;kai2* double mutant, the upregulation was as high as in *max2* (Figure 3). As such, this data suggests that the *TMO5L1* expression might be regulated via the signaling pathway that goes via D14 to MAX2, although a certain redundancy of KAI2 cannot be excluded.

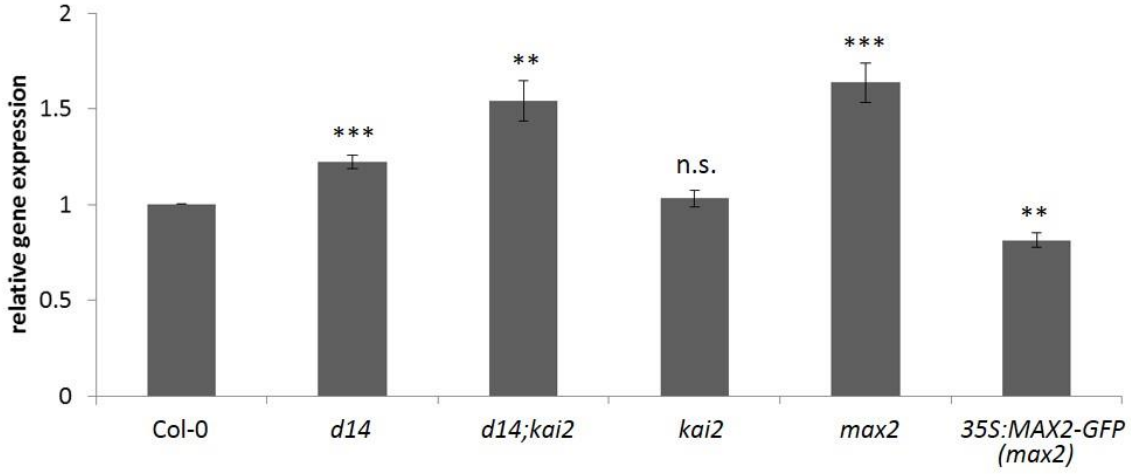

Figure3. Expression of *TMO5L1* in the root of the different SL signaling mutants. Plants of *Col-0*, *d14*, *kai2, d14;kai2, max2,* and a *MAX2*-overexpressing line in *max2* (*35S:MAX2-GFP (max2)*) were grown for 5 days and root samples were harvested. The relative gene expression was determined via qRT-PCR and the expression level was normalized via ACTIN (ACT2). Error bars represent the standard error (SE) of three independent biological repeats. Asterisks indicate statistically significant differences compared to the WT (Col-0) (** *P* <0.01; *** *P* <0.001; one-way ANOVA)

4.2.2. Overexpression of *TMO5L1* results in a large overlap with the *rac*-GR24-related transcriptome

To get a general insight into the effects of *TMO5L1* on the transcriptome, we analyzed the *TMO5L1*-overexpressing line *35S*:*TMO5L1-GFP* (*TMO5L1-OX*) via RNA-seq (E. Russinova, unpublished). With a FC cutoff of 1.2 and $P < 0.05$, overexpression of *TMO5L1* resulted in the differential expression of 3,144 genes, of which 1,869 were upregulated and 1,275 were downregulated (Supplementary Dataset 1). With a FC cutoff of 2 and $P < 0.05$, 716 genes were differentially expressed (440 upregulated, 276 downregulated). Because of the known role for TMO5L1 in vascular development, it was first analyzed if the known target genes of TMO5L1 in this process were also present in this dataset (*LOG3*, *LOG4*, *SAC51*, *SACL1*, *SACL2* and *SACL3*). Indeed, both *SAC51* (FC of 1.27) and *SACL3* (FC of 2.25) were found to be differentially expressed (Supplementary Dataset 1). For the *LOG* genes no differential expression was detected, which is in agreement with earlier findings that only a combined overexpression of TMO5L1 and LHW results in *LOG* induction; whereas for TMO5, only overexpression of TMO5 is sufficient to induce *LOG* gene expression (De Rybel et al., 2014; Ohashi-Ito et al., 2014).

Several datasets, which are broadly comparable to the setup of our TMO5L1-OX dataset, have been published: (i) inducible combined overexpression of TMO5L1 and LHW in plant cell culture (Ohashi-Ito et al., 2014); (ii) inducible overexpression of TMO5 (selective harvest of root tips) (De Rybel et al., 2014); and (iii) inducible overexpression of TMO5 combined with cycloheximide (CHX) treatment to enrich for primary response genes (selective harvest of root tips) (De Rybel et al., 2014). In order to compare the content of these datasets, an overlap of differentially expressed genes (with a FC cutoff of 2 and $P < 0.05$ for all datasets) was generated (Figure 4). The gene content of the most important overlaps can be retrieved in Supplementary Table 1.

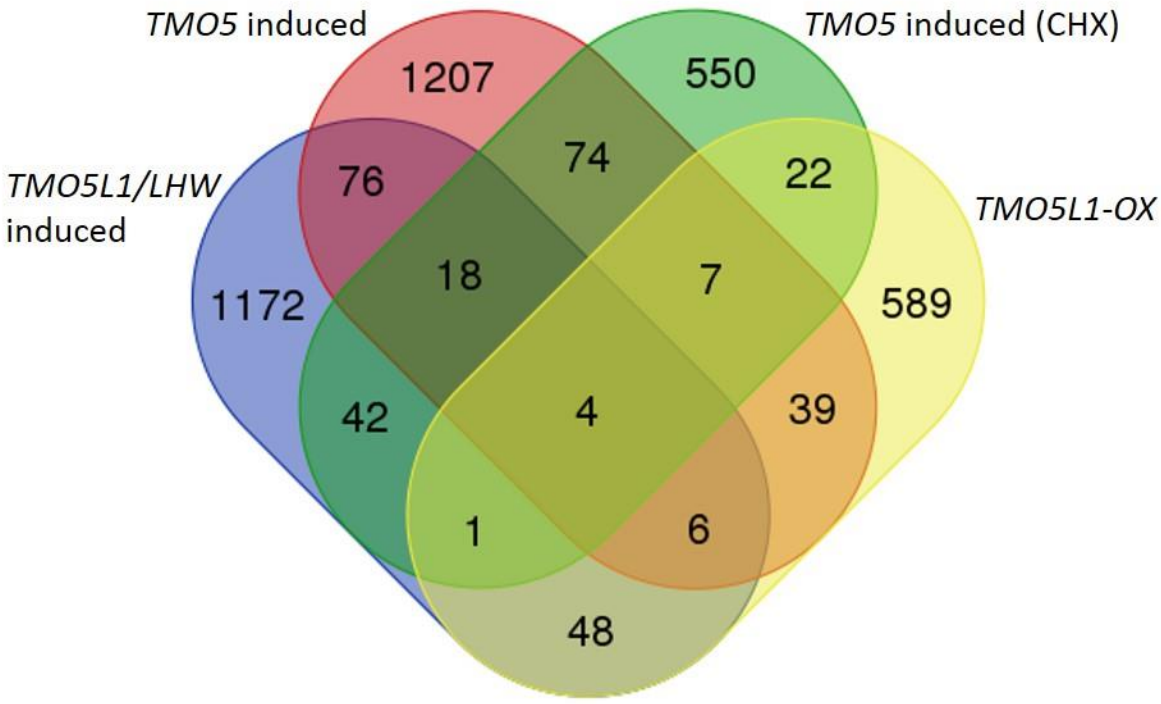

Figure 4. Overlap of the existing datasets related to the *TMO5L1-OX* dataset. Genes in the datasets were selected based on a FC cutoff of 2 and *P*-value < 0.05. Gene content of the *TMO5L1-OX* dataset was compared to three broadly related datasets: (i) inducible combined overexpression of *TMO5L1* and *LHW* in plant cell culture (*TMO5L1/LHW* induced) (Ohashi-Ito et al., 2014); (ii) inducible overexpression of *TMO5* with selective harvest of root tips (*TMO5* induced) (De Rybel et al., 2014); and (iii) inducible overexpression of *TMO5* combined with CHX treatment to enrich for primary response genes with selective harvest of root tips (*TMO5* induced (CHX)) (De Rybel et al., 2014).

In general, the majority of genes in all four datasets are unique for that specific dataset (Figure 4). This could potentially be because of the use of different tissues (cell cultures vs. whole plants vs. root tips), different gene constructs (*TMO5*, *TMO5L1*, *TMO5l1* + *LHW*) and inducible vs. constitutive overexpression of that gene construct. Clearly, there are also considerate amounts of overlaps between the different datasets, with ultimately 4 genes shared between all datasets (Figure 4). *SACL3* was one of these 4 genes, a downstream target of TMO5 and TMO5L1 in the regulation of vascular development (Katayama et al.,

2014; Vera-Sirera et al., 2014). As indicated above, also *SAC51* could have been part of this overlap, but this gene was in the TMO5L1-OX dataset induced only 1.27 times (< FC 2).

To generate an overview of the affected processes by TMO5L1-OX, we visualized the dataset with the MapMan software (Figure 5). Clearly, *TMO5L1-OX* had a large negative impact on photosynthesis, as various genes involved in light reactions and chlorophyll (tetrapyrrole) synthesis were downregulated when compared to the WT (Figure 5; Supplementary Table 2). Also many genes involved in the secondary metabolism were affected by *TMO5L1*-OX, of which the majority of the genes were upregulated in comparison with the WT (Figure 5; Supplementary Table 2). When the gene content of the published TMO5L1-related datasets was visualized, genes involved in the light reactions and secondary metabolism were also present, but not as many as in the *TMO5L1-OX* dataset, which could indicate that the *TMO5L1-OX* dataset is enriched for secondary effects (Supplementary Figure 2).

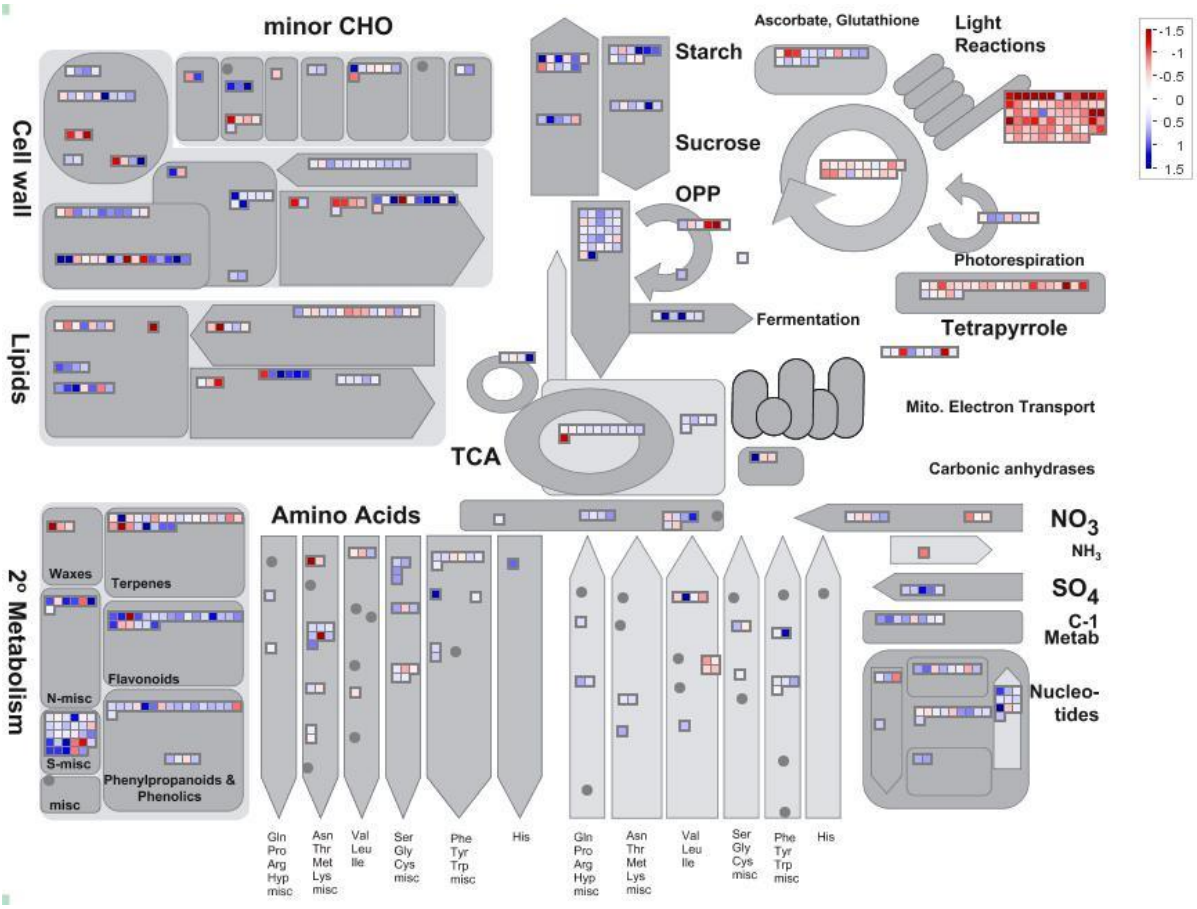

Figure 5. General overview of the transcriptomic changes after *TMO5L1*-OX. MapMan-generated overview that summarizes the cellular processes that were perturbed after *TMO5L1* overexpression. Each square represents one gene. Color coding according to the LOG2 scale: blue and red, upregulated and downregulated, respectively. For the gene identity, see Supplementary Table 2.

Interestingly, when the *TMO5L1-OX* dataset was compared with the datasets either of *rac*-GR24-treated root tissue or of the *max2* roots compared to the WT (Chapter 3), an enriched overlap in gene content could be observed in both cases (Figure 6). As such, 42% of the genes that were differentially expressed in the WT by the *rac*-GR24 treatment were also differentially expressed by the *TMO5L1-OX*, an enrichment which is statistically significant ($P = 5.2E^{-11}$) (Figure 6A; Supplementary Table 3). Similarly, 25% of the genes, of which the expression was distorted in the *max2* roots, were also distorted in the *TMO5L1-*

OX, an enrichment which is also statistically significant (P = 1.9E^{-13}) (Figure 6B; Supplementary Table 4). On the other hand, the *rac*-GR24-treated WT and the *max2*-MOCK dataset only had a small overlap with the published TMO5L1-related datasets, and were not statistically significant enriched (Supplementary Figure 3). This could indicate that the overlap with the SL-related datasets might consist of indirect effects of constitutive *TMO5L1-OX*. Alternatively, it is also possible that the genes in the overlaps are specifically differentially expressed by only overexpressing *TMO5L1*, and not by the combination of *TMO5L1* and *LHW* or by *TMO5*.

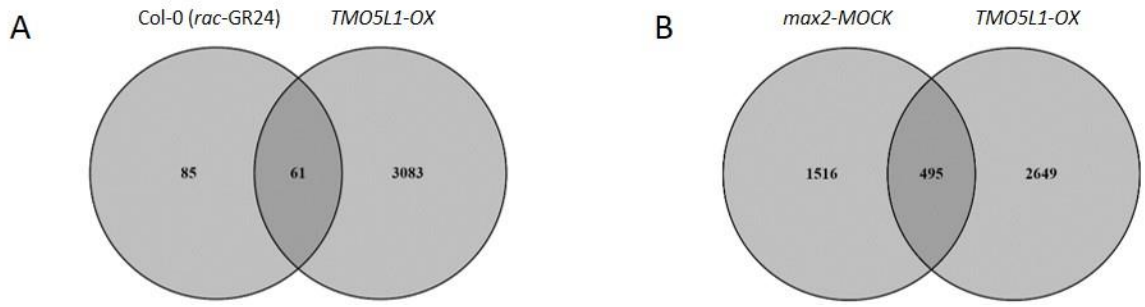

Figure 6. Overlap of differentially expressed genes between the *TMO5L1* overexpression RNA-seq dataset and the SL-related RNA-seq datasets. (A) Overlap between the set of differentially expressed genes in the WT root after *rac*-GR24 treatment and after *TMO5L1* overexpression. **(B)** Overlap between the set of differentially expressed genes in the root of *max2* under normal growth conditions and after *TMO5L1* overexpression. Statistical analysis of the overlap was done with a one-sided Fisher Exact test. Genes were selected based on a FC cutoff of 1.2 and a *P*-value < 0.05.

As the *rac*-GR24 treatment resulted in a strong downregulation of *TMO5L1*, genes that were differentially expressed in the *rac*-GR24 treated WT dataset and the *TMO5L1-OX* dataset are expected to have an opposite expression pattern: upregulated by *rac*-GR24 and downregulated by the *TMO5L1-OX*, and vice versa. Indeed, more than half of the overlapping genes followed this criterion: 36 genes had an opposite and 25 had a similar expression pattern in both datasets (Supplementary Table 3). Inversely,

because the *max2* mutant was hallmarked with an induced expression of *TMO5L1*, the genes in the overlap between this dataset and the *TMO5L1*-OX dataset are foreseen to behave similarly. Almost half of the overlapping genes (239 of 495) followed the expected expression pattern, whereas 256 genes had the opposite one (Supplementary Table 4).

When the overlap between the *rac*-GR24 dataset and the *TMO5L1*-OX dataset was visualized, an enrichment for genes related to light reactions was apparent (Figure 7, top panel). These genes were upregulated after the *rac*-GR24 treatment and downregulated in *TMO5L1*-overexpressing plants. Also genes involved in flavonoid biosynthesis were common but were upregulated in the two datasets (Figure 7, top panel). Furthermore, also an overlap between the *max2* dataset and the *TMO5L1* overexpression dataset was visualized (Figure 7, bottom panel). Common genes in the secondary metabolism and, more specifically, in flavonoid synthesis occurred (Figure 7, bottom left panel). These genes were downregulated in *max2*; but upregulated in the *TMO5L1-OX*. However, in the published TMO5L1-related datasets, genes related to light reactions and secondary metabolism were present but not as enriched as in the *TMO5L1-OX* dataset (Supplementary Figure 2). As indicated above, this could mean that the enrichment for these genes in the *TMO5L1-OX* dataset might be in part the result of secondary responses. For this we analyzed a Chromatin immunoprecipitation (ChIP)-seq dataset of *TMO5L1-OX* that contains putative primary targets of TMO5L1 (Supplementary Table 5; E. Russinova, unpublished results). Comparing these putative primary targets with the genes that are differentially expressed by *rac*-GR24 in the WT, shows an overlap of 19 genes (Supplementary Table 6). From these, two are related to light harvesting: *CHLOROPHYLL A/B BINDING PROTEIN 3* (*AT1G29910*) and a *RIBULOSE BISPHOSPHATE CARBOXYLASE FAMILY PROTEIN* (*AT5G38410*). However, no genes related to secondary metabolism were retrieved as putative primary targets of TMO5L1 in the *rac*-GR24-treated WT dataset (Supplementary Table 6).

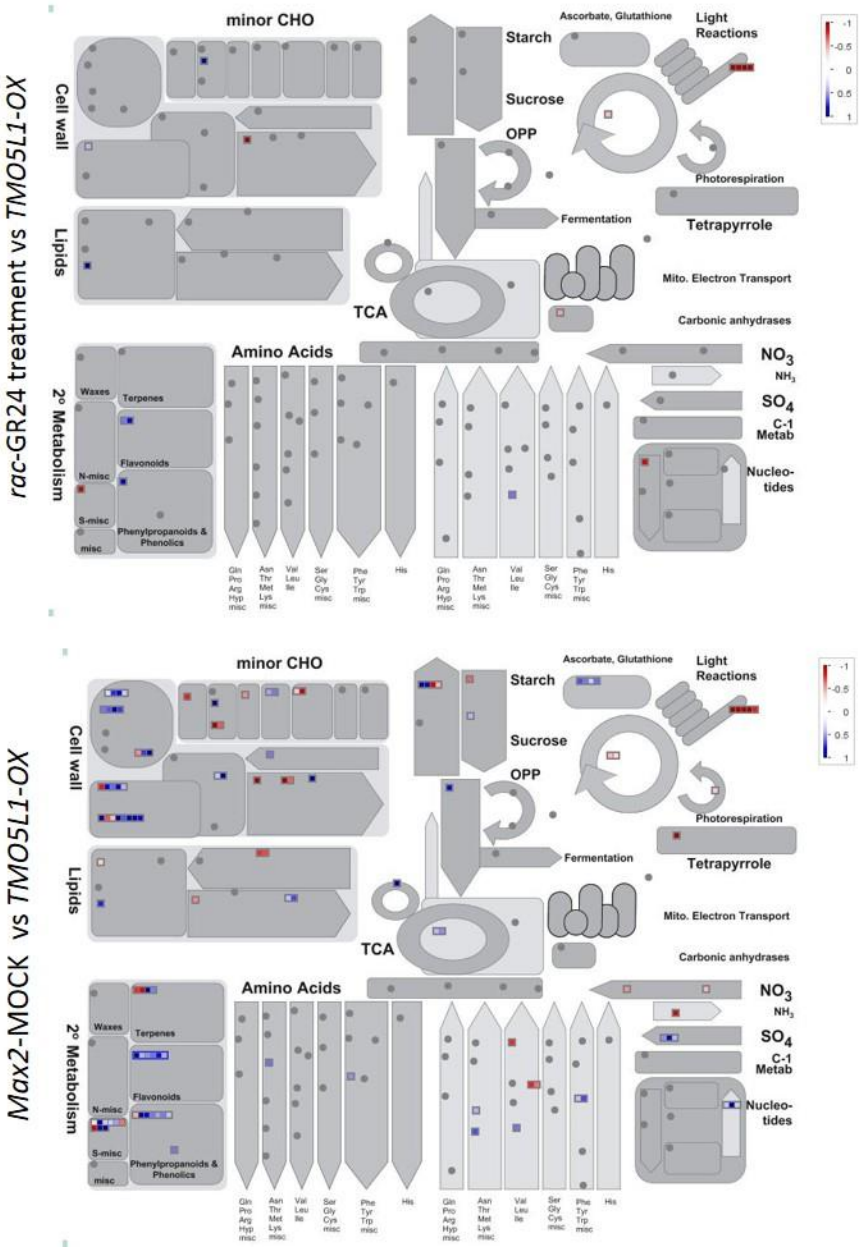

Figure 7. General overview of the overlap of differentially expressed genes between the *TMO5L1* overexpression and the SL-related RNA-seq datasets. MapMan-generated overview that summarizes the cellular processes that were common in the transcriptomes of the *rac*-GR24-treated WT and the overexpression of *TMO5L1* **(top panels)** and the cellular processes common in the transcriptomes of the *max2* root under normal growth conditions and the overexpression of *TMO5L1* **(bottom panels)**. Each square represents one gene. Color coding according to the LOG2 scale of the SL-related datasets: blue and red, upregulated and downregulated, respectively. For the gene identity, see Supplementary Tables 3 and 4.

In conclusion, many genes that are differentially expressed after *rac*-GR24 treatment or genes that are differentially expressed in *max2* roots compared to the WT, also have a distorted expression pattern when *TMO5L1* is overexpressed. From these common genes, only a few processes appeared to be enriched, namely photosynthesis and flavonoid synthesis. However, the majority of these genes might not be primary targets of TMO5L1. Nonetheless, because of the strong response of *rac*-GR24 on the expression of *TMO5L1*, a further investigation for a role for TMO5L1 in the SL responses in the root is justified.

4.2.3. Subcellular localization and expression pattern analysis of TMO5L1

TMO5L1 encodes a member of the bHLH family and, as such, probably acts as a TF in the nucleus. To verify this assumption, we determined its subcellular localization by means of a transgenic *35S:TMO5L1-GFP*-overexpressing line (*TMO5L1-OX*). In addition, we also checked whether *rac*-GR24 could have a direct impact on the subcellular localization or protein stability of TMO5L1 by treating *TMO5L1-OX* seedlings with 1 µM *rac*-GR24. Confocal microscopy images confirmed the nuclear localization of TMO5L1 (Figure 8). No difference in intensity or in localization could be observed between the *rac*-GR24-treated and untreated seedlings, indicating that *rac*-GR24 might not influence the stability or the subcellular localization of TMO5L1 (Figure 8). Regarding the GFP expression domain of this overexpressing line, it should be noted that it does not seem to correspond to the expression domain of a *35S*-promoter. This observation should be reanalyzed, but if this would be truly the case, it might provide an additional reason for the relative low overlap with the published *TMO5L1*-related datasets or might possibly even question the validity of the *TMO5L1-OX* dataset.

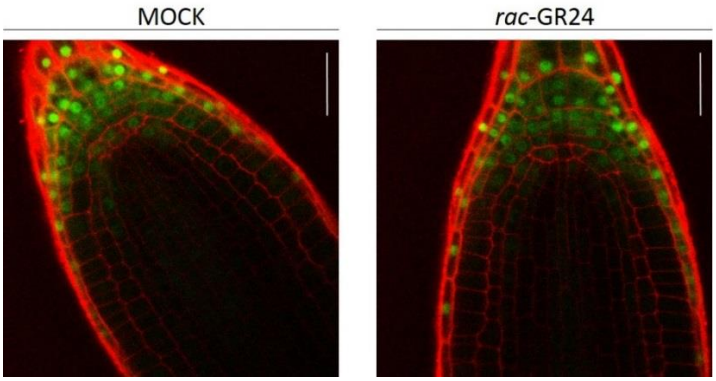

Figure 8. Subcellular localization of TMO5L1 in root tip cells. Five-day-old seedlings of a *35S:TMO5L1-GFP (TMO5L1-OX)* line were transferred for 6 h to fresh medium supplemented with 1 µM *rac*-GR24 or to control medium. The expression of the construct was visualized in the root tip by confocal laser scanning microscopy. Propidium Iodide (PI) was used to stain the cell wall. Bars = 20 µm.

Next, we examined the endogenous expression pattern of TMO5L1 in the root with a transgenic line containing a *pTMO5L1:TMO5L1-YFP* construct. In line with previous reports, a faint and nuclear localized expression could be detected in the prevascular bundle of the apical root meristem (Figure 9A) (De Rybel et al., 2013). In addition to the root tip, *TMO5L1* appeared to be also specifically expressed in LR primordia. The expression was visible from the early stages of LR primordia development on and persisted until LR emergence (Figures 9C, 9E, 9G, 9I, and 9K). This expression pattern was roughly consistent with the transcriptional high-resolution spatiotemporal expression pattern and the gravistimulus-induced LR expression pattern of *TMO5L1* that are available via the e-FP-browser (Figures 10 and 11) (Winter et al., 2007; http://bbc.botany.utoronto.ca/efp). To determine whether *rac*-GR24 influences the protein level of TMO5L1, seedlings containing the *pTMO5L1:TMO5L1-YFP* construct were treated for 24 h with 1 µM *rac*-GR24. However, no difference in intensity could be observed between the treated and the untreated plants, not in the root tip (Figures 9A and 9B), nor during any stages of LR primordia development (Figures 9C-9L).

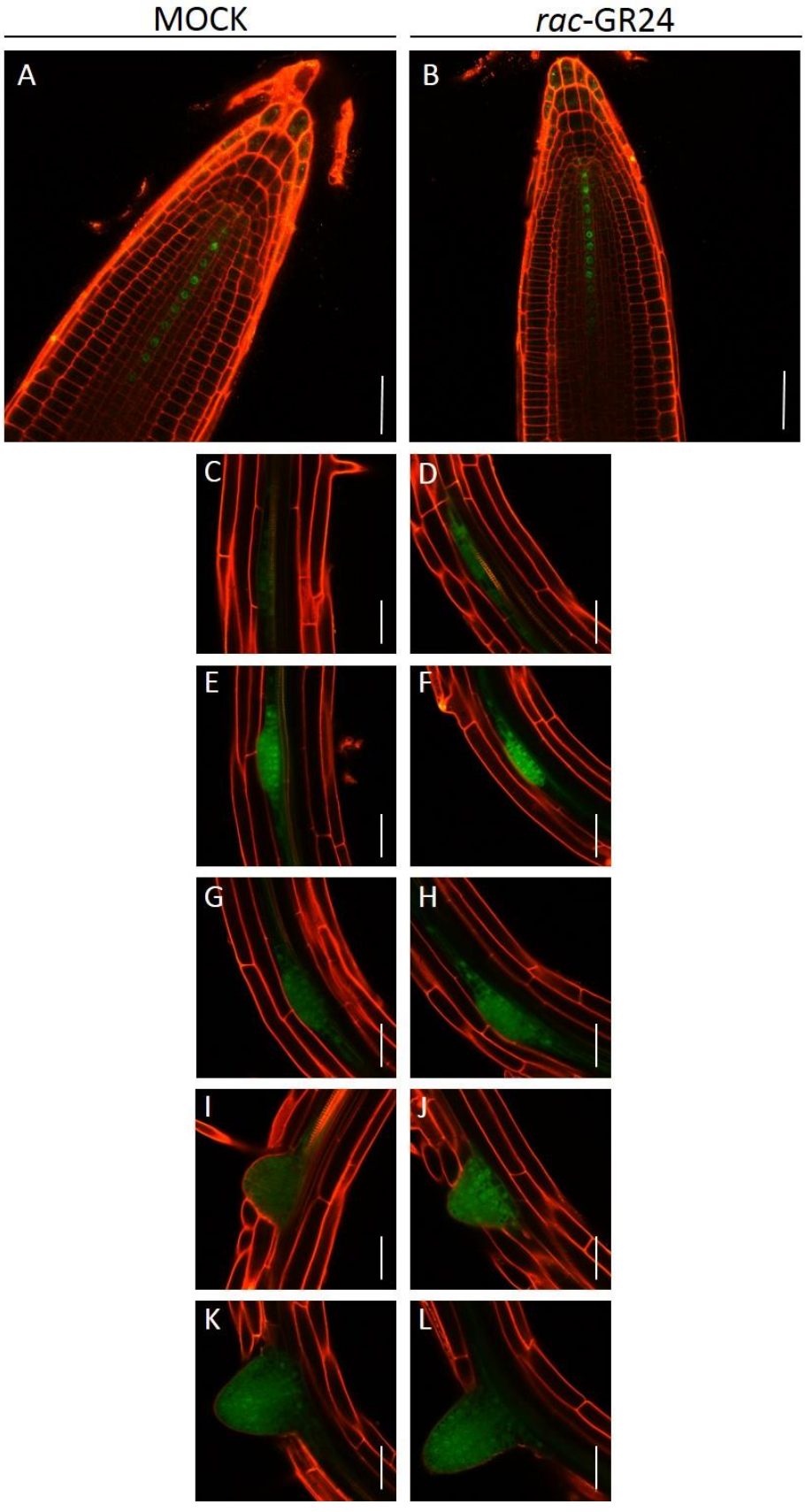
MOCK
rac-GR24
A
B
C
D
E
F
G
H
I
J
K
L

Figure 9. Endogenous expression pattern analysis of TMO5L1 in the root. Five-day-old seedlings of a *pTMO5L1:TMO5L1-YFP* line were transferred for 24 h to fresh medium supplemented with 1 µM *rac*-GR24 or to control medium. The expression was visualized by confocal laser scanning microscopy. **(A and B)** The expression of TMO5L1 with *pTMO5L1:TMO5L1-YFP* plants in the root tip **(A)** under control conditions or after *rac*-GR24 treatment **(B)**. **(C to L)** Expression of *TMO5L1* in *pTMO5L1:TMO5L1-YFP* plants during different stages of LR development under control conditions **(C, E, G, I, and K)** and after *rac*-GR24 treatment **(D, F, H, J, and L)**. Propidium Iodide (PI) was used to stain the cell wall. Bars = 30 µm.

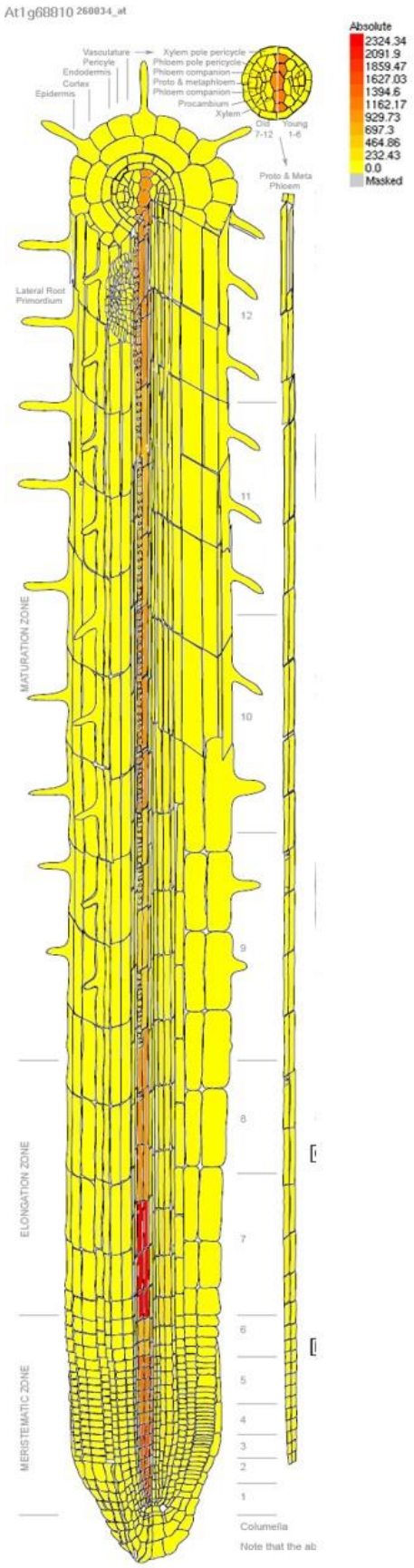
At1g68810 260834_at
Absolute
2324.34
2091.9
1859.47
1627.03
1394.6
1162.17
929.73
697.3
464.86
232.43
0.0
Masked
Vasculature
Pericyle
Endodermis
Cortex
Epidermis
Xylem pole pericycle
Phloem pole pericycle
Phloem companion
Proto & metaphloem
Phloem companion
Procambium
Xylem
Old
7-12
Young
1-6
Proto & Meta
Phloem
Lateral Root
Primordium
MATURATION ZONE
ELONGATION ZONE
MERISTEMATIC ZONE
12
11
10
9
8
7
6
5
4
3
2
1
Columella
Note that the ab

Figure 10. High-resolution transcriptional spatiotemporal map of *TMO5L1*. Root material from 5-to 6-day-old seedlings (radial data) or 7-day-old seedlings (longitudinal data) was collected by fluorescence-activated cell sorting or sectioning (Brady et al., 2007). Spatiotemporal expression levels were imputed with an EM algorithm (Cartwright et al., 2009). Data are normalized by the GCOS method, TGT value of 100. Figure adapted from e-FP Browser (Winter et al. 2007; http://bar.utoronto.ca/efp/development/).

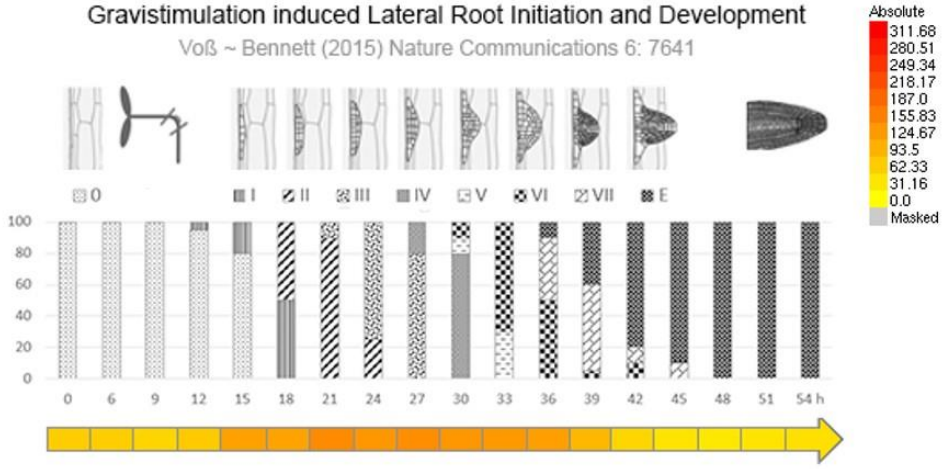

Figure 11. Expression of *TMO5L1* during gravistimulation-induced LR development. Col-0 seedlings were grown vertically on half-strength Murashige and Skoog medium in square Petri dishes for 3 days. LR induction was obtained by rotating the plates by 90 degrees. For each time point, a root segment corresponding to the bend was microdissected for RNA extraction. A mature root segment located between the bend and the shoot was harvested 9 h after gravistimulation to serve as a reference of nongravitropically stimulated root tissues devoid of LR initiation (time point 0 in the dataset) (Voβ et al., 2015). Data are normalized by the GCOS method, TGT value of 100. Figure adapted from e-FP Browser (Winter et al., 2007; http://bar.utoronto.ca/efp/development/).

4.2.4. Investigation of the *rac*-GR24-mediated effect on LR density in TMO5L1-related mutants

SLs are known to modulate the root system architecture, with one of the most pronounced effects the MAX2-dependent reduction in LRD (Kapulnik et al., 2011a; Ruyter-Spira et al., 2011). As *rac*-GR24 strongly downregulated the *TMO5L1* expression in the root and the TMO5L1 protein was specifically produced during the various stages of LR development, the effect of *rac*-GR24 on a mutant and overexpression line of *TMO5L1* was investigated. Additionally, because of a possible redundancy with *TMO5,* a double *tmo5;tmo5L1* mutant was also analyzed. The root system architecture of *tmo5l1*, *tmo5*, *tmo5;tmo5l1,* and the *TMO5L1*-OX was examined upon treatment with *rac*-GR24 (Figure 12). The primary root length of *tmo5l1* and the *tmo5;tmo5l1* double mutant, but not of *tmo5,* was shorter than that of the WT under normal growth conditions (Figures 12A, 12C, and 12E). A reduction in the primary root length was also observable in the *TMO5L1-OX* line.

Treatment with *rac*-GR24 is known to modulate the primary root length (Ruyter-Spira et al., 2011; Shinohara et al., 2013). In our hands, the reduction was very minor and could only be observed in the experiment where TMO5L1-OX plants were analyzed (Figure 12G). Nevertheless, also the *TMO5L1-OX* line had a decreased primary root length after treatment with *rac*-GR24 (Figure 12G).

Regarding the LRD phenotype, the LRD of *tmo5*, *tmo5l1,* and *tmo5;tmo5l1* was slightly smaller than that of the WT under normal growth conditions (Figures 12B, 12D, and 12F). Moreover, after treatment with *rac*-GR24, the LRD in *tmo5l1* had decreased by 47%, a reduction significantly higher than the 34% in the WT ($P < 0.01$), hinting at a hypersensitivity toward *rac*-GR24 (Figure 12B). In contrast, the LRD reduction after treatment with *rac*-GR24 treatment was similar for *tmo5* (54%) and the WT (50%) (Figure 12D). However, in the *tmo5;tmo5l1* double mutant, the *rac*-GR24 treatment resulted in a higher reduction in LRD (67%) than that in the WT (42%) ($P < 0.001$), indicative of hypersensitivity of the double

mutant to *rac*-GR24 (Figure 12F). Interestingly, the LRD reduction of *the 35S*:*TMO5L1-GFP* line was also higher after *rac*-GR24 than that of the WT (51% vs. 35%; $P < 0.01$) (Figure 12H). It should be noted that the *tmo5l1* mutant is in Nossen (No-0) background and not in Col-0. As such, the results should be confirmed with a proper control in the future.

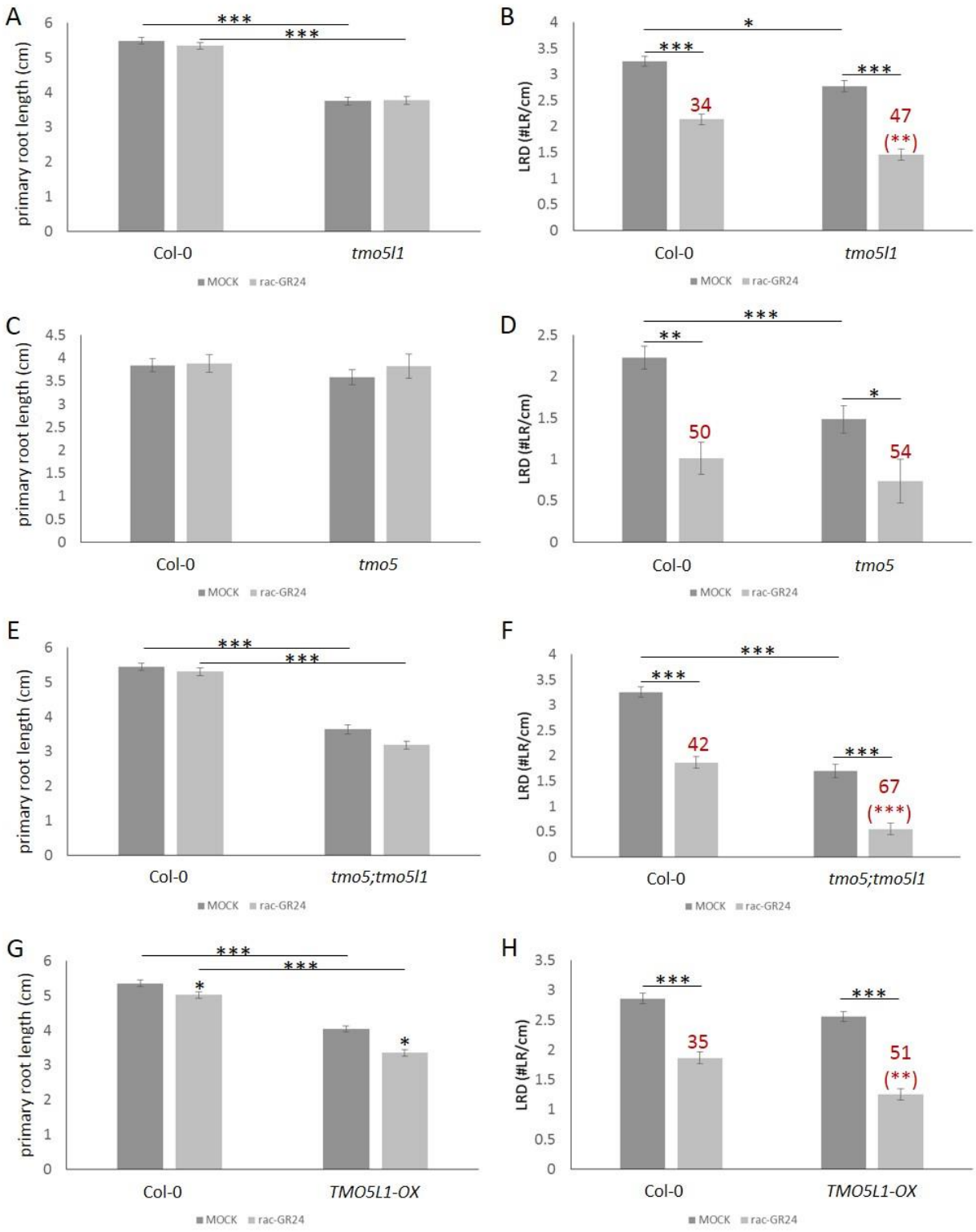

Figure 12. Effects of *rac*-GR24 on the root system architecture of *TMO5L1*-related mutants. Primary root length of *tmo5l1* **(A)**, *tmo5* **(C)**, *tmo5;tmo5l1* **(E),** and *35S*:*TMO5L1-GFP* **(G)** upon *rac*-GR24 treatment. LRD of *tmo5l1* **(B)**, *tmo5* **(D)**, *tmo5;tmo5l1* **(F),**

and *35S*:*TMO5L1-GFP* **(H)** upon *rac*-GR24 treatment. Data presented are means ± SE of three biological repeats ($n > 20$). Asterisks indicate statistically significant differences (* $P < 0.05$; ** $P < 0.01$; *** $P < 0.001$; ANOVA-mixed model for the primary root length; Poisson regression model for the LRD and LRD reductions). Numbers in far red in panels B, D, F and H indicate percentage of LRD reduction as compared to the MOCK grown control for each genotype. Asterisks in far red in panels B, D, F and H indicate statistical significant differences in LRD reduction between the WT control and the respective mutant (also indicated in the text).

In summary, lack of *TMO5L1* (and *TMO5*) expression resulted in various aberrations in root development and to hypersensitivity to *rac*-GR24 responses in the root regarding the effect on the LRD. As such, the data suggest that TMO5L1 might have an important function in the control of the *rac*-GR24-mediated effect on LR development.

4.2.5. The role of TMO5/TMO5L1 in the *rac*-GR24-regulated effect on flavonol biosynthesis gene expression in the root

Besides an effect on the root architecture, treatment with *rac*-GR24 also results in the upregulation of transcript and protein levels of various flavonol biosynthesis genes and accumulation of flavonols in the root (Walton et al., 2016). To examine whether *TMO5L1* is also involved in the control of this process, we determined the transcript levels of two key flavonol biosynthetic genes, *CHALCONE SYNTHASE* (*CHS*) and *FLAVONOL SYNTHASE* (*FLS*) in the *tmo5l1* and *tmo5;tmo5l1* mutants and the *TMO5L1-OX* line treated or not with *rac*-GR24 for 24 h (Figure 13).

In agreement with Walton et al. (2016), the expression of both genes was upregulated after *rac*-GR24 treatment in the WT (Figure 13). For *CHS*, but not for *FLS*, the expression level in the absence of *rac*-GR24 was higher in the *TMO5L1-OX* line than that in the WT, as was also the case for both genes in the *tmo5;tmo5l1* double mutant (Figure 13). Next, we investigated whether the expression changed after *rac*-

GR24 treatment and found that the upregulation of these genes, as seen in the WT, was not present in the *TMO5L1-OX* line nor in one of the mutants (Figure 13).

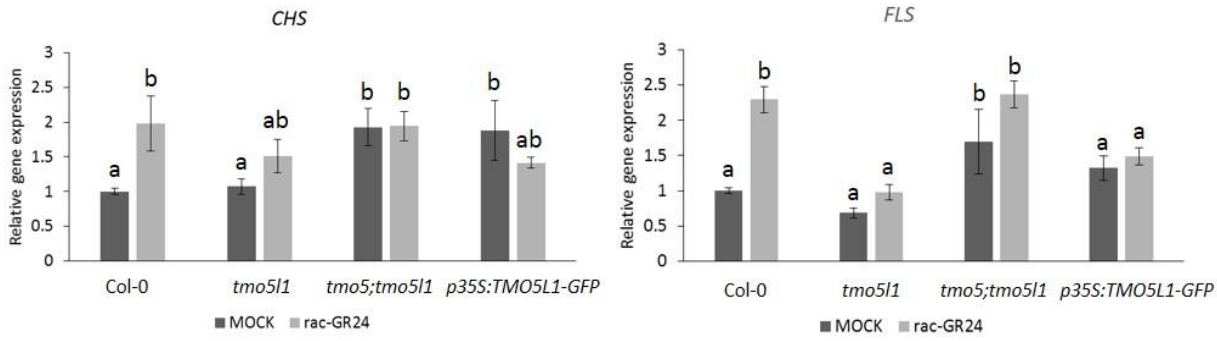

Figure 13. Effect of *rac*-GR24 treatment on the relative gene expression of key flavonol biosynthesis genes in the root of *TMO5L1*-related mutants. Five-day-old Col-0, *tmo5l1*, *tmo5;tmo5l1*, and *TMO5L1*-overexpressing (*35S*:*TMO5L1-GFP*) seedlings were transferred to fresh medium containing 1 µM *rac*-GR24 or to control medium (MOCK). Root samples were taken after 24 h of treatment. The relative gene expression of *CHS* **(A)** and *FLS* **(B)** was determined via qRT-PCR and the expression level was normalized via *ACTIN* (*ACT2*). Means of three independent biological repeats are presented. Error bars represent the standard error (SE). Letters above bars indicate statistically significant differences (bars with no common letter are significantly different from each other; ANOVA mixed model).

4.2.6. TMO5L1 is probably not implicated in the *rac*-GR24-mediated reduction of the hypocotyl

Besides reducing the LRD, treatment with *rac*-GR24 is also known to decrease the hypocotyl elongation of seedlings grown under continuous red light (Nelson et al., 2011). Recently, signaling mediated by D14 as well as KAI2 has been found to be involved in the regulation of this process, although only the *kai2,* but not the *d14,* mutant exhibits an elongated hypocotyl in the absence of exogenous *rac*-GR24 (Scaffidi et al., 2014). To determine whether *TMO5L1* also plays a role in the control of this *rac*-GR24 phenotype, we grew *tmo5l1* and *tmo5;tmo5l1* mutant plants and the *35S*:*TMO5L1-GFP* line in the

presence and absence of *rac*-GR24 under continuous red light, along with the *rac*-GR24 signaling mutants *max2*, *d14*, *kai2* and the double mutant *d14;kai2* (Figure 14).

When the hypocotyl length is considered in the absence of *rac*-GR24, the hypocotyl length was obviously longer in *max2*, *kai2,* and the *kai2;d14* double mutant than that in the WT, whereas it was indistinguishable from the WT in *d14*, corresponding with previous findings (Figure 14) (Waters et al., 2012; Toh et al. 2014) and in *tmo5l1* as well, but it was slightly shorter in *tmo5;tmo5l1* and the *35S*:*TMO5L1-GFP* than that in the WT (Figure 14). In the presence of *rac*-GR24, the hypocotyl length was clearly reduced in the WT (Figure 14). Both receptor mutants *d14* and *kai2* were also still responsive to *rac*-GR24, but only the *d14;kai2* double mutant and *max2* were fully insensitive to the *rac*-GR24 treatment, confirming previous data (Waters et al., 2012; Toh et al. 2014) (Figure 14). *tmo5l1* and the double mutant *tmo5;tmo5l1* displayed a sensitivity to *rac*-GR24, but, in contrast to the effects on the LRD, these mutants had no hypersensitive response (Figure 14).

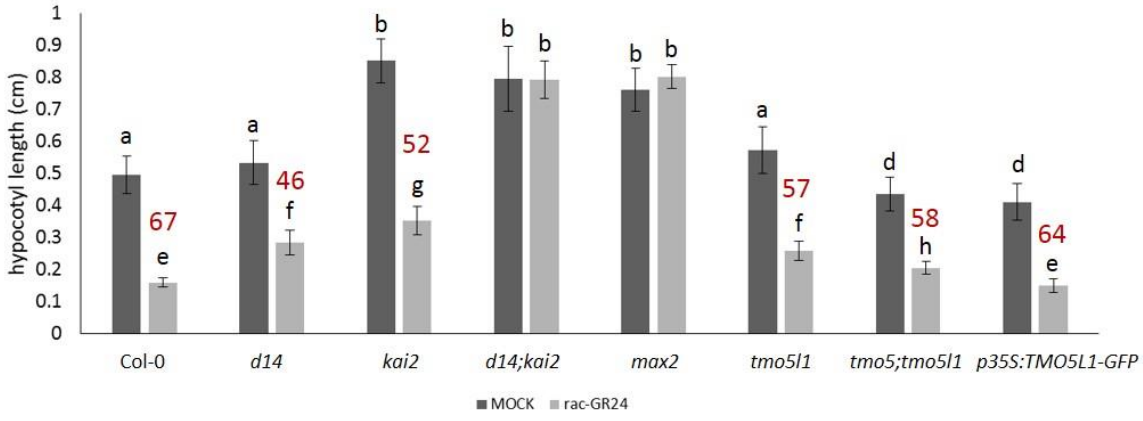

Figure 14. hypocotyl assay for *TMO5L1*-related mutants. Seeds of Col-0, *d14, kai2, d14;kai2, max2, tmo5l1, tmo5;tmo5l1,* and *TMO5L1-OX* were sown on half-strength Murashige and Skoog medium without sucrose, supplemented or not with 1 µM *rac*-GR24. After stratification, plates were exposed to white light for 3 h, followed by incubation in the dark for an additional 21 h, and ultimately to red light for 4 days. Graphs represent means of three biological repeats (n > 25). Error bars represent the standard error (SE). Letters above bars indicate statistically significant differences (bars without common letter are significantly different from each other; ANOVA-mixed model), numbers in far red indicate percentage of reduction of hypocotyl length.

4.3. Discussion

In the last years, a lot of research has been focused on unraveling the SL signaling network. Although considerate amount of progress has been made in recent years, further downstream signaling events leading to the various physiological responses are still lacking. Here, we report on the characterization of TMO5L1, a TF that likely plays a role in the SL-regulated root responses.

In a previous RNA-seq experiment on *Arabidopsis* roots treated with 1 µM *rac*-GR24, *TMO5L1* had emerged as a strongly downregulated gene. This MAX2-dependent downregulation was confirmed by qRT-PCR and persisted from 6 h until at least 48 h of treatment (Figure 2). This negative impact of the *rac*-GR24 treatment on the *TMO5L1* expression was also noted after 2 h of treatment, albeit not so strong as after 6 h (Figure 2). In comparison with other plant hormones, this event could be considered as fairly late, because for many hormones, the first transcriptional events happen within several minutes after treatment as illustrated with the jasmonate responses (Pauwels et al., 2010). The signaling cascade of SLs is not initiated so rapidly. Indeed, the degradation of the direct target proteins SMXL6, SMXL7, and SMXL8 occurs only 30 minutes to 1 hour after treatment (Zhao et al., 2013; Soundappan et al., 2015; Wang et al., 2015). As such, the downregulation of *TMO5L1* might be a primary response after SL perception and target degradation. This possibility can be investigated by the addition of the protein synthesis inhibitor cycloheximide (CHX) (Roig-Villanova et al., 2006). If the *rac*-GR24-triggered downregulation would still take place in the presence of CHX, no additional protein synthesis would be required and, hence, *TMO5L1* would be a primary target. However, a complication might be the relatively slow SL signaling cascade, because a CHX application longer than 2 h can be considered as toxic for plants (L. Pauwels, personal communication) and combined with the relatively weak *TMO5L1* downregulation after 2 h of *rac*-GR24 treatment would hinder the readout. Nevertheless, a direct target, of which the expression is downregulated by *rac*-GR24, is not in line with the current working hypothesis of the SL signaling pathway.

The SMXL family (the direct protein targets) contain an EAR motif known to be an active repression motif that mediates the interaction with TOPLESS (TPL) or members of the TPL RELATED (TPR) family (Kagale and Rozwadowski, 2011; Soundappan et al., 2015; Wang et al., 2015). Thus, the SMXL proteins are suggested to act as negative transcription regulators and, hence, SL-induced degradation of the SMXL proteins would induce, rather than repress transcription. This hypothesis implies that either the *TMO5L1* downregulation by *rac*-GR24 is not a direct transcriptional target, or that an alternative pathway, independent of the EAR domain of the SMXL proteins, is at play to regulate the *TMO5L1* expression. Indeed, recently, the EAR domain of the SMXL proteins has been demonstrated to be required for most, but not all, SL-regulated phenotypes, indicating that also EAR-independent mechanisms play a role (Liang et al., 2016).

Analysis of the *35S:TMO5L1-GFP* and *pTMO5L1:TMO5L1-YFP* lines confirmed the nuclear localization of TMO5L1, as expected for an (active) TF (Figures 8 and 9) (De Rybel et al., 2013; An et al., 2014). We could show that the TMO5L1 protein is not posttranslationally regulated by *rac*-GR24 nor that its subcellular localization is influenced by *rac*-GR24. TMO5L1 has been previously reported to be specifically expressed in the xylem precursor cells of the root apical meristem, in agreement with its role in controlling vascular cell division and differentiation (Figure 9) (De Rybel et al., 2013; Ohashi-Ito et al., 2014). We could additionally determine that TMO5L1 is also strongly expressed during all the LR development stages (Figure 9), an expression pattern that is broadly confirmed by transcript profiling during gravitropy-induced LR development (Figure 11). Despite the strong impact of *rac*-GR24 on the transcriptional expression of *TMO5L1*, no clear effect on the protein level of TMO5L1 could be seen. The *pTMO5L1:TMO5L1-YFP* line used for this study might possibly miss a regulatory element that is essential for SL regulation. To clarify this assumption, complementation of the *tmo5l1* mutant with the construct should be carried out and, additionally, the responsivity of TMO5L1 to *rac*-GR24 should be checked in more independent lines.

As TMO5L1 is most probably expressed during LR development and SLs are known LR development inhibitors, we investigated whether TMO5L1 plays a role in the *rac*-GR24-regulated LR response. As such, we found that both *tmo5l1* and *tmo5;tmo5l1*, but not *tmo5*, were hypersensitive for the LR development inhibition by *rac*-GR24.

Both TMO5L1 and TMO5 are known to form heterodimers with LHW and to control the vasculature development in the root apical meristem (De Rybel et al., 2013; Ohashi-Ito et al., 2014). These regulators function at the interplay between auxin and cytokinin, because they are induced by auxin and, in turn, directly induce cytokinin biosynthesis (Schlereth et al., 2010; De Rybel et al., 2013, 2014; Ohashi-Ito et al., 2014). During the vascular development, these hormones act in a module in which they inhibit each other and, as such, tightly regulate the vascular patterning (Mähönen et al., 2006; Bishopp et al., 2011; De Rybel et al., 2014). However, neither *LHW* nor the downstream targets of the TMO5L1/LHW heterodimer in the regulation of vascular development were differentially expressed upon *rac*-GR24 treatment or in the *max2* mutant under MOCK conditions. Indeed, if SLs would impinge on the vascular development as a manner to regulate LR development, differential expression of these genes is expected. Moreover, because TMO5L1 forms heterodimers, interaction with a bHLH TF different from LHW or its homologs, might extent the toolbox and result in a different outcome. That TMO5L1 might be expressed during all developmental LR stages and that its expression is not restricted to specific cells giving rise to the vascular system in the LR primordium (Figure 9) also support an additional role for TMO5L1.

Besides a role in the *rac*-GR24 effect on LRD, we could show that TMO5L1 might influence the SL-mediated response on the flavonoid levels in the root. Whereas SLs enhance the production of flavonoids (Walton et al., 2016), TMO5L1-related mutants might have increased levels of flavonoids, as inferred from transcript analysis (Figure 13). Especially, the *tmo5;tmo5l1* double mutant displayed high transcript levels of flavonoid biosynthetic genes that did not increase upon *rac*-GR24 treatment under normal conditions, because the levels were already the same as in the WT after treatment with *rac*-GR24. As these results

were not so clear in the *tmo5l1* mutant, redundancy between TMO5 and TMO5L1 is expected. However, based on analysis of TMO5L1-related datasets and a ChIP-Seq analysis on TMO5L1, the role of TMO5L1 on SL-regulated flavonoid levels is likely not a primary response.

As *rac*-GR24 triggers both the signaling pathways mediated by D14 and KAI2 that lead to responses regulated by SL or KAR, respectively, we analyzed in which pathway TMO5L1 acts downstream (Scaffidi et al., 2014) and found indications that TMO5L1 might function mainly in the D14-cascade. However, a certain redundancy between D14 and KAI2 is very likely, because the expression level of *TMO5L1* in the *d14;kai2* double mutant exceeds that in the *d14* mutant and equals that in the *max2* mutant (Figure 3). Although both D14 and KAI2 had previously been shown to be involved in the LR development regulation after addition of (pure enantiomers of) GR24, KAI2 might be responsible for the endogenous LR development control, because the *kai2* mutant, but not the *d14* mutant, exhibits an enhanced LRD under mock conditions (Chapter 3). Hence, at least a partial involvement of *KAI2*, instead of *D14* only, is expected upstream of *TMO5L1* as a regulator of *rac*-GR24-mediated LR inhibition.

The signaling cascade via D14 is mainly known in shoot branching regulation and the involvement of TMO5L1 in shoot branching should certainly be evaluated genetically (Bennett et al., 2016). Previously, overexpression of TMO5L1 has been found to induce various shoot-related phenotypes, among which an increase in the number of secondary inflorescences (An et al., 2014). Although enhanced branching of the inflorescences is not the same as axillary bud outgrowth, the involvement of TMO5L1 in SL-mediated inhibition of bud outgrowth should be investigated properly.

Finally, overexpression of *TMO5L1* seemed to result in various anomalies, both at the transcript level and phenotypically. Because of the downregulation of *TMO5L1* by *rac*-GR24, common genes in the *TMO5L1-OX* and in the *rac*-GR24-treated WT datasets are expected to behave inversely, but this behavior was only true for 50% of the overlap (Supplementary Table 4). Similarly, nearly 50% of the overlapping

genes between the *TMO5L1-OX* dataset and the dataset comparing *max2* with WT roots had the same behavior, despite the TMO5L1 upregulation in *max2* (Supplementary Table 4). Whereas the loss-of-function mutants *tmo5l1* and *tmo5;tmo5l1* exhibit a reduced primary root length and are hypersensitive to the *rac*-GR24-mediated LRD reduction, the *TMO5L1-OX* line acts in a similar manner, instead of a lack or opposite response (Figure 12), hinting at a dominant-negative effect of the *TMO5L1* overexpression. Indeed, under normal circumstances, TMO5L1 is transcriptionally active as a heterodimer, for which the dimerization with LHW is well documented (Ohashi-Ito and Bergmann, 2007; De Rybel et al., 2013; An et al., 2014). *In vitro*, TMO5L1 alone has no transcriptional activity and, *in vivo,* only the combined overexpression of TMO5L1 and LHW results in an induction of the cytokinin biosynthesis genes LOG3 and LOG4 (An et al., 2014; Ohashi-Ito et al., 2014). Thus, homodimers could be formed by overexpression of TMO5L1 only, preventing the creation of certain heterodimers and, hence, compelling the overexpression line to behave to a certain extent like a loss-of-function mutant. This mechanism could explain why not all the genes in the overlaps between the *TMO5L1-OX* dataset and the SL-related datasets behave as expected, as illustrated by the flavonol biosynthesis genes. Indeed, for these genes, we could show that a downregulation by the *rac*-GR24 treatment correlated with an upregulation in the loss-of-function mutants, whereas they were also upregulated (thus with an opposite pattern) in the *TMO5L1-OX* dataset. As such, it could be that the overlapping genes in the transcriptome might be valid, whether they follow an expected expression pattern or not. However, because the majority of these genes are likely not primary targets of TMO5L1, the content of these gene overlaps might possibly not be very relevant.

In conclusion, we identified the TF TMO5L1 as a likely downstream component of the SL signaling pathway in the root, controlling SL-regulated LR development and (indirectly) SL-regulated flavonol content in the root.

4.4. Materials and methods

Transcript analyses

For the expression analyses of RNA-seqencing (RNA-seq) samples treated for 2 h and 6 h with *rac*-GR24, wild-type (WT) *Arabidopsis thaliana* (L.) Heynh., accession Columbia-0 (Col-0) and *max2-1* seeds (Leyser et al., 2002) were grown together on nylon meshes (20 µm) to facilitate transfer and on half-strength Murashige and Skoog medium with 1% [w/v] sucrose in a square plate divided in two. For the time series, WT *Arabidopsis* Col-0 seeds treated for 0 h, 6 h, 24 h, and 48 h with *rac*-GR24 were set likewise on square plates. The plates were incubated at 4°C for 2 days, then transferred, and placed vertically for 5 days under continuous light conditions at 21°C. Plantlets were subsequently shifted onto either mock or medium containing 1 µM *rac*-GR24 and placed back in the growth room. Root material was harvested after the indicated time points and flash-frozen in liquid nitrogen.

To determine the expression levels of the flavonol biosynthesis genes, *Arabidopsis* Col-0, *tmo5l1* (De Rybel et al., 2013), *tmo5;tmo5l1* (De Rybel et al., 2013), and *35S:TMO5L1-GFP* expressing seeds (E. Russinova, unpublished material) were also set on square plates on 20-µm nylon meshes and grown as described above. After 5 days of growth, plants were subsequently shifted onto either mock or medium containing 1 µM *rac*-GR24 and placed back in the growth room for 24 h. Root material was harvested and flash-frozen in liquid nitrogen.

For the expression levels of *TMO5L1* in the SL/KAR signaling mutants, *Arabidopsis* Col-0, *max2-1*, *d14-1* (Arite et al., 2009)*, htl-3 (kai2* allele in Col-0 background) (Toh et al., 2014), *d14-1;htl-3* (Toh et al., 2014); and *35S:MAX2-GFP* in the *max2-1* mutant background (Kindy provided by B. Márquez-García, unpublished) were set and grown as described above. After 5 of growth, root material was harvested and flash-frozen in liquid nitrogen.

For each tissue sample, approximately 100 seedlings were used stored at –80°C until processing. The experiments were repeated three times.

Total RNA was extracted with the RNeasy Plant Mini Kit (Qiagen) according to the manufacturer's protocol. Genomic DNA was removed by DNase treatment. The RNA samples were purified through NH_4Ac precipitation (at a final concentration of 2.5 M NH_4Ac). Samples were quality-controlled and quantified with a Nano-Drop Spectrophotometer (Isogen). RNA (1 µg) was reverse-transcribed into cDNA with the iScript cDNA synthesis Kit (BioRad) and subsequently diluted 25 times. Quantitative real-time--polymerase chain reaction (qRT–PCR) was done on a LightCycler 480 (Roche Diagnostics) with SYBR Green for detection, in triplicate on a 384-multiwell plate in a total volume of 5 µl and 10% cDNA fraction. Cycle threshold (Ct) values were obtained with the accompanying software and analyzed with the $2^{-\Delta\Delta CT}$ method (Livak and Schmittgen, 2001). The obtained values were normalized against those of *ACTIN2* (ACT2, AT3G18780) that was used as an internal standard.

Transcriptome profiling of *35S:TMO5L1-GFP*-expressing seedlings

The database with differentially expressed genes between the WT *Arabidopsis* Col-0 and *TMO5L1*-overexpressing *35S:TMO5L1-GFP* seedlings (*TMO5L1-OX*) was determined via RNA-seq analysis of whole seedlings.(E. Russinova, unpublished)

Confocal microscopy

Plants expressing *35S:TMO5L1-GFP* or *pTMO5L1:TMO5L1-YFP* (De Rybel et al., 2013) were grown for 5 days under continuous white light conditions at 21°C on half-strength Murashige and Skoog medium with 1% [w/v] sucrose on nylon meshes (20 µm). Plants were subsequently shifted onto either mock or

medium containing 1 µM *rac*-GR24 and placed back in the growth room for 6 h for *35S:TMO5L1-GFP*-expressing plants or for 24 hours for *pTMO5L1:TMO5L1-YFP*-expressing plants. Seedlings were mounted on slides in liquid half-strength Murashige and Skoog medium with 1% [w/v] sucrose supplemented with propidium iodide (0.01 mg/ml). The seedling roots were examined and images were taken with a confocal laser scanning microscope (Zeiss LSM 710 confocal).

Lateral root assay

WT, *tmo5* (De Rybel et al., 2013), *tmo5l1*, *tmo5;tmo5l1,* and *35S:TMO5l1-GFP* plants were grown for 9 days under continuous light conditions at 21°C on half-strength Murashige and Skoog medium with 1% [w/v] sucrose, supplemented with 1 µM *rac*-GR24 (kind gift of F-D Boyer). LRs were counted under a S4E binocular microscope (Leica Microsystems) and root length was measured with ImageJ (http://rsb.info.nih.gov/ij). Both values were used to calculate the LR density (LRD).

Hypocotyl assay

Seeds of Col-0, *max2-1*; *d14-1*; *htl-3 (kai2* allele in Col-0 background); *d14;htl-3*; *tmo5l1*; *tmo5;tmo5l1*, and *35S:TMO5L1-GFP* were sown on half-strength Murashige and Skoog medium without sucrose, supplemented with or without 1 µM *rac*-GR24 and kept for 2 days at 4°C before exposure to white light for 3 h to induce germination. Hereafter, the seeds were kept in the dark at 21°C for an additional 21 hs by wrapping the plates in aluminum foil, followed by exposure to continuous red light at 21°C (20 PAR) in a horizontal position. Hypocotyl lengths were measured 4 days later.

Statistics

Statistics regarding the expression analyses of experiments consisting of more than one genotype or time point combined with more than one treatment (i.e. MOCK and *rac*-GR24) were done via analysis of variance (ANOVA)-mixed models as previously described (Rasmussen et al., 2012). A Student's *t*-test was used for the experiments containing only one genotype, treated or not with *rac*-GR24 at one specific time point (Excel). A one-way ANOVA was used in experiments in which expression was analyzed in multiple genetic backgrounds under normal growth conditions (i.e. one treatment) by means of the SAS Enterprise Guide Software (Cary, NC, USA), followed by a post-hoc analysis. Tukey corrections were applied to multiple testing.

The statistical significance of the created overlaps between the various RNA-seq datasets was determined via a one-sided Fisher Exact test, based on the hypergeometric distribution (R Development Core Team, 2012).

For the statistical analysis of the phenotypic root analyses, the number of LRs was modeled by Poisson regression with the root length as offset variable. In the presence of overdispersion, the negative binomial distribution was preferred over the Poisson distribution. The GLIMMIX procedure (SAS Institute) was used that allows random effects. To account for the correlation between the observations within one repeat, a random intercept for repeat was included in the model. The fixed factors were genotype and treatment. The model included both factors as well as the interaction term. User-defined contrasts were estimated with the PLM procedure. To control for a family-wise error rate of 0.05, the MAXT method was applied by means of a simulation method as implemented in the PLM procedure. For the statistical analysis of the primary root length, ANOVA-mixed models were used, as previously described (Rasmussen et al., 2013). For the statistical significance of the hypocotyl assay, a similar ANOVA-mixed model was applied.

4.5. References

Aguilar-Martínez, J.A., Poza-Carrión, C., and Cubas, P. (2007). *Arabidopsis BRANCHED1* acts as an integrator of branching signals within axillary buds. Plant Cell 19, 458-472.

An, R., Liu, X., Wang, R., Wu, H., Liang, S., Shao, J., Qi, Y., An, L. and Yu, F. (2014). *The Over-Expression of Two Transcription Factors, ABS5/bHLH30 and ABS7/MYB101, Leads to Upwardly Curly Leaves.* PloS one, 9(9), e107637.

Arite, T., Umehara, M., Ishikawa, S., Hanada, A., Maekawa, M., Yamaguchi, S., and Koyzuka, J. (2009). *d14*, a strigolactone-insensitive mutant of rice, shows an accelerated outgrowth of tillers. Plant Cell Physiol. 50, 1416-1424.

Bennett, T., Liang, Y., Seale, M., Ward, S., Müller, D., and Leyser, O. (2016). Strigolactone regulates shoot development through a core signalling pathway. Biol. Open 5, 1806-1820.

Bielach, A., Podlešákovaá, K., Marhavý, P., Duclercq, J., Cuesta, C., Müller, B., Grunewald, W., Tarkowski, P., and Benková, E. (2012). Spatiotemporal regulation of lateral root organogenesis in Arabidopsis by cytokinin. Plant Cell 24, 3967-3981.

Bishopp, A., Help, H., El-Showk, S., Weijers, D., Scheres, B., Friml, J., Benková, E., Mähönen, A.P., and Helariutta, Y. (2011). A mutually inhibitory interaction between auxin and cytokinin specifies vascular pattern in roots. Curr. Biol. 21, 917-926.

Brady, S.M., Orlando, D.A., Lee, J.-Y., Wang, J.Y., Koch, J., Dinneny, J.R., Mace, D., Ohler, U., and Benfey, P.N. (2007). A high-resolution root spatiotemporal map reveals dominant expression patterns. Science 318, 801-806.

Braun, N., de Saint Germain, A., Pillot, J.-P., Boutet-Mercey, S., Dalmais, M., Antoniadi, I., Li, X., Maia-Grondard, A., Le Signor, C., Bouteiller, N., Luo, D., Bendahmane, A., Turnbull, C., and Rameau, C. (2012). The pea TCP transcription factor PsBRC1 acts downstream of strigolactones to control shoot branching. Plant Physiol. 158, 225-238.

Cartwright, D.A., Brady, S.M., Orlando, D.A., Sturmfels, B., and Benfey, P.N. (2009). Reconstructing spatiotemporal gene expression data from partial observations. Bioinformatics 25, 2581-2587.

Cheng, X., Ruyter-Spira, C., and Bouwmeester, H. (2013). The interaction between strigolactones and other plant hormones in the regulation of plant development. Front. Plant Sci. 4, 199.

Chevalier, F, Nieminen, K, Sánchez-Ferrero, J.C., Rodríguez, M.L., Chagoyen, M., Hardtke, C.S., and Cubas, P. (2014). Strigolactone promotes degradation of DWARF14, an α/β hydrolase essential for strigolactone signaling in *Arabidopsis*. Plant Cell 26, 1134-1150.

Chevalier, F, Nieminen, K, Sánchez-Ferrero, J.C., Rodríguez, M.L., Chagoyen, M., Hardtke, C.S., and Cubas, P. (2014). Strigolactone promotes degradation of DWARF14, an α/β hydrolase essential for strigolactone signaling in *Arabidopsis*. Plant Cell 26, 1134-1150.

De Rybel, B., Abidi, M., Breda, A.S., Wendrich, J.R., Smit, M.E., Novák, O., Yamaguchi, N., Yoshida, S., Van Isterdael, G., Palovaara, J., Nijsse, B., Boekschoten, M.V., Hooiveld, G., Beeckman, T., Wagner, D., Ljung, K., and Weijers, D. (2014) Integration of growth and patterning during vascular tissue formation in *Arabidopsis*. *Science* 345, 1255215.

De Rybel, B., Möller, B., Yoshida, S., Grabowicz, Barbier de Reuille, P., Boeren, S., Smith, R.S., Borst, J.W., and Weijers, D. (2013) A bHLH complex controls embryonic vascular tissue establishment and indeterminate growth in *Arabidopsis*. *Dev. Cell* 24, 426-437.

de Saint Germain, A., Clavé, G., Badet-Denisot, M.-A., Pillot, J.-P., Cornu, D., Le Caer, J.-P., Burger, M., Pelissier, F., Retailleau, P., Turnbull, C., Bonhomme, S., Chory, J., Rameau, C., and Boyer, F.-D. (2016). An histidine covalent receptor and butenolide complex mediates strigolactone perception. Nat. Chem. Biol. 12, 787-794.

Dun, E.A., de Saint Germain, A., Rameau, C., and Beveridge, C.A. (2012). Antagonistic action of strigolactone and cytokinin in bud outgrowth control. Plant Physiol. 158, 487-498.

Flematti, G.R., Waters, M.T., Scaffidi, A., Merritt, D.J., Ghisalberti, E.L., Dixon, K.W., and Smith, S.M. (2013). Karrikin and cyanohydrin smoke signals provide clues to new endogenous plant signaling compounds. Mol. Plant 6, 29-37.

Gomez-Roldan, V., Fermas, S., Brewer, P.B., Puech-Pagès, V., Dun, EA., Pillot, J.-P., Letisse, F., Matusova, R., Danoun, S., Portais, J-C., Bouwmeester, H., Bécard, G., Beveridge, C.A., Rameau, C., and Rochange, S.F. (2008). Strigolactone inhibition of shoot branching. Nature 455, 189-194.

Hamiaux, C., Drummond, R.S.M., Janssen, B.J., Ledger, S.E., Cooney, JM., Newcomb, R.D., and Snowden, K.C. (2012). DAD2 is an α/β hydrolase likely to be involved in the perception of the plant branching hormone, strigolactone. Curr. Biol. 22, 2032-2036.

Jiang, L., Liu, X., Xiong, G., Liu, H., Chen, F., Wang, L., Meng, X., Liu, G., Yu, H., Yuan, Y., Yi, W., Zhao, L., Ma, H., He, Y., Wu, Z., Melcher, K., Qian, Q., Xu, H.E., Wang, Y., and Li, J. (2013). DWARF 53 acts as a repressor of strigolactone signalling in rice. Nature 504, 401-405.

Kagale, S., and Rozwadowski, K. (2011). EAR motif-mediated transcriptional repression in plants: an underlying mechanism for epigenetic regulation of gene expression. Epigenetics 6, 141–146.

Kapulnik, Y., Delaux, P.-M., Resnick, N., Mayzlish-Gati, E., Wininger, S., Bhattacharya, C., Séjalon-Delmas, N., Combier, J.-P., Bécard, G., Belausov, E., Beeckman, T., Dor, E., Hershenhorn, J., and Koltai, H. (2011a). Strigolactones affect lateral root formation and root-hair elongation in Arabidopsis. Planta 233, 209-216.

Kapulnik, Y., Resnick, N., Mayzlish-Gati, E., Kaplan, Y., Wininger, S., Hershenhorn, J., and Koltai, H. (2011b). Strigolactones interact with ethylene and auxin in regulating root-hair elongation in *Arabidopsis*. J. Exp. Bot. 62, 2915-2924.

Katayama, H., Iwamoto, K., Kariya, Y., Asakawa, T., Kan, T., Fukuda, H., and Ohashi-Ito, K. (2015). A negative feedback loop controlling bHLH complexes is involved in vascular cell division and differentiation in the root apical meristem. Curr. Biol. 25, 3144-3150.

Kong, X., Zhang, M., and Ding, Z. (2014). D53: the missing link in strigolactone signaling. Mol. Plant 7, 761-763.

Laplaze, L., Benkova, E., Casimiro, I., Maes, L., Vanneste, S., Swarup, R., Weijers, D., Calvo, V., Parizot, B., Herrera-Rodriguez, M.B., Offringa, R., Graham, N., Doumas, P., Friml, J., Bogusz, D., Beeckman, T., and Bennett, M. (2007). Cytokinins act directly on lateral root founder cells to inhibit root initiation. Plant Cell 19, 3889-3900.

Lavenus, J., Goh, T., Roberts, I., Guyomarc'h, S., Lucas, M., De Smet, I., Fukaki, H., Beeckman, T., Bennett, M., and Laplaze, L. (2013). Lateral root development in Arabidopsis: fifty shades of auxin. Trends Plant Sci. 18, 450 458.

Leyser, O. (2002). Molecular genetics of auxin signaling. Annu. Rev. Plant Biol. 53, 377-398.

Liang, Y., Ward, S., Li, P., Bennett, T., and Leyser, O. (2016). SMAX1-LIKE7 signals from the nucleus to regulate shoot development in Arabidopsis via partially EAR motif-independent mechanisms. Plant Cell 28, 1581-1601.

Livak, K.J., and Schmittgen, T.D. (2001). Analysis of relative gene expression data using real-time quantitative PCR and the $2^{-\Delta\Delta C}_{T}$ method. Methods 25, 402-408.

Mähönen, A.P., Bishopp, A., Higuchi, M., Nieminen, K.M., Kinoshita, K., Törmäkangas, K., Ikeda, Y., Oka, A., Kakimoto, T., and Helariutta, Y. (2006a). Cytokinin signaling and its inhibitor AHP6 regulate cell fate during vascular development. Science 311, 94-98.

Minakuchi, K., Kameoka, H., Yasuno, N., Umehara, M., Luo, L., Kobayashi, K., Hanada, A., Ueno, K., Asami, T., Yamaguchi, S., and Kyozuka, J. (2010). *FINE CULM1* (*FC1*) works downstream of strigolactones to inhibit the outgrowth of axillary buds in rice. Plant Cell Physiol. 51, 1127-1135.

Nelson, D.C., Scaffidi, A., Dun, E.A., Waters, M.T., Flematti, G.R., Dixon, K.W., Beveridge, C.A., Ghisalberti, E.L., and Smith, S.M. (2011). F-box protein MAX2 has dual roles in karrikin and strigolactone signaling in *Arabidopsis thaliana*. Proc. Natl. Acad. Sci. USA 108, 8897-8902.

Ohashi-Ito, K., and Bergmann, D.C. (2007). Regulation of the *Arabidopsis* root vascular initial population by *LONESOME HIGHWAY*. Development 134, 2959-2968.

Ohashi-Ito, K., Saegusa, M., Iwamoto, K., Oda, Y., Katayama, H., Kojima, M., Sakakibara, H., and Fukuda, H. (2014). A bHLH complex activates vascular cell division via cytokinin action in root apical meristem. Curr. Biol. 24, 2053-2058.

Pauwels, L., Fernández Barbero, G., Geerinck, J., Tilleman, S., Grunewald, W., Cuéllar Pérez, A., Chico, J.M., Vanden Bossche, R., Sewell, J., Gil, E., García-Casado, G., Witters, E., Inzé, D., Long, J.A., De Jaeger, G., Solano, R., and Goossens, A. (2010). NINJA connects the co-repressor TOPLESS to jasmonate signalling. Nature 464, 788-791.

R Development Core Team (2012). R: A language and environment for statistical computing. Vienna, Austria, R Foundation for Statistical Computing.

Rasmussen, A., Depuydt, S., Goormachtig, S., and Geelen, D. (2013). Strigolactones fine-tune the root system. Planta 238, 615-626.

Rasmussen, A., Mason, M.G., De Cuyper, C., Brewer, P.B., Herold, S., Agusti, J., Geelen, D., Greb, T., Goormachtig, S., Beeckman, T., and Beveridge, C.A. (2012). Strigolactones suppress adventitious rooting in Arabidopsis and pea. Plant Physiol. 158, 1976-1987.

Roig-Villanova, I., Bou, J., Sorin, C., Devlin, P.F., and Martínez-García, J.F. (2006). Identification of primary target genes of phytochrome signaling. Early transcriptional control during shade avoidance responses in Arabidopsis. Plant Physiol. 141, 85-96.

Ruyter-Spira, C., Kohlen, W., Charnikhova, T., van Zeijl, A., van Bezouwen, L., de Ruijter, N., Cardoso, C., Lopez-Raez, J.A., Matusova, R., Bours, R., Verstappen, F., and Bouwmeester, H. (2011). Physiological effects of the synthetic strigolactone analog GR24 on root system architecture in Arabidopsis: another belowground role for strigolactones? Plant Physiol. 155, 721-734.

Scaffidi, A., Waters, M.T., Sun, Y.K., Skelton, B.W., Dixon, K.W., Ghisalberti, E.L., Flematti, G.R., and Smith, S.M. (2014). Strigolactone hormones and their stereoisomers signal through two related receptor proteins to induce different physiological responses in Arabidopsis. Plant Physiol. 165, 1221 1232.

Schlereth, A., Möller, B., Liu, W., Kientz, M., Flipse, J., Rademacher, E.H., Schmid, M., Jürgens, G., and Weijers, D. (2010). MONOPTEROS controls embryonic root initiation by regulating a mobile transcription factor. Nature 464, 913–916.

Shen, H., Luong, P., and Huq, E. (2007). The F-Box protein MAX2 functions as a positive regulator of photomorphogenesis in Arabidopsis. Plant Physiol. 145, 1471-1483.

Shinohara, N., Taylor, C., and Leyser, O. (2013). Strigolactone can promote or inhibit shoot branching by triggering rapid depletion of the auxin efflux protein PIN1 from the plasma membrane. PLoS Biol. 11, e1001474.

Soundappan, I., Bennett, T., Morffy, N., Liang, Y., Stanga, J.P., Abbas, A., Leyser, O., and Nelson, D.C. (2015). SMAX1-LIKE/D53 family members enable distinct MAX2-dependent responses to strigolactones and karrikins in Arabidopsis. Plant Cell 27, 3143-3159.

Stanga, J.P., Smith, S.M., Briggs, W.R., and Nelson, D.C. (2013). *SUPPRESSOR OF MORE AXILLARY GROWTH2 1* controls seed germination and seedling development in Arabidopsis. Plant Physiol. 163, 318-330.

Stirnberg, P., Furner, I.J., and Leyser, H.M.O. (2007). MAX2 participates in an SCF complex which acts locally at the node to suppress shoot branching. Plant J. 50, 80-94.

Stirnberg, P., Ward, S., and Leyser, O. (2010). Auxin and strigolactones in shoot branching: intimately connected? Biochem. Soc. Trans. 38, 717-722.

Toh, S., Holbrook-Smith, D., Stokes, M.E., Tsuchiya, Y., and McCourt, P. (2014). Detection of parasitic plant suicide germination compounds using a high-throughput *Arabidopsis* HTL/KAI2 strigolactone perception system. Chem. Biol. 21, 988-998.

Tsuchiya, Y., Vidaurre, D., Toh, S., Hanada, A., Nambara, E., Kamiya, Y., Yamaguchi, S., and McCourt, P. (2010). A small-molecule screen identifies new functions for the plant hormone strigolactone. Nat. Chem. Biol. 6, 741-749.

Umehara, M., Hanada, A., Yoshida, S., Akiyama, K., Arite, T., Takeda-Kamiya, N., Magome, H., Kamiya, Y., Shirasu, K., Yoneyama, K., Kyozuka, J., and Yamaguchi, S. (2008). Inhibition of shoot branching by new terpenoid plant hormones. Nature 455, 195-200.

Vera-Sirera, Francisco, Bert De Rybel, Cristina Urbez, Evangelos Kouklas, Marta Pesquera, Juan Camilo Álvarez-Mahecha, Eugenio G. Minguet et al. "A bHLH-based feedback loop restricts vascular cell proliferation in plants." Developmental cell 35, no. 4 (2015): 432-443.

Voß, U., Wilson, M.H., Kenobi, K., Gould, P.D., Robertson, F.C., Peer, W.A., Lucas, M., Swarup, K., Casimiro, I., Holman, T.J., Wells, D.M., Péret, B., Goh, T., Fukaki, H., Hodgman, T.C., Laplaze, L., Halliday, K.J., Ljung, K., Murphy, A.S., Hall, A.J., Webb, A.A.R., and Bennett, M.J. (2015). The circadian clock rephases during lateral root organ initiation in *Arabidopsis thaliana*. Nat. Commun. 6, 7641.

Walton, A., Stes, E., Goeminne, G., Braem, L.,Vuylsteke, M., Matthys, C., De Cuyper, C., Staes, A., Vandenbussche, J., Boyer, F.-D., Vanholme, R., Fromentin, J., Boerjan, W., Gevaert, K., and Goormachtig, S. (2016). The response of the root proteome to the synthetic strigolactone GR24 in Arabidopsis. Mol. Cell. Proteomics 15, 2744-2755.

Wang, L., Wang, B., Jiang, L., Liu, X., Li, X., Lu, Z., Meng, X., Wang, Y., Smith, S.M., and Li, J. (2015). Strigolactone signaling in Arabidopsis regulates shoot development by targeting D53-like SMXL repressor proteins for ubiquitination and degradation. Plant Cell 27, 3128-3142.

Waters, M.T., Nelson, D.C., Scaffidi, A., Flematti, G.R., Sun, Y.K., Dixon, K.W., and Smith, S.M. (2012). Specialisation within the DWARF14 protein family confers distinct responses to karrikins and strigolactones in *Arabidopsis*. Development 139, 1285-1295.

Winter, D., Vinegar, B., Nahal, H., Ammar, R., Wilson, G.V., and Provart, N.J. (2007). An "electronic Fluorescent Pictograph" browser for exploring and analyzing large-scale biological data sets. PLoS ONE 2, e718.

Yao, R., Ming, Z., Yan, L., Li, S., Wang, F., Ma, S., Yu, C., Yang, M., Chen, L., Chen, L., Li, Y., Yan, C., Miao, D., Sun, Z., Yan, J., Sun, Y., Wang, L., Chu, J., Fan, S., He, W., Deng, H., Nan, F., Li, J., Rao, Z., Lou, Z., and Xie, D. (2016). DWARF14 is a non-canonical hormone receptor for strigolactone. Nature 536, 469-473.

Zhao, L.H., Zhou, X.E., Wu, Z.-S., Yi, W., Xu, Y., Li, S., Xu, T.-H., Liu, Y., Chen, R.-Z., Kovach, A., Kang, Y., Hou, L., He, Y., Xie, C., Song, W., Zhong, D., Xu, Y., Wang, Y., Li, J., Zhang, C., Melcher, K., and Xu, H.E. (2013). Crystal structures of two phytohormone signal-transducing α/β hydrolases: karrikin-signaling KAI2 and strigolactone-signaling DWARF14. Cell Res. 23, 436-439.

Zhou, F., Lin, Q., Zhu, L., Ren, Y., Zhou, K., Shabek, N., Wu, F., Mao, H., Dong, W., Gan, L., Ma, W., Gao, H., Chen, J., Yang, C., Wang, D., Tan, J., Zhang, X., Guo, X., Wang, J., Jiang, L., Liu, X., Chen, W., Chu, J., Yan, C., Ueno, K., Ito, S., Asami, T., Cheng, Z., Wang, J., Lei, C., Zhai, H., Wu, C., Wang, H., Zheng, N., and Wan, J. (2013). D14--SCF^{D3}-dependent degradation of D53 regulates strigolactone signalling. Nature 504, 406-410.

4.6. Supplementary data

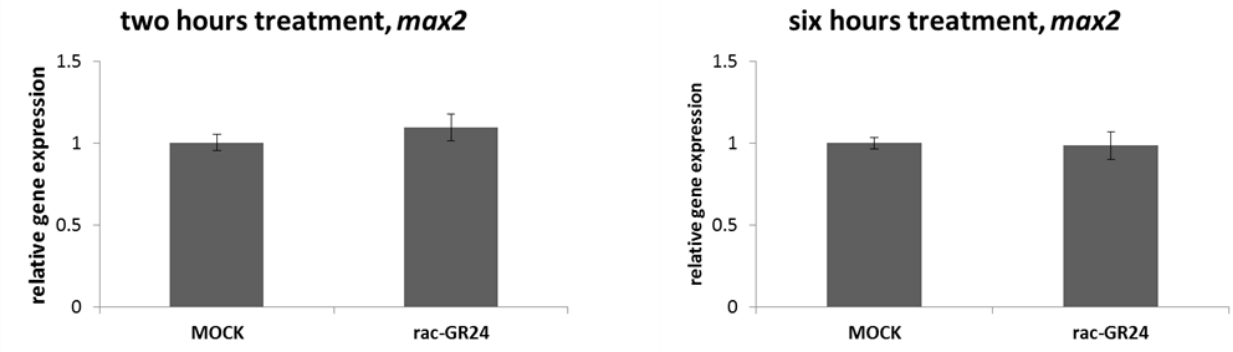

Supplementary Figure 1. Effect of *rac*-GR24 treatment on the relative gene expression of *TMO5L1* in *max2*. Five-day-old *max2* seedlings were transferred to fresh medium containing 1 µM *rac*-GR24 or to control medium (MOCK). Root samples were taken after 2 h **(left)** and after 6 h **(right)** of treatment. The relative gene expression was determined via qRT-PCR and the expression level was normalized via *ACTIN* (*ACT2*). Means of three independent biological repeats are presented. Error bars represent the standard error (SE). Statistically significance was determined via Student's *t*-test.

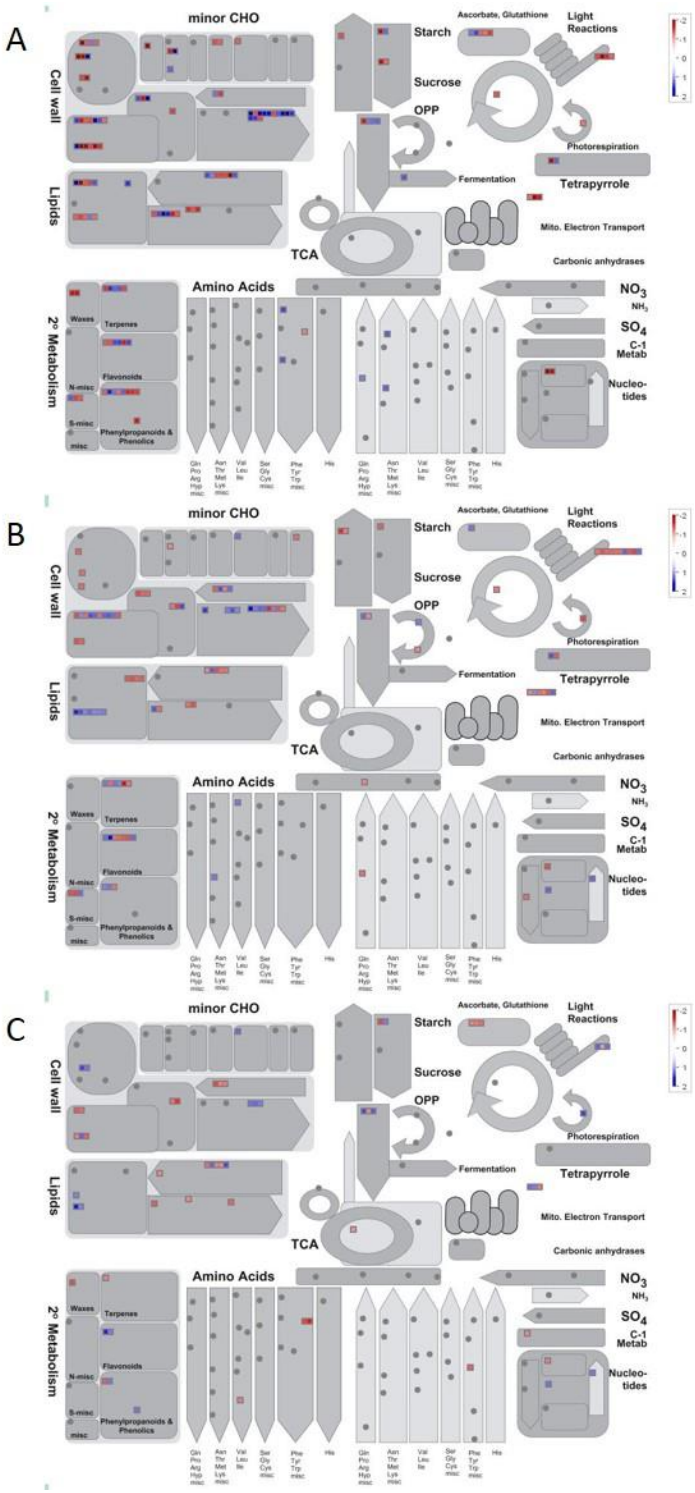

Supplementary Figure 2. General overview of the transcriptomic changes in published TMO5L1-related datasets. MapMan-generated overview that summarizes the cellular processes that were perturbed after in the various published *TMO5L1*-related datasets. **(A)** inducible combined overexpression of *TMO5L1* and *LHW* in plant cell culture (Ohashi-Ito et al., 2014); **(B)** inducible overexpression of *TMO5* (selective harvest of root tips) (De Rybel et al., 2014); and **(C)** inducible overexpression of *TMO5*

combined with cycloheximide (CHX) treatment to enrich for primary response genes (selective harvest of root tips) (De Rybel et al., 2014). Each square represents one gene. Color coding according to the LOG2 scale: blue and red, upregulated and downregulated, respectively.

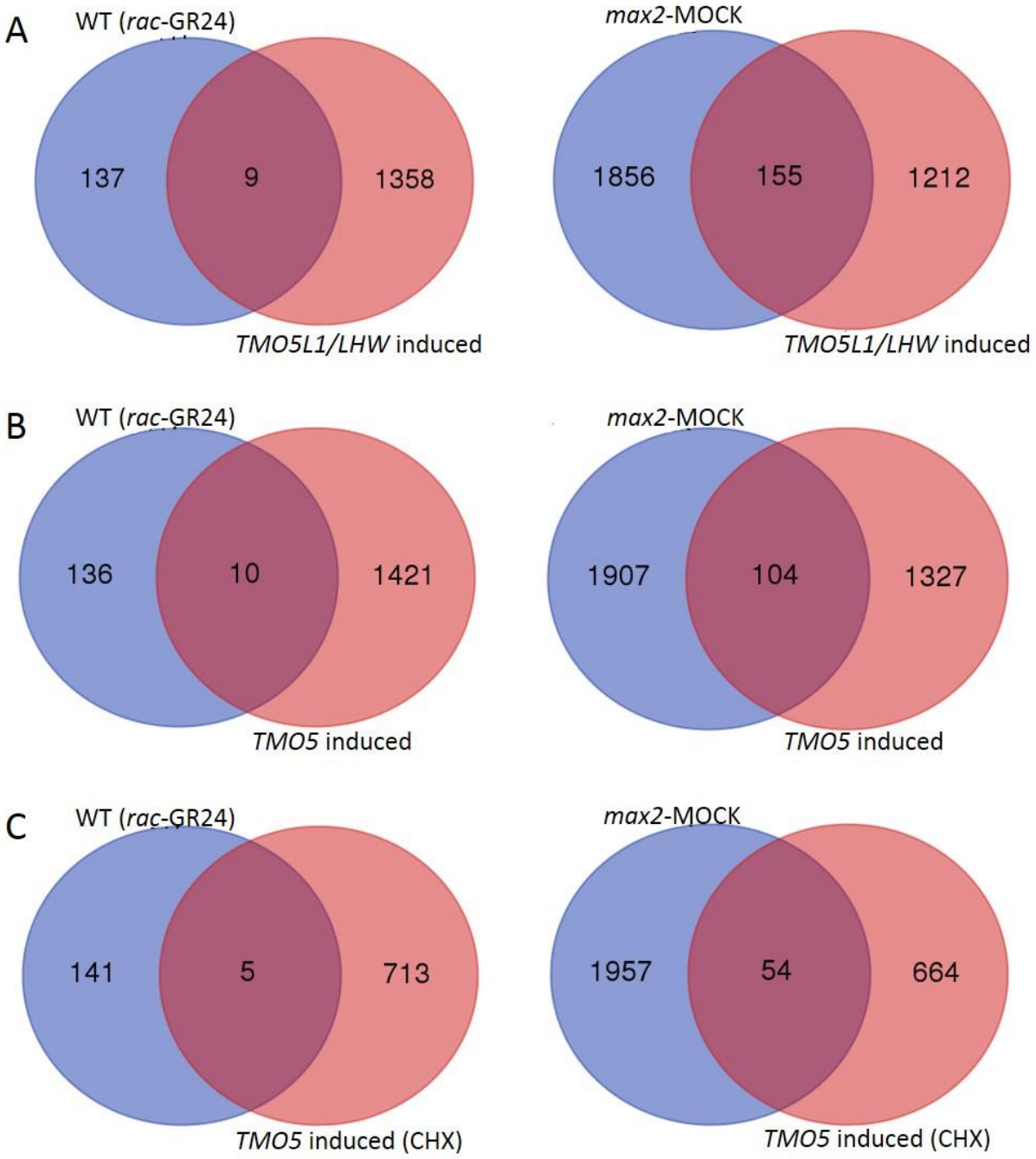

Supplementary Figure 3. Overlap of differentially expressed genes between the published *TMO5L1-related datasets* and the SL-related RNA-seq datasets. Left: overlaps with *rac*-GR24 treated WT; **Right:** overlaps with the *max2-MOCK* dataset with **(A)** inducible combined overexpression of *TMO5L1* and *LHW* in plant cell culture (Ohashi-Ito et al., 2014); **(B)** inducible overexpression of *TMO5* (selective harvest of root tips) (De Rybel et al., 2014); and **(C)** inducible overexpression of *TMO5* combined with

cycloheximide (CHX) treatment to enrich for primary response genes (selective harvest of root tips) (De Rybel et al., 2014). Selection of the genes in the TMO5L1-related datasets is based on a FC-cutoff of 2 and *P*-value < 0.05.

Supplementary Table 1. Gene content of the overlaps between the TMO5L1-related datasets. Available via https://goo.gl/ckowXg

Supplementary Table 2. Identity of genes covered in Figure 5. Available via https://goo.gl/ckowXg

Supplementary Table 3. Overview of the overlap between the *rac*-GR24 treatment dataset (WT) and the *TMO5L1-OX* dataset. Available via https://goo.gl/ckowXg

Supplementary Table 4. Overview of the overlap between the *max2*-MOCK dataset and the *TMO5L1-OX* dataset. Available via https://goo.gl/ckowXg

Supplementary Table 5. List of potentially directly regulated genes by TMO5L1 (ChIP-seq) (E. Russinova, Unpublished data). Available via https://goo.gl/ckowXg

Supplementary Table 6. Overlap of *rac*-GR24 treated WT dataset with potentially directly regulated genes by TMO5L1 (ChIP-seq). Available via https://goo.gl/ckowXg

Supplementary Dataset 1. Differentially Expressed genes in *p35S:TMO5L1-GFP (TMO5L1-OX)* vs. WT seedlings. Available via https://goo.gl/ckowXg

CHAPTER 5

WORK IN PROGRESS: UNDERSTANDING THE ROLE OF STRIGOLACTONES IN PLANT DEVELOPMENT BY THE USE OF CHEMICAL GENETICS

CEDRICK MATTHYS, ANDZREJ DROŻDŻECKI, LONG NGUYEN, DANNY VEREECKE, STEFAAN WERBROUCK, DOMINIQUE AUDENAERT, TOM BEECKMAN, AND SOFIE GOORMACHTIG.

In preparation

Author's contribution: Cedrick Matthys was the main researcher involved in the work displayed in this chapter.

Abstract

Strigolactones (SLs) are a group of phytohormones that regulate various aspects of shoot and root development, but had initially been discovered because of their role in rhizosphere interactions. However, a lot about the SL signaling cascades still needs to be discovered. Here, we report on the initiation of a chemical genetics approach in *Arabidopsis thaliana* to obtain a better insight into the molecular mechanisms of SL sensing and signaling by screening a compound library for molecules that inhibit the reduction in hypocotyl elongation induced by the synthetic racemic SL *rac*-GR24. We identified 10 putative lead SL antagonists and tested their effects on various SL related physiological responses. In addition to the effect on the hypocotyl length, three were also shown to prevent the *rac*-GR24-induced germination of parasitic seeds, whereas two others might influence the impact of *rac*-GR24 on lateral root development. Hence, after validation, the new lead compounds will help to provide more knowledge on the molecular mechanisms by which SL signaling results in the various physiological outcomes.

5.1. Introduction

Strigolactones (SLs), which had initially been discovered for their role in rhizosphere interactions (Xie and Yoneyama, 2010), have become a cutting-edge topic in plant biology and agronomy, with a great potential in modern agriculture because of their various physiological responses. SLs influence root and shoot architecture (Gomez-Roldan et al., 2008; Umehara et al., 2008; Tsuchiya et al., 2010; Kapulnik et al., 2011; Ruyter-Spira et al., 2011). In addition, they induce arbuscular mycorrhization and induce germination of parasitic weeds, such as *Striga* spp. and members of the *Orobanchaceae* family (Yoder and Scholes, 2010). Knowledge on the regulation of plant architecture is essential to improve crop yield in an ever-changing environment. Moreover, parasitic weeds still cause world-wide crop losses (Yoder and Scholes, 2010) and understanding the mycorrhizal symbiosis might lead to agricultural practices with a reduced input of chemical fertilizers. Hence, it is important to understand how SL signaling results in their various physiological outcomes.

MORE AXILLARY GROWTH2 (MAX2), a nuclear localized leucine-rich repeat F-box protein, is a key player in SL signaling in *Arabidopsis thaliana* (Stirnberg et al., 2007; Gomez-Roldan et al., 2008; Umehara et al., 2008). In the presence of SLs, MAX2 forms a complex with the SL receptor DWARF14 (D14) that eventually results in the ubiquitination and subsequent degradation of their direct protein targets of the SUPPRESSOR OF SMAX1 LIKE (SMXL) family (Stanga et al., 2013; Soundappan et al., 2015; Wang et al., 2015; Liang et al., 2016). Interestingly, MAX2 is also recruited in the signaling pathway of karrikins, smoke-derived compounds that induce germination (Nelson et al., 2011). These karrikins bind to a protein that is closely related to D14, KARRIKIN INSENSITIVE2 (KAI2). In analogy to the D14 pathway, it is believed that this might also lead to the recruitment of MAX2 and the degradation of other members of the SMXL family. This duality is all the more relevant, because the commonly used SL analog *rac*-GR24 activates both signaling via the D14 and the KAI2 pathway (Scaffidi et al. 2014).

Chemical genetics is a technique that makes use of small molecules that alter protein function to study biological processes and that has proven to be very powerful in deciphering plant hormone signaling pathways (Armstrong et al., 2004; Gendron et al., 2008; Savaldi-Goldstein et al., 2008; De Rybel et al., 2009b). It provides complementary information to that results obtained by molecular genetics and often overcomes its limitations, such as redundancy, lethality, and pleiotropic effects (Tóth and van der Hoorn, 2009). The discipline often utilizes classical forward genetics screens for chemical resistance or hypersensitivity to identify target proteins and pathways. The use of small molecules is an integrated part of, for instance, auxin research, because it allows researchers to pinpoint specific pathways and decipher the pleiotropic effects of this versatile hormone (De Rybel et al., 2009a). Because SLs have diverse effects, chemical genetics will greatly help to unravel the unknown signaling nodes and networks on which SLs act. Several years ago, compounds have been identified that inhibit SL biosynthesis or enhance SL levels (Sergeant et al., 2009; Tsuchiya et al., 2010). Additionally, a yeast-based chemical screen has revealed several SL agonists, and more recently, an inhibitor of KAI2 activity in *Arabidopsis* and *Striga* could be identified via chemical genetics (Toh et al., 2014; Holbrook-Smith et al., 2016).

By developing a chemical screen based on the *rac*-GR24-induced reduction in hypocotyl length, we identified 10 lead compounds that possibly interfere with SL signaling, of which three also prevented the *rac*-GR24-induced germination of parasitic seeds and two others might also influence the impact of *rac*-GR24 on the lateral root development. After further validation, these new compounds will help us understand the molecular mechanisms of the various physiological consequences triggered by the SL signaling.

5.2. Results and discussion

5.2.1. A bioassay for high-throughput screening

For a successful chemical genetics screen, a well-characterized and robust bioassay needs to be established, based on either phenotype or on expression of marker genes (Tóth and van der Hoorn, 2009). This bioassay will be used for a high-throughput screen of a chemical compound library of 12,000 compounds to yield hit compounds. To screen for compounds that interfere with the *rac*-GR24 signaling, we optimized a protocol based on the observation that *rac*-GR24 enhances the red light-mediated inhibition of the hypocotyl elongation (Figure 1) (Shen et al., 2007; Nelson et al., 2011; Waters et al., 2012). For this assay, seeds were sown on solid medium either supplemented or not with *rac*-GR24. After a 2-day stratification period, they were exposed to 3 h of white light to induce germination followed by a 21-h dark period, whereafter the plates were exposed to continuous red light for 4 days to allow seedling development (Figure 1A). As such, the *rac*-GR24 treatment resulted in a reduced hypocotyl length in a MAX2-dependent manner; whereas under MOCK conditions, the hypocotyl of the *max2* mutant was longer than that of the WT (Figures 2B and 2C), in agreement with previous findings (Shen et al., 2007; Nelson et al., 2011).

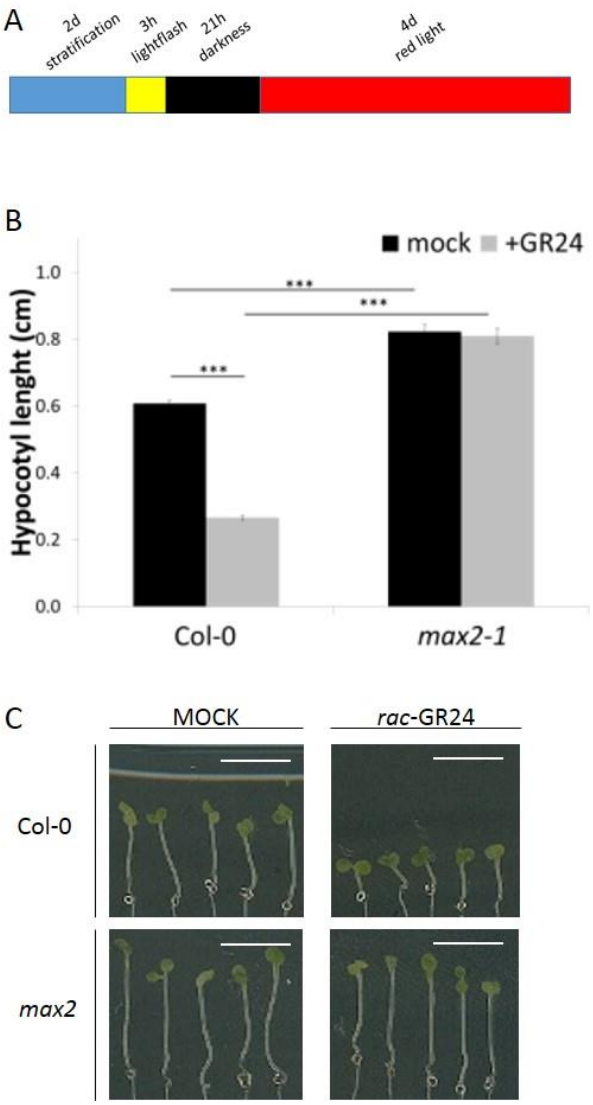

Figure 1. *rac*-GR24 hypocotyl assay. Seeds of Col-0 and *max2-1* were sown on half-strength Murashige and Skoog medium without sucrose, supplemented or not with 1 µM *rac*-GR24. After stratification, plates were exposed to white light for 3 h, followed by incubation in the dark for an additional 21 h and were ultimately exposed to red light for 4 days. **(A)** Visual representation of the followed protocol. **(B)** Graphs represent means of three biological repeats ($n > 25$). Error bars represent the standard error (SE). Asterisks indicate statistically significant differences (*** $P < 0.001$; ANOVA-mixed model). **(C)** Five representative seedlings are shown. Bars = 0.5 cm.

As a chemical screen requires a small-scale assay, we investigated whether similar results could be obtained when this assay was done in a microtiter plate. To this end, we examined various concentrations of *rac*-GR24 and tested them on both solid and liquid growth medium in 96-well plates, while the other parameters of the assay were kept unchanged (Figure 2). After the treatment with red light, seedlings were individually spread on a thin layer of agar to allow the hypocotyl measurement. The hypocotyl length was clearly reduced in both medium types containing 1 µM and 2 µM *rac*-GR24, with almost no difference between the two concentrations (Figure 2). Additionally, in liquid medium the hypocotyl length was also slightly reduced with 0.1 µM *rac*-GR24 (Figure 2). Previous studies only report the use of 1 µM or 10 µM *rac*-GR24 in solid medium and the reductions were similar as those after treatment with 1 µM or 2 µM *rac*-GR24 (Nelson et al., 2011; Waters et al., 2012; Toh et al., 2014). The fact that treatment with 0.1 µM *rac*-GR24 only in liquid medium resulted in a length reduction, might indicate that the *rac*-GR24 uptake is enhanced in liquid medium. This could perhaps be because the full seedling is in contact with the growth medium, instead of solely the root in the case of solid medium.

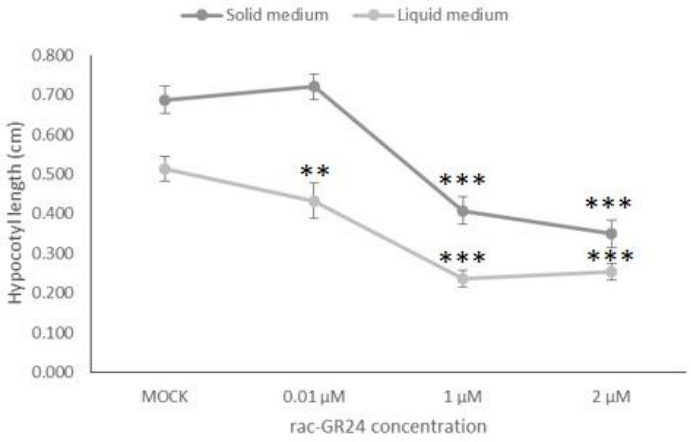

Figure 2. Optimizations of the hypocotyl assay for high-throughput screening. Seeds of Col-0 and *max2-1* were sown in multiple wells in a 96-well format on half-strength Murashige and Skoog medium without sucrose (solidified or not with 0.8% [w/v] plant tissue culture agar), supplemented or not with 0.1, 1, or 2 µM *rac*-GR24. 3-5 seeds were sowed per well. After stratification,

plates were exposed to white light for 3 h, followed by incubation in the dark for an additional 21 h and ultimately exposed to red light for 4 days. Graphs represent means of three biological repeats (n > 25). Error bars represent the standard error (SE). Asterisks indicate statistically significant differences within the medium type for each concentration compared to the respective MOCK condition (** P < 0,01; *** P <0.001; ANOVA-mixed model).

To avoid compound interference with seed germination during a chemical screen, the library is generally preferably added after germination and, thus, an assay in liquid medium is favored. As our aim was to find antagonists of the SL signaling, the presence of *rac*-GR24 in the growth medium long before addition of the compound library had to be avoided. To investigate whether *rac*-GR24 (and at a later stage also the compound library) could be added after the germination without influencing the outcome of the assay, we sowed *Arabidopsis* seeds in the absence of *rac*-GR24 and added it only after the incubation time in the dark. To ensure that all seeds had germinated, we extended this dark incubation from 21 h to 27 h, or 42 h and visually confirmed the progression of the germinating seeds (data not shown). Even after a delayed treatment of 42 h, *rac*-GR24 was still able to inhibit the hypocotyl length (Figure 3). As the hypocotyl reduction after treatment with 1 µM and 2 µM *rac*-GR24 is almost indistinguishable, the following experiments were done with 1 µM. Thus, these modifications resulted in a compatible and robust assay for an optimal high-throughput chemical screen.

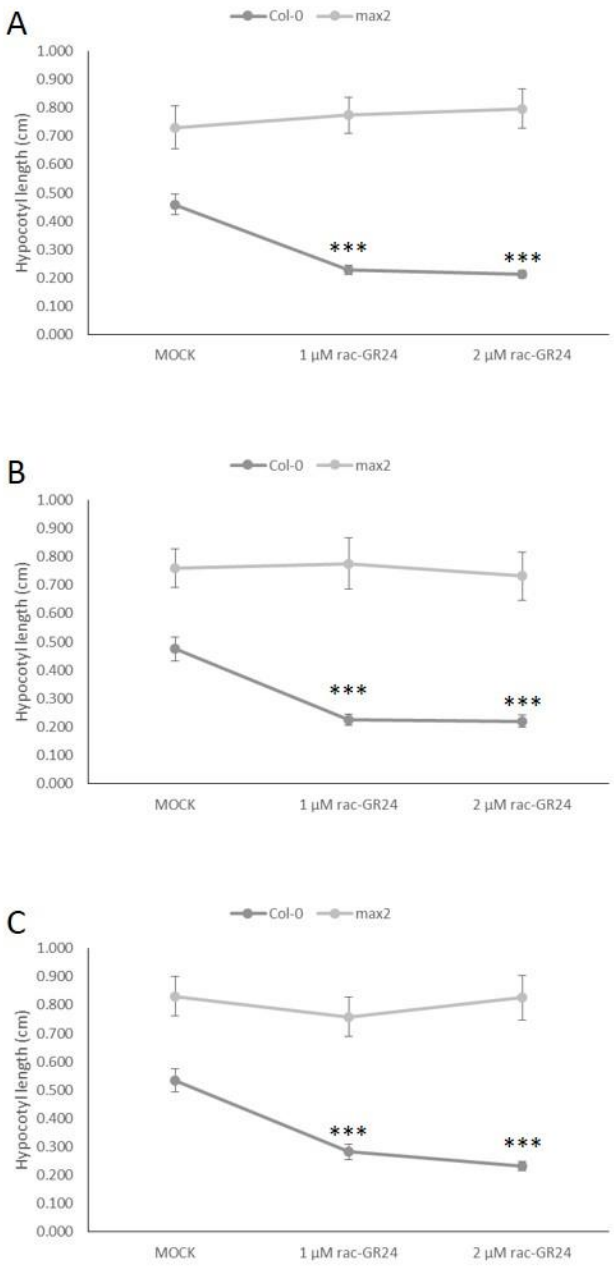

Figure 3. Effect of delayed addition of *rac*-GR24 on the reduction in hypocotyl elongation. Seeds of Col-0 and *max2-1* were sown in a 96-well format on liquid half-strength Murashige and Skoog medium in the absence of *rac*-GR24. After stratification, plates were exposed to white light for 3 h, followed by incubation in the dark for an additional 21 h **(A)** 27 h **(B),** or 42 h **(C)**. Then, fresh medium supplemented or not with *rac*-GR24 was added to the wells (1 µM or 2 µM final *rac*-GR24 concentrations) and were ultimately exposed to red light for 4 days. Graphs represent means of three biological repeats ($n > 25$). Error bars represent the standard error (SE). Asterisks indicate statistically significant differences within the genotype compared to the respective MOCK condition (*** $P < 0.001$; ANOVA-mixed model).

5.2.2. Chemical screening and the selection of hit compounds

Using the optimized hypocotyl bioassay, we want to screen for compounds that antagonize *rac*-GR24 signaling. Recently, *rac*-GR24 has been shown to trigger both the D14- and the KAI2-signaling pathway via MAX2, whereby D14 preferentially binds to and hydrolyzes (+)GR24 and KAI2 preferentially to (-)GR24 (Figure 4) (Scaffidi et al., 2014; Flematti et al., 2016). Additionally, both signaling pathways were shown to be involved in the regulation of the hypocotyl length by *rac*-GR24 (Figure 4) (Chapter 4; Nelson et al., 2011; Waters et al., 2012; Toh et al., 2014). As such, only when the two signaling pathways are blocked (e.g. genetically by a mutation in *MAX2*, or by a mutation of both *D14* and *KAI2*), plants are fully insensitive to the *rac*-GR24-effect on hypocotyl length. On the other hand, when only one of the two pathways is blocked, this results in a reduced sensitivity towards the *rac*-GR24 effect on hypocotyl length, so *d14* or *kai2* are not completely insensitive. In other words, *rac*-GR24 still causes a certain reduction of the hypocotyl length in *d14* and in *kai2*, but this reduction is weaker compared to the WT (Nelson et al., 2011; Waters et al., 2012; Toh et al., 2014). As such, we will screen for antagonists of *rac*-GR24 signaling, thus compounds that partially or fully prevent the *rac*-GR24-mediated reduction of hypocotyl length.

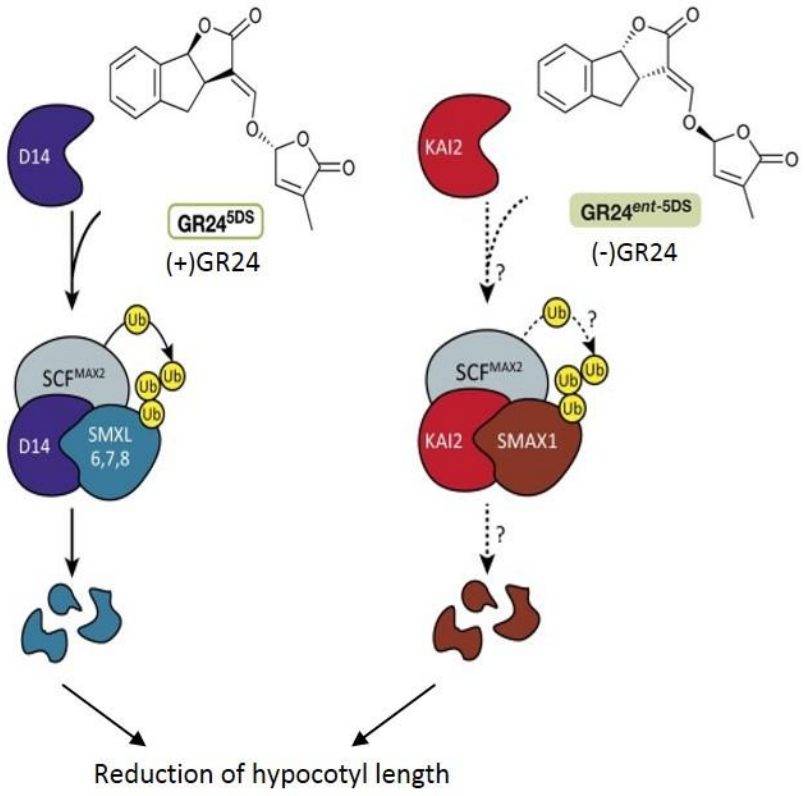

Figure 4. Schematic representation of hypocotyl length reduction by *rac*-GR24. rac-GR24 consists of two enantiomers. (+)GR24 is preferentially recognized by D14, triggering an association of D14 with SCF^{MAX2} and the SMXL6,SMXL7,SMXL8/D53 proteins that are then targeted for proteasomal degradation, eventually enabling a reduction of the hypocotyl length. (-)GR24 is preferentially recognized by KAI2, likely triggering the formation of a SCF^{MAX2}–KAI2–SMAX1 complex, allowing responses, such as reduction of hypocotyl length. Dashed lines and question marks indicate that the KAI2-dependent signaling mechanism is an untested hypothesis. Figure modified from Morffy et al. (2016).

To screen for putative SL antagonists, we used a ChemBridge™ chemical library of 12,000 compounds. The workflow of the screening procedure is summarized in Figure 5. First, *Arabidopsis* seeds were sown in liquid medium in 96-well plates. After 2 days of stratification, the plates were incubated for 3 h in white light to induce germination. Next, the plates were put in the dark for 42 h, whereafter both *rac*-GR24 and one of the 12,000 compounds from the ChemBridge™ chemical library were added in each well (final concentrations 50 µM and 1 µM of compound and *rac*-GR24, respectively). For the sake of

comparison, no *rac*-GR24 nor any compound were added (MOCK control) in one row of wells, whereas *rac*-GR24 was added without any compound (*rac*-GR24 control) in another row, allowing the testing of 80 compounds per plate. Finally, the plates were incubated for 4 days in continuous red light and the hypocotyl length was analyzed qualitatively under a binocular by comparing with the MOCK and *rac*-GR24 control wells. As such, compounds that resulted in seedlings with a hypocotyl that was clearly longer than the *rac*-GR24 treated control plants were retained as hit compounds.

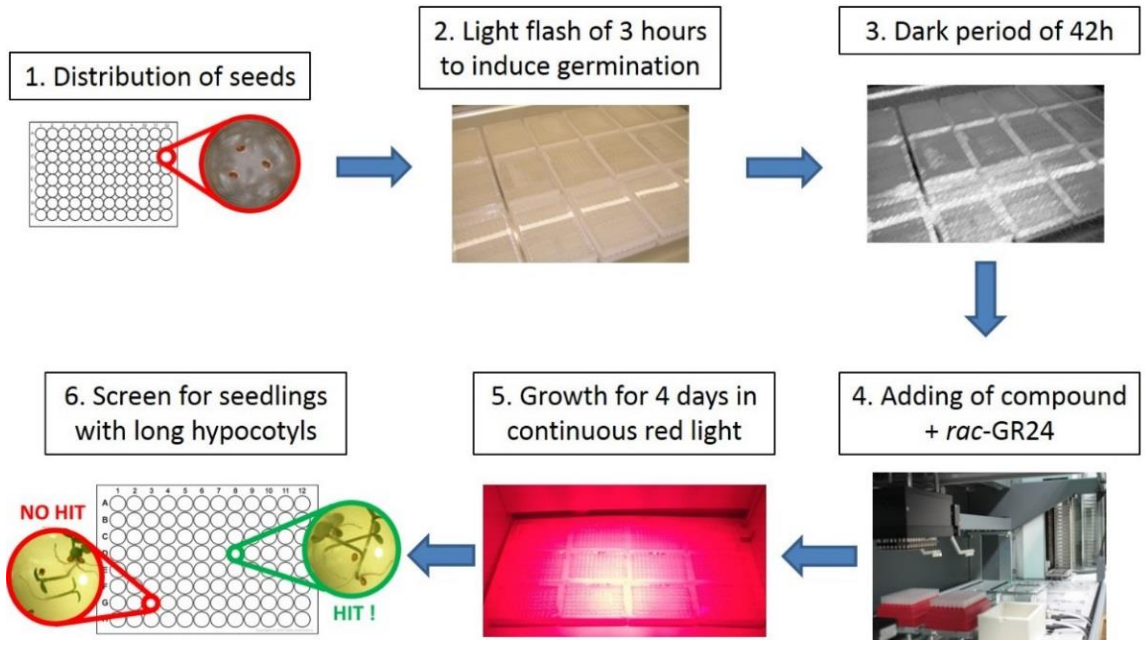

Figure 5. Workflow of the chemical screening procedure. For details, see text.

From the 12,000 tested compounds, 490 resulted in a long hypocotyl phenotype in the presence of *rac*-GR24 in the primary screen. To reduce this amount, we performed a structure-based clustering of the hit compounds prior to a confirmation screen (Supplementary Table 1). Thus, a representative compound from each cluster was selected, resulting in 168 compounds. These 168 compounds were confirmed by means of the same setup as the primary screen, except that after 4 days of growth in

continuous red light, the seedlings were transferred from the wells and spread on a thin layer of agar to allow the quantitative hypocotyl measurements. As a result, 58 compounds were validated (Supplementary Figure 1; Supplementary Table 2). From the remaining compounds, any compound that resembled the so-called pro-auxins was discarded. These molecules had been discovered in a chemical screen based on the promotion of hypocotyl elongation (Savaldi-Goldstein et al., 2008) and shared structural characteristics with synthetic and natural auxins, such as 2,4-dichlorophenoxyacetic acid (2,4D) or 1-naphthaleneacetic acid (1-NAA) or do so only when they are metabolized into active auxin inside the cells. Indeed, bioconversion of compounds into an auxin due to hydrolytic cleavage events by amidases or esterases has been frequently reported (Dai et al., 2005; Sungur et al., 2007; Christian et al., 2008; Savaldi-Goldstein et al., 2008). Hence, these compounds do not act by directly antagonizing the *rac*-GR24 signaling. For this selection, any compound that contained the structure of 2,4D; 1-NAA or indole-3-acetic acid (IAA) (Supplementary Figure 2) connected to a 'carrier' structure via an easily hydrolysable bond, were considered as pro-auxins and were discarded. Finally, 30 compounds were retained for further analysis (Supplementary Table 3). Recently, KAI2 inhibitors were reported, but none of the compounds are structurally similar to the hits that we have identified (Supplementary Table 4) (Holbrook-Smith et al., 2016). This was done by visually comparing the 30 remaining hit compounds with the structures published by Holbrook-Smith (2016). However, a comparison is somewhat complicated by the fact that the active moieties of the (putative) KAI2 inhibitors are not yet identified.

The hypocotyl length is known to be regulated by a complex network of both endogenous (such as various hormones) and environmental (such as light) cues (for a review, see Vandenbussche et al. 2005; Boron and Vissenberg, 2014). With a secondary screen on the remaining compounds, we aimed at discarding compounds that act independently of *rac*-GR24. Indeed, in order to derive whether a specific hit compound truly antagonizes the effect of *rac*-GR24, one should be able to compare the reduction in hypocotyl length between absence and presence of *rac*-GR24 treatment on the one hand; with the

reduction in hypocotyl length between the compound alone and the compound in the presence of *rac*-GR24 on the other hand. In the initial screen, the growth condition where only the compound was present in the absence of *rac*-GR24 was not included. As such, one could only screen for compounds that resulted in a longer hypocotyl in the presence of *rac*-GR24 compared to *rac*-GR24 treatment alone. Determining the differences in reduction of hypocotyl length between absence or presence of compound was not possible.

In order to determine the differences in reduction, and as such infer if the compounds are able to completely or incompletely antagonize the *rac*-GR24-mediated reduction in hypocotyl length, we carried out the hypocotyl assay on Col-0 and *max2* seeds in a 24-well plate under four different conditions: (i) in the absence of both *rac*-GR24 and the compound; (ii) only in the presence of *rac*-GR24; (iii) only in the presence of the compound; and (iv) in the presence of both *rac*-GR24 and the compound.

As such, by comparing the reduction in hypocotyl length between condition (i) and (ii), with the reduction in hypocotyl length between condition (iii) and (iv) for each hit compound, it can be determined whether the specific hit compound results in an equal sensitivity (i.e. not antagonistic); partial or complete insensitivity towards *rac*-GR24 treatment. As mentioned earlier in the hypothesis at the beginning of this section, both the D14- and the KAI2-signaling pathway are involved in the response of the hypocotyl to *rac*-GR24. As such, the receptor mutants *d14* and *kai2* are not fully insensitive to the *rac*-GR24 treatment when the reduction in hypocotyl length is analyzed, whereas the *d14;kai2* double mutant and the *max2* mutant are fully insensitive (Nelson et al., 2011; Waters et al., 2012; Toh et al., 2014). Hence, compounds that only antagonize one specific signaling pathway would result in only partial insensitivity, whereas compounds that are able to antagonize both pathways would result in a complete insensitivity towards *rac*-GR24.

Additionally, only the *kai2* mutant exhibited an elongated hypocotyl likewise the *max2* mutant under MOCK conditions (Chapter 4; Nelson et al., 2011; Waters et al., 2012; Toh et al., 2014). As a result, compounds that do not cause an enlargement of the hypocotyl length of WT seedlings, but antagonize the effect of *rac*-GR24 on the hypocotyl length might interfere with D14-dependent signaling, while compounds that do enlarge the WT hypocotyl might affect both D14 and KAI2-mediated effects, or might be specific for KAI2. Additionally, we hypothesized that hit compounds should not change the hypocotyl length of *max2*, as this mutant is flawed in *rac*-GR24 signaling.

Without compounds, the *rac*-GR24 treatment reduced the hypocotyl length in a MAX2-dependent fashion; whereas under MOCK conditions the hypocotyl was longer in the *max2* mutant than that in the WT (Figure 6A), in agreement with the results obtained on solid medium and with previous findings (Shen et al., 2007; Nelson et al. 2011). From the 30 compounds, 10 (partially) prevented the strong reduction in hypocotyl length that is normally caused by the *rac*-GR24 treatment (Figure 6). Indeed, the MAX2-dependent reduction in hypocotyl length was less pronounced in the presence of compound 5, 7, 8, 9, 21, 26, 27, or 30 or was completely absent in the presence of compound 10 or 24 (Figure 6). Thus, these compounds might function as *rac*-GR24 antagonists, because they made the WT insensitive or partially insensitive to the *rac*-GR24 treatment. The remaining 20 compounds were unable to fully or partially antagonize the *rac*-GR24 treatment, because the reduction in hypocotyl length in the presence of these compounds was indistinguishable from the control treatment with *rac*-GR24 (Supplementary Figure 3).

For compounds 7 and 8, additionally, the hypocotyl length of the WT slightly increased (P <0.001) (Figure 6). Because the mutation in *kai2* (but not in *d14*) leads to an elongated hypocotyl phenotype, compounds 7 and 8 might at least antagonize the KAI2 signaling pathway (Chapter 4, Nelson et al., 2011; Waters et al., 2012; Toh et al., 2014). However, they also slightly increased the hypocotyl length of the *max2* mutant (P <0.001) (Figure 6). This is unexpected and could imply two things: (i) the impact of these compounds on the hypocotyl length could be off-target effects, or (ii) the *max2*-mutant might not be

completely flawed in *rac*-GR24 signaling (as discussed in Chapter 3) and the compounds antagonize the remaining *rac*-GR24 signaling, resulting in a slight increase of the hypocotyl length.

For compounds 5, 9, 26, 27, and 30, no effect on the hypocotyl length of the WT and *max2* was found in the absence of *rac*-GR24 (Figure 6). As these compounds provoked a partial insensitivity to *rac*-GR24, they could antagonize signaling via D14, because a mutation in *d14* does not result in an elongated hypocotyl phenotype (Chapter 4, Nelson et al., 2011; Waters et al., 2012; Toh et al., 2014).

Finally, also special care should be taken for compounds 10, 21, and 24. Although compounds 10 and 24 resulted in a complete insensitivity, thus hinting at their antagonism of both D14 and KAI2, and compound 21 in a partial insensitivity, they had a negative impact on the hypocotyl length of the *max2* mutant under MOCK conditions ($P < 0.001$) (Figure 6). Also this effect is unexpected, and can currently not be explained.

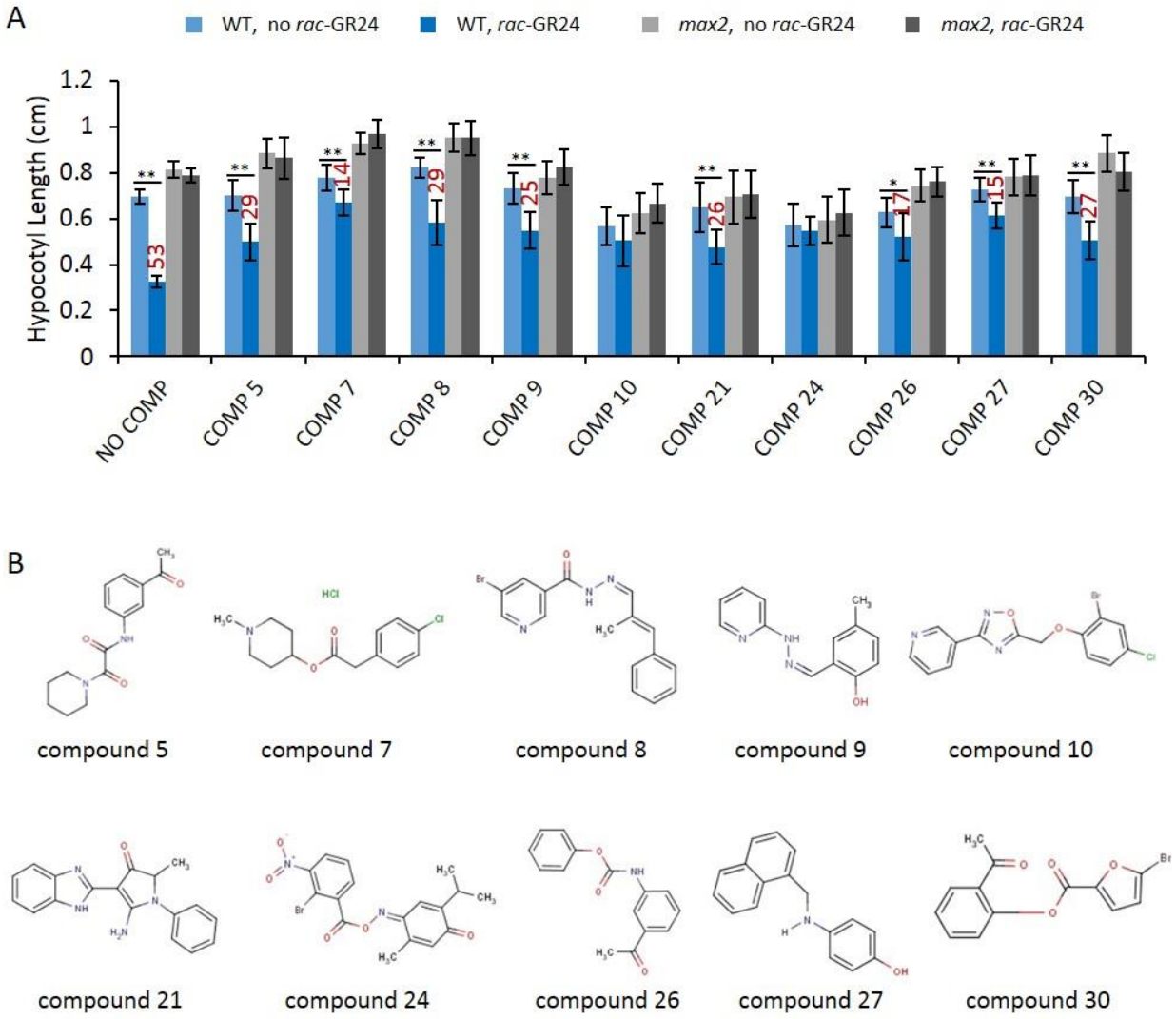

Figure 5. Positive hits of a secondary screen based on the hypocotyl phenotype. Seeds of WT and *max2-1* were sown in a 24-well format on liquid half-strength Murashige and Skoog medium in the absence of *rac*-GR24. After stratification, plates were exposed to white light for 3 h, followed by incubation in the dark for an additional 42 h. Then, the compounds and fresh medium supplemented with or without *rac*-GR24 were added to the wells (1 µM and 50 µM final concentrations of *rac*-GR24 and of the compounds, respectively) and were ultimately exposed to red light for 4 days. **(A)** Graphs represent means of three biological repeats ($n > 25$). Error bars represent the standard error (SE). Asterisks indicate statistically significant differences compared to the respective no-rac-*GR24* condition (* $P < 0.05$; ** $P < 0.001$; ANOVA-mixed model). Other relevant statistically significant effects are indicated in the text in order to keep the figure clear. Numbers in far red indicate the percentage of reduction in hypocotyl length (comparing 'no *rac*-GR24' treatment with '*rac*-GR24' treatment). **(B)** Structure of the positive-hit compounds shown in **(A)**.

In conclusion, 10 lead compounds were retained after the secondary screening. Compounds 5, 9, 26, 27, and 30 might be antagonists of the D14 signaling pathway, whereas compounds 7 and 8 might antagonize the KAI2 signaling or both KAI2 and D14 signaling. Compounds 10, 21, and 24 also antagonized the *rac*-GR24 effect on the hypocotyl length, but given their negative effect on *max2,* care should be taken when further analyzing these hits.

5.2.3. Effects of the lead compounds on *Phelypanche aegyptiaca* germination

Besides their role in the regulation of hypocotyl elongation, SLs also impact various physiological responses, such as lateral shoot branching, LR development, and germination of parasitic weeds. To check whether the newly discovered putative antagonists acted specifically on the hypocotyl effect of *rac*-GR24 or whether they were able to antagonize SLs in a broader way, we investigated their impact on some other SL-controlled phenotypes. As mentioned, SLs had been initially discovered because of their role in rhizosphere interactions. They induce germination of harmful root parasitic weeds that results in huge agricultural losses worldwide (Yoder and Scholes, 2010). Hence, we explored whether the 10 remaining antagonists were also able to prevent the SL-induced germination of *P. aegyptiaca* seeds. Generally, the seeds of this parasite remain dormant until their germination is triggered by the presence of SLs in the medium. Here, we exposed *P. aegyptiaca* seeds to a combined treatment of *rac*-GR24 with one of the antagonists and checked the effect on their germination. As expected, under control conditions, the *P. aegyptiaca* seeds did not germinate, but approximately 80% germinated by *rac*-GR24 treatment (Figure 7). Interestingly, co-treatment of *rac*-GR24 with compounds 24, 27, or 30 strongly reduced the impact of *rac*-GR24 on the germination (Figure 7). For compounds 24, 27, and 30, the germination was reduced to 31%, 51%, and 38%, respectively, compared to the 80% germination when treated with *rac*-GR24 only, suggesting that these three compounds might antagonize SL signaling over the species border. Indeed,

recent research has revealed that SLs are perceived by parasitic plants through several KAI2 paralogs, rather than by D14, as is the case in other land plants (Conn et al., 2015; Toh et al., 2015; Tsuchiya et al., 2015). The *KAI2* gene has undergone extensive gene duplication in parasites, whereas D14 remained as a single copy (Conn et al., 2015). The divergent clade (KAI2d) of paralogs has an extended ligand-binding cavity that can be compared to that of D14 in *Arabidopsis*. As such, the *KAI2* gene seems to have undergone extensive duplication in the parasite to obtain novel ligand specificities, enabling the parasite to respond to various germination stimulants that, in turn, may influence the host range of the parasite (Conn et al., 2015). As compounds 24, 27, and 30 could reduce the germination of the parasites, they might antagonize signaling via one or more members of the KAI2d clade.

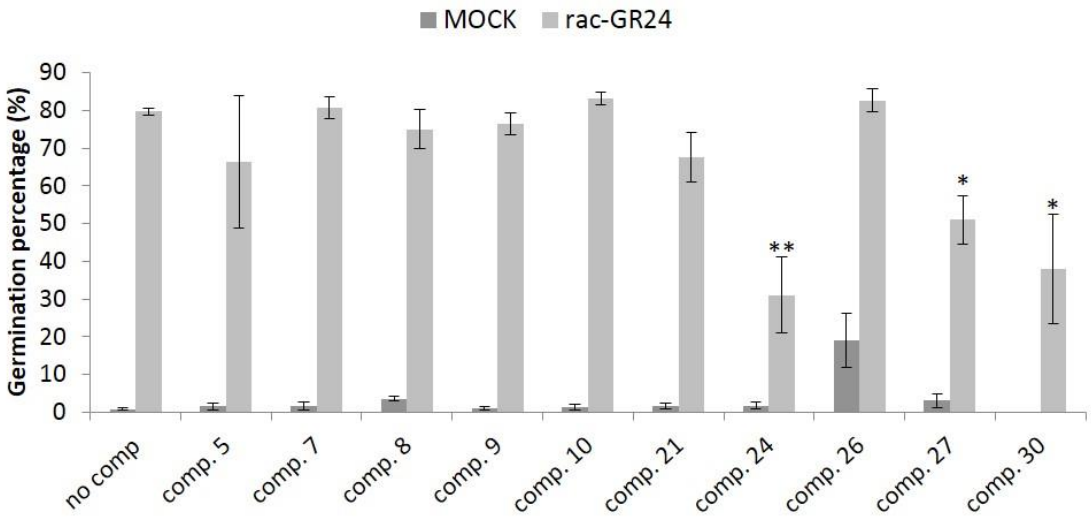

Figure 6. *Phelipanche aegyptiaca* seed germination assay in the presence of the selected hit compounds. After preconditioning of the seeds, the compounds (50 µM final concentration) were administered either with or without 0.1 µM *rac*-GR24. For the positive control, *rac*-GR24 solution was added and for the negative control, 1 ml of H_2O. After 7 days, the germination percentage was determined. Graphs represent means of three biological repeats. Error bars represent the standard error (SE) of three biological repeats. Asterisks indicate statistically significant differences compared to *rac*-GR24 treatment in the absence of compounds (* P <0.05; ** P <0.01; one-way ANOVA).

Thus far, the lead compounds were tested at the concentration that had originally been used during the chemical screening procedure. To investigate whether the compounds were also active at low concentrations, we conducted a dose response analysis. The antagonistic activity of compounds 24, 27, and 30 on the *rac*-GR24-induced germination of *P. aegyptiaca* seeds was tested in concentrations ranging between 1 µM and 50 µM (Figure 8). For compound 24, a dose-dependent antagonistic effect could be observed starting from 10 µM toward 50 µM, but the effect was only significant at 50 µM (Figure 8) and, similarly, for compound 27 from 10 µM onward but significant at both 10 µM and 50 µM (Figure 8). Also treatment with compound 30 resulted in a concentration-dependent reduction in germination and the impact was significant at 50 µM (Figure 8).

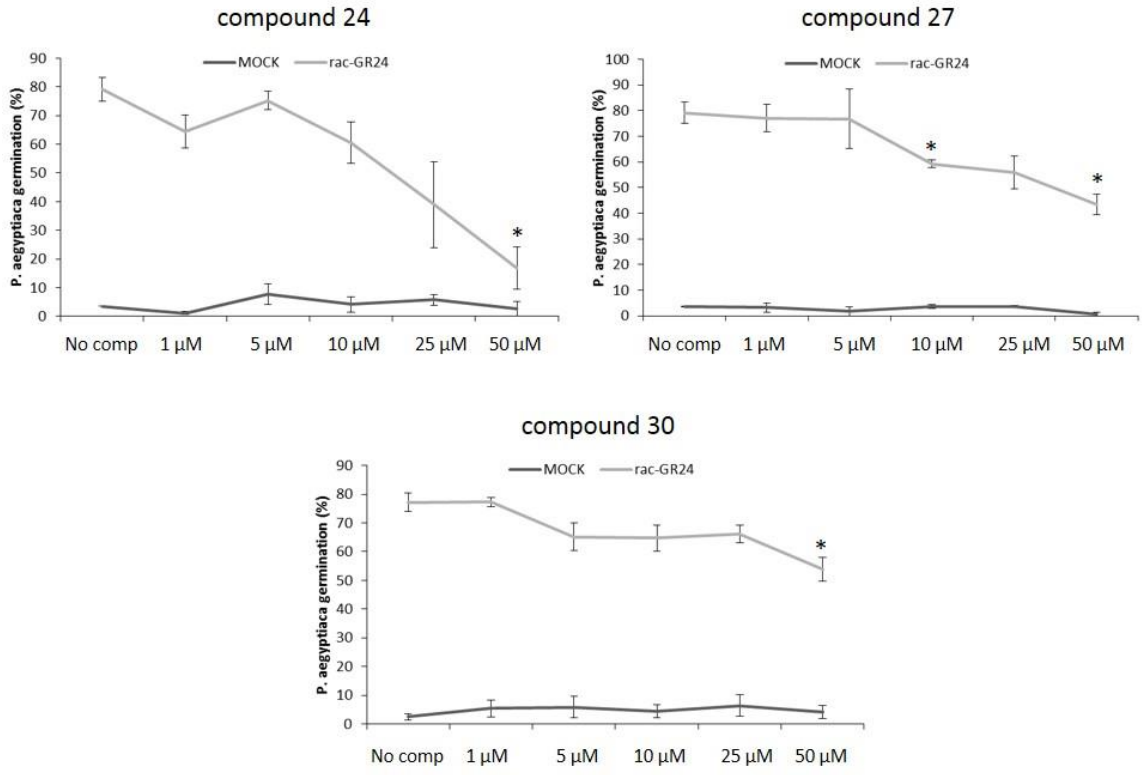

Figure 8. Dose response analyses of compounds 24, 27, and 30 on *P. aegyptiaca* seed germination. After preconditioning of the seeds, the compounds (final concentrations ranging from 1, 5, 10, 25 to 50 µM) were administered either with or without 0.1 µM *rac*-GR24. For the positive control, *rac*-GR24 solution was added and for the negative control, 1 ml of H_2O. After 7 days, the

germination percentage was determined. Graphs represent means of three (for compound 30) and two (for compounds 24 and 27) biological repeats. Error bars represent the standard error (SE) for the respective amount of biological repeats. Asterisks indicate statistically significant differences compared to *rac*-GR24 treatment in the absence of compounds (* P <0.05; one-way ANOVA).

Hence, the tested compounds seem to be the most potent as antagonists the higher the concentrations, but almost ineffective at low concentrations (Figure 8), indicating that the activity of these compounds might still be improved, for instance by structure-activity relationship (SAR) studies (Tóth and van der Hoorn, 2009). Via SAR studies, various functional groups of a specific molecule are replaced by other groups and their effect on the activity is evaluated. The bioactive moiety of the molecule can be identified and the structure can be altered in such manner as to enhance the biological activity.

5.2.4. Effects of the lead compounds on the lateral root phenotype

To investigate whether the 10 lead compounds could also impact on the *rac*-GR24-mediated reduction of the LRD, we grew WT and *max2* seeds for 9 days on growth medium either supplemented with or without *rac*-GR24 together with absence or presence of the compound (applied concentrations of *rac*-GR24 and compounds were 1 µM and 50 µM respectively). As the effects of the compounds on the root system architecture is so far only repeated once, the obtained results below should be interpreted with care.

This preliminary experiment indicated that in *Arabidopsis*, the compounds 7, 10, 24, 26, 27, and 30 caused a serious growth defect when seeds were directly exposed to the compound prior to germination, although the germination itself was not affected (Supplementary Figure 4), but their effect on the *rac*-GR24-mediated LRD reduction could not be inferred. Treatment with compounds 5, 8, and 21

also resulted in a reduction of the primary root length, albeit less serious, whereas treatment with compound 9 did not (Figure 9A and 9C; Supplementary Figure 5A and 5C). Currently, the role of SLs in the regulation of the primary root length is a matter of debate, because both positive (Ruyter-Spira et al., 2011) as negative (Shinohara et al., 2013) effects have been reported. As such, it is difficult to assess whether the reduced primary root length after treatment with compound 5, compounds 8 and compound 21, is a SL-related effect or not. Additionally, the effect of the compounds on the root system architecture should be repeated in order to confirm or reject these findings.

In agreement with previous studies, in the absence of compounds, treatment with *rac*-GR24 resulted in a MAX2-dependent reduction of the LRD when compared to control conditions (Figure 9) (Chapter 2; Chapter 4; Ruyter-Spira et al., 2011; Kapulnik et al., 2011). Our preliminary data suggest that when *rac*-GR24 was administered together with compound 5, the LRD was largely restored to the level in the presence of compound 5 without *rac*-GR24, which could imply an antagonistic effect of compound 5 on the *rac*-GR24 effect on the LRD (Figure 9B). Compound 5 also had a positive impact on LR development, because under MOCK conditions the LRD had increased by the addition of compound 5, both in the WT and in *max2* (Figure 9B). This could potentially point to an antagonism of compound 5 to endogenous SL signaling occurring in the WT. However, because this increase in LRD under MOCK conditions was also present in the *max2* mutant, this effect could be independent of SLs, unless the *max2* mutant is not fully flawed in SL signaling (see Chapter 3). Likewise as for the hypocotyl, the preliminary results for compound 5 seem to indicate an incomplete insensitivity of *rac*-GR24 on the LRD, possibly reconfirming an antagonistic effect specific for the D14 signaling pathway, because previously the *d14* mutant had been shown to be also partially insensitive at the LRD level to the *rac*-GR24 treatment (Chapter 3). Again here, the results of the compound on root system architecture should first be confirmed in additional repeats before clear conclusions can be drawn.

Treatment with compound 8 together with *rac*-GR24 seems to prevent the *rac*-GR24-mediated reduction in the LRD (Figure 9D). However, the preliminary experiment seems to indicate that compound 8 might have a very strong positive effect on the LR development, because under MOCK conditions the LRD strongly increased by the addition of compound 8, both in the WT and in *max2* (Figure 9D). Although the preliminary experiment seems to indicate that compound 8 might cause an insensitivity to *rac*-GR24, the general phenotype induced by compound 8 might not match a SL-related, but more an auxin effect (Boerjan et al., 1995; Himanen et al., 2002; Ruyter-Spira et al., 2011). Additionally, a high auxin level has been shown to overrule the *rac*-GR24 impact (Chapter 2; Ruyter-Spira et al., 2011). Hence, based on the results of this preliminary experiment, compound 8 might act as an auxin and, as such, cancels the *rac*-GR24 effect. However, the effect of compound 8 should be repeated to confirm or reject these initial findings.

Finally, treatment with compounds 9 or 21 does not seem to reduce the sensitivity to the *rac*-GR24 effect on the LRD. Thus, these compounds are likely not SL antagonists for this specific phenotype (Supplementary Figure 5).

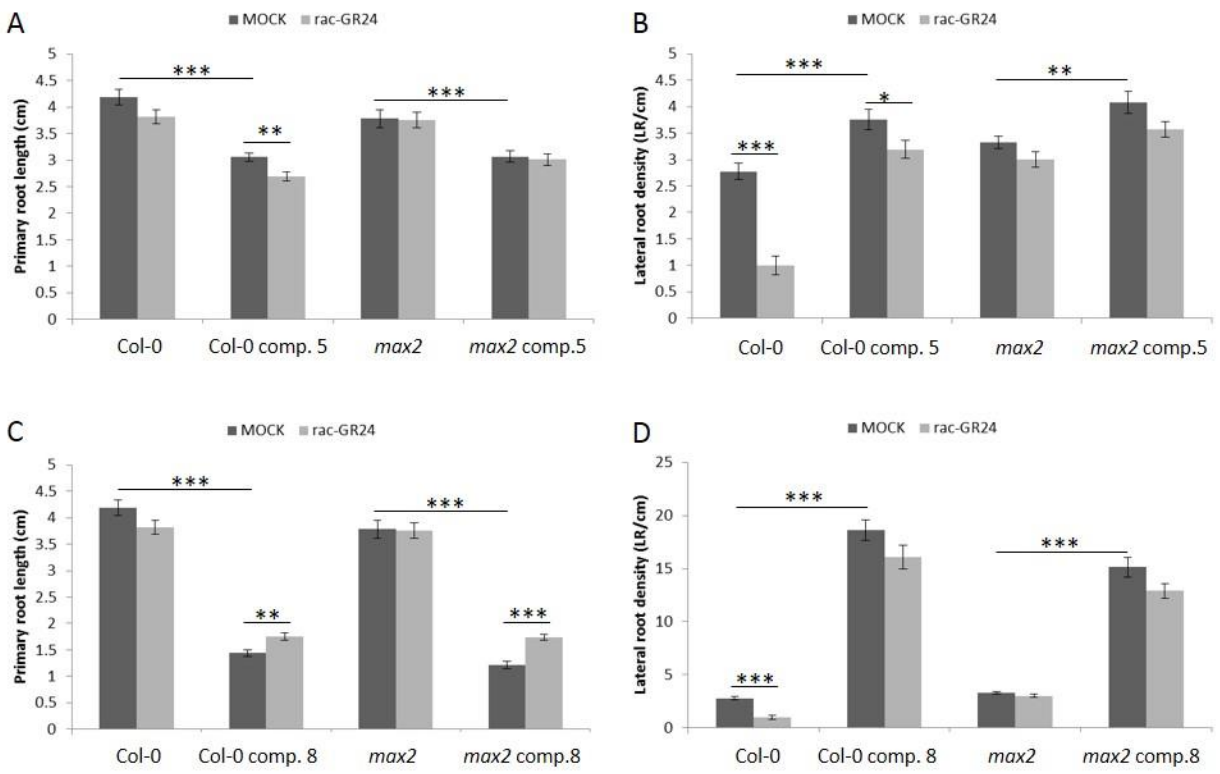

Figure 9. Preliminary results on the effects of compounds 5 and 8 on primary root length and on the *rac*-GR24-mediated reduction in lateral root density. Primary root length of Col-0 (WT) and *max2-1* after treatment with *rac*-GR24 and compound 5 **(A)** or compound 8 **(B)**. LRD of Col-0 and *max2-1* after treatment with *rac*-GR24 and compound 5 **(C)**, or compound 8 **(D)**.Data presented are means ± SE of one biological repeat ($n > 20$). Asterisks indicate statistically significant differences (* $P < 0.05$; ** $P < 0.01$; *** $P < 0.001$; Student's *t*-test).

To further investigate the growth defect caused by compounds 7, 10, 24, 26, 27, and 30, we sowed Col-0 WT seeds expressing the auxin reporter *pDR5:GUS* on growth medium supplemented with the compounds. For plants grown in the presence of compounds 5, 8, 9, and 21, no obvious differences could be observed compared to the control plants, both regarding the general morphology as the *pDR5:GUS* expression pattern (Figure 10). For compound 8, these results are in contradiction to the observed preliminary effects on the root system architecture above (Figure 9). There, compound 8 was shown to highly induce the LRD and hence could potentially be considered as an auxin-like molecule. However, in

seedlings expressing the *pDR5:GUS* construct treated with compound 8, no obvious induction of the construct, nor excessive formation of LR primordia could be observed (Figure 10). As the experiments on the *pDR5:GUS* expression pattern were repeated, and the effects on the RSA were the observations of only one biological repeat, the observed effects of compound 8 on the latter should be questioned. For compound 5, an induction of the *pDR5:GUS* expression pattern could be observed near the shoot-root junction (Figure 10). This is in *Arabidopsis* the location where adventitious roots are formed. As SLs are also known to inhibit adventitious root formation, this observation could suggest that compound 5 might also possibly antagonize this SL-effect and should be further investigated (Rasmussen et al., 2012).

However, for compounds 7, 10, 24, and 30, the growth inhibition of the primary root was accompanied with a strong induction of the *pDR5:GUS* expression in the cotyledons, the root tip, the hypocotyl, and near the shoot-root junction. Compound 7 contains a structure that is highly similar to the synthetic auxin phenylacetic acid, linked via a hydrolysable bond to another structure (Figure 5B). As such, it also has the characteristics of a pro-auxin molecule, and should have been discarded in an earlier elimination step (Savaldi-Goldstein et al., 2008). Similar for compound 10, a structure similar to the synthetic auxin 2,4D is present (Figure 5B; Supplementary Figure 2). During the initial selection to remove pro-auxin-like compounds it was argued that this molecule might not be a pro-auxin-like compound, because the auxin-moiety was linked to a ring structure and not via a (easily) hydrolysable bond. Nevertheless, the compound strongly induces *pDR5:GUS*. Additionally, treatment with compounds 26 and 27 resulted in a reduced primary root length and induction of the *pDR5:GUS* expression pattern near the shoot-root junction and in the root tip. Thus, compounds 7, 10, 24, 26, 27, and 30 cause serious growth defects of the primary root, accompanied with a strong induction of *pDR5:GUS*, hinting at elevated auxin levels and/or signaling. As high auxin levels are known to strongly reduce the primary root growth, they might explain the serious growth defects caused by these compounds (Himanen et al., 2002; Müssig et al., 2003; Rahman et al., 2007). Hence, these compounds likely distort the auxin homeostasis in *Arabidopsis,*

causing elevated auxin accumulation and/or signaling. Based on this result, their antagonistic effect on the *rac*-GR24-regulated hypocotyl length should be treated with care, because it has been reported that high auxin levels overrule the *rac*-GR24 effects (Chapter 2; Ruyter-Spira et al., 2011). On the other hand, compound 24, 27 and 30 were also shown to antagonize the *rac*-GR24-mediated germination of *P. aegyptiaca* seeds (Figure 7). This could indicate that they might be true SL antagonists in addition to their possible effect on the auxin homeostasis in *Arabidopsis*. Such a dual activity for chemical compounds has been reported earlier, exemplified by the compound brassinopride that has been shown to affect both brassinosteroid and ethylene signaling (Gendron et al., 2008).

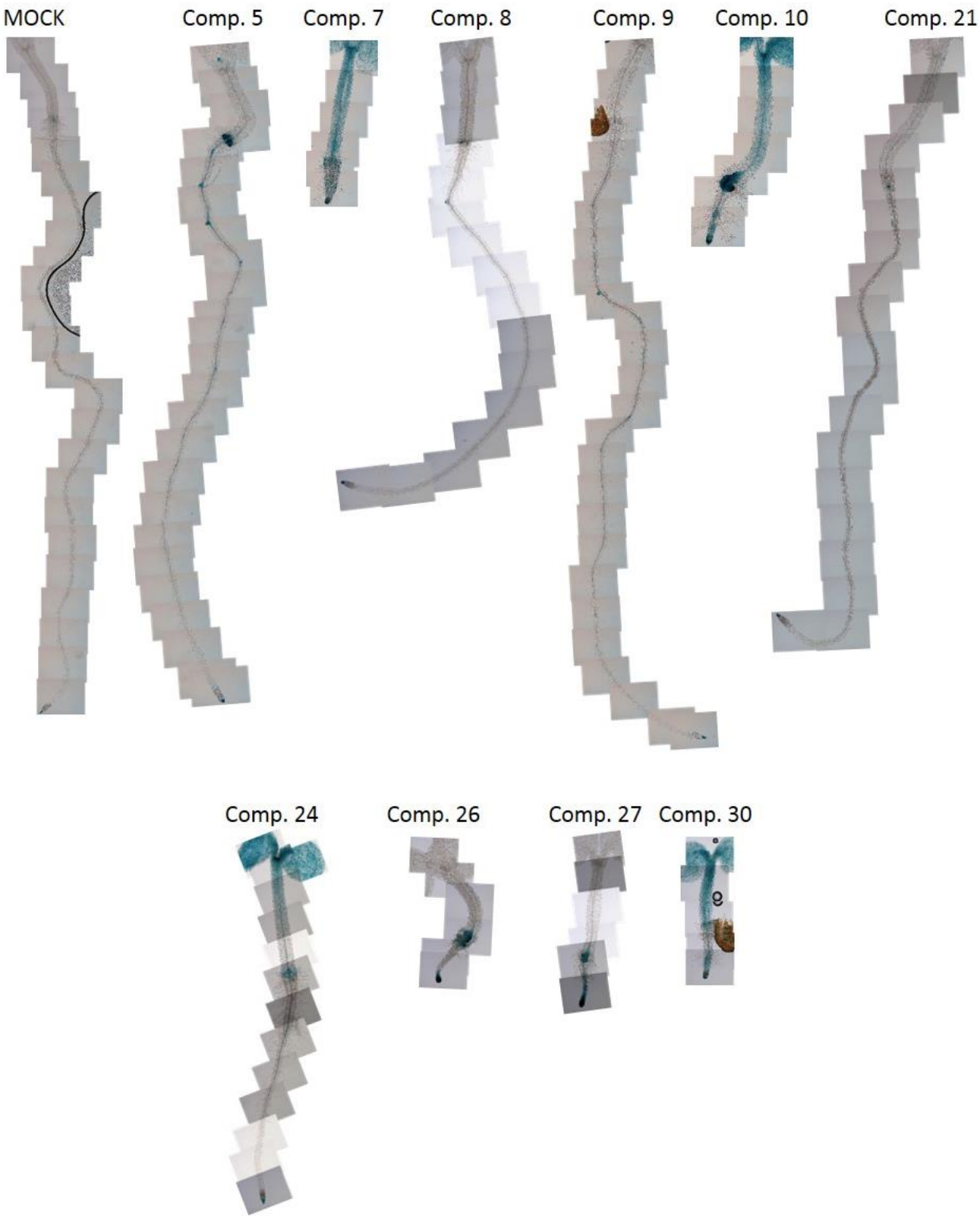
MOCK
Comp. 5
Comp. 7
Comp. 8
Comp. 9
Comp. 10
Comp. 21
Comp. 24
Comp. 26
Comp. 27
Comp. 30

Figure 10. Effect of the hit compounds on the general root development and the p*DR5:GUS* expression pattern. p*DR5:GUS* expression patterns of plants grown in the presence of 50 µM of the different compounds, 5 days after growth. This experiment was done in two biological repeats, with similar results (*n* = 7). The expression pattern was similar in all investigated seedlings, and one representative seedling was selected for imaging.

Finally, also for compounds 5 and 8, a dose response analysis was done, based on their inhibition of the *rac*-GR24-mediated reduction of the hypocotyl in *Arabidopsis*. Concentrations ranging between 1 µM and 50 µM were tested. The antagonistic effect of compound 5 on the *rac*-GR24 effect became slightly apparent from treatment with 5 µM onward and became stronger with increasing concentrations (Figure 11), whereas for compound 8, it started at a concentration of 10 µM and intensified with increasing concentrations (Figure 11). At 50 µM, compound 8 also had a positive impact on the hypocotyl length in the absence of *rac*-GR24, confirming the results obtained during the secondary screen (Figure 6).

Hence, as for compounds 24, 27, and 30, the compounds seem to be most potent as antagonists at high concentrations, whereas they had almost no effect at low concentrations (Figures 8 and 11). For compounds 5 and 8 too, the bioactivity might still be improved by SAR studies. Unlike phytohormones that are active at low concentrations, compounds used in a chemical screen did not undergo a strong evolutionary pressure and are, as such, not yet optimized to work in a highly efficient way.

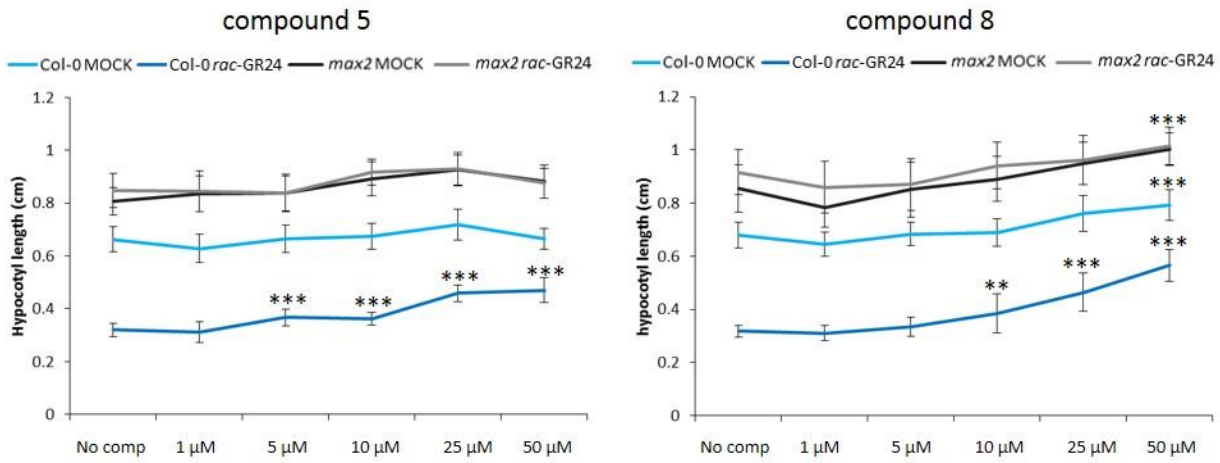

Figure 11. Dose response analyses of compounds 5 and 8 on the hypocotyl phenotype. Seeds of Col-0 and *max2-1* were sown in a 24-well format on liquid half-strength Murashige and Skoog medium. After stratification, plates were exposed to white light for 3 h, followed by incubation in the dark for an additional 42 h. Then, the compounds (at concentrations ranging from 1, 5, 10, 25 to 50 µM) and fresh medium supplemented with or without *rac*-GR24 (final concentration of 1 µM) were added to the wells and were ultimately exposed to red light for 4 days. Graphs represent means of three biological repeats (n > 25). Error bars represent the standard error (SE). Asterisks indicate statistically significant differences compared to the respective condition in the absence of compound (No comp) (** P <0,01; *** P <0.001; ANOVA-mixed model).

In conclusion, a chemical genetics screen was initiated, and 10 hit compounds could be identified as putative antagonists of the *rac*-GR24 inhibition of hypocotyl elongation. However, further analyses revealed that six of these compounds (compounds 7, 10, 24, 26, 27, and 30) might alter the auxin homeostasis in Arabidopsis, and might as such overrule the *rac*-GR24 effect. As discussed above, the results on the effect of compound 8 on the root system architecture are currently contradictory and should first be repeated. Of the remaining compounds, compound 5 could potentially be a general antagonist of *rac*-GR24 signaling, because it has an impact on both the hypocotyl and possibly also the LRD phenotype. In contrast, the antagonizing effect of compounds 9 and 21 is most probably restricted to the *rac*-GR24 effect on the hypocotyl. Although compounds 24, 27, and 30 possibly affect the auxin

homeostasis in *Arabidopsis*, they had a strong inhibitory effect on the *rac*-GR24-induced germination of *P. aegyptiaca* seeds. Thus far, a negative effect of auxin on the germination of *P. aegyptiaca* has not been reported yet. If auxin would seemingly not affect their germination, compounds 24, 27, and 30 would be valid SL antagonists, besides influencing the auxin homeostasis in *Arabidopsis*. In addition to the optimization of their bioactivity and the identification of their bioactive moiety, SAR has also been proven useful for the uncoupling of different phenotypes caused by a lead compound (Rojas-Pierce et al., 2007; Gendron et al., 2009). Hence, derivates might be found that no longer have auxin activities, but still antagonize the germination of parasitic weeds by SLs.

Table 1 summarizes the different effects of the compounds that have been investigated so far. A next step would be to validate if these compounds are true antagonists of *rac*-GR24 signaling. This could be done by analysis of various SL-related mutants, by checking their effect on SL-marker gene expression and by SAR studies. Besides a SAR study, unraveling the mode-of-action of the remaining lead compounds by identification of their target proteins will be the next challenge. Likewise, new insight will be obtained into how SL signaling triggers the various physiological responses and the identification of chemicals might be useful to modify SL-dependent processes for biotechnological applications.

Table 1. summary on the different effects of the compounds

Comp.	*rac-GR24 mediated reduction of hypocotyl lenght*	*rac-GR24 mediated P. aegyptiaca germination*	*rac-GR24 mediated reduction of LRD*	*effect on DR5:GUS expression*
5	Partial insensitive: 29% reduction instead of 53% reduction	/	Partial insensitive? * reduction of primary root length? * increase on LRD?	No strong induction
7	Partial insensitive: 14% reduction instead of 53% reduction * Causes slight increase in hypocotyl length	/	n.a.	Strong induction in the cotyledons, root tip, hypocotyl and near the shoot-root junction
8	Partial insensitive: 29% reduction instead of 53% reduction * Causes slight increase in hypocotyl length	/	Fully insensitive? * reduction of primary root length? * Increase on LRD??	No strong induction
9	Partial insensitive: 25% reduction instead of 53% reduction	/	Fully sensitive? * decrease on LRD?	No strong induction
10	Fully insensitive: no significant reduction * Causes slight decrease in *max2* hypocotyl length	/	n.a.	Strong induction in the cotyledons, root tip, hypocotyl and near the shoot-root junction
21	Partial insensitive: 26% reduction instead of 53% reduction * Causes slight decrease in *max2* hypocotyl length	/	Fully sensitive? * reduction of primary root length? * decrease on LRD?	No strong induction
24	Fully insensitive: no significant reduction * Causes slight decrease in *max2* hypocotyl length	31% germination instead of 80% germination	n.a.	Strong induction in the cotyledons, root tip, hypocotyl and near the shoot-root junction
26	Partial insensitive: 17% reduction instead of 53% reduction	/	n.a.	Strong induction in the root tip and near the shoot-root junction
27	Partial insensitive: 15% reduction instead of 53% reduction	51% germination instead of 80% germination	n.a.	Strong induction in the root tip and near the shoot-root junction
30	Partial insensitive: 27% reduction instead of 53% reduction	38% germination instead of 80% germination	n.a.	Strong induction in the cotyledons, root tip, hypocotyl and near the shoot-root junction

/: no effect; n.a. : not analyzed; ?: uncertain effect, preliminary; ??: uncertain effect, preliminary and contradicting data present

5.3. Materials and methods

Hypocotyl assays

Wild-type (WT) *Arabidopsis thaliana* (L.) Heynh., accession Columbia-0 (Col-0) and *max2-1* seeds (Leyser et al., 2002) were sown on half-strength Murashige and Skoog medium (0.8% [w/v] plant tissue culture agar) without sucrose, supplemented with or without 1 µM *rac*-GR24 (kindly provided by Prof. Dr. F.-D. Boyer) and kept for 2 days at 4°C before exposure to white light for 3 h to induce germination. Thereafter, the seeds were kept in the dark at 21°C for an additional 21 h by wrapping the plates in aluminum foil. Then, the seeds were grown horizontally in continuous red light at 21°C (20 photosynthetically active radiation [PAR]). Hypocotyl lengths were measured 4 days later.

For optimization, 3-6 seeds were sown in each well of a 96-well plate with 100 µL solid or 200 µL liquid half-strength Murashige and Skoog medium without sucrose. Concentrations of 0.1, 1, and 2 µM *rac*-GR24 were used. For the delayed addition of *rac*-GR24, seeds were sown in 100 µL liquid medium. After the exposure to white light for 3 h and dark incubation for either 21, 27, or 42 h, the plates were unwrapped and an extra 100 µL of fresh medium supplemented with or without *rac*-GR24 was added to the wells, resulting in a total volume of 200 µL medium (final concentrations of 1 or 2 µM of *rac*-GR24) prior to the red-light exposure. For the hypocotyl measurements, the medium was replaced first by a 70% ethanol solution to stop growth. Seedlings were carefully transferred on a thin layer of agar to allow scanning and subsequent measurement of the hypocotyl by means of the ImageJ software (http://rsb.info.nih.gov/ij).

Chemical screening

The ChemBridge™ DiverSet 3 chemical library containing 12,000 compounds was employed. The compounds were dissolved in dimethyl sulfoxide (DMSO) to a final concentration of 5 mM. Three to 6 Col-0 seeds were sown per well containing 100 µL of liquid medium and were handled as described above. After a 42-h dark incubation, the plates were unwrapped and the compounds were distributed, whereafter 100 µL of liquid medium supplemented with *rac*-GR24 was added, resulting in a final concentration of 50 µM compound, 1 µM *rac*-GR24, and 1% (v/v) DMSO. As a negative control, in the first row of each 96-well plate, no compound was administered. As a positive control, 100 µL of liquid medium without *rac*-GR24 or compound was added to the last row of each 96-well plate. After this procedure, plates were resealed and exposed to continuous red light for 4 days (20 PAR). The seedling growth was stopped by replacing the growth medium by a 70% ethanol solution. The hypocotyls were scored qualitatively under a binocular.

The structure-based clustering of the hit compounds was carried out with the KNIME workflow with the CDK extension (https://tech.knime.org/community/cdk). The input of the chemical structures and generation of the fingerprints was done via CDK nodes, whereas the distance matrix and clustering were done by means of the KNIME software itself.

For the confirmation screen, seedlings were carefully transferred on a thin layer of agar to allow quantitative measurements of the hypocotyl length.

Secondary screening

Confirmed hit compounds were ordered via the ChemBridge™ Chemical store (www.hittolead.com®) and were dissolved in DMSO to a final concentration of 20 mM (except for 10 mM for compound 20) and were stored at -20°C. Approximately 20 *Arabidopsis* Col-0 and *max2-1* seeds were

sown in each well of a 24-well plate containing 400 µL liquid half-strength Murashige and Skoog medium without sucrose. The plates were incubated as described above and after 42 h of dark incubation, the plates were unwrapped and compounds and 400 µL of fresh medium supplemented or not with *rac*-GR24 were added to each well (final concentrations 50 µM and 1 µM of compound and *rac*-GR24, respectively). In the absence of compound, DMSO was added as a control. After the further growth procedure, seedlings were carefully transferred to a thin layer of agar to allow hypocotyl length measurements. The procedure was done in three biological repeats.

For the hypocotyl-based dose response analyses, seeds were likewise sown. The compounds were added to a final concentration of 1 µM, 5 µM, 10 µM, 25 µM, and 50 µM or only DMSO as a control.

Phelypanche aegyptiaca germination assays

The *Phelypanche aegyptiaca* (broomrape) seeds (kindly provided by Dr. Radi Aly, Newe Yaar Research Center, Ramat Yeshai, Israel) were surface sterilized with 70% (v/v) ethanol containing 0.05% (v/v) sodium dodecyl sulfate for 5 min and then washed with 95% (v/v) ethanol for 5 min and air dried. For the preconditioning, the seeds were sprinkled on a filter paper humidified with 1 ml of sterile water containing 1% (v/v) 4-(2-hydroxyethyl)-1-piperazineethanesulfonic acid (HEPES) buffer and 0.1% (v/v) Plant Preservative Mixture (Plant Cell Technology®) in a 5-cm Petri dish, sealed with parafilm, and kept in the dark at 24°C for 7 days. Excess water was removed as much as possible. For the positive control, 1 ml of the solution was added and for the negative control, 1 ml of water. The compounds (50 µM final concentration) were administered as a 1-ml solution either supplemented or not with 0.1 µM *rac*-GR24. The Petri dishes were resealed with parafilm and incubated in the dark at 24°C. After 7 days, the germination percentage was determined. All incubations were done in triplicate. The dose response

analyses for *P. aegyptiaca* were carried out as described above and concentrations of the compounds were 1 µM, 5 µM, 10 µM, 25 µM, and 50 µM or only DMSO as a control.

Lateral root density assay

WT and *max2-1* plants were grown for 9 days under continuous light conditions at 21°C on half-strength Murashige and Skoog medium with 1% (w/v) sucrose, supplemented or not with 1 µM *rac*-GR24 in the absence (DMSO) or presence of the compounds (50 µM final concentration for the compounds). Laterals roots (LRs) were counted under a binocular S4E microscope (Leica Microsystems) and root length was measured with ImageJ. Both values were used to calculate the LR density (LRD).

pDR5:GUS analysis and clearing

Seeds of *pDR5:GUS* were sown on medium supplemented with 50 µM compound or with the same volume of DMSO as control and were stratified for 2 days at 4°C. Square 8-well plates (Nunc) were utilized. Seedlings were grown vertically under continuous white light at 21°C. After 5 days, the seedlings were harvested for analysis and were stained for 90 min in multiwell plates as described (Jefferson et al., 1987). Samples were cleared as described (Malamy and Benfey, 1997) and were analyzed by a differential interference contrast BX51 microscope (Olympus).

Statistics

Statistics regarding the hypocotyl length in the various experiments were done by means of analysis of variance (ANOVA)-mixed models as previously described with slight modifications (Rasmussen et al., 2012). A Student's *t*-test was used for the experiments on the impact on the root system

architecture (Excel, Microsoft Office 2013). A one-way ANOVA was done for the *P. aegyptiaca* germination assays according to the Enterprise Guide Software (SAS, Cary, NC, USA). A *post-hoc* analysis and Tukey corrections were applied to correct for multiple testing.

5.4. References

Aguilar-Martínez, J.A., Poza-Carrión, C., and Cubas, P. (2007). *Arabidopsis BRANCHED1* acts as an integrator of branching signals within axillary buds. Plant Cell 19, 458-472.

Arite, T., Umehara, M., Ishikawa, S., Hanada, A., Maekawa, M., Yamaguchi, S., and Koyzuka, J. (2009). *d14*, a strigolactone-insensitive mutant of rice, shows an accelerated outgrowth of tillers. Plant Cell Physiol. 50, 1416-1424.

Armstrong, J.I., Yuan, S., Dale, J.M., Tanner, V.N., and Theologis, A. (2004). Identification of inhibitors of auxin transcriptional activation by means of chemical genetics in Arabidopsis. Proc. Natl. Acad. Sci. USA 101, 14978-14983 [Erratum Proc. Natl. Acad. Sci. USA 101, 17565].

Boerjan, W., Cervera, M.-T., Delarue, M., Beeckman, T., Dewitte, W., Bellini, C., Caboche, M., Van Onckelen, H., Van Montagu, M., and Inzé, D. (1995). *superroot*, a recessive mutation in Arabidopsis, confers auxin overproduction. Plant Cell 7, 1405-1419.

Boron, A.K., and Vissenberg, K. (2014). The *Arabidopsis thaliana* hypocotyl, a model to identify and study control mechanisms of cellular expansion. Plant Cell Rep. 33, 697-706.

Christian, M., Hannah, W.B., Lüthen, H., and Jones, A.M. (2008). Identification of auxins by a chemical genomics approach. J. Exp. Bot. 59, 2757-2767.

Conn, C.E., Bythell-Douglas, R., Neumann, D., Yoshida, S., Whittington, B., Westwood, J.H., Shirasu, K., Bond, C.S., Dyer, K.A., and Nelson, D.C. (2015). Convergent evolution of strigolactone perception enabled host detection in parasitic plants. Science 349, 540-543.

Crawford, S., Shinohara, N., Sieberer, T., Williamson, L., George, G., Hepworth, J., Müller, D., Domagalska, M.A., and Leyser, O. (2010). Strigolactones enhance competition between shoot branches by dampening auxin transport. Development 137, 2905-2913.

Dai, X., Hayashi, K.-i., Nozaki, H., Cheng, Y., and Zhao, Y. (2005). Genetic and chemical analyses of the action mechanisms of sirtinol in Arabidopsis. Proc. Natl. Acad. Sci. USA 102, 3129–3134.

De Rybel, B., Audenaert, D., Beeckman, T., and Kepinski, S. (2009a). The past, present and future of chemical biology in auxin research. ACS Chem. Biol. 4, 987-998.

De Rybel, B., Audenaert, D., Vert, G., Rozhon, W., Mayerhofer, J., Peelman, F., Coutuer, S., Denayer, T., Jansen, L., Nguyen, L., Vanhoutte, I., Beemster, G.T.S., Vleminckx, K., Jonak, C., Chory, J., Inzé, D., Russinova, E., and Beeckman, T. (2009b). Chemical inhibition of a subset of *Arabidopsis thaliana* GSK3-like kinases activates brassinosteroid signaling. Chem. Biol. 16, 594-604.

Flematti, G.R., Scaffidi, A., Waters, M.T., and Smith, S.M. (2016). Stereospecificity in strigolactone biosynthesis and perception. Planta 243, 1361-1373.

Gendron, J.M., Haque, A., Gendron, N., Chang, T., Asami, T., and Wang, Z.-Y. (2008). Chemical genetic dissection of brassinosteroid-ethylene interaction. Mol. Plant 1, 368-379.

Gomez-Roldan, V., Fermas, S., Brewer, P.B., Puech-Pagès, V., Dun, EA., Pillot, J.-P., Letisse, F., Matusova, R., Danoun, S., Portais, J-C., Bouwmeester, H., Bécard, G., Beveridge, C.A., Rameau, C., and Rochange, S.F. (2008). Strigolactone inhibition of shoot branching. Nature 455, 189-194.

Himanen, K., Boucheron, E., Vanneste, S., de Almeida Engler, J., Inzé, D., and Beeckman, T. (2002). Auxin-mediated cell cycle activation during early lateral root initiation. Plant Cell 14, 2339-2351.

Holbrook-Smith, D., Toh, S., Tsuchiya, Y., and McCourt, P. (2016). Small-molecule antagonists of germination of the parasitic plant *Striga hermonthica*. Nat. Chem. Biol. 12, 724-729.

Jefferson, R.A., Kavanagh, T.A., and Bevan, M.W. (1987). GUS fusions: β-glucuronidase as a sensitive and versatile gene fusion marker in higher plants. EMBO J. 6, 3901-3907.

Jia, K.-P., Luo, Q., He, S.-B., Lu, X.-D., and Yang, H.-Q. (2014). Strigolactone-regulated hypocotyl elongation is dependent on cryptochrome and phytochrome signaling pathways in *Arabidopsis*. Mol. Plant 7, 528-540.

Kapulnik, Y., Delaux, P.-M., Resnick, N., Mayzlish-Gati, E., Wininger, S., Bhattacharya, C., Séjalon-Delmas, N., Combier, J.-P., Bécard, G., Belausov, E., Beeckman, T., Dor, E., Hershenhorn, J., and Koltai, H. (2011). Strigolactones affect lateral root formation and root-hair elongation in Arabidopsis. Planta 233, 209-216.

Leyser, O. (2002). Molecular genetics of auxin signaling. Annu. Rev. Plant Biol. 53, 377-398.

Liang, Y., Ward, S., Li, P., Bennett, T., and Leyser, O. (2016). SMAX1-LIKE7 signals from the nucleus to regulate shoot development in Arabidopsis via partially EAR motif-independent mechanisms. Plant Cell 28, 1581-1601.

Malamy, J.E., and Benfey, P.N. (1997). Organization and cell differentiation in lateral roots of *Arabidopsis thaliana*. Development 124, 33-44.

Müssig, C., Shin, G.-H., and Altmann, T. (2003). Brassinosteroids promote root growth in Arabidopsis. Plant Physiol. 133, 1261-1271.

Nelson, D.C., Scaffidi, A., Dun, E.A., Waters, M.T., Flematti, G.R., Dixon, K.W., Beveridge, C.A., Ghisalberti, E.L., and Smith, S.M. (2011). F-box protein MAX2 has dual roles in karrikin and strigolactone signaling in Arabidopsis thaliana. Proc. Natl. Acad. Sci. USA 108, 8897-8902.

Rahman, A., Bannigan, A., Sulaman, W., Pechter, P., Blancaflor, E.B., and Baskin, T.I. (2007). Auxin, actin and growth of the *Arabidopsis thaliana* primary root. Plant J. 50, 514-528.

Rasmussen, A., Mason, M.G., De Cuyper, C., Brewer, P.B., Herold, S., Agusti, J., Geelen, D., Greb, T., Goormachtig, S., Beeckman, T., and Beveridge, C.A. (2012). Strigolactones suppress adventitious rooting in Arabidopsis and pea. Plant Physiol. 158, 1976-1987.

Rojas-Pierce, M., Titapiwatanakun, B., Sohn, E.J., Fang, F., Larive, C.K., Blakeslee, J., Cheng, Y., Cuttler, S.R., Peer, W.A., Murphy, A.S., and Raikhel, N.V. (2007). *Arabidopsis* P-glycoprotein19 participates in the inhibition of gravitropism by gravacin. Chem. Biol. 14, 1366-1376 [Erratum Chem. Biol. 15, 87].

Ruyter-Spira, C., Kohlen, W., Charnikhova, T., van Zeijl, A., van Bezouwen, L., de Ruijter, N., Cardoso, C., Lopez-Raez, J.A., Matusova, R., Bours, R., Verstappen, F., and Bouwmeester, H. (2011). Physiological effects of the

synthetic strigolactone analog GR24 on root system architecture in Arabidopsis: another belowground role for strigolactones? Plant Physiol. 155, 721-734.

Savaldi-Goldstein, S., Baiga, T.J., Pojer, F., Dabi, T., Butterfield, C., Parry, G., Santner, A., Dharmasiri, N., Tao, Y., Estelle, M., Noel, J.P., and Chory, J. (2008). New auxin analogs with growth-promoting effects in intact plants reveal a chemical strategy to improve hormone delivery. Proc. Natl. Acad. Sci. USA 105, 15190-15195.

Scaffidi, A., Waters, M.T., Sun, Y.K., Skelton, B.W., Dixon, K.W., Ghisalberti, E.L., Flematti, G.R., and Smith, S.M. (2014). Strigolactone hormones and their stereoisomers signal through two related receptor proteins to induce different physiological responses in Arabidopsis. Plant Physiol. 165, 1221 1232.

Sergeant, M.J., Li, J.-J., Fox, C., Brookbank, N., Rea, D., Bugg, T.D.H., and Thompson, A.J. (2009). Selective inhibition of carotenoid cleavage dioxygenases. Phenotypic effects on shoot branching. J. Biol. Chem. 284, 5257-5264.

Shen, H., Luong, P., and Huq, E. (2007). The F-Box protein MAX2 functions as a positive regulator of photomorphogenesis in Arabidopsis. Plant Physiol. 145, 1471-1483.

Shen, H., Zhu, L., Bu, Q.-Y., and Huq, E. (2012). MAX2 affects multiple hormones to promote photomorphogenesis. Mol. Plant 5, 750-762.

Shinohara, N., Taylor, C., and Leyser, O. (2013). Strigolactone can promote or inhibit shoot branching by triggering rapid depletion of the auxin efflux protein PIN1 from the plasma membrane. PLoS Biol. 11, e1001474.

Soundappan, I., Bennett, T., Morffy, N., Liang, Y., Stanga, J.P., Abbas, A., Leyser, O., and Nelson, D.C. (2015). SMAX1-LIKE/D53 family members enable distinct MAX2-dependent responses to strigolactones and karrikins in Arabidopsis. Plant Cell 27, 3143-3159.

Stanga, J.P., Smith, S.M., Briggs, W.R., and Nelson, D.C. (2013). *SUPPRESSOR OF MORE AXILLARY GROWTH2 1* controls seed germination and seedling development in Arabidopsis. Plant Physiol. 163, 318-330.

Stirnberg, P., Furner, I.J., and Leyser, H.M.O. (2007). MAX2 participates in an SCF complex which acts locally at the node to suppress shoot branching. Plant J. 50, 80-94.

Sungur, C., Miller, S., Bergholz, J., Hoye, R.C., Brisbois, R.G., and Overvoorde; P. (2007). The small molecule 2-furylacrylic acid inhibits auxin-mediated responses in *Arabidopsis thaliana*. *Plant Cell Physiol*. 48, 1693-1701.

Toh, S., Holbrook-Smith, D., Stogios, P.J., Onopriyenko, O., Lumba, S., Tsuchiya, Y., Savchenko, A., and McCourt, P. (2015). Structure-function analysis identifies highly sensitive strigolactone receptors in Striga. Science 350, 203-207.

Toh, S., Holbrook-Smith, D., Stokes, M.E., Tsuchiya, Y., and McCourt, P. (2014). Detection of parasitic plant suicide germination compounds using a high-throughput *Arabidopsis* HTL/KAI2 strigolactone perception system. Chem. Biol. 21, 988-998.

Tóth, R., and van der Hoorn, R.A.L. (2010). Emerging principles in plant chemical genetics. Trends Plant Sci. 15, 81-88.

Tsuchiya, Y., Vidaurre, D., Toh, S., Hanada, A., Nambara, E., Kamiya, Y., Yamaguchi, S., and McCourt, P. (2010). A small-molecule screen identifies new functions for the plant hormone strigolactone. Nat. Chem. Biol. 6, 741-749.

Tsuchiya, Y., Yoshimura, M., Sato, Y., Kuwata, K., Toh, S., Holbrook-Smith, D., Zhang, H., McCourt, P., Itami, K., Kinoshita, T., and Hagihara, S. (2015). Probing strigolactone receptors in *Striga hermonthica* with fluorescence. Science 349, 864-868.

Umehara, M., Hanada, A., Yoshida, S., Akiyama, K., Arite, T., Takeda-Kamiya, N., Magome, H., Kamiya, Y., Shirasu, K., Yoneyama, K., Kyozuka, J., and Yamaguchi, S. (2008). Inhibition of shoot branching by new terpenoid plant hormones. Nature 455, 195-200.

Vandenbussche, F., Verbelen, J.-P., and Van Der Straeten, D. (2005). Of light and length: regulation of hypocotyl growth in *Arabidopsis*. BioEssays 27, 275-284.

Wang, L., Wang, B., Jiang, L., Liu, X., Li, X., Lu, Z., Meng, X., Wang, Y., Smith, S.M., and Li, J. (2015). Strigolactone signaling in Arabidopsis regulates shoot development by targeting D53-like SMXL repressor proteins for ubiquitination and degradation. Plant Cell 27, 3128-3142.

Waters, M.T., Nelson, D.C., Scaffidi, A., Flematti, G.R., Sun, Y.K., Dixon, K.W., and Smith, S.M. (2012). Specialisation within the DWARF14 protein family confers distinct responses to karrikins and strigolactones in Arabidopsis. Development 139, 1285-1295.

Xie, X., Yoneyama, K., and Yoneyama, K. (2010). The strigolactone story. Annu. Rev. Phytopathol. 48, 93-117.

Yoder, J.I., and Scholes, J.D. (2010). Host plant resistance to parasitic weeds; recent progress and bottlenecks. Curr. Opin. Plant Biol. 13, 478-484.

5.5. Supplementary data

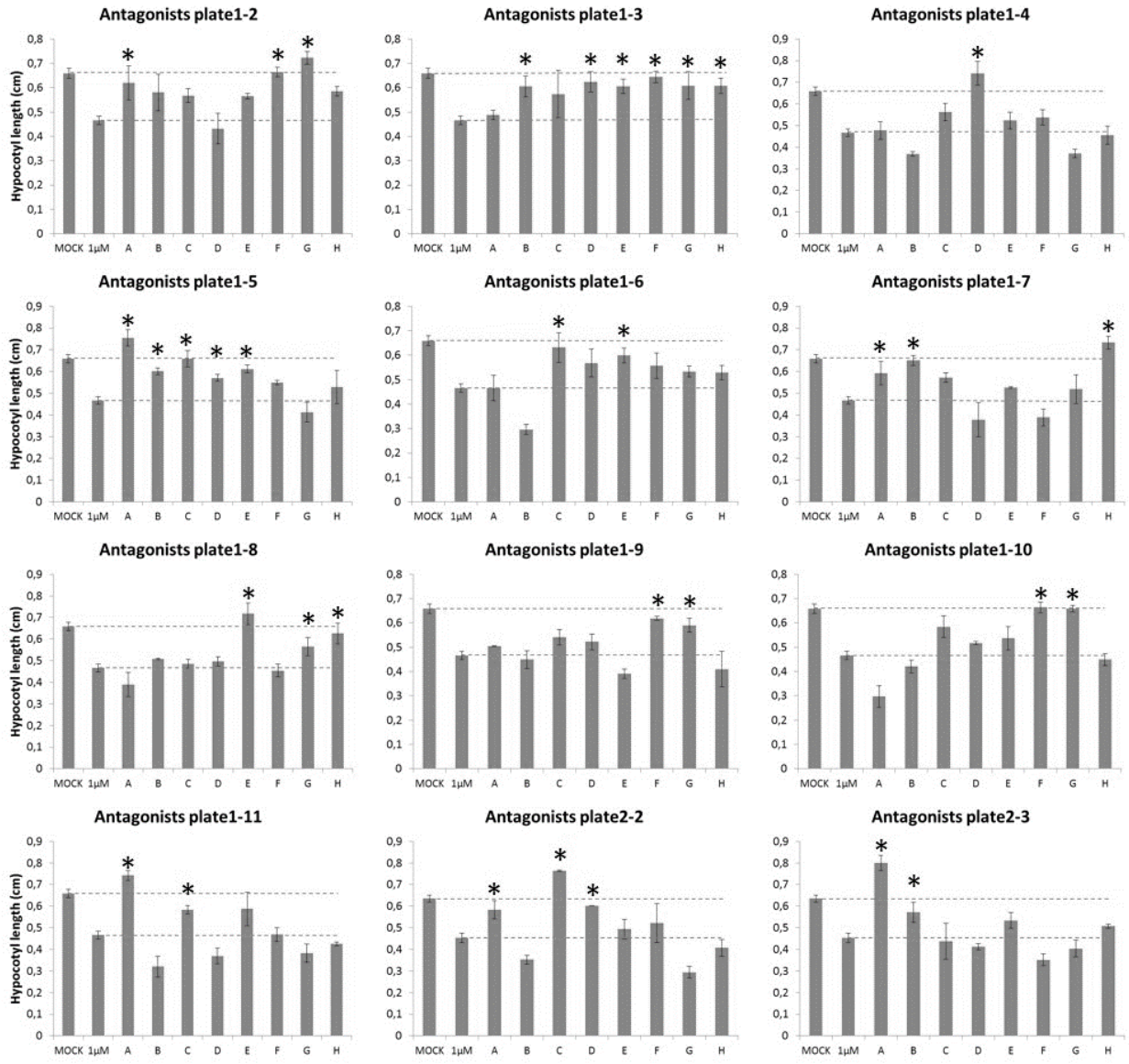

Supplementary Figure 1. Confirmation screen of hit compounds. *(Part 1)*

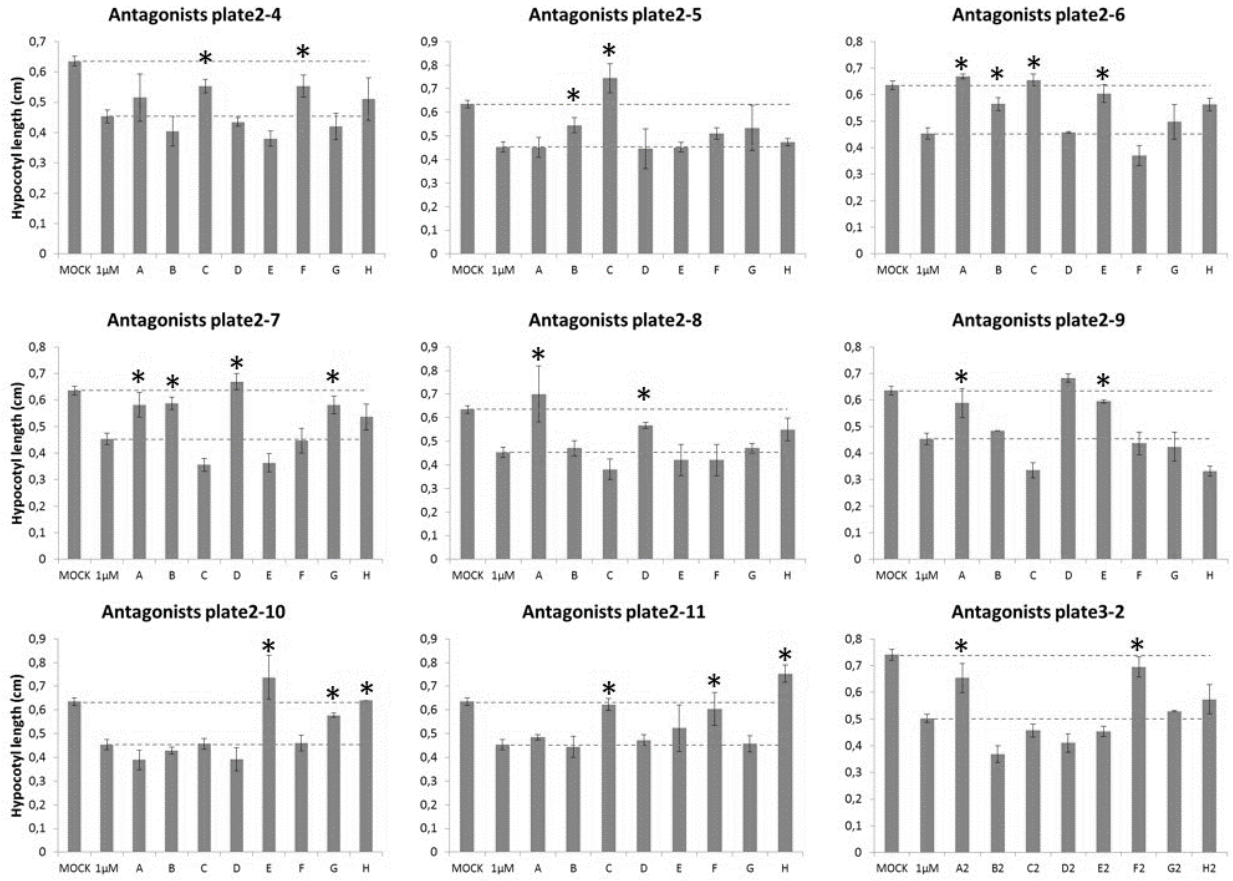

Supplementary Figure 1. Confirmation screen of hit compounds. *(Part 2)* Col-0 seeds were sown and treated as described for the chemical screen (1 µM *rac*-GR24 and 50 µM of compound). As a negative control, *rac*-GR24, without compound was administered in the first row of each 96-well plate and as a positive control, medium lacking *rac*-GR24 and compound was added to the last row of each 96-well plate. After this procedure, plates were resealed and exposed to continuous red light for 4 days. The growth of the seedlings was stopped by replacing the growth medium by a 70% (v/v) ethanol solution. Seedlings were carefully transferred on a thin layer of agar to allow quantitative measurements of the hypocotyl length. Graphs represent means of 3 to 6 seedlings. Error bars represent the standard error (SE). Asterisks indicate confirmed hits.

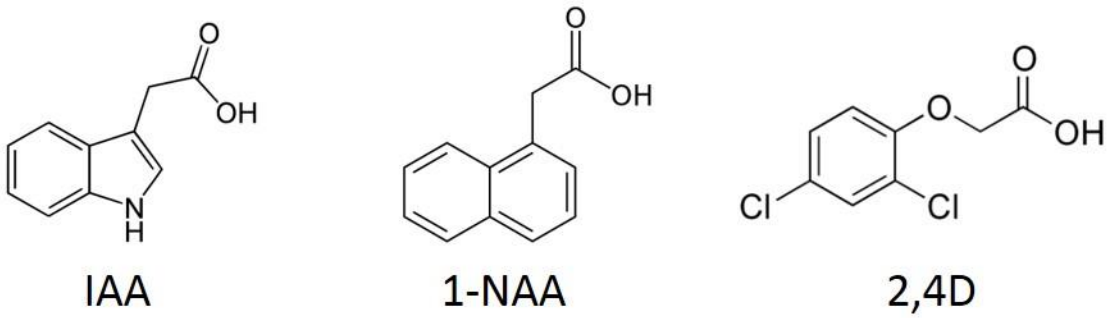

Supplementary Figure 2. Chemical structure of natural and synthetic auxins used for discarding pro-auxin-like compounds.

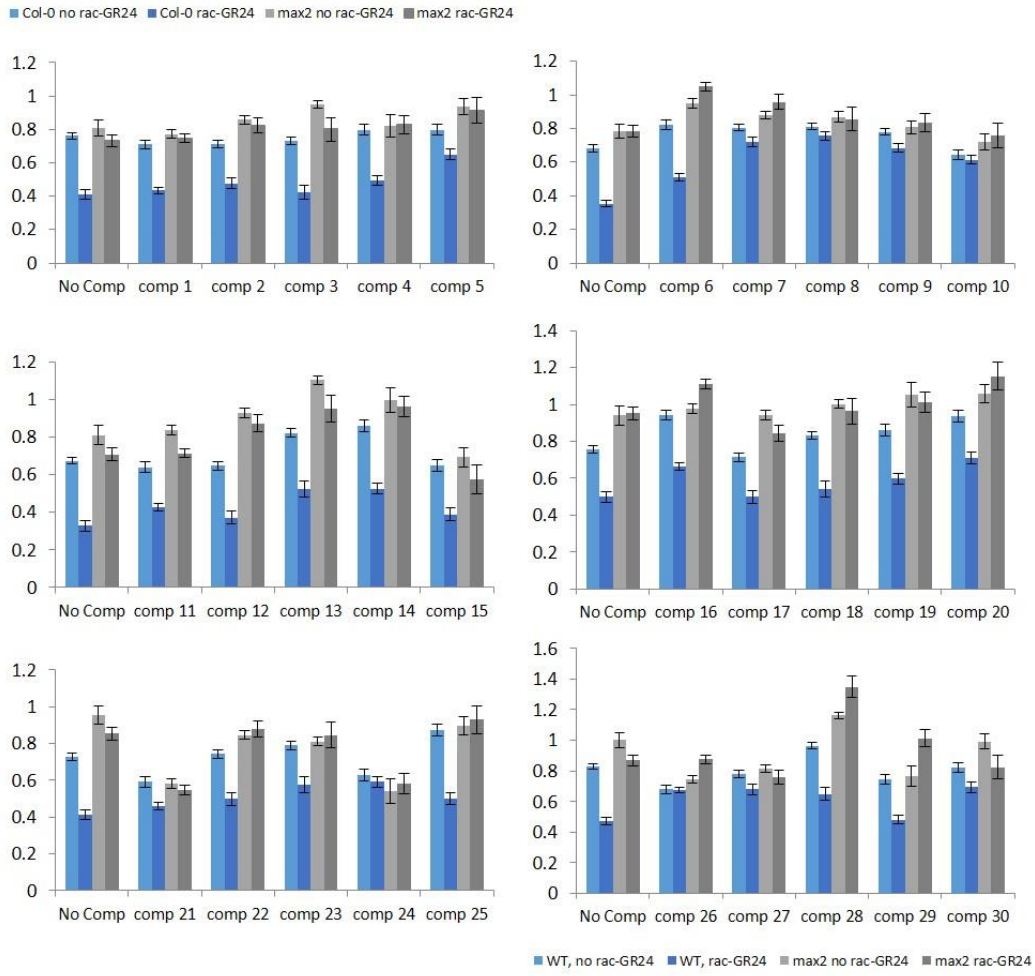

Supplementary Figure 3. Secondary screening results of all 30 hit compounds. Seeds of WT and *max2-1* were sown in a 24-well format on liquid half-strength Murashige and Skoog medium in the absence of *rac*-GR24. After stratification, plates were exposed to white light for 3 h, followed by incubation in the dark for an additional 42 h. Then, the compounds and fresh medium supplemented with or without *rac*-GR24 were added to the wells (final concentrations of 1 µM and of 50 µM for *rac*-GR24 and the compounds, respectively) and were ultimately exposed to red light for 4 days. In the graphs, the effect of all 30 compounds are depicted. For the positive results only, see Figure 6.

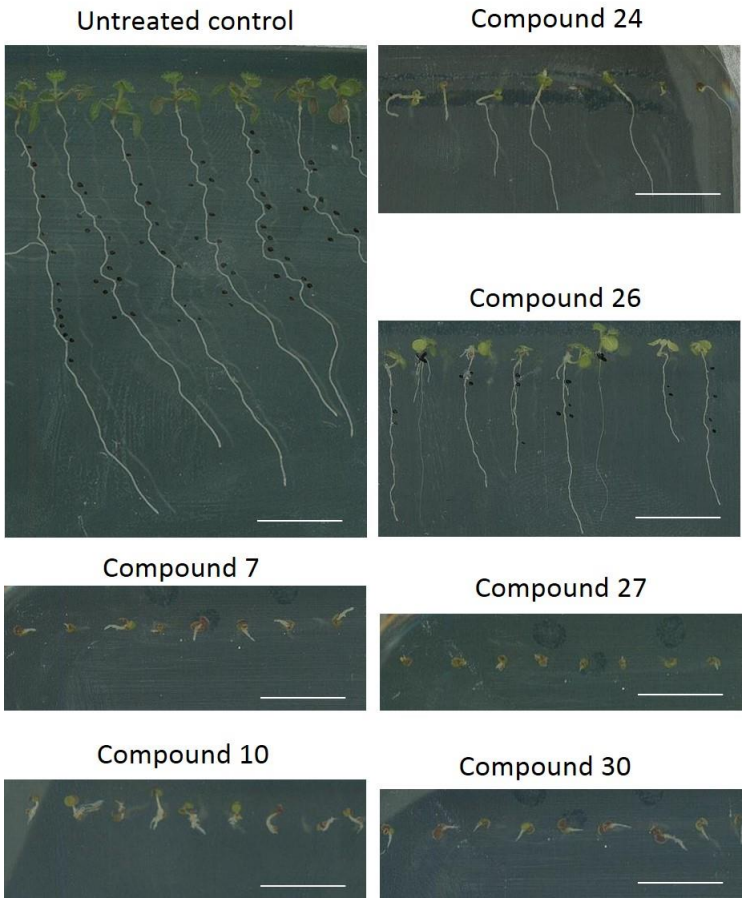

Supplementary Figure 4. Effect on the root development of seedlings germinated in the presence of the hit compounds. Plants were grown for 9 days under continuous light conditions at 21°C on half-strength Murashige and Skoog medium with 1% (w/v) sucrose in the absence (DMSO) or presence of compounds (50 µM final concentration). Effects of compounds 7, 10, 24, 26, 27, and 30 on the root development are depicted. Bars = 1 cm.

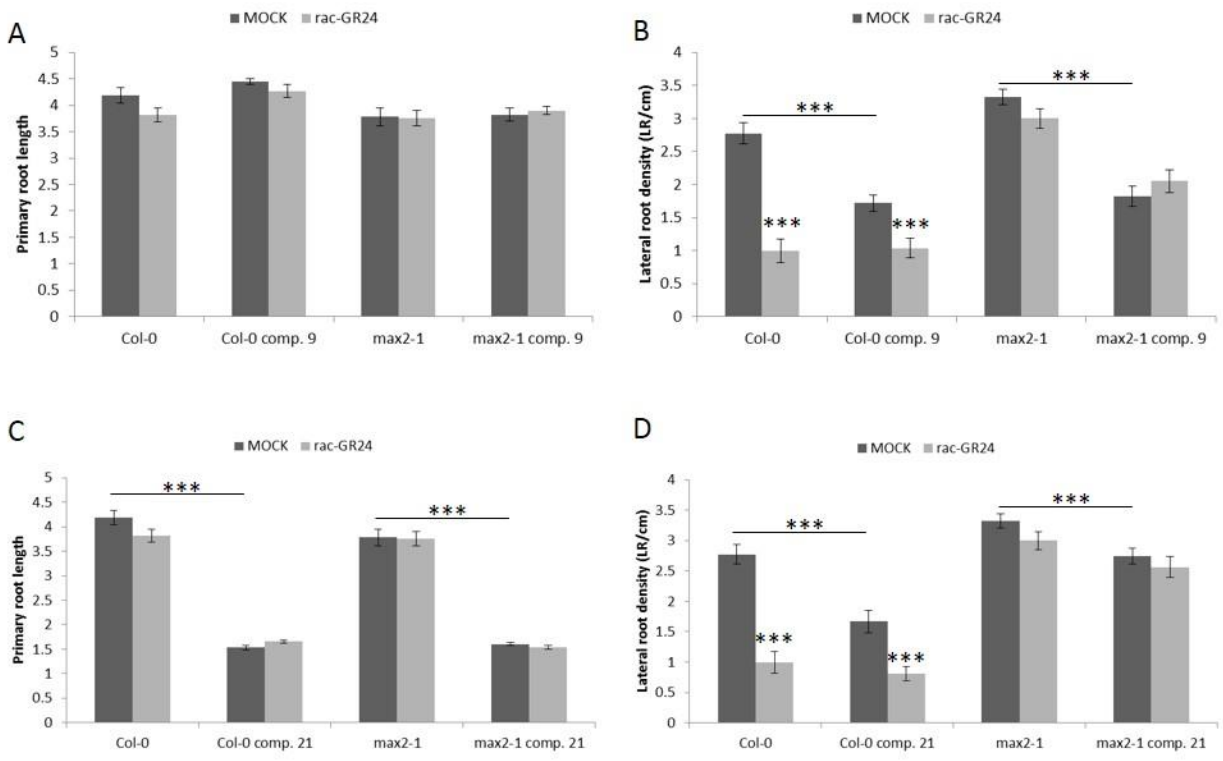

Supplementary Figure 5. Effects of compounds on the *rac*-GR24-mediated reduction in LRD and the primary root length. Primary root length of Col-0 and *max2-1* after treatment with *rac*-GR24 and compound 9 **(A)** and compound 21 **(B)**. LRD of Col-0 and *max2-1* after treatment with *rac*-GR24 and compound 9 **(C)**, and compound 21 **(D)**. Data presented are means ± SE of one biological repeat ($n > 20$). Asterisks indicate statistically significant differences (*** $P < 0.001$; Student's *t*-test).

Supplementary Table 1. Structure-based clustering of the SL antagonist hit compounds. Available via https://goo.gl/gQpr37

Supplementary Table 2. Structure of the 58 confirmed hit compounds. Available via https://goo.gl/gQpr37

Supplementary Table 3. Structure of the selected 30 lead compounds

Structure	ID	ChemBridge ID	Mol. Mass (g/mol)	Mol. Formula
	1	5103619	203.2	$C_9 H_{10} N O S . Na$
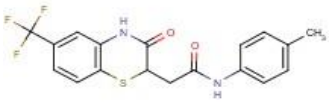	2	6383233	380.4	$C_{18} H_{15} F_3 N_2 O_2 S$
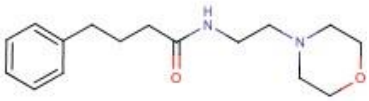	3	6636623	276.4	$C_{16} H_{24} N_2 O_2$
	4	6998095	339.3	$C_{19} H_{17} N O_5$
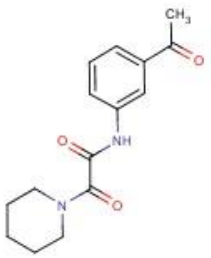	5	7584981	274.3	$C_{15} H_{18} N_2 O_3$

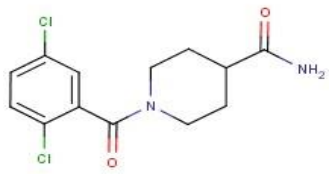	6	7630348	301.2	$C_{13}\ H_{14}\ Cl_2\ N_2\ O_2$
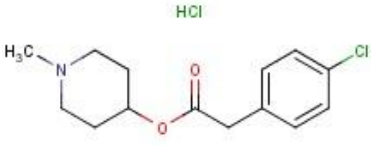	7	7703113	304.2	$C_{14}\ H_{18}\ Cl\ N\ O_2$. Cl H
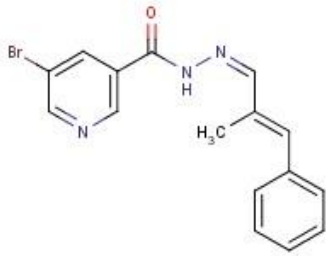	8	5231863	344.2	$C_{16}\ H_{14}\ Br\ N_3\ O$
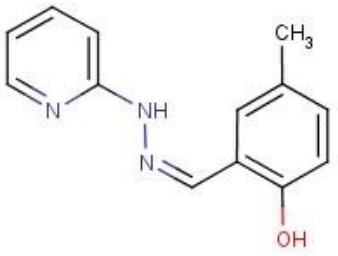	9	5109873	227.3	$C_{13}\ H_{13}\ N_3\ O$
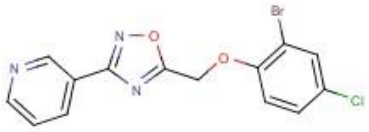	10	5802987	366.6	$C_{14}\ H_9\ Br\ Cl\ N_3\ O_2$

	11	7686962	304.4	$C_{13}\ H_{12}\ N_4\ O\ S_2$
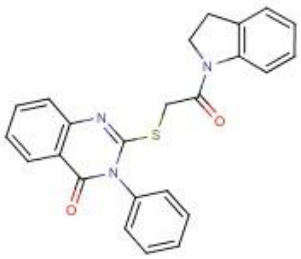	12	7685891	413.5	$C_{24}\ H_{19}\ N_3\ O_2\ S$
	13	6665489	216.2	$C_{11}\ H_{12}\ N_4\ O$
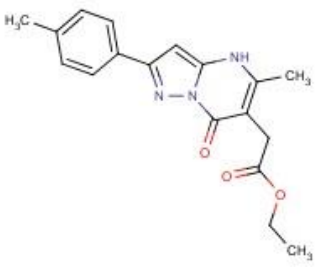	14	7152390	325.4	$C_{18}\ H_{19}\ N_3\ O_3$
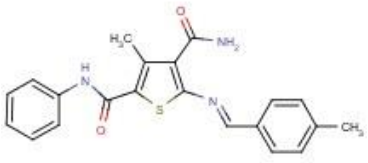	15	5665502	377.5	$C_{21}\ H_{19}\ N_3\ O_2\ S$

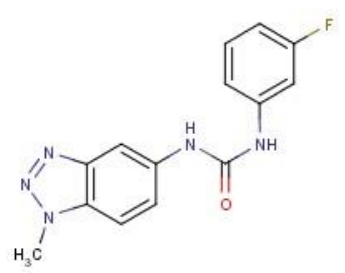	16	7579153	285.3	$C_{14}\ H_{12}\ F\ N_5\ O$
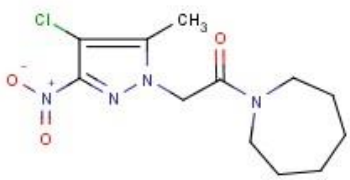	17	5667077	300.7	$C_{12}\ H_{17}\ Cl\ N_4\ O_3$
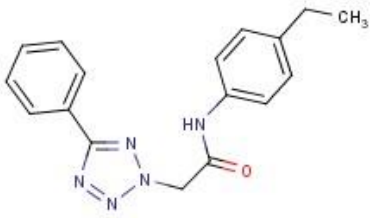	18	5842609	307.4	$C_{17}\ H_{17}\ N_5\ O$
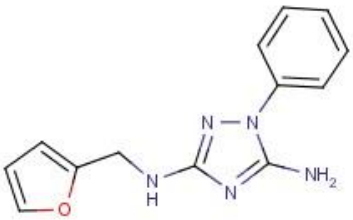	19	6614368	255.3	$C_{13}\ H_{13}\ N_5\ O$
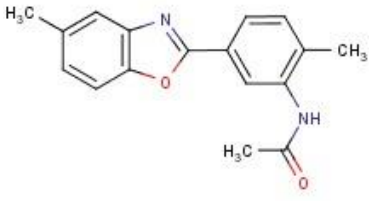	20	7590055	280.3	$C_{17}\ H_{16}\ N_2\ O_2$

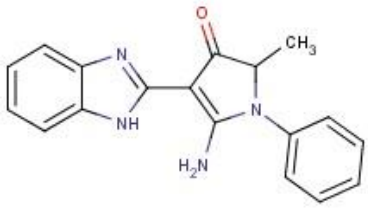	21	7488890	304.4	$C_{18}\ H_{16}\ N_4\ O$
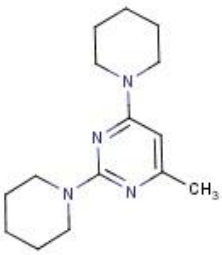	22	7592791	260.4	$C_{15}\ H_{24}\ N_4$
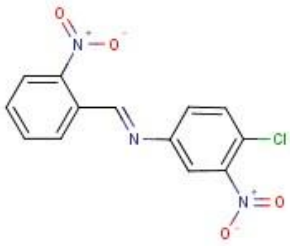	23	5314166	305.7	$C_{13}\ H_8\ Cl\ N_3\ O_4$
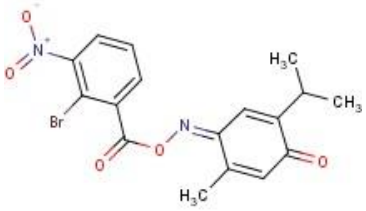	24	6623567	407.2	$C_{17}\ H_{15}\ Br\ N_2\ O_5$
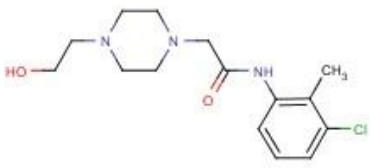	25	7492232	311.8	$C_{15}\ H_{22}\ Cl\ N_3\ O_2$

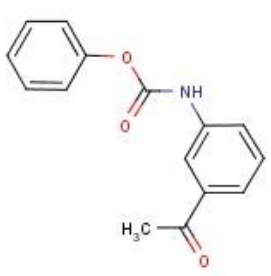	26	6943235	255.3	$C_{15}\ H_{13}\ N\ O_3$
	27	7744338	249.3	$C_{17}\ H_{15}\ N\ O$
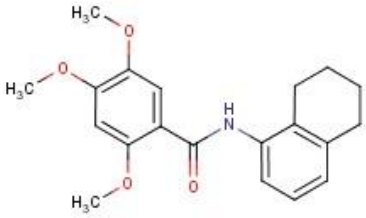	28	7728103	341.4	$C_{20}\ H_{23}\ N\ O_4$
	29	7701077	282.3	$C_{16}\ H_{14}\ N_2\ O_3$
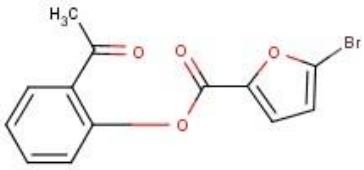	30	7668807	309.1	$C_{13}\ H_9\ Br\ O_4$

Supplementary Table 4. Structures of all (putative) KAI2 inhibitors identified by Holbrook-Smith et al. (2016). Available via https://goo.gl/gQpr37

PART IV

CHAPTER 6

DISCUSSION AND PERSPECTIVES

Plants produce a wide variety of chemical compounds, primary and secondary metabolites, of which some act as hormones. Generally, hormones are small signaling molecules that are active at very low concentrations and support communication between cells and organs. As such, they play a pivotal role in optimizing plant growth and development, but they often have different functions and, additionally, their effects can be influenced by the activity of other hormones. Therefore, it is very important to unravel the complex hormonal signaling pathways that result in various physiological responses. To date, many signaling components remain elusive and, besides the 'classic' hormones (auxin, cytokinins, ethylene, gibberellins, and abscisic acid), new endogenous molecules are often expanding the list of phytohormones. Strigolactones (SLs) have been detected as ones of the latest.

Strigolactones, compounds with a past

The study of SLs is hallmarked by its rich history of discoveries that have impacted on various agricultural aspects. At first, in 1966, they had been depicted as malignant molecules, inducing the germination of parasitic weeds, with serious loss in crop yields all over the world as a consequence (Cook et al., 1966). This negative image was counterbalanced in 2005 by the discovery that SLs were also able to enhance the symbiotic interaction between plants and arbuscular mycorrhizal fungi, resulting in a more efficient uptake of water and nutrients (Akiyama et al., 2005). However, because plant species that do not undergo arbuscular mycorrhization, such as *Arabidopsis thaliana,* also produced SLs, an endogenous function was expected. Indeed, in 2008, a function for SLs as inhibitors of shoot branching was uncovered, adding them as the most recent members to the list of plant hormones (Gomez-Roldan et al., 2008; Umehara et al., 2008). Later on, additional roles of SLs in the regulation of plant physiology have been described, such as the control of the root system architecture (Chapter 2; Kapulnik et al., 2011a, 2011b; Ruyter-Spira et al., 2011; Shinohara et al., 2013). As lot of research has been focused on the elucidation of the SL signaling network behind the various physiological responses, a considerate amount of progress

has been made in recent years. DWARF14 (D14) has been identified as a SL receptor that -after binding and hydrolysis of a SL molecule- brings the MORE AXILLARY BRANCHING2 (MAX2) complex with Skp, Cullin, F-box (SCF^{MAX2}) in the proximity of the SUPPRESSOR OF MAX2 1 LIKE (SMXL) family target proteins, enabling their polyubiquitination and subsequent degradation (Soundappan et al., 2015; Wang et al., 2015; Bennett et al., 2016). However, further downstream signaling events leading to the different physiological responses are lacking.

In this PhD, we aimed at getting a profound molecular insight into how SL signaling results in the downstream physiological outcomes, with a focus on the root system architecture of *Arabidopsis thaliana*. To this end, we studied the effect of *rac*-GR24 on the lateral root (LR) development in an in-depth spatiotemporal manner and its crosstalk with cytokinin and auxin. In addition, we performed RNA sequencing (RNA-seq) on root tissue to obtain a transcriptome-wide overview of the changes brought about by treatment with *rac*-GR24 and to identify downstream players in the physiological responses of SLs on the root system architecture. Finally, we also initiated a chemical screen for which our goal was the detection of new SL antagonists that could be helpful in the further deciphering of SL actions.

Toward a better understanding of the SL effects on LR development

In 2011, SLs were found to have a MAX2-dependent negative impact on LR development (Kapulnik et al., 2011a; Ruyter-Spira et al., 2011). Both an impact on the initiation and blockage of LR development around stage V were reported. However, in-depth phenotypical insights on the effect of *rac*-GR24 on LR development were still lacking. By means of the early LR marker *GATA23*, we were able to follow the effect of *rac*-GR24 on LR development in a spatiotemporal manner (Chapter 2). A developmental map of all possible LR primordia and prebranch sites, i.e. pericycle-derived LR founder cells that are predestined to start cell division for LR development, positioned along the primary root could be constructed (Malamy

and Benfey, 1997; De Rybel et al., 2010). A dual effect of *rac*-GR24 on the development of LRs was revealed: a minor one on the prebranch site development and a main one on LR outgrowth. The latter observation corresponds with previous observations, although the proposed specific interruption at stage V of the LR development was not detected (Ruyter-Spira et al., 2011). This map also showed that the impact of *rac*-GR24 was most pronounced on the first developing LR primordia that are located in the older root part. This spatiotemporal effect was also visible on the *PINFORMED 1* (*PIN1)* expression pattern. As a dependence on the shoot-derived auxin could be demonstrated for the *rac*-GR24 treatment on the LRs, this effect might be partially explained by the low dependency of the LR development on shoot-derived auxin at later stages of seedling development (Bhalerao et al., 2002). An alternative explanation for the weaker effect of *rac*-GR24 on younger root tissue might lie in the reported disappearance of the SL receptor D14 in the root after the *rac*-GR24 treatment (Chevalier et al., 2014).

However, an effect on LR initiation, as reported previously (Kapulnik et al., 2011a), was not confirmed by our analysis, but this might be due to the impact of *rac*-GR24 on prebranching. The formation of prebranch sites occurs in the basal meristem and is the result of an auxin-induced oscillatory gene expression (De Smet et al., 2007; Moreno-Risueno et al., 2010; Xuan et al., 2015). This oscillating pattern was shown to be regulated by a still unknown carotenoid-derived signal (Van Norman et al., 2014). Despite the increased root-forming potential of the *max2* mutant, a function for SLs as the carotenoid-derived signal was excluded, mainly because this effect was absent in the SL biosynthesis mutants (Van Norman et al., 2014). Nevertheless, it might be that the KAI2 ligand (KL), which is the unknown endogenous ligand of KARRIKIN INSENSITIVE2 (KAI2) (and which is probably also perceived by D14, see below) might be this unknown carotenoid-derived signal. Efforts to reveal the identity of this KL molecule have been initiated. Recently, the presence of the presumed KL molecule has recently been detected in *Arabidopsis* leaf extracts by means of a novel reporter-gene assay (Sun et al., 2016). Awaiting the identification of KL, it would be interesting to analyze the effect of *rac*-GR24 as a mimic of SLs or related

compounds on the periodic oscillations in the basal meristem via the use of the *pDR5:LUCIFERASE* reporter line. In addition, the *GATA23* marker should also be crossed in the receptor mutants *d14* and *kai2* and the *d14;kai2* double mutant to investigate any spatiotemporal effect of *rac*-GR24 or its pure enantiomers on the LR development and to investigate the lateral root forming potential in these mutants. The obtained results should be compared with those in the wild type (WT) and *max2*. Furthermore, the basic-HELIX-LOOP-HELIX (bHLH) transcription factor (TF) TARGET OF MONOPTEROS5 LIKE1 (TMO5L1), discovered as a downstream signaling component of SLs in the roots, is expressed in the protoxylem (Chapter 5; De Rybel et al., 2013). As this TF is located near the oscillation zone of the basal meristem, it would be worthwhile to examine a possible role for TMO5L1 in LR priming, for instance, by mutant analyses.

Although the involvement of MAX2 and the effect of *rac*-GR24 on the LR development is well established, *rac*-GR24 has recently been shown to activate SL signaling both via D14 and KAI2 (Scaffidi et al., 2014). Based on the hypocotyl phenotype, (-)GR24 has been suggested to specifically trigger KAI2 signaling and (+)GR24 the D14 signaling (Scaffidi et al., 2014), but biochemically the separation does not seem to be strict. In rice (*Oryza sativa*) and pea (*Pisum sativum*), the D14 ortholog binds and hydrolyzes both enantiomers, but with a higher specificity to (+)GR24 (Nakamura et al., 2013; de Saint Germain et al., 2016). In *Arabidopsis*, D14 and KAI2 hydrolyze both enantiomers, but the reactions are much more for efficient to (+)GR24 and (-)GR24 for D14 and KAI2, respectively (Flematti et al., 2016). In contrast to the effects on the hypocotyl (Scaffidi et al., 2014), these biochemical data fit with the physiological outcome of the pure enantiomers on the LR density (LRD) of the SL signaling mutants (Chapter 3). Here we could show that the WT was equally sensitive to both pure enantiomers and to *rac*-GR24. However, the *d14* mutant was still partially sensitive to (+)GR24, probably because of partial signaling of (+)GR24 via the active KAI2 receptor and, *vice versa*, for the *kai2* mutant to (-)GR24 via the D14 activity. Indeed, only a mutation of both receptors leads to a full insensitivity toward both enantiomers and *rac*-GR24. These results put both D14 and KAI2 central in the LRD regulation. Nevertheless, endogenously seen, KAI2 could

be considered as the main receptor for the LR phenotype, because only *kai2* and not *d14* exhibits an increased LRD comparable to that of *max2*. However, determining the lateral root potential of the various mutants by staging might provide additional information. Interestingly, genetic evidence revealed that *smxl6;smxl7;smxl8* and not *smax1* could suppress the high LRD phenotype of *max2* (Soundappan et al., 2015). As SMXL6, SMXL7, and SMXL8 are known to be downstream of D14, and SMAX1 downstream of KAI2, these data demonstrate that D14 is also involved (Stanga et al., 2013; Soundappan et al., 2015; Wang et al., 2015; Bennett et al., 2016). Indeed, both receptors are very probably truly implicated in the regulation of the LRD phenotype, endogenous SLs are perhaps not, because SL biosynthesis mutants do not exhibit an induced LRD (reviewed in Chapter 1). In other words, *rac*-GR24 might serve as a mimic of the endogenous KL molecule that will be the *bona fide* KAI2 and D14 ligand, at least for the regulation of the LRD.

To get a better molecular understanding of how *rac*-GR24 influences the root system architecture, we determined the transcriptome via RNA-seq (Chapter 3). For our setup, we used Columbia-0 (Col-0) and *max2* seedlings that were transiently treated with *rac*-GR24 for 6 hours. A much earlier timepoint would not have been appropriate, because, in comparison to other hormones, the SL signaling cascade is not initiated so rapidly. Indeed, the degradation of the direct target proteins SMXL6, SMXL7, and SMXL8 occurs only 30 minutes to 1 hour after treatment (Zhao et al., 2013; Soundappan et al., 2015; Wang et al., 2015). Thus, harvesting after 6 hours of treatment ensured picking up transcriptional responses, based on the effects of *rac*-GR24 on the expression of previously published SL marker genes. The fact that the SL signaling pathway seems to start slower than other hormonal pathways might be because of the non-natural nature of *rac*-GR24. It is possible that this synthetic analog, which is commonly used in SL research, might not be as powerful as naturally occurring SLs for initiating the molecular signaling cascade. Natural SLs might be more efficiently in initiating the response and might result in stronger transcriptional responses than *rac*-GR24. Further research will be required to investigate this possibility.

Treatment with *rac*-GR24 resulted in a restricted amount of 146 differentially expressed genes, generally with a limited fold change. Selection of this fold change cut-off was confirmed by the occurrence of genes known to be regulated by *rac*-GR24 in the root, such as the flavonol biosynthesis genes and genes of the SMXL family (Walton et al., 2016). For the SMXL genes, the effect of *rac*-GR24 on the *GUS* reporter lines provided extra validation (L. Jiang, unpublished data). In contrast to the *rac*-GR24 treatment, 2,011 genes were differentially expressed in *max2* roots grown under MOCK conditions. By combining the information present in both datasets, we found that SLs influenced various pathways, such as the hormonal crosstalk, drought responses, and light harvesting and sensitivity, and modulated the plant's secondary metabolism (flavonol biosynthesis). Although previously a crosstalk had been reported between SLs and cytokinins in the LRD regulation via the ARABIDOPSIS HISTIDINE KINASE3 (AHK3)/ARABIDOPSIS RESPONSE REGULATOR1(ARR1)/ARR12/SHORT HYPOCOTYL2 (SHY2) module (Chapter 2), a strong crosstalk was not retrieved on the transcriptional level, based on the results from our RNA-seq. This is probably because the insensitivity to *rac*-GR24 of mutants in the AHK3/ARR1/ARR12/SHY2 module had been shown to result from an enhanced auxin transport flux in these mutants. However, strong transcriptional effects, as described for *PIN1* (Chapter 2), were not obtained as well, probably due to the spatiotemporally restricted effect of *rac*-GR24 (on *PIN1* expression) to the upper root part. Hence, sampling of the whole root might have diluted the signal.

Besides the gene classes that were both differentially expressed after *rac*-GR24 and in the *max2* roots under MOCK conditions, various other genes were upregulated in *max2* only, pointing to an increased cellular activity in the *max2* mutant. As this transcriptional effect did not proceed via the D14 or KAI2 signaling, the involvement of another receptor for this response, such as D14 LIKE2 (DLK2), was hypothesized. To confirm this possibility, gene expression analyses should be carried out in a *dlk2* mutant line. Furthermore, because these genes were not differentially expressed after the *rac*-GR24 treatment, this pathway might possibly be triggered by a different, endogenous ligand that cannot be mimicked by

rac-GR24. This ligand could be the still unknown KL molecule, if DLK2 were highly specific toward KL perception of KL and not toward *rac*-GR24. Identification of the KL molecule will be crucial to study this pathway in detail.

Among the TFs present in the *rac*-GR24 dataset (Chapter 3 and 4), *TMO5L1* was found the most repressed. A role for *TMO5L1* in the *rac*-GR24 response in the root was suggested based on genetic and molecular approaches. We could show that TMO5L1 might act mainly via the D14 pathway, but a certain redundancy with the KAI2 pathway could not be excluded. For detailed investigation, the expression of *TMO5L1* could be checked in the *d14* and *kai2* mutants and in the *d14;kai2* double mutant treated with *rac*-GR24. The downregulation of *TMO5L1* by *rac*-GR24 should be abolished in the signaling mutants, in which it acts downstream. The use of pure GR24 enantiomers could also be considered. Additionally, to investigate the position of *TMO5L1* downstream of the SMXL family, its expression should be checked in these mutants as well. Depending on the downstream position of *TMO5L1* action, *smax1* or *smax1;smxl2* (for the KAI2 pathway) or *smxl6;smxl7;smxl8* (for the D14 pathway) should be analyzed by molecular as well as genetical analyses. Via the generation of a *max2;tmo5l1* double mutant, it would be possible to investigate whether *tmo5l1* can suppress the increased LRD phenotype of *max2*. Likewise, because *smxl6;smxl7;smxl8* can also rescue this *max2* phenotype (Soundappan et al., 2015), crossing in *tmo5l1* will be informative to know whether they work in the same genetic pathway or not.

Although *TMO5L1* is transcriptionally strongly downregulated by the *rac*-GR24 treatment, thus far, this mechanism could not be confirmed at the protein level and should be investigated, because this result is completely unexpected. First, the effect of *rac*-GR24 on the expression pattern of a transcriptional *TMO5L1* reporter line should be examined. Besides the corroboration of the downregulation of *TMO5L1* by *rac*-GR24, this experiment would also confirm the expression of *TMO5L1* in the LR primordia. Alternatively, *in situ* hybridization could be employed to confirm the expression pattern and the transcriptional effect of *rac*-GR24 on *TMO5L1*. As already discussed, the *pTMO5L1:TMO5L1-YFP*

translational line might not be completely *bona fide,* for instance by missing SL-regulatory signals in the cloned promoter. First, complementation of the *tmo5l1* mutant should be checked, together with an analysis of independent lines. After confirmation, the effect of *rac*-GR24 on the TMO5L1 protein level should be re-investigated in these lines.

Regarding the functional role of *TMO5L1* in the SL network of the roots, several options can be formulated. Because of the well described role of TMO5L1 in the regulation of vascular development in the primary root (De Rybel et al., 2013, 2014; Ohashi-Ito et al., 2014; Katayama et al., 2015), the very same process can very well be regulated by SLs during LR development and, as such, slow down the further development of the LR primordia. However, the other key players during vascular development, such as the cytokinin biosynthesis genes of the *LONELY GUY* (*LOG*) family, *SUPPRESSOR OF ACAULIS 51* (*SAC51*), *SAC51 LIKE's* and LONESOME HIGHWAY (LHW) families, seemed unaffected by *rac*-GR24 or in *max2* roots under MOCK condition. Moreover, because TMO5L1 forms heterodimers, interaction with a bHLH TF different from LHW or its homologs, might extend the toolbox and have another outcome. To investigate a potentially different role for TMO5L1 in the SL signaling network in the root, the primary targets of TMO5L1 should be carefully investigated. Crucial will be the identification of novel bHLH interaction partners of TMO5L1, possibly resulting in different TMO5L1 functionalities. To this end, tandem affinity purification or green fluorescent protein (GFP)-trapping can be utilized as a technique to find new interaction partners. Alternatively, a candidate-gene approach can be set up by specifically looking for bHLH proteins that are expressed in the *Arabidopsis* (lateral) root and inferring their interaction with TMO5L1, for example by means of yeast two-hybrid screening. If interaction partners could be selected, identification of the genes they regulate will greatly broaden our knowledge on how LR development is regulated by the SL signaling network.

Chemical genetics to decipher the role of SLs in plant development

As an alternative to mutational genetics, chemical genetics has been used to understand various plant hormone signaling pathways (Armstrong et al., 2004; Gendron et al., 2008; Savaldi-Goldstein et al., 2008; De Rybel et al., 2009). Because chemical genetics provides complementary information and often overcomes redundancy, lethality, and pleiotropic effects, it is a valuable approach to decipher the SL signaling network. To this end, a well-characterized and robust bioassay, based on either phenotype or on marker gene expression is a must (Tóth and van der Hoorn, 2010).

Although SLs influence various physiological responses, such as axillary bud outgrowth, secondary stem thickening, leaf senescence, hypocotyl elongation, adventitious and LR development, and root hair elongation (for a review, see Al-Babili and Bouwmeester, 2015), many of these phenotypes are difficult -if not impossible- to assess via a small-scale setup or do not allow efficient high-throughput screening. Additionally, screening for compounds with a positive outcome (i.e., a positive screen) is preferred to avoid that compounds are collected that cause the effect due to toxicity or lethality. For example, a screen based on the effect of SLs on parasitic seed germination to find SL antagonists would have resulted in a negative screen and, additionally, entailed the risk that the impact of the compound could not be translated to *Arabidopsis* for further research. Moreover, because SL agonists had already been screened (Toh et al., 2014), we selected the inhibitory effect of SLs on the hypocotyl length as a suitable phenotype to allow a positive screen for antagonists. Recently, a direct antagonist of the KAI2 protein had been identified via a similar assay, proving its usefulness for antagonist screening (Holbrook-Smith et al., 2016).

Alternatively, a screen based on marker gene expression could be considered. However, at the time we initiated a chemical genetics approach to identify SL signaling antagonists, no valuable SL markers were available. Even to date, not many ideal markers are obtainable. Recently, *DLK2* has been used in a reporter-assay to demonstrate the presence of the KL molecule in leaf extracts (Sun et al., 2016). However,

the use of this marker to identify SL antagonists would result in a negative screen, namely inhibition of gene expression. Likewise, a screen based on the downregulation of the *TMO5L1* expression by *rac*-GR24, would not be ideal, because it is known to be induced by auxin (Schlereth et al., 2010). Indeed, compounds that act like an auxin or are bioconverted into an auxin are frequently found during a chemical genetics screen (Sungur et al., 2007; Christian et al., 2008; Savaldi-Goldstein et al., 2008). Especially in the case of SLs, these auxin-like compounds form a major hurdle, because high auxin levels mask the SL effects (Chapter 2, Ruyter-Spira et al., 2011). After removal of the hits with proauxin-like characteristics, still six of the 10 lead compounds identified appeared to have a strong impact on auxin homeostasis. Based on this observation, any future chemical genetics approach to identify SL antagonists should include a control for auxin-like behavior of the compounds. In the case of the hypocotyl, for instance, an *Arabidopsis* line containing a *pDR5:GUS* construct could be used to screen the compounds and good candidates should result in an elongated hypocotyl without induction of the GUS reporter.

By not taking into account the compounds that seem to influence the auxin homeostasis, we could identify at least three (or four, as also compound 8 might possibly not influence the auxin homeostasis) putative lead SL antagonists. Although their discovery was based on a similar assay, none of the newly identified lead compounds presented here are structurally similar to the recently published KAI2 protein inhibitors (Holbrook-Smith et al., 2016), probably because our compounds might act via the D14 pathway or possibly further downstream of KAI2 and/or D14. Certainly, these compounds first need to be validated as true SL antagonists by SAR analysis, SL mutant analysis and inferring their effect on SL marker gene expression. After that, the next challenge will be to find the mode of action of these compounds by identifying their target proteins. Compound 5 could probably act as a general SL antagonist, because it affects both the hypocotyl and possibly also the LRD phenotype and, thus, has likely an impact on a protein quite upstream in the SL signaling complex. In contrast, the antagonizing effect of compounds 9 and 21 might probably be more restricted to the effect of *rac*-GR24 on the hypocotyl, hinting at an impact on a

molecular player further downstream of the SL signaling network. To confirm a function for compounds 24, 27, and 30 in the SL signaling network of parasitic seed germination, this effect should first be further investigated.

To identify the target of compound 5, a candidate approach could be considered. Binding of SLs slightly destabilizes the D14 protein, as visualized by differential scanning fluorimetry (DSF) (Hamiaux et al., 2012; Abe et al., 2014; de Saint-Germain et al., 2016). DSF is a fast method to detect compounds that bind and, hence, (de)stabilize purified proteins (Niesen et al., 2007). Thus, it is relatively easy to assess whether compound 5 can prevent the SL binding to D14 or whether the compound itself can bind with any of the known SL signaling components. Alternatively, compound 5 could possibly target an unknown protein of the SL signaling network. Therefore, more general approaches should be taken to identify the target proteins, and especially for compounds 9 and 21, because they could probably target a protein that is further downstream of the core SL signaling pathway.

In plant chemical biology, commonly used strategies include transcriptome analyses to define target pathways and off-target effects (Goda et al., 2002; Manabe et al., 2007; De Rybel et al., 2009; Park et al., 2009) and forward-genetic screens for compound resistance (Rojas-Pierce et al., 2007; Park et al., 2009; De Rybel et al., 2012). Besides these classical approaches, also various identification strategies emerge, such as Yeast 3-Hybrid, affinity-based technologies, or label-free compound-based technologies (for a review, see Dejonghe and Russinova; 2014). Indeed, many options are available for the ultimate finding of the targets of our identified SL antagonists.

Concluding remarks

Although SLs had already been discovered in 1966, only recently major breakthroughs have been made in the unraveling of the early signaling events, but it is still currently unclear what happens

thereafter. In this PhD, we obtained valuable new insights into how SLs regulate their physiological responses, with a main focus on the root system architecture. On top of that, we have initiated a chemical genetics screen that resulted in the identification of various putative SL antagonists. Nevertheless, many questions remain unanswered yet, offering challenging opportunities for future research.

References

Abe, S., Sado, A., Tanaka, K., Kisugi, T., Asami, K., Ota, S., Kim, H.I., Yoneyama, K., Xie, X., Ohnishi, T., Seto, Y., Yamaguchi, S., Akiyama, K., Yoneyama, K., and Nomura, T. (2014). Carlactone is converted to carlactonoic acid by MAX1 in *Arabidopsis* and its methyl ester can directly interact with AtD14 in vitro. Proc. Natl. Acad. Sci. USA 111, 18084-18089.

Akiyama, K., Matsuzaki, K.-i., and Hayashi, H. (2005). Plant sesquiterpenes induce hyphal branching in arbuscular mycorrhizal fungi. Nature 435, 824-827.

Al-Babili, S., and Bouwmeester, H.J. (2015). Strigolactones, a novel carotenoid-derived plant hormone. Annu. Rev. Plant Biol. 66, 161-186.

Armstrong, J.I., Yuan, S., Dale, J.M., Tanner, V.N., and Theologis, A. (2004). Identification of inhibitors of auxin transcriptional activation by means of chemical genetics in Arabidopsis. Proc. Natl. Acad. Sci. USA 101, 14978-14983 [Erratum Proc. Natl. Acad. Sci. USA 101, 17565].

Bennett, T., Liang, Y., Seale, M., Ward, S., Müller, D., and Leyser, O. (2016). Strigolactone regulates shoot development through a core signalling pathway. Biol. Open 5, 1806-1820.

Bhalerao, R.P., Eklöf, J., Ljung, K., Marchant, A., Bennett, M., and Sandberg, G. (2002). Shoot-derived auxin is essential for early lateral root emergence in *Arabidopsis* seedlings. Plant J. 29, 325-332.

Chevalier, F, Nieminen, K, Sánchez-Ferrero, J.C., Rodríguez, M.L., Chagoyen, M., Hardtke, C.S., and Cubas, P. (2014). Strigolactone promotes degradation of DWARF14, an α/β hydrolase essential for strigolactone signaling in *Arabidopsis*. Plant Cell 26, 1134-1150.

Christian, M., Hannah, W.B., Lüthen, H., and Jones, A.M. (2008). Identification of auxins by a chemical genomics approach. J. Exp. Bot. 59, 2757-2767.

Cook, C.E., Whichard, L.P., Turner, B., Wall, M.E., and Egley, G.H. (1966). Germination of witchweed (*Striga lutea* Lour.): isolation and properties of a potent stimulant. Science 154, 1189-1190.

De Rybel, B., Abidi, M., Breda, A.S., Wendrich, J.R., Smit, M.E., Novák, O., Yamaguchi, N., Yoshida, S., Van Isterdael, G., Palovaara, J., Nijsse, B., Boekschoten, M.V., Hooiveld, G., Beeckman, T., Wagner, D., Ljung, K., and Weijers, D. (2014) Integration of growth and patterning during vascular tissue formation in *Arabidopsis*. *Science* 345, 1255215.

De Rybel, B., Audenaert, D., Vert, G., Rozhon, W., Mayerhofer, J., Peelman, F., Coutuer, S., Denayer, T., Jansen, L., Nguyen, L., Vanhoutte, I., Beemster, G.T.S., Vleminckx, K., Jonak, C., Chory, J., Inzé, D., Russinova, E., and Beeckman, T. (2009). Chemical inhibition of a subset of *Arabidopsis thaliana* GSK3-like kinases activates brassinosteroid signaling. Chem. Biol. 16, 594-604.

De Rybel, B., Audenaert, D., Xuan, W., Overvoorde, P., Strader, L.C., Kepinski, S., Hoye, R., Brisbois, R., Parizot, B., Vanneste, S., Liu, X., Gilday, A., Graham, I.A., Nguyen, L., Jansen, L., Njo, M.F., Inzé, D., Bartel, B., and

Beeckman, T. (2012). A role for the root cap in root branching revealed by the non-auxin probe naxillin. Nat. Chem. Biol. 8, 798-805.

De Rybel, B., Möller, B., Yoshida, S., Grabowicz, Barbier de Reuille, P., Boeren, S., Smith, R.S., Borst, J.W., and Weijers, D. (2013). A bHLH complex controls embryonic vascular tissue establishment and indeterminate growth in *Arabidopsis*. Dev. Cell 24, 426-437.

De Rybel, B., Vassileva, V., Parizot, B., Demeulenaere, M., Grunewald, W., Audenaert, D., Van Campenhout, J., Overvoorde, P., Jansen, L., Vanneste, S., Möller, B., Wilson, M., Holman, T., Van Isterdael, G., Brunoud, G., Vuylsteke, M., Vernoux, T., De Veylder, L., Inzé, D., Weijers, D., Bennett, M.J., and Beeckman, T. (2010). A novel Aux/IAA28 signaling cascade activates GATA23-dependent specification of lateral root founder cell identity. Curr. Biol. 20, 1697-1706.

de Saint Germain, A., Clavé, G., Badet-Denisot, M.-A., Pillot, J.-P., Cornu, D., Le Caer, J.-P., Burger, M., Pelissier, F., Retailleau, P., Turnbull, C., Bonhomme, S., Chory, J., Rameau, C., and Boyer, F.-D. (2016). An histidine covalent receptor and butenolide complex mediates strigolactone perception. Nat. Chem. Biol. 12, 787-794.

De Smet, I., Tetsumura, T., De Rybel, B., Frey dit Frei, N., Laplaze, L., Casimiro, I., Swarup, R., Naudts, M., Vanneste, S., Audenaert, D., Inzé, D., Bennett, M.J., and Beeckman, T. (2007). Auxin-dependent regulation of lateral root positioning in the basal meristem of *Arabidopsis*. Development 134, 681-690.

Dejonghe, W., and Russinova, E. (2014). Target identification strategies in plant chemical biology. Front. Plant Sci. 5, 352.

Flematti, G.R., Scaffidi, A., Waters, M.T., and Smith, S.M. (2016). Stereospecificity in strigolactone biosynthesis and perception. Planta 243, 1361-1373.

Gendron, J.M., Haque, A., Gendron, N., Chang, T., Asami, T., and Wang, Z.-Y. (2008). Chemical genetic dissection of brassinosteroid-ethylene interaction. Mol. Plant 1, 368-379.

Goda, H., Shimada, Y., Asami, T., Fujioka, S., and Yoshida, S. (2002). Microarray analysis of brassinosteroid-regulated genes in Arabidopsis. Plant Physiol. 130, 1319-1334.

Gomez-Roldan, V., Fermas, S., Brewer, P.B., Puech-Pagès, V., Dun, EA., Pillot, J.-P., Letisse, F., Matusova, R., Danoun, S., Portais, J-C., Bouwmeester, H., Bécard, G., Beveridge, C.A., Rameau, C., and Rochange, S.F. (2008). Strigolactone inhibition of shoot branching. Nature 455, 189-194.

Hamiaux, C., Drummond, R.S.M., Janssen, B.J., Ledger, S.E., Cooney, JM., Newcomb, R.D., and Snowden, K.C. (2012). DAD2 is an α/β hydrolase likely to be involved in the perception of the plant branching hormone, strigolactone. Curr. Biol. 22, 2032-2036.

Holbrook-Smith, D., Toh, S., Tsuchiya, Y., and McCourt, P. (2016). Small-molecule antagonists of germination of the parasitic plant *Striga hermonthica*. Nat. Chem. Biol. 12, 724-729.

Jia, K.-P., Luo, Q., He, S.-B., Lu, X.-D., and Yang, H.-Q. (2014). Strigolactone-regulated hypocotyl elongation is dependent on cryptochrome and phytochrome signaling pathways in *Arabidopsis*. Mol. Plant 7, 528-540.

Kapulnik, Y., Delaux, P.-M., Resnick, N., Mayzlish-Gati, E., Wininger, S., Bhattacharya, C., Séjalon-Delmas, N., Combier, J.-P., Bécard, G., Belausov, E., Beeckman, T., Dor, E., Hershenhorn, J., and Koltai, H. (2011a). Strigolactones affect lateral root formation and root-hair elongation in Arabidopsis. Planta 233, 209-216.

Kapulnik, Y., Resnick, N., Mayzlish-Gati, E., Kaplan, Y., Wininger, S., Hershenhorn, J., and Koltai, H. (2011b). Strigolactones interact with ethylene and auxin in regulating root-hair elongation in *Arabidopsis*. J. Exp. Bot. 62, 2915-2924.

Katayama, H., Iwamoto, K., Kariya, Y., Asakawa, T., Kan, T., Fukuda, H., and Ohashi-Ito, K. (2015). A negative feedback loop controlling bHLH complexes is involved in vascular cell division and differentiation in the root apical meristem. Curr. Biol. 25, 3144-3150.

Malamy, J.E., and Benfey, P.N. (1997). Organization and cell differentiation in lateral roots of *Arabidopsis thaliana*. Development 124, 33-44.

Manabe, Y., Tinker, N., Colville, A., and Miki, B. (2007). CSR1, the sole target of imidazolinone herbicide in *Arabidopsis thaliana*. Plant Cell Physiol. 48, 1340-1358.

Mayzlish-Gati, E., LekKala, S.P., Resnick, N., Wininger, S., Bhattacharya, C., Lemcoff, J.H., Kapulnik, Y., and Koltai, H. (2010). Strigolactones are positive regulators of light-harvesting genes in tomato. J. Exp. Bot. 61, 3129-3136.

Moreno-Risueno, M.A., Van Norman, J.M., Moreno, A., Zhang, J., Ahnert, S.E., and Benfey, P.N. (2010). Oscillating gene expression determines competence for periodic *Arabidopsis* root branching. Science 329, 1306-1311.

Nakamura, H., Xue, Y.-L., Miyakawa, T., Hou, F., Qin, H.-M., Fukui, K., Shi, X., Ito, E., Ito, S., Park, S.-H., Miyauchi, Y., Asano, A., Totsuka, N., Ueda, T., Tanokura, M., and Asami, T. (2013). Molecular mechanism of strigolactone perception by DWARF14. Nat. Commun. 4, 2613.

Niesen, F.H., Berglund, H., and Vedadi, M. (2007). The use of differential scanning fluorimetry to detect ligand interactions that promote protein stability. Nat. Protoc. 2, 2212-2221.

Ohashi-Ito, K., Saegusa, M., Iwamoto, K., Oda, Y., Katayama, H., Kojima, M., Sakakibara, H., and Fukuda, H. (2014). A bHLH complex activates vascular cell division via cytokinin action in root apical meristem. Curr. Biol. 24, 2053-2058.

Park, S.-Y., Fung, P., Nishimura, N., Jensen, D.R., Fujii, H., Zhao, Y., Lumba, S., Santiago, J., Rodrigues, A., Chow, T.-f.F., Alfred, S.E., Bonetta, D., Finkelstein, R., Provart, N.J., Desveaux, D., Rodriguez, P.L., McCourt, P., Zhu, J.-K., Schroeder, J.I., Volkman, B.F., and Cutler, S.R. (2009). Abscisic acid inhibits type 2C protein phosphatases via the PYR/PYL family of START proteins. Science 324, 1068–1071.

Rojas-Pierce, M., Titapiwatanakun, B., Sohn, E.J., Fang, F., Larive, C.K., Blakeslee, J., Cheng, Y., Cuttler, S.R., Peer, W.A., Murphy, A.S., and Raikhel, N.V. (2007). Arabidopsis P-glycoprotein19 participates in the inhibition of gravitropism by gravacin. Chem. Biol. 14, 1366-1376 [Erratum Chem. Biol. 15, 87].

Ruyter-Spira, C., Kohlen, W., Charnikhova, T., van Zeijl, A., van Bezouwen, L., de Ruijter, N., Cardoso, C., Lopez-Raez, J.A., Matusova, R., Bours, R., Verstappen, F., and Bouwmeester, H. (2011). Physiological effects of the synthetic strigolactone analog GR24 on root system architecture in Arabidopsis: another belowground role for

strigolactones? Plant Physiol. 155, 721-734.

Savaldi-Goldstein, S., Baiga, T.J., Pojer, F., Dabi, T., Butterfield, C., Parry, G., Santner, A., Dharmasiri, N., Tao, Y., Estelle, M., Noel, J.P., and Chory, J. (2008). New auxin analogs with growth-promoting effects in intact plants reveal a chemical strategy to improve hormone delivery. Proc. Natl. Acad. Sci. USA 105, 15190-15195.

Scaffidi, A., Waters, M.T., Sun, Y.K., Skelton, B.W., Dixon, K.W., Ghisalberti, E.L., Flematti, G.R., and Smith, S.M. (2014). Strigolactone hormones and their stereoisomers signal through two related receptor proteins to induce different physiological responses in Arabidopsis. Plant Physiol. 165, 1221 1232.

Schlereth, A., Möller, B., Liu, W., Kientz, M., Flipse, J., Rademacher, E.H., Schmid, M., Jürgens, G., and Weijers, D. (2010). MONOPTEROS controls embryonic root initiation by regulating a mobile transcription factor. Nature 464, 913–916.

Shen, H., Luong, P., and Huq, E. (2007). The F-Box protein MAX2 functions as a positive regulator of photomorphogenesis in Arabidopsis. Plant Physiol. 145, 1471-1483.

Shen, H., Zhu, L., Bu, Q.-Y., and Huq, E. (2012). MAX2 affects multiple hormones to promote photomorphogenesis. Mol. Plant 5, 750-762.

Shinohara, N., Taylor, C., and Leyser, O. (2013). Strigolactone can promote or inhibit shoot branching by triggering rapid depletion of the auxin efflux protein PIN1 from the plasma membrane. PLoS Biol. 11, e1001474.

Soundappan, I., Bennett, T., Morffy, N., Liang, Y., Stanga, J.P., Abbas, A., Leyser, O., and Nelson, D.C. (2015). SMAX1-LIKE/D53 family members enable distinct MAX2-dependent responses to strigolactones and karrikins in Arabidopsis. Plant Cell 27, 3143-3159.

Stanga, J.P., Smith, S.M., Briggs, W.R., and Nelson, D.C. (2013). *SUPPRESSOR OF MORE AXILLARY GROWTH2 1* controls seed germination and seedling development in Arabidopsis. Plant Physiol. 163, 318-330.

Sun, Y.K., Flematti, G.R., Smith, S.M., and Waters, M.T. (2016). Reporter gene-facilitated detection of compounds in *Arabidopsis* leaf extracts that activate the karrikin signaling pathway. Front. Plant Sci. 7, 1799.

Sungur, C., Miller, S., Bergholz, J., Hoye, R.C., Brisbois, R.G., and Overvoorde; P. (2007). The small molecule 2-furylacrylic acid inhibits auxin-mediated responses in Arabidopsis thaliana. Plant Cell Physiol. 48, 1693-1701.

Toh, S., Holbrook-Smith, D., Stokes, M.E., Tsuchiya, Y., and McCourt, P. (2014). Detection of parasitic plant suicide germination compounds using a high-throughput *Arabidopsis* HTL/KAI2 strigolactone perception system. Chem. Biol. 21, 988-998.

Tóth, R., and van der Hoorn, R.A.L. (2010). Emerging principles in plant chemical genetics. Trends Plant Sci. 15, 81-88.

Tsuchiya, Y., Vidaurre, D., Toh, S., Hanada, A., Nambara, E., Kamiya, Y., Yamaguchi, S., and McCourt, P. (2010). A small-molecule screen identifies new functions for the plant hormone strigolactone. Nat. Chem. Biol. 6, 741-749.

Umehara, M., Hanada, A., Yoshida, S., Akiyama, K., Arite, T., Takeda-Kamiya, N., Magome, H., Kamiya, Y., Shirasu, K., Yoneyama, K., Kyozuka, J., and Yamaguchi, S. (2008). Inhibition of shoot branching by new terpenoid plant

hormones. Nature 455, 195-200.

Van Norman, J.M., Zhang, J., Cazzonelli, C.I., Pogson, B.J., Harrison, P.J., Bugg, T.D.H., Chan, K.X., Thompson, A.J., and Benfey, P.N. (2014). Periodic root branching in *Arabidopsis* requires synthesis of an uncharacterized carotenoid derivative. Proc. Natl. Acad. Sci. USA 111**,** E1300-1309.

Walton, A., Stes, E., Goeminne, G., Braem, L.,Vuylsteke, M., Matthys, C., De Cuyper, C., Staes, A., Vandenbussche, J., Boyer, F.-D., Vanholme, R., Fromentin, J., Boerjan, W., Gevaert, K., and Goormachtig, S. (2016). The response of the root proteome to the synthetic strigolactone GR24 in *Arabidopsis*. Mol. Cell. Proteomics 15, 2744-2755.

Wang, L., Wang, B., Jiang, L., Liu, X., Li, X., Lu, Z., Meng, X., Wang, Y., Smith, S.M., and Li, J. (2015). Strigolactone signaling in Arabidopsis regulates shoot development by targeting D53-like SMXL repressor proteins for ubiquitination and degradation. Plant Cell 27, 3128-3142.

Xuan, W., Audenaert, D., Parizot, B., Möller, B.K., Njo, M.F., De Rybel, B., De Rop, G., Van Isterdael, G., Mähönen, A.P., Vanneste, S., and Beeckman, T. (2015). Root cap-derived auxin pre-patterns the longitudinal axis of the *Arabidopsis* root. Curr. Biol. 25, 1381-1388.

Zhao, L.H., Zhou, X.E., Wu, Z.-S., Yi, W., Xu, Y., Li, S., Xu, T.-H., Liu, Y., Chen, R.-Z., Kovach, A., Kang, Y., Hou, L., He, Y., Xie, C., Song, W., Zhong, D., Xu, Y., Wang, Y., Li, J., Zhang, C., Melcher, K., and Xu, H.E. (2013). Crystal structures of two phytohormone signal-transducing α/β hydrolases: karrikin-signaling KAI2 and strigolactone-signaling DWARF14. Cell Res. 23, 436-439.

DANKWOORD / ACKNOWLEDGEMENTS

EIN-DE-LIJK! Het is zover: de thesis is geschreven, de laatste aanpassingen zijn doorgevoerd, de eindsprint is ingezet. Het hele proces is zeker niet zonder slag of stoot verlopen, en zonder de hulp en steun van velen zou dit allemaal niet mogelijk geweest zijn. Daarom is het niet meer dan normaal om dit droge wetenschappelijke deel af te sluiten met woorden van dank en met enkele mensen welgemeend in de bloemetjes te zetten.

Eerst en vooral zou ik mijn promotoren **Prof. Dr. Sofie Goormachtig** en **Prof. Dr. Tom Beeckman** willen bedanken voor de kansen die ze me gaven om op dit onderwerp te kunnen werken. In het bijzonder wil ik Sofie mijn dank betuigen. Sofie, het is niet altijd gelopen zoals we het gehoopt hadden, maar toch bleef je geduld en vooral positivisme uitstralen waar velen –mezelf inbegrepen– een voorbeeld aan kunnen nemen. Ik bewonder je niet alleen als promotor, maar vooral ook als persoon. Je staat altijd klaar voor je mensen, wat onder andere geïllustreerd wordt door het feit dat je deur steeds open staat voor iedereen. Daarnaast stel je bijvoorbeeld maar al te graag je eigen huis ter beschikking voor onze jaarlijkse labo zomerbarbecues en kerstdinertjes. Door die vlotte omgang ben je erin geslaagd om een werkomgeving te creëren waar men zich thuis voelt en iedereen met iedereen collegiaal om gaat. Respect.

Next, I would also like to thank the chairman and my jury members: ***Prof. Dr. Lieven De Veylder****,* ***Prof. Dr. Bartel Vanholme****,* ***Dr. Sandrine Bonhomme****,* ***Dr. Danny Vereecke****,* ***Prof. Dr. Bert De Rybel*** *and* ***Dr. Boris Parizot****. Thank you for your time and efforts for reading my manuscript, your critical assessment, and your interesting questions during the discussions at the closed defense. Dr. Sandrine Bonhomme and Dr. Danny Vereecke, it's really a pity that both of you cannot make it to the public defense.*

Een volgende groep van mensen die ik welgemeend wil bedanken zijn de ex- en huidige '*Rhizosphere*' lab members: **Alan**, **Lukas**, **Sylwia**, **Justine**, **Belen**, **Annick**, **Tom**, **Tibby**, **Stien**, **Sarah**, **Anse** and **Dexian**. Wat een ongelooflijke sfeer heerst er in het rhizosphere labo: naast fijne collega's mogen we elkaar ook gerust stuk voor stuk vrienden noemen. Niemand viel of valt uit de boot en nieuwe groepsleden

werden warm opgenomen in de groep. Een unieke situatie als je het mij vraagt! *Alan, my English/half-Scottish/French(? ;-)) 'island'-colleague who unfortunately already left the lab to return to France. Damn boy, I miss you!* Lukas, ik herinner me nog goed de eerste keer dat ik je ontmoette: het was op de posterbeurs waar Alan en ik een poster deelden om masterstudenten te ronselen. Nick zou je introduceren als kandidaat voor het project van Alan. Ik denk dat de eerste ontmoeting direct een schot in de roos was: een enthousiaste student, vlot in de omgang. Gaandeweg leerde ik je beter kennen, startte je ook als doctoraatstudent in het labo en kunnen we onszelf intussen ook echt vrienden noemen. Wanneer is de volgende game time ☺ ? *For some reason Lukas, when I think of Lukas, I think of Justine. Justine, I really enjoyed our time together in the lab, the funny (and sometimes serious) conversations and the reciprocal pep talks now and then. Luckily, this is now continued with fun times outside the lab environment! Sylwia, also for you I'm really glad that I got the chance to get to know you. You're an awesome friend with a heart of gold (and cherry wodka :-P). I guess you're the next in line to start writing and to defend. You'll do great, I'm sure of that. Good luck!* Annick –*the queen of cloning*–, voor mij ben je altijd een beetje de 'mama' van het labo geweest. Je stond altijd klaar met raad en daad als de kloneringen eens niet lukten, of als er weer eens een groot experiment gepland stond en een extra paar handen welkom was om snel te kunnen oogsten en de daarmee gepaard gaande grote hoeveelheden RNA bereidingen te helpen verwerken,... Niet alleen langs de praktische kant stond je paraat, maar ook voor een gewone aangename babbel was je steeds te vinden. Bedankt voor de aangename tijden in het labo! Tibby, het was aangenaam om je helemaal te zien openbloeien in het labo. Ik wens jou en Tom veel succes met jullie nieuwe avontuur en dat jullie grootse dingen mogen verwezenlijken met Aphea.Bio! Anse, Sarah en Stien –*ik zen ne wolf*–, de (relatief) nieuwe aanwinsten van het labo. Ik ben blij dat ik ook jullie heb leren kennen, in het labo en daarbuiten. Wie weet, Stien, begin je gezelschapspelletjes binnenkort wel écht leuk te vinden!

Naast de 'vaste' –voor zover je het vast kan noemen, met het continue komen en gaan van mensen– labo partners, heb ik ook nog het geluk gehad om twee fantastische masterstudenten te kunnen begeleiden tijdens hun masterthesis: **Lien** en **Nick**. Lien, ik vond het zeer aangenaam om jou te begeleiden, je was steeds je immer positieve en gemotiveerde zelve. Vastberaden wist je maar al te goed wat je wilde, en vooral wat je niet wilde: les geven en doctoreren, respectievelijk ☺. Ik wens je nog veel succes verder! Nick, jou begeleiden tijdens je thesis was eveneens zeer aangenaam. Het was leuk om je te zien groeien in je wetenschappelijke doen en denken. Tegen het einde van je thesis kwam een assistentenpositie vrij in Tom's labo. Met een licht dubbel gevoel bracht ik je hiervan op de hoogte: ik wist dat die positie je op de buik geschreven stond; de perfecte combinatie tussen doctoreren en les geven/studenten begeleiden, ook al betekende dat je afscheid binnen het 'Rhizosphere' labo. Ik ben oprecht blij voor je dat je die positie meer dan verdiend gekregen hebt!

Daarnaast zijn er ook nog een heleboel mensen binnen het PSB die ik wil bedanken voor de leuke samenwerkingen, babbels, activiteiten,… Sowieso ga ik nu een heleboel namen vergeten vermelden. Alvast mijn oprechte excuses hiervoor. Neem het niet persoonlijk, diep vanbinnen weet je –ja, jij daar die nu dit dankwoord zit te lezen ;-) – dat ik je zeer dankbaar ben. **Stefanie** –*bestie*–, **Toon**, **Fien, Alex et al**.,: bedankt voor onder andere de hartelijke adoptie van mij binnen jullie labo en jullie labo feestjes ;-). Stefanie, hopelijk ben je snel weer helemaal hersteld zodat je weer vlot kan eten en drinken! Nog even 'op je tanden bijten' ;-). Bedankt **Christa** om je queeste en verwoede pogingen tot een nettere en veiligere werkomgeving niet te staken. Er komt een dag waarop iedereen (of toch bijna iedereen) je zomaar zal gehoorzamen ;-). **Kristof**, **Jackie**, **An**, **Peter**, **Nico**, **Thomas** en **Miguel**, bedankt voor de goede zorgen op technisch vlak. Bedankt **Nancy** voor de ontspannende babbels tijdens het medium maken. ***Dominique**, **Long** and **Andrzej**, thanks for sharing the chemical library with me and for making sure that the pipetting robot was doing what he needed to do. Andrzej, an additional thank you for your help with the clustering of my hit compounds etc,…* ☺. Een extra woord van dank voor **Martine** is hier ook zeker op zijn plaats.

Martine, het is ongelooflijk met welke passie en overgave je manuscripten naleest en bibliografielijsten samen stelt. Een dikke merci om dit ook zo voor mijn thesis te willen doen! **Veronique**, mede-Deinzenaar, bedankt voor je hulp bij de statistische analyses en je *custom-made* scriptjes. Je hebt statistiek voor mij net weer wat duidelijker kunnen maken ;-)!

Ook buiten het labo zijn er een heleboel mensen die ik graag wil bedanken: bedankt aan **al mijn vrienden**. Jullie hebben me de laatste tijd nogal wat moeten missen, maar onze schade halen we snel weer in. Beloofd! Bcbt-vrienden **Silvie**, **Giel**, **Koen**, **Lisa**, **Mieke**, **Niels**,… Bedankt voor alle fijne momenten de voorbije jaren! De meeste onder jullie liep ik ook geregeld tegen het lijf op het VIB, gepaard gaande met zowel wetenschappelijke (we konden geregeld wel eens tegen elkaar klagen over onze resultaten,… :-P) als niet-wetenschappelijke gesprekken. Silvie en Lisa, extra bedankt voor al de steun, de leuke tijden, en de nodige motiverende woorden zo nu en dan, ze hebben echt geholpen! Koen, binnenkort is het aan jou om je doctoraat af te leggen. Dat komt sowieso goed; geef er een lap op, veel succes. **Sven**, **Sander & Lisa**, **Joke & Kjell**, **Tine & Koen**, **Sisi & Fred**, **Lien & Tom**, **Jolanda**, bedankt voor alle leuke tijden die we al samen beleefd hebben en die we nog zullen beleven; we zijn een hechte, leuke vriendengroep. Ook bedankt om af en toe mijn klaagzang te aanhoren en vooral voor de ontspanning waarvoor jullie zorgden tijdens mijn doctoraat: de ideale afleiding.

Ook het thuisfront mag uiteraard niet ontbreken in dit dankwoord. **Ma & Pa**, bedankt voor al de kansen die jullie mij al gegeven hebben en om altijd en onvoorwaardelijk in mij te blijven geloven. Mede dankzij jullie steun is ook dit verhaal tot een goed einde gekomen! Bedankt voor het warme nest dat jullie gevormd hebben, waar het leuk is om geregeld naar terug te keren. Jullie zijn fantastisch. Daarnaast heb ik ook het geluk gehad om met Thomas er een extra familie erbij te krijgen: **Brigitte & Karl**, **Noël & Ann**, bedankt om me hartelijk op te nemen in jullie gezin, voor jullie steun en de gezellige momenten samen.

De laatste –en belangrijkste– persoon die ik hier nog wil bedanken is **Thomas**. Thomas, je bent mijn onvoorwaardelijke steun en toeverlaat. Ik denk wel dat je beseft dat dit alles zonder jou niet mogelijk was. Bedankt om er steeds voor mij te zijn. Samen met jou ben ik klaar voor een nieuwe uitdaging!

Scientific resume

CEDRICK MATTHYS

° 28/01/1987, Aalst

Aaltersesteenweg 35D, B-9800 Deinze, Belgium

+32 472 22 52 72

cedrick.matthys@hotmail.com

Work experience

2011 - 2017	**Doctoral researcher in Biochemistry and Biotechnology** Faculty of Sciences, Ghent University VIB Center of Plant Systems Biology Topic: *Understanding the physiology of strigolactones in Arabidopsis thaliana: a multi-angle approach* Promoters: Prof. Dr. Sofie Goormachtig & Prof. Dr. Tom Beeckman
2009 - 2011	**Summer student at Devgen NV** (now Syngenta Ghent Innovation Center)

Education

2006 - 2011	**Master of Science in Biochemistry and Biotechnology** Faculty of Sciences, Ghent University *Summa cum laude* Major: Plant Biotechnology – Minor: Biomedical Biotechnology Bayer Award for best master thesis Master thesis: *The role of strigolactones in the root architecture of* Arabidopsis thaliana, promoter: Prof. Dr. Sofie Goormachtig
2011 - 2017	**PhD in Biochemistry and Biotechnology** Faculty of Sciences, Ghent University VIB Center of Plant Systems Biology Topic: *Understanding the physiology of strigolactones in Arabidopsis thaliana: a multi-angle approach* Promoters: Prof. Dr. Sofie Goormachtig & Prof. Dr. Tom Beeckman

Skills

Languages	Dutch – native proficiency

	English – professional working proficiency French – limited working proficiency Spanish - elementary
Software	Microsoft Windows • MS Office (Word, Excel, PowerPoint) • various (online) bioinformatic tools • ImageJ • CLC Main Workbench and CLC Sequence Viewer (sequence analysis and design) • SAS Enterprise Guide (statistical analysis)
Techniques	(Gateway) cloning • PCR • qRT-PCR • genotyping • high quality RNA and DNA preparation and handling • chemical genetics • analysis and interpretation of RNAseq data • expression pattern analyses • development and optimization of bioassays • high-throughput screening • Aseptic working • microbiological handling • plant tissue culture • plant transformation • (confocal) microscopy • plant phenotyping

Courses and trainings

December 2011	Getting started with CLC Bio DWB (VIB – BITS)
January 2012	Microscopy basic training (VIB – Microscopy Core Facility)
April 2012	QPCR training session (Bioline – Steve Hawkins)
October 2012	Basic bioinformatics concepts, databases and tools (VIB – BITS)
December 2012	Hands-on session in SAS/EG (VIB – Veronique Storme)
February 2013	RNAseq training (VIB – Frederik Coppens)
October 2015	EXPANDER workshop (VIB – Oren Tzfadia)
January 2016	Confocal microscopy training – Zeiss 710 (VIB – Daniel Van Damme)

Personal skills

Meticulous • analytical • curious • enthusiastic • autonomous • self-motivated • good social skills

Publications in peer-reviewed journals

Rasmussen A, Heugebaert T, **Matthys C**, Van Deun R, Boyer F-D, Goormachtig S, et al. A fluorescent alternative to the synthetic strigolactone GR24. MOLECULAR PLANT. 2013;6(1):100–12.

Stes E, Depuydt S, De Keyser A, **Matthys C**, Audenaert K, Yoneyama K, et al. Strigolactones as an auxiliary hormonal defence mechanism against leafy gall syndrome in Arabidopsis thaliana. JOURNAL OF EXPERIMENTAL BOTANY. 2015;66(16):5123–34.

Jiang L*, **Matthys C***, Marquez-Garcia B, De Cuyper C, Smet L, De Keyser A, et al. Strigolactones spatially influence lateral root development through the cytokinin signaling network. JOURNAL OF EXPERIMENTAL BOTANY. 2016;67(1):379–89.

Matthys C*, Walton A*, Struk SM, Stes E, Boyer F-D, Gevaert K, et al. The whats, the wheres and the hows of strigolactone action in the roots. PLANTA. 2016;243(6):1327–37.

Walton A, Stes E, Goeminne G, Braem L, Vuylsteke M, **Matthys C**, et al. The response of the root proteome to the synthetic strigolactone GR24 in Arabidopsis. MOLECULAR & CELLULAR PROTEOMICS. 2016;15(8):2744–55.

Presentations and posters at international conferences

Carolien De Cuyper, **Cedrick Matthys**, Michiel Vandecasteele, Annick De Keyser, Stephen Depuydt, Geert De Jaeger and Sofie Goormachtig – Unraveling the strigolactone signal transduction cascade, poster at Frontiers in plant biology, from discovery to applications (October 2012 – Ghent, Belgium)

Cedrick Matthys, Carolien De Cuyper, Linxian Jiang, Annick De Keyser, Stephen Depuydt and Sofie Goormachtig – Elucidating strigolactone signaling via marker genes and interaction with other hormones, poster at Frontiers in plant biology, from discovery to applications (October 2012 – Ghent, Belgium)

Cedrick Matthys, Stephen Depuydt, Marlies Demeulenaere, Tom Beeckman and Sofie Goormachtig – Strigolactones and root architecture: where do they meet?, poster at First COST meeting on Strigolactone action (STREAM) (November 2013 – Jerusalem, Israel) – *Award for best paper*

Cedrick Matthys, Dominique Audenaert, Tom Beeckman and Sofie Goormachtig – Understanding strigolactone signaling by the use of chemical genetics, poster at 25th International Conference on Arabidopsis Research (ICAR) (July 2014 – Vancouver, Canada)

Cedrick Matthys, Dominique Audenaert, Tom Beeckman and Sofie Goormachtig – Understanding the role of GR24 in plant development by the use of chemical genetics, poster and flash talk at 1st International Congress on Strigolactones (March 2015 – Wageningen, The Netherlands)

Sylwia Struk, Alan Walton, Carolien De Cuyper, **Cedrick Matthys**, Lukas Braem, Annick De Keyser and Sofie Goormachtig - Molecular insight into strigolactone signaling network in Arabidopsis thaliana, poster at the bi-annual PhD Symposium 2016 of the faculty of Sciences (March 2016 – Ghent, Belgium)

Teaching experience

2012-2013

- Supervision master dissertation Lien Smet (2nd Master in Biochemistry and Biotechnology): De rol van strigolactonen in de wortelarchitectuur van *Arabidopsis thaliana*
- Supervision master project Nick Vangheluwe (1st Master in Biochemistry and Biotechnology): The hormonal crosstalk between strigolactones and jasmonates and the resulting effects on root architecture of *A. thaliana*
- Practical course 'Genetica en moleculaire technieken'; Prof. Dr. S. Goormachtig – 2nd bachelor Biology students

2013-2014

- Supervision master dissertation Nick Vangheluwe (2nd Master in Biochemistry and Biotechnology): De analyse van strigolactonresponsieve genen in het wortelsysteem van *Arabidopsis thaliana*
- Practical course 'Plantenfysiologie'; Prof. Dr. D. Inze and Prof. Dr. B. Vanholme – 2nd bachelor Biology students

- Practical course 'Genetica en moleculaire technieken'; Prof. Dr. S. Goormachtig – 2nd bachelor Biology students

2014-2015

- Practical course 'Plantenfysiologie'; Prof. Dr. D. Inze and Prof. Dr. B. Vanholme – 2nd bachelor Biology students – Head responsible

Publications

1. Rasmussen A, Heugebaert T, **Matthys C**, Van Deun R, Boyer F-D, Goormachtig S, et al. A fluorescent alternative to the synthetic strigolactone GR24. MOLECULAR PLANT. 2013;6(1):100–12.

2. Stes E, Depuydt S, De Keyser A, **Matthys C**, Audenaert K, Yoneyama K, et al. Strigolactones as an auxiliary hormonal defence mechanism against leafy gall syndrome in Arabidopsis thaliana. JOURNAL OF EXPERIMENTAL BOTANY. 2015;66(16):5123–34.

3. Jiang L*, **Matthys C***, Marquez-Garcia B, De Cuyper C, Smet L, De Keyser A, et al. Strigolactones spatially influence lateral root development through the cytokinin signaling network. JOURNAL OF EXPERIMENTAL BOTANY. 2016;67(1):379–89.

4. **Matthys C***, Walton A*, Struk SM, Stes E, Boyer F-D, Gevaert K, et al. The whats, the wheres and the hows of strigolactone action in the roots. PLANTA. 2016;243(6):1327–37.

5. Walton A, Stes E, Goeminne G, Braem L, Vuylsteke M, **Matthys C**, et al. The response of the root proteome to the synthetic strigolactone GR24 in Arabidopsis. MOLECULAR & CELLULAR PROTEOMICS. 2016;15(8):2744–55.

Molecular Plant • Volume 6 • Number 1 • Pages 100–112 • January 2013 RESEARCH ARTICLE

A Fluorescent Alternative to the Synthetic Strigolactone GR24

Amanda Rasmussen[a], Thomas Heugebaert[b], Cedrick Matthys[c,d], Rik Van Deun[e], Francois-Didier Boyer[f], Sofie Goormachtig[c,d], Christian Stevens[b] and **Danny Geelen[a,1]**

a Plant Production, Faculty of Bioscience Engineering, Ghent University, Coupure links 653, Ghent 9000, Belgium
b Research Group SynBioC, Department of Sustainable Organic Chemistry and Technology, Faculty of Bioscience Engineering, Ghent University, Coupure links 653, B-9000 Gent, Belgium
c Department of Plant Systems Biology, VIB, Ghent 9052, Belgium
d Department of Plant Biotechnology and Bioinformatics, Ghent University, Ghent 9052, Belgium
e f-element Coordination Chemistry Lab, Inorganic and Physical Chemistry Department, Ghent University, Krijgslaan 281—S3, 9000 Gent, Belgium
f Centre de Recherche de Gif, Institut de Chimie des Substances Naturelles, UPR2301 CNRS, INRA, 1 avenue de la Terrasse, F-91198 Gif-sur-Yvette Cedex, France

ABSTRACT Strigolactones have recently been implicated in both above- and below-ground developmental pathways in higher plants. To facilitate the molecular and chemical properties of strigolactones *in vitro* and *in vivo*, we have developed a fluorescent strigolactone molecule, CISA-1, synthesized via a novel method which was robust, high-yielding, and used simple starting materials. We demonstrate that CISA-1 has a broad range of known strigolactone activities and further report on an adventitious rooting assay in *Arabidopsis* which is a highly sensitive and rapid method for testing biological activity of strigolactone analogs. In this rooting assay and the widely used Orobanche germination assay, CISA-1 showed stronger biological activity than the commonly tested GR24. CISA-1 and GR24 were equally effective at inhibiting branching in *Arabidopsis* inflorescence stems. In both the branching and adventitious rooting assay, we also demonstrated that CISA-1 activity is dependent on the max strigolactone signaling pathway. In water methanol solutions, CISA-1 was about threefold more stable than GR24, which may contribute to the increased activity observed in the various biological tests.

Key words: strigolactones; adventitious rooting; branching; fluorescent markers; parasitic weed seed germination.

INTRODUCTION

Strigolactones are a class of signaling molecules emitted by host plants that control in the rhizosphere the germination of parasitic plant seeds (Cook et al., 1966), hyphal branching in arbuscular mycorrhizal fungi (Akiyama et al., 2005), as well as several developmental processes in higher plants including germination, branching, and root development (Matusova et al., 2005; Gomez-Roldan et al., 2008; Umehara et al., 2008; Kapulnik et al., 2011; Koltai, 2011; Rasmussen et al., 2012). Typically, natural strigolactones are composed of a tricyclic lactone (A-, B-, and C-rings) connected via an enol ether bridge to a D-ring. This generalized core structure contains four structural regions (Figure 1). The structural features which are conserved in all natural strigolactones and which are generally regarded as the bioactiphore are the lactone D-ring, connected through an enol ether to an α,β-unsaturated ester (or ketone) (Mangnus and Zwanenburg, 1992; Zwanenburg et al., 2009). The A- and B-rings allow a large degree of structural freedom, as observed in the great variety of naturally occurring strigolactones. There are some indications that the presence of H-bond acceptors on the A- and B-rings enhances the biological activity; however, this effect remains to be validated for models other than parasitic seed germination (Kim et al., 2010; Malik et al., 2011). Moving forward from the natural strigolactones, synthetic efforts have shown, through the generation of non-naturally occurring strigolactones, that the bioactiphore can be further simplified. First, the lactone contained within the C-ring is unimportant for biological activity. Furthermore, the synthesis of non-natural strigolactones has shown an even higher-than-expected structural freedom. In fact, it was recently shown (Boyer et al., 2012) that the D-ring contains the essence of the biological activity and that the whole of

[1] To whom correspondence should be addressed. E-mail danny.geelen@ugent.be, tel. +32 9 2646076, fax +32 9 2646225.

doi:10.1093/mp/sss110, Advance Access publication 30 September 2012

Received 3 August 2012; accepted 19 September 2012

Journal of Experimental Botany, Vol. 66, No. 16 pp. 5123–5134, 2015
doi:10.1093/jxb/erv309 Advance Access publication 30 June 2015
This paper is available online free of all access charges (see http://jxb.oxfordjournals.org/open_access.html for further details)

RESEARCH PAPER

Strigolactones as an auxiliary hormonal defence mechanism against leafy gall syndrome in *Arabidopsis thaliana*

Elisabeth Stes[1,2,3,4*], Stephen Depuydt[1,2,5*], Annick De Keyser[1,2], Cedrick Matthys[1,2], Kris Audenaert[6], Koichi Yoneyama[7], Stefaan Werbrouck[6], Sofie Goormachtig[1,2], and Danny Vereecke[6†]

[1] Department of Plant Systems Biology, VIB, 9052 Gent, Belgium
[2] Department of Plant Biotechnology and Bioinformatics, Ghent University, 9052 Gent, Belgium
[3] Department of Medical Protein Research, VIB, 9000 Gent, Belgium
[4] Department of Biochemistry, Ghent University, 9000 Gent, Belgium
[5] Ghent University Global Campus, Incheon 406-840, Republic of Korea
[6] Department of Applied Biosciences, Ghent University, 9000 Gent, Belgium
[7] Center for Bioscience Research & Education, Utsunomiya University, Utsunomiya 321–8505, Japan

* These authors contributed equally to this work.
† To whom correspondence should be addressed. E-mail: danny.vereecke@ugent.be.

Received 11 May 2015; Revised 1 June 2015; Accepted 1 June 2015

Editor: Angus Murphy

Abstract

Leafy gall syndrome is the consequence of modified plant development in response to a mixture of cytokinins secreted by the biotrophic actinomycete *Rhodococcus fascians*. The similarity of the induced symptoms with the phenotype of plant mutants defective in strigolactone biosynthesis and signalling prompted an evaluation of the involvement of strigolactones in this pathology. All tested strigolactone-related *Arabidopsis thaliana* mutants were hypersensitive to *R. fascians*. Moreover, treatment with the synthetic strigolactone mixture GR24 and with the carotenoid cleavage dioxygenase inhibitor D2 illustrated that strigolactones acted as antagonistic compounds that restricted the morphogenic activity of *R. fascians*. Transcript profiling of the *MORE AXILLARY GROWTH1* (*MAX1*), *MAX2*, *MAX3*, *MAX4*, and *BRANCHED1* (*BRC1*) genes in the wild-type Columbia-0 accession and in different mutant backgrounds revealed that upregulation of strigolactone biosynthesis genes was triggered indirectly by the bacterial cytokinins via host-derived auxin and led to the activation of *BRC1* expression, inhibiting the outgrowth of the newly developing shoots, a typical hallmark of leafy gall syndrome. Taken together, these data support the emerging insight that balances are critical for optimal leafy gall development: the long-lasting biotrophic interaction is possible only because the host activates a set of countermeasures—including the strigolactone response—in reaction to bacterial cytokinins to constrain the activity of *R. fascians*.

Key words: Apical dominance, Gram-positive phytopathogen, witches' broom.

Introduction

Leafy gall syndrome is an infectious plant disease that affects a wide range of plants, primarily dicotyledonous herbs (for recent reviews, see Stes *et al.*, 2011*b*, 2013). The pathology is caused by the Gram-positive actinomycete *Rhodococcus*

Abbreviations: 2-iP, 2-isopentenyladenine; 2MeS, 2-methylthio; AHK, *Arabidopsis* histidine kinase, BRC, BRANCHED; CCD, carotenoid cleavage dioxygenase; CKX, CYTOKININ DEHYDROGENASE/OXIDASE; *cZ*, *cis*-zeatin; D27, DWARF27; DAD, DECREASED APICAL DOMINANCE; DMSO, dimethylsulfoxide; dpi, days post infection; GR24, strigolactone analogue; GUS, β-glucuronidase; LC-MS/MS, liquid chromatography-tandem mass spectrometry; MAX, MORE AXILLARY GROWTH; qRT-PCR, quantitative reverse-transcription-polymerase chain reaction; SCF, Skp-Cullin-F-box; TAA, TRYPTOPHAN AMINOTRANSFERASE; TAR, TAA1-RELATED; *tZ*, *trans*-zeatin; WEI, WEAK ETHYLENE INSENSITIVE.

Journal of Experimental Botany, Vol. 67, No. 1 pp. 379–389, 2016
doi:10.1093/jxb/erv478 Advance Access publication 31 October 2015
This paper is available online free of all access charges (see http://jxb.oxfordjournals.org/open_access.html for further details)

RESEARCH PAPER

Strigolactones spatially influence lateral root development through the cytokinin signaling network

Lingxiang Jiang[1,2,*], Cedrick Matthys[1,2,*], Belen Marquez-Garcia[1,2], Carolien De Cuyper[1,2], Lien Smet[1,2], Annick De Keyser[1,2], François-Didier Boyer[3,4], Tom Beeckman[1,2], Stephen Depuydt[1,2,5,†] and Sofie Goormachtig[1,2,†,§]

[1] Department of Plant Systems Biology, VIB, 9052 Gent, Belgium
[2] Department of Plant Biotechnology and Bioinformatics, Ghent University, 9052 Gent, Belgium
[3] Institut Jean-Pierre Bourgin, Unité Mixte de Recherche 1318, Institut National de la Recherche Agronomique-AgroParisTech, 78026 Versailles Cedex, France
[4] Centre de Recherche de Gif, Institut de Chimie des Substances Naturelles, Unité Propre de Recherche 2301, Centre National de la Recherche Scientifique, 91198 Gif-sur-Yvette, France
[5] Ghent University Global Campus, Incheon 406–840, Korea

* These authors contributed equally to this manuscript.
† These authors contributed equally to this manuscript.
§ To whom correspondence should be addressed. E-mail: sofie.goormachtig@psb.vib-ugent.be.

Received 16 July 2015; Revised 1 October 2015; Accepted 12 October 2015

Editor: Hitoshi Sakakibara, RIKEN Center for Sustainable Resource Science

Abstract

Strigolactones are important rhizosphere signals that act as phytohormones and have multiple functions, including modulation of lateral root (LR) development. Here, we show that treatment with the strigolactone analog GR24 did not affect LR initiation, but negatively influenced LR priming and emergence, the latter especially near the root–shoot junction. The cytokinin module *ARABIDOPSIS HISTIDINE KINASE3* (*AHK3*)/*ARABIDOPSIS RESPONSE REGULATOR1* (*ARR1*)/*ARR12* was found to interact with the GR24-dependent reduction in LR development, because mutants in this pathway rendered LR development insensitive to GR24. Additionally, pharmacological analyses, mutant analyses, and gene expression analyses indicated that the affected polar auxin transport stream in mutants of the *AHK3*/*ARR1*/*ARR12* module could be the underlying cause. Altogether, the data reveal that the GR24 effect on LR development depends on the hormonal landscape that results from the intimate connection with auxins and cytokinins, two main players in LR development.

Key words: *Arabidopsis thaliana*, cytokinin signaling, lateral root development, polar auxin transport, strigolactones.

Introduction

Strigolactones (SLs) are phytohormones that affect lateral branching of the shoot (Gomez-Roldan *et al.*, 2008; Umehara *et al.*, 2008) and many other processes, such as photomorphogenesis, drought tolerance, leaf senescence, and secondary growth, among others (Woo *et al.*, 2001; Snowden *et al.*, 2005; Shen *et al.*, 2007, 2012; Tsuchiya *et al.*, 2010;

Abbreviations: AHK, ARABIDOPSIS HISTIDINE KINASE; ARR, ARABIDOPSIS RESPONSE REGULATOR; BAP, 6-benzylaminopurine; BES, BRASSINOSTEROID INSENSITIVE--EMS-SUPPRESSOR; BRC, BRANCHED; CRE, CYTOKININ RESPONSE; D14, DWARF14; DAG, days after germination; EMS, ethyl methanesulfonate; GUS, β-glucuronidase; IAA, indole-3-acetic acid; LR, lateral root; LRD, lateral root density; MAX, MORE AXILLARY GROWTH; NPA, 1-*N*-naphthylphthalamic acid; PIN, PIN-FORMED; SCF, Skp-Cullin-F-box; SHY, SHORT HYPOCOTYL; SL, strigolactone; WT, wild-type; XPP, xylem pole pericycle.

Planta (2016) 243:1327–1337
DOI 10.1007/s00425-016-2483-9

REVIEW

The Whats, the Wheres and the Hows of strigolactone action in the roots

Cedrick Matthys[1,2] · Alan Walton[1,2,3,4] · Sylwia Struk[1,2] · Elisabeth Stes[1,2,3,4] · François-Didier Boyer[5,6] · Kris Gevaert[3,4] · Sofie Goormachtig[1,2]

Received: 7 December 2015 / Accepted: 29 January 2016 / Published online: 19 February 2016

Abstract
Main conclusion **Strigolactones control various aspects of plant development, including root architecture. Here, we review how strigolactones act in the root and survey the strigolactone specificity of signaling components that affect root development.**
Strigolactones are a group of secondary metabolites produced in plants that have been assigned multiple roles, of which the most recent is hormonal activity. Over the last decade, these compounds have been shown to regulate various aspects of plant development, such as shoot branching and leaf senescence, but a growing body of literature suggests that these hormones play an equally important role in the root. In this review, we present all known root phenotypes linked to strigolactones. We examine the expression and presence of the main players in biosynthesis and signaling of these hormones and bring together the available information that allows us to explain how strigolactones act to modulate the root system architecture.

Keywords *rac*-GR24 · Root system architecture · Strigolactone · Strigolactone-related compounds

Abbreviations

D	DWARF
KAI	KARRIKIN INSENSITIVE
LR	Lateral root
LRD	Lateral root density
MAX	MORE AXILLARY GROWTH
PIN	PIN-FORMED
rac-GR24	RACEMIC GR24
SCF	Skp, Cullin, F-box
SL	Strigolactone
SMAX1	SUPPRESSOR OF MAX2 1
SMXL	SUPPRESSOR OF MAX2 1 LIKE
TIR1	TRANSPORT INHIBITOR RESPONSE1
WT	Wild type

Introduction

Strigolactones (SLs) are carotenoid-derived metabolites originally identified as signals that stimulate seed germination of plant-parasitic weeds, such as *Striga* sp. and *Orobanche* sp. (Cook et al. 1966). Additionally, within the rhizosphere, these molecules have been found to enhance the initiation of arbuscular mycorrhization, a plant-fungal

C. Matthys and A. Walton contributed equally to this work.

✉ Sofie Goormachtig
sofie.goormachtig@psb.vib-ugent.be

[1] Department of Plant Systems Biology, VIB, Technologiepark 927, 9052 Ghent, Belgium

[2] Department of Plant Biotechnology and Bioinformatics, Ghent University, Technologiepark 927, 9052 Ghent, Belgium

[3] Department of Medical Protein Research, VIB, Albert Baertsoenkaai 3, 9000 Ghent, Belgium

[4] Department of Biochemistry, Ghent University, Albert Baertsoenkaai 3, 9000 Ghent, Belgium

[5] Institut Jean-Pierre Bourgin, Unité Mixte de Recherche 1318, Institut National de la Recherche Agronomique-AgroParisTech, 78026 Versailles Cedex, France

[6] Centre de Recherche de Gif, Institut de Chimie des Substances Naturelles, Unité Propre de Recherche 2301, Centre National de la Recherche Scientifique, 91198 Gif-Sur-Yvette, France

Research

The Response of the Root Proteome to the Synthetic Strigolactone GR24 in *Arabidopsis*

Alan Walton‡§¶‖[c], Elisabeth Stes‡§¶‖[c], Geert Goeminne‡§, Lukas Braem‡§, Marnik Vuylsteke, Cedrick Matthys‡§, Carolien De Cuyper‡§, An Staes¶‖, Jonathan Vandenbussche¶‖, François-Didier Boyer‡‡§§¶¶, Ruben Vanholme‡§, Justine Fromentin‡§‖‖[a], Wout Boerjan‡§, Kris Gevaert¶‖[bc], and Sofie Goormachtig‡§[bc]**

Strigolactones are plant metabolites that act as phytohormones and rhizosphere signals. Whereas most research on unraveling the action mechanisms of strigolactones is focused on plant shoots, we investigated proteome adaptation during strigolactone signaling in the roots of *Arabidopsis thaliana.* Through large-scale, time-resolved, and quantitative proteomics, the impact of the strigolactone analog *rac*-GR24 was elucidated on the root proteome of the wild type and the signaling mutant *more axillary growth 2 (max2)*. Our study revealed a clear MAX2-dependent *rac*-GR24 response: an increase in abundance of enzymes involved in flavonol biosynthesis, which was reduced in the *max2–1* mutant. Mass spectrometry-driven metabolite profiling and thin-layer chromatography experiments demonstrated that these changes in protein expression lead to the accumulation of specific flavonols. Moreover, quantitative RT-PCR revealed that the flavonol-related protein expression profile was caused by *rac*-GR24-induced changes in transcript levels of the corresponding genes. This induction of flavonol production was shown to be activated by the two pure enantiomers that together make up *rac*-GR24. Finally, our data provide much needed clues concerning the multiple roles played by MAX2 in the roots and a comprehensive view of the *rac*-GR24-induced response in the root proteome. ***Molecular & Cellular Proteomics 15: 10.1074/mcp.M115.050062, 2744–2755, 2016.***

Root development is pivotal for plant survival, providing anchorage, ensuring water and nutrient uptake, and allowing the plant to engage in beneficial interactions with soil microorganisms. Root growth is modulated in response to numerous abiotic and biotic environmental cues, which are interpreted and transduced by hormonal pathways. Besides the well-known regulators of root development, such as auxin and cytokinin, a group of carotenoid-derived terpenoid lactones, coined strigolactones, have been described to play a role in the regulation of root architecture. The influence of strigolactones on the lateral root density (LRD)[1], adventitious root formation, and induction of root hair elongation has been demonstrated, but the molecular networks ruling these belowground effects are still not well understood (1–7).

Multiple research teams have contributed to a better understanding of the strigolactone biosynthesis pathway, early signaling processes, and transport mechanisms (8–14). Early signaling occurs mainly through the action of an α/β-hydrolase DWARF14 (D14)/DECREASED APICAL DOMINANCE2 (DAD2) that interacts with an F-box protein, MORE AXILLARY GROWTH2 (MAX2) (15). MAX2 together with an additional α/β-hydrolase and a D14 paralog, KARRIKIN INSENSITIVE2

From the ‡Department of Plant Systems Biology, VIB, 9052 Ghent, Belgium; §Department of Plant Biotechnology and Bioinformatics, Ghent University, 9052 Ghent, Belgium; ¶Medical Biotechnology Center, VIB, 9000 Ghent, Belgium; ‖Department of Biochemistry, Ghent University, 9000 Ghent, Belgium; **Gnomixx, 9000 Ghent, Belgium; ‡‡Institut National de la Recherche Agronomique, Institut Jean-Pierre Bourgin, Unité Mixte de Recherche 1318, Equipe de Recherche Labellisée Centre National de la Recherche Scientifique 3559, Saclay Plant Sciences, 78026 Versailles, France; §§AgroParisTech, Institut Jean-Pierre Bourgin, Unité Mixte de Recherche 1318, Equipe de Recherche Labellisée Centre National de la Recherche Scientifique 3559, Saclay Plant Sciences, 78026 Versailles, France; ¶¶Centre de Recherche de Gif, Institut de Chimie des Substances Naturelles, Unité Propre de Recherche 2301, Centre National de la Recherche Scientifique, 91198 Gif-sur-Yvette, France, ‖‖Laboratoire des Interactions Plantes-Microorganismes, Unité Mixte de Recherche 441, Institut National de la Recherche Agronomique, 31326 Castanet-Tolosan, France; and [a]Laboratoire des Interactions Plantes-Microorganismes, Unité Mixte de Recherche 2594, Centre National de la Recherche Scientifique, 31326 Castanet-Tolosan, France

Received March 30, 2015, and in revised form, June 9, 2016
Published, MCP Papers in Press, June 17, 2016, DOI 10.1074/mcp.M115.050062
Author contributions: A.W., E.S., K.G., and S.G. designed research; A.W., E.S., G.G., L.B., M.V., C.M., C.D.C., A.S., J.V., F.-D.B., and J.F. performed research; A.W., E.S., G.G., and R.V. analyzed data; A.W., E.S., K.G., and S.G. wrote the paper.

[1] The abbreviations used are: C4H, cinnamate-4-hydroxylase; CFI, chalcone flavone isomerase; CHS, chalcone synthase; D14, DWARF14; DAD, DECREASED APICAL DOMINANCE; DPBA, diphenylboric acid 2-amino ethyl ester; F3H, flavanone 3-hydroxylase; FLS, flavonol synthase; GO, gene ontology; HPLTC, high-performance thin-layer chromatography; hpt, hours post treatment; HTL, HYPOSENSITIVE TO LIGHT; KAI, KARRIKIN INSENSITIVE; LRD, lateral root density; LTQ, linear trap quadrupole; MAX, MORE AXILLARY GROWTH; MS, Murashige and Skoog; NAP, nonintrinsic ABC protein; PAL, phenyl ammonia-lyase; PIN, PIN-FORMED; *rac*-GR24, strigolactone analog; UGT, UDP-glucosyl transferase; ULPC, ultra-performance liquid chromatography; WT, wild type.